Mobile EV Charging

Design, Optimization and Evaluation of Battery-Integrated Robots to Improve Electric Mobility

Arda Fikret Sülecik

Delft University of Technology

TU Delft

Mobile EV Charging

Design, Optimization and Evaluation of Battery-Integrated Robots to Improve Electric Mobility

by

Arda Fikret Sülecik

to obtain the degree of Master of Science
at the Delft University of Technology,
to be defended publicly on Monday March 26, 2024 at 13:00.

Student number:	4851234	
Project duration:	July 1, 2023 – March 26, 2024	
Thesis committee:	Prof. dr. ir. P. Bauer,	TU Delft, supervisor
	Dr. ir. G. R. Chandra Mouli,	TU Delft
	Dr. ir. D. van der Born,	TU Delft
Daily Supervisor:	Alvaro Menendez Agudin	TU Delft

Cover: Cover image created using design tools on Canva.com

An electronic version of this thesis is available at http://repository.tudelft.nl/.

TU Delft

Summary

This thesis explores the development of mobile charging systems, which could significantly ease the challenges associated with current electric vehicle charging methods. The purpose of this thesis is to develop an autonomous system to fulfil estimated charging demand on a typical day under different conditions to exemplify how mobile charging systems can address these issues.

The research is mainly motivated by the limitations of conventional charging poles, such as their scarcity, lengthy charging times, unregulated demand, and urban space conflicts as EV usage grows. Future EV statistics and charging station projections are presented underscoring how these challenges can be amplified shortly. As an alternative solution, mobile charging systems are introduced highlighting products, prototypes, and studies in the market and literature. Through stakeholder analysis, these systems are shown to benefit investors, consumers, and the public, supporting the grid, facilitating convenient charging, and offering solid financial returns.

The thesis incorporates a charging demand estimation algorithm to simulate the charging tasks on a typical day. This demand estimation is represented as private, public, and workspace charging load, sampled by considering the probability of energy demand and connection times. Next, the study integrates an iterative optimization process to simulate how effectively this demand can be addressed by a robot-like mobile charging system. Furthermore, the system is simulated with different price scenarios, grid capacity values of 50 and 100 kW, varying the number of units between 3 and 5, and adjusting battery sizes between 70 and 400 kWh. As a result, it is demonstrated that mobile charging systems can effectively reduce peak demand by decoupling charging demand from the grid while offering a more convenient charging experience. The profitability is assessed through energy arbitrage, operational revenues, and energy costs, noting improvements with seasonal effects and higher grid capacity. However, life expectancy assessments using Li-ion battery degradation models show that while higher grid capacity slightly boosts profits, it reduces peak demand benefits and accelerates battery wear if used heavily for energy arbitrage, limiting lifetime returns. Furthermore, investment costs associated with the system are calculated and compared to a system with charging poles. The results show that the switchable battery configuration can effectively minimise the required investment costs because of the smaller number of necessary carrier units mobilising the battery units. A switchable battery setup with 3x270 kWh batteries and 2 carriers is identified as cost-effective for public and workplace demand, with a potential increase to 340 kWh for higher returns despite 20% more investment. The sizing process is reiterated for another demand scenario consisting of a private charging load and 260 kWh capacity is highlighted as a cost-effective choice, while the profits can be improved with 310 kWh capacity.

The thesis further discusses the mobility necessities of the system and the performance requirements of the powertrain. To maintain grounding, the study simulates the parking service area of P1 at the TU Delft campus. A driving cycle is developed by taking site measurements and also considering safety concerns and standards. Consequently, energy consumption and maximum power requirement are calculated by also integrating a weight estimation methodology regarding the main components of the system. As a result of analysing different traction machines, an induction motor is found as a suitable solution fulfilling the performance criteria and minimizing the investment costs.

Lastly, the thesis introduces different power converter topologies that can act as a bridge between the system and EVs. As a consequence of a comprehensive analysis of different converters and the findings reported in the literature, various topologies are suggested to be used in different cases. In particular, DAB and full-bridge converters are highlighted due to their relative simplicity and outstanding high-power performance in stationary applications where efficient packaging is not the priority. On the other hand, in a mobile onboard charger where the dimensions of the converter play a key role, the LLC Resonant converter becomes prominent due to its high power density and efficiency.

As a result, the findings reveal that mobile charging systems could offer a significant improvement over charging poles by providing flexible, on-demand services that reduce charging times and space requirements. These systems can adapt to the dynamic demands of urban environments, offering a competitive and convenient solution which could be attractive to the investors and public.

Contents

List of Figures

List of Tables

Nomenclature

Abbreviations

Abbreviation	Definition
AC	Alternating Current
BESS	Battery Energy Storage System
BEV	Battery Electric Vehicle
BMS	Battery Management System
CC	Constant Current
CCS	Combined Charging System
CS	Charging Station
CV	Constant Voltage
DAB	Dual Active Bridge
DC	Direct Current
EU	European Union
EV	Electric Vehicle
IP	Ingress Protection
IoT	Internet of Things
LiDAR	Light Detection and Ranging
LV	Low Voltage
MILP	Mixed Integer Linear Programming
OEM	Original Equipment Manufacturer
PMSM	Permanent Magnet Synchronous Motor
PWM	Pulse Width Modulation
ROI	Return on Investment
SoC	State of Charge
SoH	State of Health
THD	Total Harmonic Distortion
V2G	Vehicle to Grid

Symbols

Symbol	Definition	Unit
A_f	Frontal Area	$[m^2]$
C_{cal}	Calendar Aging	$[-]$
C_{cyc}	Cycling Aging	$[-]$
C_D	Drag Coefficient	$[-]$
C_{battery}	Battery Cost	[\$]
C_{D}	Total Cost of Degradation	[€]
C_{G2B}	Total Cost of Electricity	[€]
E_r	Regenerated Energy	$[J]$
E_t	Total Energy Consumed	$[kWh]$
F_a	Acceleration Force	$[N]$
F_{ad}	Aerodynamic Drag Force	$[N]$
F_g	Gradient Force	$[N]$
F_{rr}	Rolling Resistance Force	$[N]$
F_t	Total Force Exerted on the Vehicle	$[N]$

Symbol	Definition	Unit
f_r	Rolling Resistance Coefficient	$[-]$
GC	Grid Capacity	$[kW]$
g	Gravitational Acceleration	$[m/s^2]$
h	Altitude Above Sea Level	$[m]$
L	Temperature Lapse Rate	$[-]$
L	Degradation Cost per Energy Transfer	$[€/kWh]$
$M_{BatteryUnit}$	Mass of the Battery Unit	$[kg]$
$M_{MainUnit}$	Mass of the Main Unit	$[kg]$
P_b	Power Drawn from the Battery	$[W]$
$P_{\mathsf{B_{MAX}}}$	Maximum Charging Power	$[kW]$
$P_{\mathsf{M_{avg}}}$	Average Powertrain Power	$[kW]$
P_r	Power Required for Travel	$[W]$
$Price_{\mathsf{C}}$	Electricity Price Offered for Charging EVs	$[€/kWh]$
$Price_{\mathsf{G}}$	Electricity Price Asked by the Grid	$[€/kWh]$
Q	Battery Capacity	$[kWh]$
R	Ideal Gas Constant	$[J/molK]$
R_{B2G}	Total Revenue of Grid Arbitrage	$[€]$
R_{B2V}	Total Revenue of Charging	$[€]$
T	Absolute Pressure	$[K]$
T_0	Standard Temperature at Sea Level	$[K]$
V	Velocity of the Unit	$[m/s]$
W	Wind Speed	$[m/s]$
p	Absolute Pressure	$[Pa]$
p_0	Standard Atmospheric Pressure at Sea Level	$[Pa]$
α	Gradient Angle	$[°]$
Δt	Timestep	$[h]$
η_{B2G}	Discharging Efficiency of Batteries	$[-]$
η_{B2V}	Charging Efficiency of EVs	$[-]$
η_{G2B}	Charging Efficiency of Batteries	$[-]$
η_{M}	Powertrain Efficiency of Units	$[-]$
η_{reg}	Regenerative Braking Factor	$[-]$
ρ	Air Density	$[kg/m^3]$

1

Introduction

Technology, business, and policy concepts are evolving due to the climate crisis that nature and humanity have been experiencing. Global carbon emissions in 2022 reached 36.8 $GtCO_2$, an all-time high, urging stakeholders to act more environment responsibly and consciously [78], [102]. This alarming trend of emissions and the climatic consequences has resulted in a policy shift towards sustainability, along with vast technological and regulatory developments in almost every sector. Mostly powered by fossil fuels, the mobility and transportation sector is one of the most significant contributors to global emissions. In 2022, motorised transport by road, rail, shipping, air and pipeline accounted for 7.95 $GtCO_2$ of emissions [103]. In detail, road transportation by itself was responsible for 73.8% of CO_2 emitted into the atmosphere by the transportation sector [103]. Sustainable transportation therefore holds significant value in the reduction of greenhouse emissions, and making this sector emission-free would lead to a remarkable decrease in environmental damage.

As a response to the need to decrease the carbon footprint globally, the Paris Agreement was adopted by 196 Parties at the UN Climate Change Conference (COP21) on 12 December 2015 [190]. Consequently, the parties pledged to decrease their emissions in order to keep the global average temperature increase below 2°C compared to the pre-industrial levels [190]. This pledge implies an array of advancements in the global infrastructure, reshaping not only how the energy is generated and transmitted, but also how it is stored and ultimately used. Moreover, the technology playing a part in these advancements is constantly being redefined due to policy frameworks. One of the most important examples of this revolution is the European Union's (EU) restriction on fossil fuel-powered cars. According to the regulation, in order to reach carbon neutrality by 2050, the sale of new road vehicles equipped with internal combustion engines will be banned by 2035 [58]. Some of the countries with more ambitious targets such as the Netherlands, Iceland, Sweden, Ireland and Slovenia even bring this deadline forward to 2030 [144], [17]. This has prompted global automotive manufacturers to adjust their production lines and their product catalogues in order to catch up with the sustainable mobility revolution [185]. In 2022, the total number of passenger cars registered in the EU was 253,305,631 [59]. Moreover, considering that 21.6% of all registered vehicles in 2022 were electric vehicles (EVs), it is foreseeable that this percentage will heavily increase in light of the adoption policies implemented [57].

Another consequence of the countries' adoption of the Paris Agreement was a shift toward more sustainable energy generation methodologies. Primarily, the deployment of solar and wind power plants has picked up globally. With cumulative power capacity shares in 2023 of 14.7% and 11.4% respectively, solar and wind energy are expected to dominate the energy landscape, driving a significant shift away from traditional fossil fuel sources and playing a pivotal role in global endeavours to address the climate crisis [100]. Furthermore, by 2027 these shares are predicted to reach 22.2% and 14.4% respectively, as shown in Figure 1.1 [100].

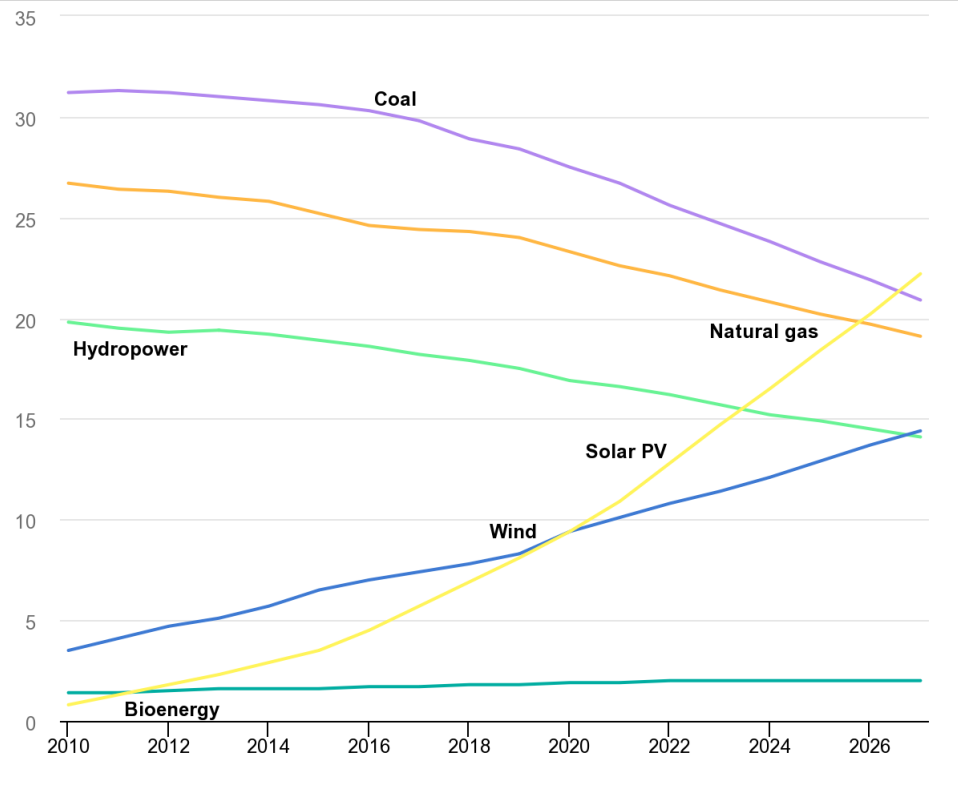

Figure 1.1: Share of cumulative power capacity by technology, 2010-2027[100]

1.1. Electric Vehicles and Charging Infrastructure

Today, significant barriers are making the EV market penetration limited, even though they play a pivotal role in the sustainable mobility transition and their use is encouraged by policy and business perspectives. Remarkably, charging infrastructure is one of those challenges making potential drivers question if they will be able to charge their cars whenever they wish and as quickly as they desire. Addressing this issue requires a wide-scale cooperation between the government-owned and private entities. For example, in February 2023, the total number of charging stations in the Netherlands was announced as 128,032, which 4,376 of are equipped with fast charging [138]. This number is a result of a strong collaboration among the Dutch Government, local governments, and public-private partnerships to reach ambitious climate goals set by the Dutch National Climate Agreement which concluded in 2019 and Fit for 55 package [137]. In this regard, The Dutch National Charging Infrastructure Agenda aims to further develop the charging infrastructure in the Netherlands, and widen the coverage of the network to increase accessibility.

In a broader perspective, the number of battery electric vehicle registrations in the EU is announced as 1,126,682 in 2022 [57]. Meanwhile, the number of charging stations in Europe is also growing in parallel, surpassing 500,000 units in 2022 [175]. Aligned with the EU climate goals, the number of charging stations is expected to reach 5 million by 2030, and then increase to 10.4 million by 2035 to serve an estimated 131 million EVs, following the implementation of vehicle sale restrictions, as shown in Figure 1.2 [187].

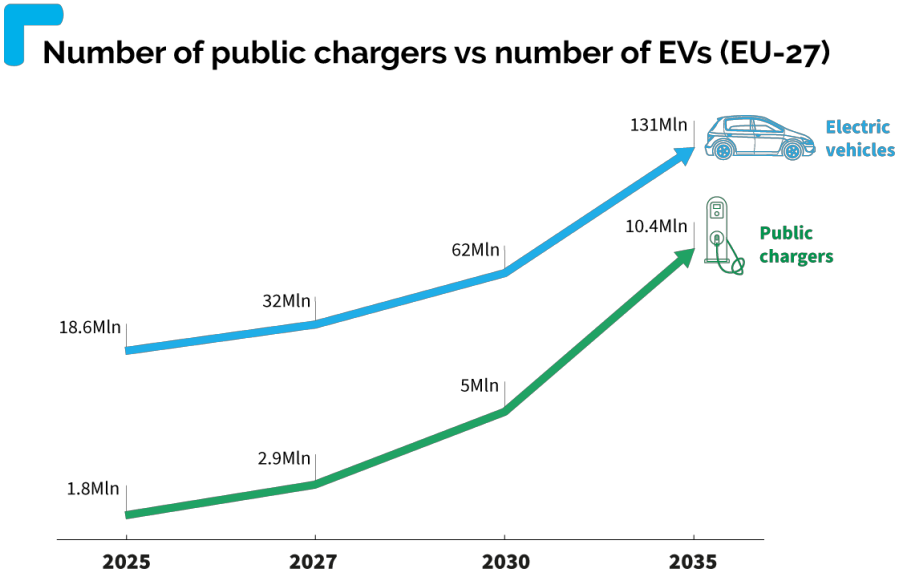

Figure 1.2: Number of public charging stations and EVs in the EU [187]

Furthermore, in a more conservative scenario, the minimum number of public charging stations that should be installed in the EU is predicted as 3.4 million by 2030 in order to develop the charging network in parallel to the increasing demand and climate goals [37]. Nevertheless, the European Automobile Manufacturers' Association (ACEA) has proposed the installation of 7 million charging stations across the EU by 2030 to lower market barriers, boost EV sales, and ensure an infrastructure capable of meeting drivers' needs following the sale [56].

Even though the significant increase in the number of charging stations has lots of advantages for sustainable mobility, it also brings about certain challenges. First, the instalment itself requires a remarkable investment. In 2032, the global charging station market is estimated to reach 280.6 billion $[80]. Furthermore, it is estimated that the number of installations proposed by ACEA will result in utilization rates as low as 5% [187]. Considering that these investments stem from both public and private capital, any unprofitable deployments would need to be subsidized, leading to substantial public expenditure [187]. Hence, the deployment should be able to pay off itself in order to reveal a sustainable business model. Second, one should pay attention that each charging station takes up a significant space in the urban environment. Although current figures do not indicate any conflict between urban space and the occupation of charging stations, it is foreseeable that a significant amount of urban space will be required for charging purposes when the number of EVs scales up to 131 million.

Another challenge to be addressed is the lengthy duration of EV charging [50], [165]. Extensive development is underway to offer drivers shorter waiting times. Specifically, the solution largely depends on the charging power used during the process. At this juncture, DC fast charging emerges as a notable solution, significantly reducing waiting times. For instance, a Tesla Model 3 can gain up to 322 km of range in just 15 minutes under optimal conditions using Supercharger technology, which is equipped with Level 3 DC charging [183]. Increasing the power of charging stations shortens the charging time. However, there is still a significant gap to bridge before EV charging can match the speed of today's refuelling times. Additionally, higher charging powers necessitate cables with larger cross-sections for insulation, resulting in heavier cables [197]. This makes cable handling a challenge for some drivers, thereby impacting the accessibility and convenience of EV technology. Furthermore, due to their high power demand, the fast charging technology requires a significant improvement in the grid management side. It poses challenges to the power grid, including potential voltage drops that could threaten system stability [1], [4]. A large number of fast chargers may strain the current power grid beyond capacity, leading to possible rapid failures and putting immense strain on the power grid [120].

Even if the higher charging powers allow a significant reduction in waiting times, there are also additional bottlenecks experienced by EV drivers regarding the charging infrastructure. For example,

it is reported that the drivers have sometimes difficulties due to the queues at the charging locations [165]. In detail, according to the survey conducted in the Netherlands, 46% of the people reported they face the issues due to the insufficient number of public charging stations in the area which could be the root cause of these queues [156]. Moreover, the effect of this insufficiency is further amplified when the charging station is blocked. This blockage can be caused by another EV which is left plugged in but not charging anymore since its battery is full. On the other hand, this could be an ICE vehicle which uses the charging location as a parking place. In the same survey, 43% of the respondents reported that they witness such incidents in their daily lives [156].

1.2. Mobile EV Chargers

The deployment of mobile chargers stands out as an innovative solution to overcome the current barriers to EV adoption and address some of the problems that today's EV owners face. These mobile chargers can either be in the form of battery units supporting or undertaking the charging activities, or grid-connected systems. Primarily, these systems enable more strategic planning of charging operations, leading to improved utilization rates. For instance, charging tasks that would typically require a large network of fixed stations can be efficiently managed by a smaller fleet of mobile units, thereby optimizing resource use and increasing utilization [4]. This advantage fundamentally paves the way for a more efficient use of urban space. However, the utility of mobile charging systems extends beyond merely offering EVs a charging solution. By their inherent flexibility, if they are equipped with batteries, they can function as mobile energy storage units, absorbing excess energy generated during periods of low demand and dispensing it during peak times [4], [131], [198], [194]. When the increasing portion of renewable sources in the energy mix is considered, the storage functionality even becomes more significant. This dual capability allows them to play a pivotal role in the broader context of the renewable energy transition, positioning them as a critical component in the effort to mitigate emissions from two of the largest contributing sectors: transportation and energy production. By acting as a dynamic buffer for the energy grid, mobile charger robots not only facilitate a more resilient and adaptable charging infrastructure for EVs but also enhance the integration of renewable energy sources, smoothing out the variability of supply and demand when they are considered battery units connected to the grid [41]. This synergy has the potential to accelerate the decarbonization of these sectors, marking a substantial stride towards achieving a sustainable, low-carbon future. This battery integration also helps to decouple charging demand from the grid, operating in a more network-friendly manner, mitigating the necessity of significant investments to improve grid capacity [120]. These systems can fulfil the charging tasks, supplying high charging powers while using a lower grid capacity and reducing the effects of fast charging [120], [160]. Moreover, drivers are responsible for plugging in their vehicles currently, which inherently restricts the physical properties of the charging cables and hence the charging power to what is manageable by human strength and skill [197]. With mobile EV chargers, the connection process is managed by a fully automated system, which becomes increasingly important to address the challenges of heavier cables and increasing safety concerns associated with the higher charging powers to reduce the charging times. Ultimately, this system could greatly enhance smart charging capabilities through its potential flexibility. Charging sessions can be optimally timed, and the interaction between the charger, the electric vehicle, and the power grid can be efficiently managed in real-time through live data acquisition.

1.3. Research Objectives

This thesis aims to investigate the main challenges associated with today's charging solutions from different perspectives to analyse an alternative solution, mobile charging, which can mitigate the related problems. To determine the scope of the research, the research gaps are identified as a result of a literature review presented in Section 2. Following these gaps, the goal of the designed framework is expressed as one general question in Section 1.3.2, while the main idea is branched under Section 1.3.3, to fully convey the details and distinguish the related disciplines of the position of this study.

1.3.1. Research Gaps

There is extensive research and development on mobile charging systems highlighting academic and corporate interest towards this area. In the literature, different studies are focusing on the practicality of such solutions, proposing designs and discussing the outcomes. These studies are grouped under

two categories depending on their focus, such as Mobile Charging System Configurations and System Optimization Studies on Mobile Charging Techniques in the literature analysis reported in Section 2. As a consequence of the literature analysis, the following research gaps can be identified:

- **Lack of Performance Assessment in Different System Configurations**
  The system configurations mainly describe the alternative approaches studied to substitute the regular charging poles. These approaches are pronounced as Battery-less Systems [92], [36], [143], [15], [49], [121], [197], [152], [114] [90], [97], Large Scale Battery Integrated Systems [25], [162], [116], Battery Swapping Systems, [168], [25] and Robot-like Systems with Batteries, [16], [111], [70], [135], [8], [71], [53], [196]. Generally, even if these studies and products demonstrate an effective use of mobile charging systems and share valuable insights on their designs, they lack a comprehensive attitude towards the designs introduced, without sharing any operational assessment or critical methodology to numerically test and verify the system's performance under various parameters. Therefore, such studies do not go beyond demonstrating prototypes, conceptually highlighting the benefits and reviewing the state-of-the-art, except one of them analysing the effect of different parameters under an assumed fixed battery capacity [111].
- **Limited Focus on Robot-Like Solutions in Urban Setting**
  Most of the reported studies focus on battery-less, grid-connected systems, undervaluing the challenges associated with the electricity grid as a consequence of substantial charging load. Furthermore, among the ones focusing on battery-integrated systems to address additional challenges related to the grid, it is found that the academic interest rather focuses on large-scale systems such as vans or trailers loaded with batteries to operate remote locations or provide emergency charging services or battery-swapping stations. Therefore, only a limited number of papers address the scalable systems that suit the urban environment and potentially substitute the regular charging poles, meanwhile, it is found that corporate interest is growing in this area as different partnerships and startups reveal robot-like systems to operate inner-city parking places. As a result, this thesis sets a unique example to focus on robot-like systems with batteries that will suit well urban charging, critically evaluate the options in terms of configurations and system sizes and assess the attractiveness of the solution from different perspectives.
- **Limited Analysis in Mobile System Sizing**
  Moreover, the studies focusing on sizing the mobile systems generally approach those systems in a complementary layout, either focusing on systems like delivery vans, mobile swapping stations or on-site charging services operating besides regular charging poles [181], [210], [160], [29], [153], [95], [120]. That means, they often realise a system made up of regular charging poles which are supported with the use of mobile batteries or chargers in a city or neighbourhood. Furthermore, such studies sometimes use assumptions on the battery capacity of the system, lacking a critical approach to reveal the effect of sizing on the final result. Even if some papers set the system size as a decision variable, the robustness of the system is not evaluated by using different price scenarios, grid capacities and charging demand patterns. Therefore, it is also aimed to assess the system's performance depending on its size under different conditions.
- **Lack of Focus on Energy Arbitrage**
  Such studies generally disregard the possibility of energy arbitrage which can bring along extra benefits for the grid and the investors, since it is more difficult to achieve so in a relatively large operational area like a city or a remote place. On the other hand, when robot-like systems are studied in a smaller operational area than a typical city, energy arbitrage becomes easily achievable, unlike delivery vans or emergency charging services. As a result, the thesis also establishes a distinctive methodology with enhanced system integration with the help of bidirectional energy flow between the batteries and the grid. This way also can pave the way for a better integration of renewable energy generation, allowing the storage in the batteries to be used when there is a deficit.
- **Need for Computational Efficiency and Trustability in Sizing Methodologies**
  The necessity of the minimization of the computational requirements also emerges as a key issue as a result of the literature analysis. The optimization studies often rely on computationally expensive methodologies such as Reinforcement Learning and heuristics or even complex custom-made combinatorial optimization algorithms. For such algorithms, the factor of explainability frequently emerges to be able to trust the results. When the tool solving the algorithms can

not claim global optimality or does not allow an understanding of why the output is returned in a certain way, a comprehensive verification process becomes necessary. Therefore, by utilizing a framework whose accuracy and performance are verified while also not compromising global optimality, the designed methodology sets a basis for formulating optimization problems whose solutions can be claimed as global optimum points by employing linearization techniques.

- **Insufficient Focus on Financial Analysis and Comparative Studies**
  As the literature does not generally focus on fulfilling the charging demand by only using mobile charging systems, it offers limited analysis of the financial performance and competitiveness compared to today's solutions. However, these factors often determine the viability of applications for different stakeholders. Furthermore, a comprehensive comparison of the advantages and disadvantages of different mobile charging system configurations such as robot-like units with built-in and switchable batteries, using numerical examples and frameworks is also missing. Hence, it is essential to test and verify the system's performance in different practical scenarios to highlight operational necessities and assess its capabilities, while proposing a system sizing and configuration.
- **Absence of Multidisciplinary Approach**
  Lastly, the related studies often approach this topic from a single discipline, such as reviewing the literature for reporting the state of the art, optimising the system's parameters such as pricing or service location, designing mechanisms, components or algorithms to implement, and proposing a prototype. Especially, it is noted that the literature does not extensively address the powertrain and power electronics requirements of the system due to the absence of comprehensive analysis focusing on robot-like systems. Therefore, the lack of a multidisciplinary approach, addressing the ideal configurations, and parameters, suggesting design solutions focusing on various aspects such as powertrain and power conversion and testing the outcoming performance of the system in various scenarios contributes to this research gap and the main motivation behind this thesis. To address this gap, a multisided framework is created to evaluate the status quo, report the potential solutions, create scenarios and discuss the results as a consequence of a comprehensive analysis.

1.3.2. Main Research Question

Bearing in mind the upcoming restrictions on road vehicles and the increasing demand for EVs, sufficient charging infrastructure is crucial to encourage the expansion of sustainable mobility in the short term and to make the charging process more convenient. Today, the insufficiency of charging infrastructure can be attributed to occupied charging spaces, lack of charging stations and overall long charging duration. All those challenges cause the charging process to become something planned, instead of being intuitive and user friendly. Challenges encountered and testimonies given by EV users set a significant barrier against the transportation sector to become more sustainable. Furthermore, heavy adoption of EVs requires a great number of charging station installations which will occupy too much space and eventually start conflict with urban life, when today's chargers are scaled according to the number of passenger vehicles. This expansion also raises concerns about the utilization ratio of the installed systems and questions about the self-sufficiency of the business scheme. Moreover, uncontrolled charging also poses a threat to the efficient management of energy and causes unpredictable power peaks and valleys.

Regarding the setbacks emphasized above the main research question can be expressed as follows.

How can the development of an effective mobile charging system be compared in terms of performance outcomes to the regular charging poles from the perspectives of the public, investors, and EV drivers while

- **Promoting the widespread adoption of EVs in urban settings,**
- **Addressing the current challenges experienced by EV drivers and grid management?**

1.3.3. Research Sub-Questions

Considering the complexity and how multi-faced the research question is, the main question can be divided into several subquestions to analyze the domains clearly, identify the trade-offs associated with

the system's development and evaluate the performance of the design in a more organised framework. These subquestions are listed below.

1. What are the challenges associated with today's EV charging systems? What alternative methods can be proposed instead of charging poles to address these challenges? What potential benefits can mobile charging bring along, compared to regular charging poles?
2. What is the optimal configuration that can be suggested as a mobile charging solution in the urban setting?
3. How can a realistic demand estimation be conducted to identify the charging tasks the mobile system fulfils in a typical day?
4. What could be an effective sizing strategy for this proposed mobile charging system? How many units should be considered and what should be the size of their batteries in the proposed configuration?
5. How does the powertrain system need to be built to achieve the expected functionality and performance requirements, and what characteristics should the system possess to ensure suitability?
6. How can the power conversion topology be implemented to act as a bridge between the system and EVs?

As the goal of the thesis is to address the identified Research Gaps in Section 1.3.1, the Research Sub-Questions are directed to tackle these gaps and pave the way for a unique and comprehensive analysis. In this regard, Research Sub-Question 1 aims to deepen the focus on Robot-like Systems with batteries, requesting an introduction of alternative charging methodologies and a comparison of these techniques to highlight their advantages. Given the operational area of the urban setting, Research Sub-Question 2 takes this analysis further to demonstrate the effective use of such systems to substitute regular charging poles. Furthermore, as the identified gaps point out a necessity of comprehensive performance and sizing analysis, Research Sub-Question 3 lays the foundation to create realistic charging demand scenarios to demonstrate the effect of different parameters on the proposed system parameters to enlarge the depth of the performance assessment. Moreover, Research Sub-Question 4 sets a basis to decide on an effective system size by analysing the influence of the number of units and the battery capacities on financial outcomes, also paying attention to the energy arbitrage. The answer to this question potentially fills various research gaps because it exhibits a comprehensive sizing analysis by accounting for various scenarios to further process the outputs to present a comparison and financial analysis, revealing the advantages and disadvantages of the system. In addition, the employed methodology to answer this Sub-Question also uses computational resources efficiently as well as employing techniques whose outputs can be verified and explainable to prove optimality. Finally, Research Sub-Questions 5 and 5 aim to enlarge the scope of the thesis to come up with a multidisciplinary approach, and address two more main technical points of the system, thus contributing to the uniqueness of the study.

1.4. Thesis Outline

This thesis consists of 7 Sections. In Section 2, today's charging solutions are introduced. In addition, challenges associated with these solutions are identified. Following that, alternative charging solutions that can potentially address these challenges are exemplified and mobile charging systems are described by using concrete example products in the market and taken from the studies in the literature. The section ends with a discussion of the potential benefits of mobile charging systems from different stakeholders' perspectives. Next, an algorithmic framework for charging demand estimation is introduced and the results are given in Section 3. Meanwhile, Section 4 mainly demonstrates a framework to size the mobile system while discussing the advantages and disadvantages of different mobile charging configurations. In order to come up with a comprehensive analysis, different inputs such as various electricity price and demand scenarios, grid capacity, number of units and battery capacity values are iterated in a Mixed Integer Linear Programming (MILP) problem. Consequently, the results are presented and the trade-offs are identified. The financial performance of the proposed system is assessed by processing the results and comparing them to traditional charging poles with the help of a business evaluation metric, considering the profitability, investment cost and product life of the system determined by the battery degradation. Furthermore, Section 5 describes the powertrain requirements of the system by first distinguishing the performance criteria. These requirements are transformed

into numbers in the form of maximum power and energy consumption per driving cycle following a weight estimation. Taking the numbers into account, a traction motor selection procedure is exhibited by discussing the advantages and disadvantages of the potential electric machine types. Moreover, power conversion topologies that can act as a bridge between the system and EVs are introduced and discussed in Section 6. In light of reported experimental values in the literature, adequate converter topologies for stationary and mobile applications are suggested. Lastly, in Section 7, the discussion is wrapped up and key findings are concluded also by emphasizing the future work.

2

State-of-the-Art

This section presents a comprehensive state-of-the-art analysis made up of the studies reported in the literature and the products developed as an alternative to charging poles. First, regular charging stations, which are grouped as private and public, are introduced. Next, mobile charging systems are described and alternative charging methodologies are demonstrated as well as discussing their advantages and disadvantages in accordance with Research Sub-Question 1. Consequently, the challenges associated with today's EV charging systems are highlighted and matched with the solutions that mobile charging systems bring along to fully answer this question. Finally, the benefits of the introduced methodologies are emphasized from different perspectives and matched with the challenges they potentially address. As a result of this comparative analysis, an optimal methodology well-suited to urban settings is introduced to answer the Research Sub-Question 2.

2.1. Fixed Charging Stations

Fixed charging stations, taking the form of standard electrical plugs or buildings equipped with multiple charging outlets, serve as enduring fixtures powered by the electricity grid or local energy sources [12]. These stations, distinguished by their accessibility, are divided into two primary categories: private charging stations and public charging stations, both of which are also called charging poles[4].

2.1.1. Private Charging Stations

Private charging stations are set up in places that demand restricted entry, such as private residential complexes and business parking lots accessible solely to authorized individuals, whether residents, employees, or visitors [33], [104], [4]. Meanwhile, many residential charging stations, typically operate at a slow charging pace [4].

In the realm of private charging infrastructure, three tiers define the charging rate: AC Level 1 (slow charging), AC Level 2 (moderate-speed charging), and Level 3 (fast charging) [7]. For home charging setups, there is a choice between the relatively slow Level 1 charger equipment or the slightly more powerful Level 2 [4]. Despite the declining prevalence of Level 1 chargers due to their limited charging power, they still constitute a significant proportion of charging instances and remain pivotal in driving EV adoption [169], [4].

2.1.2. Public Charging Stations

EV owners often rely on home charging for its affordability, yet the scarcity of private parking in urban centres and lengthy charging times propel the necessity for public charging stations [29]. These stations, typically equipped with Level 2 or Level 3 chargers, are situated in various public venues like parking lots, malls, and eateries [4]. While slow charging predominates in private and public settings, fast chargers are also geared towards commercial and public use [104], [117], [4].

Governments worldwide envision a significant expansion in public charging infrastructure, with projections ranging from 14 million slow to 2.3 million fast chargers by 2030, potentially surpassing 24 million public chargers and 4 million fast chargers under more ambitious climate goals following the Paris Agreement's Climate goals [104], [190]. Considering this drastic expansion of the charging network,

these numbers also highlight the public space requirement in the urban setting to meet the charging demand.

Public charging infrastructure is also instrumental in supporting the EV market and facilitating faster charging times, notably through advancements in DC fast charging technology, which could cut charging durations to less than 30 minutes [89], [34], [128], [4].

However, the implementation of fast chargers poses challenges to the power grid due to their high power demand and notably variable loading characteristics [128], [2]. Consequently, the power distribution network must adapt to accommodate the demands of fast-charging stations through capacity improvements [109], [4].

2.2. Mobile Charging System Configurations

This section introduces mobile charging systems studied in the literature to address the challenges of the regular EV charging process. Primarily, the studies and development are exemplified along with the solutions they bring along by matching them to the setbacks associated with today's EV charging procedures. The goal of this section is to set a basis to introduce these alternative solutions and demonstrate the potential benefits of these systems Research Sub-Question 1 considers.

As the transition to a zero-emission future accelerates, mobile EV charging systems are increasingly recognized as a promising solution to meet the evolving demands of electric EV infrastructure. In this dynamic arena, automobile manufacturers, Original Equipment Manufacturers (OEMs), and innovative start-ups are intensively researching and developing to integrate these systems into the EV technology landscape. The field showcases a wide variety of projects, each highlighted by distinctive approaches and considerations that regard strategic objectives. Subsequent sections will explore each categorised approach in detail, shedding light on the cutting-edge advancements and their potential impact on the future of EV charging. These solutions can be highlighted as alternative charging approaches that can be proposed instead of regular charging poles.

Mobile EV chargers can primarily be categorized under 4 different titles as shown in Figure 2.1, namely Battery-less Systems, Large Scale Battery Integrated Systems, Mobile Battery-Swapping Station Systems and Robot-like Systems [25]. The first category mainly describes the systems equipped with power converters to establish the connection between the EV and the grid, providing extra convenience compared to a regular charging station. Furthermore, the second category generalizes the mobile battery services fulfilling charging demand at the desired location and time. These systems mainly charge their batteries from the grid and act like an energy delivery system by request. The third category of systems can also be proposed which are capable of providing the delivery of mobile and switchable batteries, fulfilling the requested operation faster on-site, instead of charging the EVs. Meanwhile, the fourth option depicts the autonomous robotic systems which are capable of travelling to the location requested, managing the plugging process and handling the charging demand by the stored energy in the batteries. The fourth option is suggested as an effective solution when the study area can be contained in a relatively smaller area such as a parking place [25].

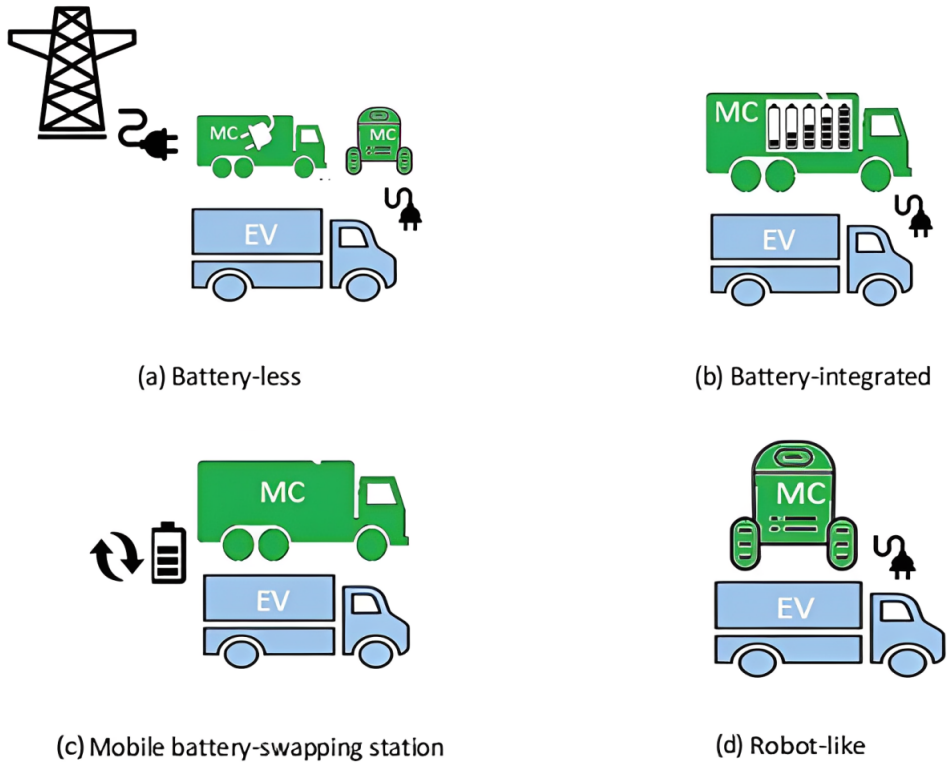

Figure 2.1: Categories of Mobile EV Charging Systems [25]

2.2.1. Battery-less Systems

EV charging cables are designed to handle substantial currents, ranging from several tens to hundreds of amperes. To minimize the charging duration and make it comparable to the refuelling process of vehicles using internal combustion engines, the implementation of high-power charging systems is crucial. These systems enable the rapid recharging of electric vehicles within a time frame closer to conventional refuelling, as the waiting time is one of the major concerns raised by the drivers [50]. The Society of Automotive Engineers establishes the specifications of Level III DC Charging, capable of delivering currents up to 400A and voltage up to 600V [186], [46]. At the core of the matter, heat generation from high currents and safety considerations stemming from accelerated ageing lead to the production of thicker cables, which in turn significantly increases their weight and stiffness. Currently, the fact that the plugging operation is performed manually by individuals imposes considerable ergonomic limitations on the design of these cables. For example, lengthy and bulky cables with a restricted bending radius occupy significant space [197]. A CCS-Type 2 (Combined Charging System) charging cable, used for charging capacities up to 106.25 kW, weighs 1.7 kg/m and has an external diameter of 28.2 mm [197]. This issue of cable handling can be addressed by some of the battery-less systems. At the centre of these configurations is a robotic, actuated arm that takes over the connection process, executing this task with enhanced safety compared to human operation. However, the platform that supports the arm is stationary and linked to the grid, making these units dedicated to their designated charging zones. Furthermore, this system generally benefits from artificial intelligence-powered cameras, sensors, and LiDAR (Light Detection and Ranging) systems to recognize the vehicle dimensions, place the charging inlet and protective lid, and identify the type of inlet and its precise location implemented in the EV.

The lack of automation in the charging process appears as a setback, affecting the convenience of EV charging. An alternative battery-less system could be underbody conductive charging units. Hirz et al. discuss the use of such charging systems for enhanced convenience [92]. The primary objectives of this study are to evaluate the mobile EV charging systems and develop a conductive charging system that is capable of working with different EV models, both human-driven or autonomous, safely operating without unexpected consequences, designed simply so that it does not require frequent maintenance and realizable by using today's technological developments. In this regard, they discuss an underbody

coupling solution. In this type of system, two complementary units are used and one of them is connected to the EV's battery, while the other is connected to the charging stations. The connection is established by coupling the EV and charging stations via these units. For coupling to happen, at least one of these units should be movable, while the other one can be fixed. These systems have a certain operation range, hence they should be aligned by the driver, still requiring human intervention, even though such systems have a typical alignment error tolerance of 0.5 m in both horizontal and vertical dimensions, according to the study. However, it is further concluded that even though such systems improve safety because the connection is done via a coupling instead of cables, it is not a scalable solution because of the challenges of integration. Because there is still no standardized, widespread, and recognized under-body charging interface used by EV manufacturers, a tailored design for each battery and EV type is necessary for these systems to become practical [92].

Another example of the underbody coupling systems is developed by the fixed charging robot produced by Continental Engineering Services (CES) incorporated in Continental AG and its startup partner Volteiro [36]. While the product is planned to be manufactured in 2024 in Germany, the charging solution consists of two parts: one attached to the vehicle's underbody and the other placed on the garage floor. When the vehicle is parked, these components automatically connect via a smart system, using a short-range data transmission technology utilizing radio-based communication. This system's advantage is that it can tolerate imprecise parking since the charging robot can compensate for a deviation of up to 30 centimetres and can connect regardless of the vehicle's angle to the floor unit. The conical connector design allows for flexibility in the connection orientation. The charging robot offers several key benefits. Unlike wireless inductive charging, it uses a physical connection, ensuring minimal energy loss and greater efficiency and sustainability [36]. The automated process removes the need for manual handling of charging cables, making it more convenient, especially in tight spaces. The ultra-broadband communication allows for precise alignment between the vehicle and the charging unit. Additionally, the system is easy to install, with options like simply placing the floor unit on the garage floor. Initially designed for private use with a 22 kW Alternating Current (AC) rating, the solution is adaptable to existing vehicle models. Plans include developing a fast-charging version for public spaces, capable of supplying over 50 kW DC, which will be especially useful for parking garages, filling stations, and fleet management of commercial vehicles [36]. The product is illustrated in Figure 2.2.

Figure 2.2: Fixed Charging Robot Developed by Continental Engineering Services and Volteiro. [36]

Some of the inconveniences of traditional EV charging can also be addressed by inductive charging systems. There is extensive research going on developing such systems even though they are not very widespread. In addition, some of the challenges created by the absence of standardization can be fixed by inductive charging systems. For example, since there is no physical coupling required between the charging station and the EV, identification and precise detection of inlet location and type requirements can be bypassed with the help of inductive charging systems.

As an example of such systems, Padmavathi et al. developed an alternative use of a wireless charging system [143]. In this study, a robotic arm carrying transmitter coils capable of locating receiving coils on the EV by using an advanced mathematical adaptive algorithm based on extremum seeking is proposed. It also discusses the use of silicon carbide metal-oxide-semiconductor field-effect tran-

sistors (MOSFETs) in the power converter to maintain high frequency, aiming to reduce charging time. Furthermore, to address the waiting times and range anxiety, a road charging methodology is also introduced. In this system, the road is equipped with wireless power transmitters and the driver receives assistance on the direction the EV should cruise towards for the most effective charging resulting from the correct alignment of the transmitter and receiver [143]. The concept is illustrated in Figure 2.3.

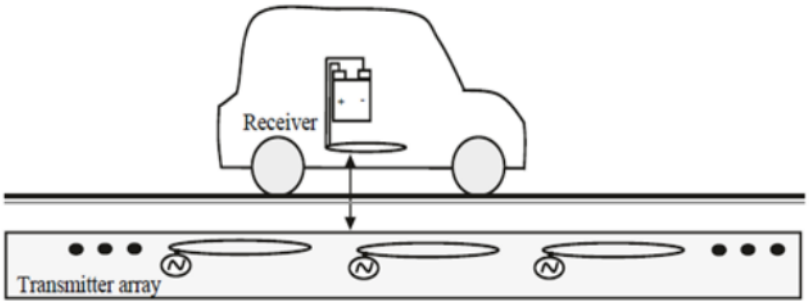

Figure 2.3: Wireless Road Charging System Studied by Padmavathi et al.[143]

In addition, Barzegaran et al. also study a conductive charging system [15]. The authors propose a novel solution leveraging transformer induction principles. Differently, this involves an autonomous robotic arm equipped with sensors, mounted under the vehicle, to precisely position a receiving coil. Hence, the moving part is mounted on the vehicle instead of the charging station itself in this approach. Accordingly, the integration of silicon carbide MOSFETs in the power converter is key to this solution, aiming to sustain high frequencies and thereby reduce charging times significantly by allowing high power densities [15]. The system design includes an object vision detection system using the vehicle's cameras to control the robot arm, ensuring the coil is placed optimally for efficient power transfer. This approach is designed to overcome obstacles like large non-permeable air gaps and electromagnetic interference [15]. The proposed schematic is illustrated in Figure 2.4.

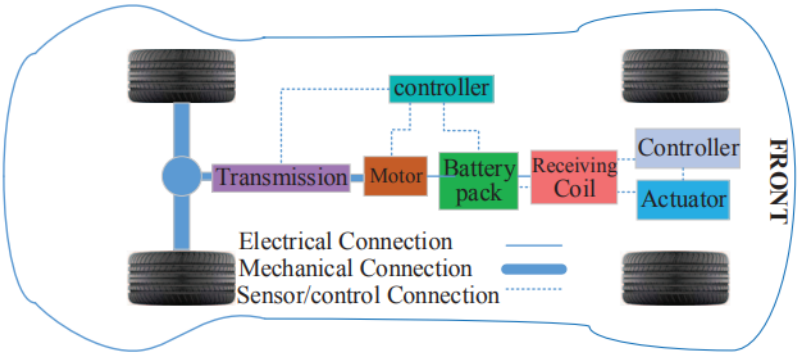

Figure 2.4: Schematic of the Wireless Charging System studied by Barzegaran et al.[15]

Moreover, there are also some private companies working on robotic inductive charging applications as well as the academy. EFI Automotive is one of those companies working on leveraging wireless autonomous charging in commercial applications [49]. EFI Automotive has developed an innovative wireless charging robot that streamlines the process of charging electric vehicles. This robot is capable of autonomously locating a vehicle and positioning itself underneath for charging, eliminating the need for precise parking or user intervention. It is designed with safety in mind, featuring obstacle avoidance and a halt function if any movement is detected. The robot employs wireless inductive charging technology, eliminating the cable handling and offering a considerable range of 5-10 meters. This allows it to charge multiple vehicles sequentially, making it highly efficient for both home and business applications. Enhancing user convenience, the robot is remotely controllable through an app and boasts a charging power of 7 kW. Lastly, it is also stated that the planned manufacturing of this product will start in 2025 [48]. The product is shown in Figure 2.5.

Figure 2.5: Inductive Charging Robot Developed by EFI Automotive [48]

On the other hand, the side coupling connection, which has been used for years in lots of different EVs and conventionalized over time could also address the issue of reported scalability and standardization associated with underbody coupling in conductive charging applications [92]. The connectors used by different EV models are shown in Figure 2.6. This shows that certain connector layouts make a side-coupled connection to be easily integrated and more advantageous than under-body connections. Moreover, since there is already a charging inlet in every single Battery Electric Vehicle(BEV), there is no additional attachment needed to couple the EV and charging station, as it is required in the under-body coupling unless they are wireless systems.

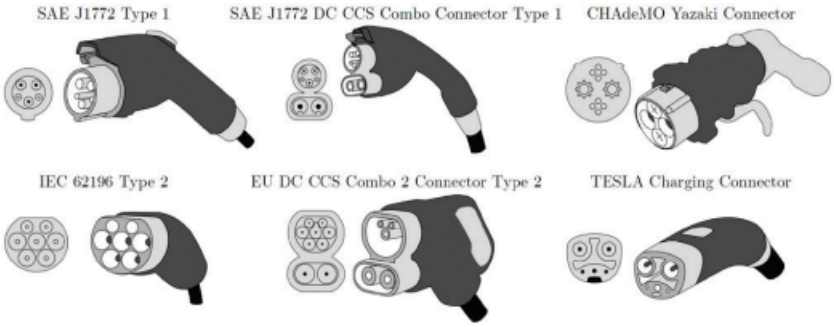

Figure 2.6: Different EV Side-Coupling Connectors [92]

As an example of the side coupling systems, Lou and Di propose the use of a fixed robotic arm to improve the charging experience [121]. In this study, battery-less mobile EV charging systems are primarily categorized under 2 different groups, namely traditional articulated manipulators, and bionic manipulators. Traditional articulated manipulators typically consist of a fixed and grid-connected robotic arm that can automatically plug and unplug charging outlets to EV inlets while the second category includes fixed systems with a bionic, snake-like arm, that plugs in EVs automatically. Consequently, the paper studies the design of a low-cost and high-flexibility robotic arm with 3 degrees of freedom to substitute human intervention during the connection process and further experiments with the developed system [121]. The proposed design is illustrated in Figure 2.7.

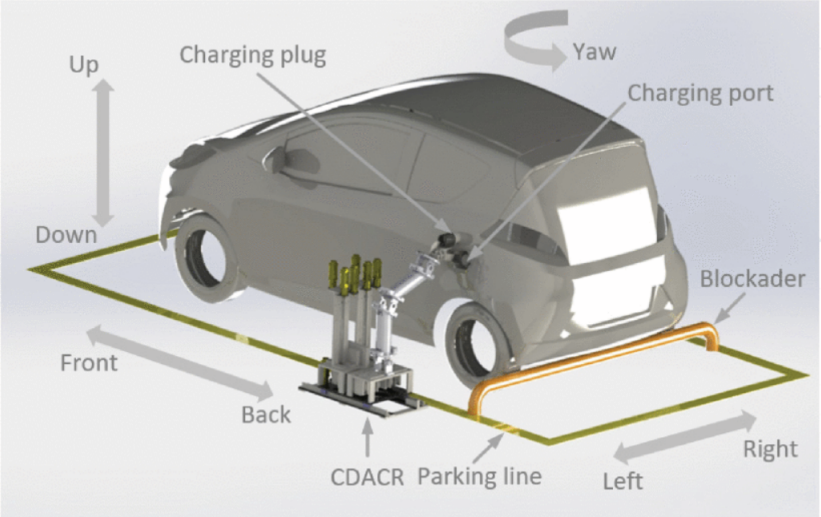

Figure 2.7: Computer Aided Drawing of the proposed robotic arm system by Lou and Di [121]

Furthermore, another product that is classified as a bionic manipulator according to Lou and Di is under development by Tesla Motor Company [121], [197]. Differently, this design incorporates a snake-like arm carrying the connector with higher degrees of freedom compared to the other alternatives reported [197]. Except for this distinguishable mechanical design, the operation logic is the same as a typical grid-connected charging robot. The fundamental advantage of this system is that since Tesla cars are standardized, they have the same inlet type with pre-designed placement on the car. Therefore, the robot can easily be integrated into all Tesla cars, even though this might not apply to the other cars manufactured by different companies [197]. The image of the product taken on the prototype testing published by Tesla Motor Company is shown below in Figure 2.8.

Figure 2.8: Bionic Charging Robot Prototype Developed by Tesla Motor Company [182]

Next, Hirz et al. propose a side-coupled battery-less system prototype with a CCS Type 2 connector, allowing the charging power to reach up to 30 kW for AC and 350 kW for DC charging [92]. The developed prototype by Hirz et al. is shown in Figure 2.9. In the Figure, the robot is shown with the number 1, while 2 shows the structural frame to carry the components. 3 and 4 show the cameras, one for detecting the vehicle and the other for precisely locating the inlet, respectively. 5 shows a box where the controllers are stored for the robot, while 6 and 7 are LED lights to increase the image quality

in case it is dark. 8 shows the actuator and 9 shows CCS Type 2 connector. 10 and 11 are carrier adapters while 13 is a rubber damper. Finally, 12 shows a microcontroller.

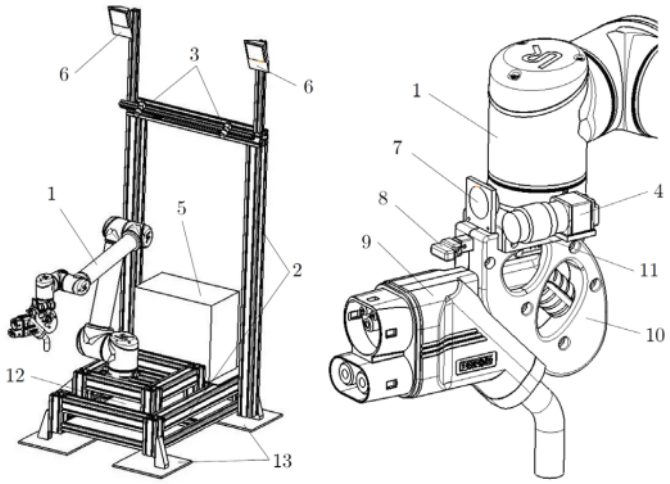

Figure 2.9: Mobile Conductive Charging System designed by Hirz et al. [92]

According to the experiments, the prototype can successfully conduct the operation in 99% of the test instances. Hence, it proves that today's technology is sufficient to develop such systems with high accuracy even though there is significant room for further development [92].

One important challenge reported by this study is that even though there are standards such as IEC 61196 and certifications such as IP (Ingress Protection) 44, directing charging systems, there are no regulations and standards published regarding automated charging systems [92]. Thus, the absence of standardization results in additional difficulties. For example, since there is no standard location for the charging inlet on an EV, advanced computer vision algorithms are required to successfully and precisely locate the charging port [92].

There are also alternative methods proposed to overcome this complexity. For example, Quilez et al. propose the use of QR codes to facilitate the docking process and guide the autonomous robots more easily while locating targets [152]. Another reported challenge comes from the absence of standardization of inlet lids. Some EVs are equipped with electronic lids that require the driver to press a button, while some of them are equipped with press and release mechanisms [152]. This also limits the integration of the system, adding additional complexities and steps to the process. Consequently, EV manufacturers' involvement in developing such systems can be attributed to this fact as they generally use standardized tools to reduce manufacturing costs.

As an example of EV manufacturers' interest in such systems, Volkswagen AG and Kuka AG signed a partnership to develop a fixed automatic charging robot [114]. The e-smart Connect initiative offers a convenient and user-oriented approach for charging the high-voltage batteries of electric vehicles from the Volkswagen Group. It features a KUKA robot that autonomously links the vehicle to a charging station using a specially designed application. Drivers only need to park the electric vehicle in a specified area, and the robot then handles the task of attaching the charging cable, providing ease and convenience for the driver [114]. Volkswagen reports that a common concern often voiced regarding e-mobility is the potential difficulty in locating a charging station during travel, or encountering stations that are incompatible or unsuitable in terms of power infrastructure and connector type [90]. Therefore, one of the primary objectives of this project is to address this inconvenience acting as a significant barrier. It is further reported that the vehicle's charging port needs to be within a 20 x 20 centimetre target zone [197]. Then, a camera mounted on the robot pinpoints the precise location of the charging socket, determining its position with millimetre accuracy. Subsequently, the robot's manipulator connects the DC Link to the vehicle's charging socket to establish the coupling. When the battery is completely charged, the robot autonomously disconnects the DC connector [197]. The developed system is shown in Figure 2.10.

Figure 2.10: E-smart Connect Charging Robot Developed by Volkswagen AG and Kuka AG. [90]

Another remarkable example of these systems is the Automatic Charging Robot (ACR) designed by Robotics Lab incorporated in Hyundai Motor Group in 2022 [97]. This system is equipped with 2 different computer vision systems powered by artificial intelligence. The first system detects the incoming vehicle and communicates with the charging station. Meanwhile, the second system is responsible for detecting the inlet and perfectly aligning the connector for successful plugging. Once the connector carried by the robotic arm is connected to the EV, the charging starts and the connection equipment is unplugged when the charging is finished. During the charging process, the first system continuously monitors the vehicle and surroundings to check if there is any anomaly in the environment to stop the charging in case of any. Furthermore, the drivers are provided with real-time information on the charging status via a mobile application such that important data such as the instantaneous state of charge (SoC) of the EV is streamed live. The system is fully waterproof and dustproof with IP 65 certification, enabling seamless operation in different outdoor and weather conditions [98]. It is further stated that the system is capable of working with any type of charger, providing the drivers with flexibility and adequate integration. At this point, the company accounts for a gravitational compensation methodology as different chargers can have significantly different weights causing the material to flex due to its elasticity. Furthermore, Hyundai Robotics Lab announces that even though the system can tolerate bad parking up to some margin, the system has a charging port locating error below 10 mm. The robot can operate in various temperature conditions between -15°C and 60°C. The maximum power that can be fed into EVs is announced around 400 kW [99]. The product is shown in Figure 2.11.

Figure 2.11: ACR developed by Hyundai Robotics Lab. [98]

2.2.2. Large Scale Battery Integrated Systems

Large Scale Battery Integrated Systems emerge as a remarkable solution to act as an emergency charging service or serve drivers in remote locations. Often, battery swapping systems which are

discussed in Section 2.2.3, are referred to as a solution to operate at the requested site. Compared to these systems, a battery-integrated system could be an adequate choice for large and heavy batteries that could cause difficulties during swapping operation [25]. Especially, for electric vans or trucks used in the logistics sector, it is not very convenient to swap these large and heavy batteries implemented in logistics EVs [25]. This operation could even become more difficult to conduct in remote locations. Nevertheless, these systems can be separated into 2 different categories regarding battery integration. The first system mainly describes the service vehicles in which batteries are directly embedded, while the second one depicts articulated vehicles in which the battery in a trailer is towed by another vehicle as shown in Figure 2.12. This reserve capacity can be used to store energy to charge the vehicles in the requested location. It is further reported that using battery-integrated mobile charging services can reduce energy costs by up to 42% [25].

(a) Battery embedded (b) Battery on trailer

Figure 2.12: Categories of Battery Integrated Vehicles [25]

Furthermore, the size of these systems can be as large as a trailer [162]. These systems set an example of large-scale charging alternatives which can decouple charging demand from the grid. As the packaging area allocated for the equipment is relatively larger, it is much easier to implement large-capacity batteries and high-power onboard chargers on these types of systems. For example, Tesla achieved to implement a 3 MWh battery storage system with 125 kW chargers on such a large scale battery integrated system to serve EVs in remote locations [4], [116]. It is also important to note that the implemented batteries can serve multiple EVs at the same time. Meanwhile, the mobility of these systems is rather limited and relatively costly compared to the other types due to their large size and heavy weight. Especially, due to the size requirements, it is challenging to navigate and deploy these units in an urban setting because of the narrow streets and limited manoeuvrability area. In addition, their application is restrained as the service area must have adequate space to facilitate the deployment of these units and accommodate the connected EVs. Given the operational challenges, including the need for a large area, these solutions are not ideal for urban settings but are more suitable for remote locations or emergency services. A sample schematic of such systems is illustrated in Figure 2.13, [162], [151].

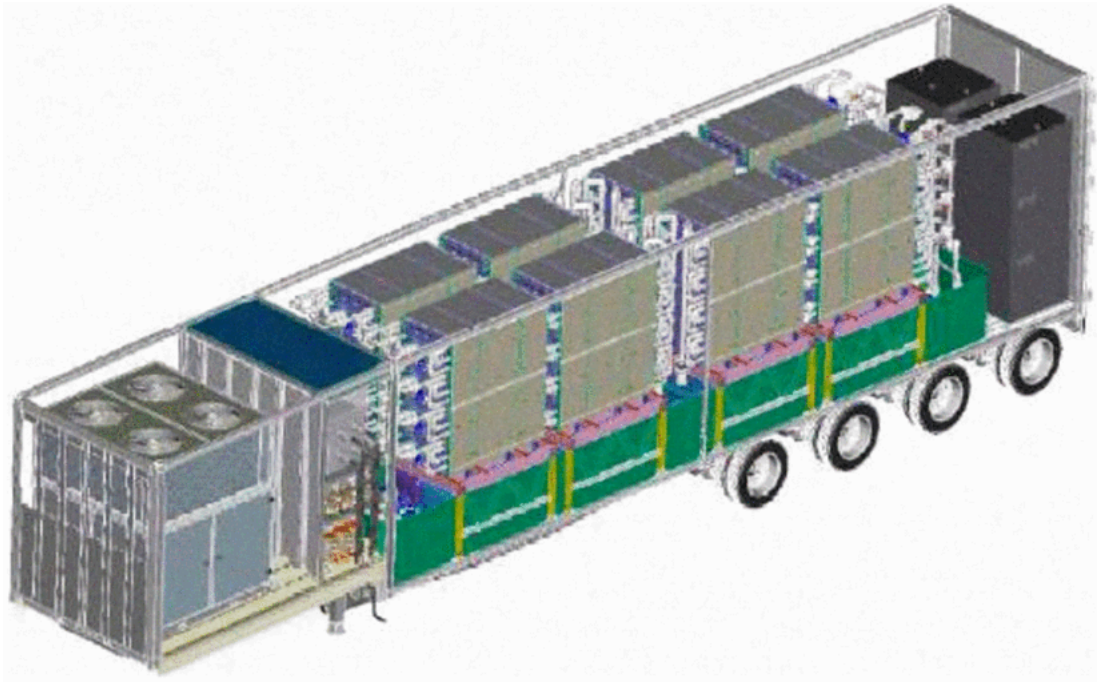

Figure 2.13: Schematic of Battery Integrated Charging Trailer [151][162]

2.2.3. Battery Swapping Systems

Another alternative to regular charging poles is the battery-swapping system. These systems include the replacement of the depleted batteries with charged ones, either at a designated station or at the requested location. An alternative solution is studied by Shukla et al., investigating the feasibility of swappable battery stations [168]. In this study, battery swapping stations are proposed as a promising solution to keep the recharging duration low, offering drivers the opportunity to replace their batteries with a fully charged one in a short amount of time, comparable to refuelling times. Furthermore, the study primarily focuses on optimizing the number of service stations affecting the vehicle interception rates in a case study focusing on Alexandria, USA.

In addition, Çatay and Sadati take this battery-swapping concept to the next step and study battery-swapping vans in the form of Electric Vehicle Routing Problem with Time Windows and Mobile Charging Stations [25]. In this study, the use of mobile charging stations, swapping or charging batteries, are proposed as a solution to the problems brought up by the utilization of EVs in the logistics sector such as long waiting times, and lack of adequate charging infrastructure and range. However, the focus of the study is rather larger areas shaped by the routes where the logistics operations take place. At this point, mobile battery swapping stations are proposed to increase the convenience of the battery swapping operation by taking the service to the point of request [25].

Regarding these systems, public acceptance and integration challenges emerge as a key issue. In this case, because battery performance and condition depend on numerous parameters, including driving behaviour, it becomes challenging to ensure batteries provided to drivers have uniform State of Health (SoH) conditions. This raises questions regarding the public acceptance of such solutions. Furthermore, the varying physical properties of batteries, such as dimensions, capacity, and ratings, across EV models make it challenging to develop a scalable business that offers easily integratable solutions.

2.2.4. Robot-like Systems with Batteries

Mobile robot-like battery-integrated charging systems generally take autonomous robots into account, which are capable of reaching designated locations and charging EVs without any human intervention as well as charging themselves from the grid. These systems mainly fall under 2 different categories. First, the robot is equipped with a built-in battery which can only charge and discharge itself to fulfil the demand. The second one takes one more degree of freedom into account and allows the robots to swap their batteries, increasing the overall flexibility of the system.

As an example of robots with battery swapping, Behl et al. study the design and development of a robot-like charging system with objectives of EV plug recognition, autonomous navigation, and implementing switchable batteries [16]. EV plug recognition aspects expect the robot to be able to identify the charging inlet location of different EV models and successfully plug the charger in by using computer vision algorithms fed by live images. In the navigation perspective, the robot is expected to continuously monitor its location in the parking place, identify the separate parking lots and hence its service locations, and distinguish the obstacles to avoid safety concerns that can arise in a parking place full of cars, passengers, and walls. Lastly, using a switchable battery approach aims to reduce the service disruptions due to the discharged batteries and enable more continuous and smooth operation because switching a battery costs significantly less time than recharging [16]. The concept studied is described in Figure 2.14.

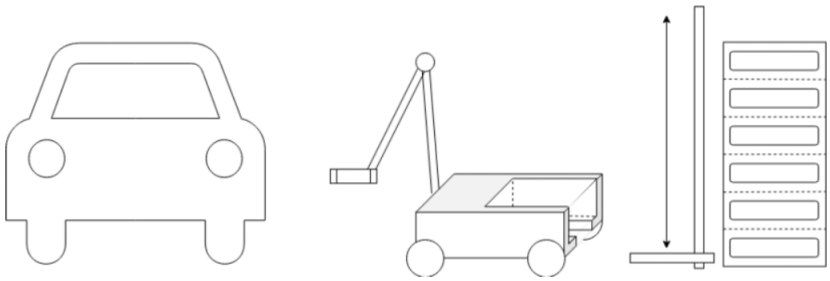

Figure 2.14: Mobile Conductive Charging System with Switchable Battery System Schematic Studied by Behl et al. [16]

Furthermore, the study experiments the use of such a system on a prototype built by using Turtle-Bot 3 WafflePi, a robotic 4-wheeled platform allowing the development of such delivery projects [16]. Furthermore, the prototype has a LiDAR sensor to chart its environment and identify proximate objects in the designated area. On the other hand, to maximize the space that can effectively be used in the robot to fit the power conversion equipment and battery mainly, and also to reduce weight, the duty of replacing batteries is fulfilled by the charging hub itself. Hence, all the moving parts responsible for taking the battery away from the robot, carrying it up to the vertical charging space, and establishing the grid connection are implemented in the hub's structure. Even though this design layout results in a more compound mechanical design, it is also concluded that the framework increases the scalability and flexibility while emphasizing the potential for an overall cost reduction [16].

An example of a robotic system with built-in batteries is studied by Kong to highlight an alternative charging system that can address the issues associated with today's charging process [111]. In the proposed system, units with 225 kWh battery capacity are simulated to fulfil the charging tasks in a parking lot. The studied system can charge the EVs with 135 kW power, while they can be charged from the grid with 348 kW. The paper estimates the system costs and presents a comparison to the regular charging poles to highlight the design's advantages in terms of initial investment. It further claims that the system can demonstrate a more cost-effective solution if it can operate for 5 years compared to the charging poles. On the other hand, the paper's main focus is to analyse the system performance under stochastic charging demand, while also using an empirical battery degradation model to estimate the operational life of the batteries, varying according to different system parameters determining how much they are used during the day [111].

Ziggy produced by EV Safe Charge company sets another example of robot-like systems with built-in batteries [70]. Ziggy is an autonomous mobile charging robot equipped with 4 cameras for obstacle detection on every side. It is equipped with 4 wheels capable of separately steering, allowing sharp manoeuvres in a packed area such as an underground parking place. Users can order the charging robot to the parking lot through a mobile app or the in-vehicle infotainment system, allowing them to either reserve a charging time slot in advance or request a charging robot on-demand, without any prior reservation. If the driver reserves a charging slot, the robot reserves a parking lot for the driver before the arrival and waits for it. After charging, ZiGGY can return to its base to recharge from the grid, battery storage, solar energy, or a combination of these. EV Safe Charge plans to offer ZiGGY robots under a Charging-as-a-Service model, which includes ongoing technical support and maintenance [70]. In

addition, the robots feature large screens for information or interactive advertising, providing additional revenue streams for parking operators to balance the costs associated with the implementation of such systems. Initially, the company offers Level 2 charging power and also plans to upgrade to Level 3 charging within the first year of operation [70]. The service is set to launch in selected locations like San Francisco and Brooklyn's Williamsburg neighbourhood, and reservations are currently open [42]. However, the robot is not equipped with an arm or any mechanism automating the plugging process. Hence, the utilization of the robot requires human intervention to initiate charging, pointing out cable management, safety, and convenience issues, while reducing the overall cost of the system due to the lack of advanced and precise detection and moving mechanisms. The product is demonstrated in Figure 2.15.

Figure 2.15: Ziggy Autonomous Charging Robot developed by EV Safe Charging Company [70]

Another autonomous conductive charging robot was introduced by NaaS Technology Inc. in March 2023 based in China [135]. This robot demonstrates advanced features like active vehicle tracking, intelligent charging, and automated payment processing, addressing the growing need for mobile EV charging. Unlike Ziggy, the robot employs mechanical arms to automatically connect to EV charging ports, handling the charging seamlessly. Incorporating advanced technologies like deep learning, 5G, V2X, and simultaneous localization and mapping, the robot is also designed to be waterproof and shock-proof, offering functionalities such as one-click ordering, precise vehicle locating and parking, automatic docking and undocking, and self-recharging [135]. Available in various power and battery capacities, it integrates with major OEMs through an open API, providing EV owners with unmanned charging services at any time. Capable of interfacing with EV systems via an API, the robot can autonomously locate vehicles with low batteries and accurately connect to the charging ports [135]. In the future, self-driving vehicles will be able to autonomously recharge, leveraging data interconnectivity between the vehicle and robot, with the help of this online integration possibility [135]. However, as the primary communication mechanism used is internet-based, this robot requires continuous internet connection and communication with EVs which can not apply to old-generation vehicles without an adequate level of smartness [135]. Furthermore, one should not forget the significance of cyber security measures as this sensitive data transaction will take place online. Therefore, data security precautions should also grow parallel to the developments in the interconnected vehicles to avoid potential vulnerabilities and breaches. The product is illustrated in Figure 2.16.

Figure 2.16: Autonomous Charging Robot developed by Naas Inc. [135]

Aiways, a personal mobility company based in Shanghai, has secured seven patents in Europe and China for the development of its autonomous charging robot, CARL [8]. This innovation includes patents for its intelligent design and charging technique. CARL is designed to address the challenges of charging electric vehicles and it is available with 30kWh and 60kWh battery capacities [8]. The company states that the robot can rapidly charge any EV compatible with standard charging protocols. It can recharge an EV battery to 80% in less than 50 minutes, offering a convenient and cost-effective charging option for both individual and business customers, as well as for infrastructure developers and operators [8]. EV owners can easily summon CARL to their vehicles in public, home, or workplace parking areas using a smartphone app. The robot utilizes GPS data to locate and autonomously charge the vehicle. After charging, CARL moves on to the next customer or returns to its base station. The product is illustrated below in Figure 2.17.

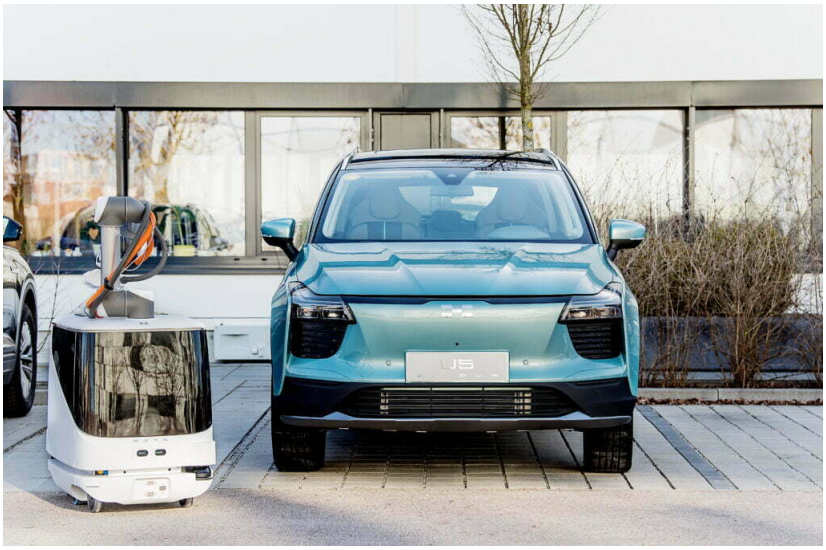

Figure 2.17: Autonomous Charging Robot developed by Aiways [8]

Parky also introduces the world's first autonomous EV recharging robot, revolutionizing the way electric vehicles are charged [71]. With its innovative use of image marker references, Parky's robot can autonomously locate the EVs for recharging. This eliminates the need for drivers to search for an EV charger as they can simply park their car, use Near-Field Communication (NFC) to summon the charging robot, and let it handle the rest [71]. The robot is capable of navigating through parking lots, using image markers to find and guide itself to the car. QR codes on the connector assist in directing the robot accurately to the vehicle as this solution is also studied by Quilez et al. [152]. For safety, the autonomous robot is equipped with triple sensors: LiDAR, Ultrasonic, and Bumpers [71]. These sensors enable the robot to detect and stop to avoid obstacles, ensuring a safe charging process. To use this service, drivers just need to park their car in any spot within the parking lot, attach the nearest connector to the charging port, and send a charge request via NFC [71]. This process is primarily

different from the fully autonomous solutions developed or studied. In detail, there are bridges mounted on the parking place walls and a connector attached. Driver still needs to be involved in the process since the connector has to be plugged in and out by human effort. After the connector is plugged in, Parky docks into the bridge to charge the EV from its battery. Hence, at least one connector and bridge are still required for each parking lot to fully allow every car parked in the designated area to charge, requiring a substantial amount of investment. Moreover, the technology behind this service is protected by a Class A patent application, showcasing its innovative approach to EV charging [71]. The product is shown in Figure 2.18.

Figure 2.18: Parky Charging Robot developed by EVAR [71]

On April 22, 2021, in Shanghai, Envision Group, a leading green technology company, introduced Mochi, the world's initial mass-produced, mobile smart charging robot [53]. The most remarkable feature of this robot is that it is fully powered by renewable energy. Even though there are a lot of active projects and research focusing on powering EVs with renewable sources, Mochi is one of the first projects realizing this concept in practice. Mochi utilizes Envision Group's EnOS, an intelligent operating system that oversees over 200GW of renewable energy assets globally [53]. This system ensures Mochi exclusively uses green electricity, contributing to an eco-friendly EV charging experience. Mochi is compatible with a wide range of mainstream EVs. It has a 70 kWh battery capacity and a 42 kW power output, making it capable of charging an EV in just two hours for up to 600km range [53]. Mochi's mobility allows it to locate and charge EVs in various locations, offering a convenient and time-saving service for drivers. Mochi features accurate location-sensing technology and can swiftly halt within 0.1 seconds from its top speed of 1 m/s if it encounters obstacles [53]. EV drivers can subscribe to the service via a mobile application, and Mochi will autonomously develop a charging plan, locate the EV, and initiate the charging. This system also provides real-time monitoring and a comprehensive health check of the battery during charging [53]. Furthermore, the robot is equipped with a robotic arm handling the connection task autonomously. The product is illustrated in the image shown in Figure 2.19.

Figure 2.19: Mochi Charging Robot Developed by Envision Group [53]

Finally, Volkswagen Group is exploring an innovative approach: autonomous charging robots that refill themselves at a central location and then deliver power to individual vehicles in an autonomous

manner, using wireless communication [196]. The charging robot navigates itself to the vehicle and communicates with the EV to request the car to open its charging socket. It then aligns its plug to connect with the vehicle, carrying out the entire charging process without human intervention. This robot is capable of charging several vehicles sequentially [196]. It transports a trailer, acting as a mobile energy storage unit, to a vehicle, connects it, and then proceeds to another vehicle while the first one is charging. In this regard, the robot is equipped with switchable batteries. Using multiple trailers, the robot can service various cars and later return the trailers to the central charging station. A key obstacle to the widespread adoption of this charging technology is the advancement of car-to-X communication, which involves vehicles using networks like 5G to interact with other vehicles and devices [196]. While some new EV models come equipped with but not yet activated Car-to-X capabilities, older models may lack this feature as this is also a valid concern for the robot developed by Naas Technology Inc.[135]. Again, it is vital to address the potential cybersecurity concerns while building a network with mobile nodes, such as autonomous robots and EVs. Moreover, Volkswagen reports that its mobile charging robot is currently in the prototype phase and is being further developed [206]. The product is demonstrated in the image shown in Figure 2.20.

Figure 2.20: Autonomous Charging Robot and Battery under development by Volkswagen [206]

2.3. System Optimization Studies on Mobile Charging Techniques

Since one of the primary objectives of this thesis work is to optimize the number of components in the system including robot and battery units, similar studies in the literature are reviewed.

The design and planning of mobile charging systems for electric vehicles are crucial in transitioning from fossil fuels to electricity. Given that existing road and grid infrastructures were not designed with EVs in mind, creating accessible and reliable charging infrastructure is vital. This shift requires a significant investment in the EV charging sector. Addressing the challenges and costs of establishing a charging infrastructure is fundamental to facilitating EV adoption. Furthermore, since this investment might require a notable amount of public and private capital, the system must be optimized to necessarily address today's EV drivers' necessities and the challenges encountered to promote the widespread use of e-mobility, encouraging potential customers as well as not putting the investors at stake. Hence, the system should maximize the service quality, fulfil the demand and also realize a profitable and feasible solution in the investor ground.

The primary capital costs in mobile charging station development include the battery and carrier, with the high cost of the Battery Energy Storage System (BESS) being a particular challenge. Subsequently, the power profile incorporated into the system should also be investigated critically, affecting power converter topology and associated costs from the investor perspective as well as the charging duration from the customer's point of view. The high cost of this technology plays an important role, causing the overall cost and the required investment of this kind of system to increase substantially. For example, in 2020, a start-up called FreeWire Technologies, developing mobile charging systems with a built-in battery, raised $25M investment, pointing out how high spending can be required for large-scale applications [171]. Extensive research has introduced metrics to determine the optimal battery pack capacity and number of units in mobile charging systems. Primarily, these optimization studies revolve

around finding the number of stations with an assumed capacity, optimizing the service routes in a given scenario, and optimizing the energy transfer by taking the benefits on the grid into account.

Tang et al. introduce the concept of Online to Offline service and further evaluate the mobile charging services according to this business model [181]. As mobile internet becomes more prevalent, it is transforming how various industries operate. A notable example of this is the rise of the online-to-offline (O2O) business model [181]. In this new paradigm, customers no longer need to visit physical stores to buy products. Instead, they can simply order what they want online, and the items will be delivered to their location within hours, or sometimes even minutes [181]. Applying this concept to electric vehicle recharging, it suggests that charging services could be brought directly to the EV user on demand. This approach would allow drivers to recharge their vehicles wherever they are parked, eliminating the need to search for a charging station and wait in line, thereby streamlining the recharging process [181]. However, in this study, mobile charging systems are not only considered battery-carrying or grid-connected robots but rather generalized over any type of remote charging service [181]. To this extent, this service can also be offered as an emergency road service, rescuing cars with a dead battery at remote locations.

Consequently, two primary challenges faced in the deployment and planning of mobile charging services are referred to in this study [181]. First, the system must be ready to respond to unpredictable and dynamically changing demands. Deployed finite mobile charging resources are needed to effectively be managed to achieve certain objectives, such as lowering operational costs, enhancing service quality, or a blend of both. Second, considering the nature of demand, operators must strategically plan the infrastructure of the mobile charging system. This includes determining the quantity and locations of depots, the size of the mobile charger fleet, and the battery capacity, all aimed at optimizing social welfare. To address these two points, the paper presents a two-layer simulation-based model for strategic planning and online operation of the mobile charging system. The first layer, the operational level, focuses on optimizing the scheduling of the mobile charger fleet to enhance the efficiency of the service. Secondly, at the planning level, the paper aims to refine system design by determining the optimal number and locations of depots, fleet size, and battery size, taking into account the operational performance. To realize these objectives, the paper models the mobile charging service as a dynamic vehicle routing problem and proposes an online operation policy for efficient scheduling of the fleet to maximize operational utility.

Another optimization problem focusing on mobile charging systems is studied by Zhang et al. [210]. In this study, mobile battery piles transported by vans or trucks are analyzed and compared to the regular charging poles from the user's perspective in terms of practicality and service cost paid and levelized cost of electricity (LCOE) [189]. This practicality is primarily associated with the charging duration dependent on the hub location, delivery speed, charging power, and energy demand. Meanwhile, the costs associated with the users are primarily defined as a function of time and money they spend on charging. The time is monetized by taking the average salary earned by the residents living in the study area of Xiamen, China. Finally, LCOE is calculated with and without including land cost for fixed charging stations with different utilization rates and mobile charging stations.

In addition, Chen et al. introduce a novel approach for improving the EV charging experience using mobile charging stations within heterogeneous networks composed of macro cells and small cells [31]. It proposes an optimal model for scheduling EV charging tasks and utilizes the Chaotic Evolution Particle Swarm Optimization (CEPSO) algorithm to optimize the placement of mobile charging stations, taking user demand and station capacity into account. In another study, the authors explore the integration of EVs with the Internet of Things (IoT), emphasizing the rapid adoption of EVs in urban settings, especially when combined with renewable energy sources [30]. The limitations of regular charging poles, notably the challenges posed by the unpredictable arrival times of EV users, and the necessity for refined power management strategies are pointed out. Then, the focus shifts to mobile charging stations, which are increasingly recognized for their superior charging services such as including effective communication between stations and EV users for optimal power supply decisions, reduced concerns about battery charge states due to their flexibility, and shorter waiting times for charging enabled by real-time data acquisition [30].

However, the paper also identifies significant challenges in power distribution for mobile chargers, such as limited power supply and the diverse power needs of EV users [30]. These challenges are amplified by the dynamic nature of renewable energy and the randomness of EV user arrivals. To tackle these issues, the paper proposes a stochastic optimization method for power supply in IoT contexts.

This method accounts for the fluctuating nature of renewable power and the behaviours of EV users. It transforms the economic challenge into a stochastic optimization problem minimising the operational costs, solvable through subproblems based on Lyapunov theory. The effectiveness of the proposed algorithm is analyzed and demonstrated, showing its capability to lower investment costs [30].

Proposing an autonomous robot-like charging unit with batteries, Kong simulates the use of a mobile system in a parking lot with different stochastic charging demands dependent on arrival and departure times [111]. In this study, the author uses the Markov Chain model to create this stochasticity and analyses the system's performance with a 225 kWh fixed-capacity battery. The performance metrics used in the study are charging delay and blocking probability to make sure the system can fulfil the demand under the given circumstances. It further optimizes the system's service by taking throughput, number of parking places and EV penetration rate into account. The paper further employs a semi-empirical battery degradation model to investigate the effect of these various parameters on the operational life and calculates the probability densities of different service durations. The obtained average service lives with the highest probabilities are 5.02, 2.64 and 2.07 years when a 50% capacity retention is marked as an end-of-life point, varying according to different system parameters [111].

Cui et al. aim to determine the optimal mix of charging station sizes and charger numbers, considering a fixed budget in a study [38]. It divides BEV charging time into three components: queuing, fixed preparation time, and charging time dependent on the amount of energy transferred and power. The study finds that more chargers can reduce queue times significantly.

Furthermore, the paper investigates the effect of the location of charging stations of various sizes and types, taking into account BEV users' routing choices [38]. The goal is to aid government planners in situating diverse BEV charging stations within a budget to minimize public and social costs. This includes considering travel, charging, and queuing times for network users. The proposed optimization model aims to cater to different BEV charging needs and enhance service levels, while also considering the economic aspect of public facility investment and aiding in government decision-making. The study's findings are relevant for future studies, such as driving behaviour analysis of BEVs, and traffic planning and management. Finally, the reconstruction-linearization technique is applied to transform the resulting non-convex and computationally demanding problem into a Mixed Integer Linear Program [38].

Another contribution in the literature is studied by Saboori et al., aiming to realize an EV charging network based on regular charging poles, supported by mobile charging stations [160]. However, the mobile charging system introduced in this paper consists of battery units with a 200 kW power rating and 800 kWh capacity carried by trucks. The paper further assumes that each EV connected demands 25 kWh of energy from the grid per hour. In light of these assumptions and introductions, the study aims to develop and optimize an energy management model for this introduced combined EV charging network, which also includes charging poles. The focus is on enhancing the overall efficiency of the EV charging process within a distribution network, considering both economic and operational aspects. By introducing a mobile charging solution, the paper seeks to alleviate peak load pressures on the fixed stations and improve the energy distribution within the network as well as reduce the charging queues, increasing the convenience of the overall process from the drivers' point of view. The core of the research revolves around an optimization problem that addresses the efficient allocation of mobile charging stations. This problem involves determining the most effective spatial and temporal deployment of the mobile units, considering their charging and discharging cycles, and balancing their operational costs. Key elements of this problem include scheduling the location and timing of the mobile charger's movements, managing its battery charge levels, ensuring it meets the varying EV charging demand, and minimizing the overall operation costs while adhering to network constraints. The optimization methodology is applied to processing various data points, such as electricity prices, EV charging demand patterns, mobile battery capacity, and the operational costs associated with charging and transportation. The study concludes that the strategic deployment of mobile charging systems significantly enhances the efficiency of the EV charging network. It achieves a notable reduction in the total daily operational costs by 3.46% and drastically decreases the EV charging queue at fixed stations by approximately 94% [160]. Additionally, the energy demand during peak periods is significantly reduced, leading to improved voltage stability and reduced network strain [160]. This not only reduces the operational costs but also contributes positively to the overall performance and reliability of the electric distribution network.

In parallel to Saboori et al., Chauhan and Gupta explore a hybrid charging grid model that integrates

mobile charging trucks [29], [160]. The central challenge addressed in their research is the strategic distribution and timing of mobile deployments. Given the charging requests from EVs at various locations and times, the study seeks to optimally position mobile charging stations, which are essentially vehicles equipped with large battery storage. Such mobile units are designed to enhance the capabilities of fixed charging stations, especially during times of high demand, thereby easing wait times for EV users and lessening the burden on the electrical grid. Additionally, the study underscores the complexity of this problem. To address this complex scheduling problem, the authors propose two heuristic strategies, namely the slotMCS-Allocation Algorithm and the reduced-slotMCS-Allocation Algorithm. The first approach constructs a charge-conflict graph representing potential charging slots for EVs. It then employs graph colouring techniques to identify independent sets of charging tasks that can be handled by individual mobile units. As an extension of the first, the second algorithm initially reduces the size of the problem by assigning a single potential charging pole to each EV. This streamlines the charge-conflict graph, making the scheduling task more manageable. Simulation results, based on the road map and charging station data of Los Angeles, reveal that both algorithms effectively manage the scheduling of mobile units. The analysis reveals that while the slotMCS-Allocation Method is more effective in charging a greater number of EVs, it does so at the expense of increased computational demands. In contrast, the reduced-slotMCS-Allocation Algorithm offers faster computation but may charge fewer EVs due to its initial reduction phase. The research concludes with an affirmation of the significant role these algorithms can play in boosting the efficiency of mobile charging station operations within the charging grids, thus advancing the objective of sustainable urban transit [29].

Răboacă et al. focus on optimizing the operation and placement of temporary mobile charging stations for electric vehicles in urban areas, specifically examining the Brooklyn neighbourhood in New York City [153]. The primary objective is to enhance the efficiency and accessibility of EV charging infrastructure by determining optimal locations for these mobile stations without classifying how they are transported. This is achieved through a comprehensive approach involving simulation, optimization, and comparative analysis.

The article investigates two distinct operational modes for mobile charging stations: the traditional moving operational mode and the proposed temporary location strategy. The moving operational mode involves the charging station relocating itself according to the EV's request, while the temporary location strategy positions charging stations at strategic locations for a fixed duration. The study's primary aim is to ascertain which mode is more effective in terms of service quality and operational efficiency [153].

A variety of methodologies are employed in this research. The authors conduct simulations to mimic the behaviour of 200 taxis in Brooklyn, capturing the dynamics of EV charging demand. They also develop nonlinear and mixed-linear optimization models to solve the location-allocation problem, considering unique probability-queuing constraints. These constraints include factors such as the number of EVs that can be queued at a charging station and the capacity limitations of these stations. In addition, location constraints are implemented aiming to position the charging stations in areas with limited access to fixed charging infrastructure, thereby filling a crucial gap in the charging network. The objective function in the optimization model is designed to minimize factors such as the time taken for an EV to receive service after making a request, operational costs considering the mobilization associated with relocating the charging stations and the electricity costs of charging EVs. It further employs a penalty term for the percentage of charging requests that cannot be satisfied within a given time frame stated as miss ratio [153].

The results indicate several key findings. Firstly, the temporary location strategy outperforms the moving operational mode in terms of response time and the ability to meet changing demands. This suggests that stationary mobile charging stations, if strategically placed, can offer more efficient service. Secondly, the optimal locations for these charging stations are typically found in areas with limited fixed charging infrastructure, highlighting their role in filling infrastructure gaps. Thirdly, the study notes that the moving operational mode incurs higher operational costs due to increased travel distances, underscoring the economic benefits of the temporary location strategy [153].

Moreover, in a novel approach to EV battery charging, Huang et al. investigate mobile charger systems, specifically focusing on two configurations such as Mobile Plug-in Chargers and Mobile Swapping Stations [95]. The study introduces a queuing-based analytical framework, central to the Next Job Nearest (NJN) service strategy. This strategy prioritizes serving the nearest EV after completing the current charging task, based on a Poisson distribution of charging requests and a uniform spatial spread across a designated service area [95]. The research includes both an idealized analytical model and a prac-

tical simulation model. The analytical model examines a hypothetical system using unit square areas, while the simulation, developed in MATLAB, realistically mimics EV charging requests in a 100 km² urban setting. Key assumptions in the simulation include a steady mobile charging speed and a uniform charging duration. The study is anchored in a case study of Singapore, where EV usage patterns are modelled to reflect daily activities such as work commutes and lunchtime errands. Local factors like traffic flow and population density are further taken into account, providing a realistic framework for estimating travel distances and corresponding energy needs [95].

The objective function in the optimization task is multi-faceted. It involves terms that represent operational metrics such as the miss ratio and response time. Additionally, economic factors like battery cost and charge fulfilment rates are also incorporated into the objective function to determine the breakeven cost per charge request. The optimization aims to balance these elements to achieve an optimal operational model. Essentially, the study seeks to identify an operation point where the system can serve efficiently without incurring excessive costs. Hence, the goal can be summarized as, finding the optimal battery capacity and charging rate for the mobile plug-in configuration, or determining the ideal number of battery swaps and swap times for the mobile swapping configuration [95].

Liu et al. introduce mobile charging vehicles as a flexible and dynamic solution to augment existing charging infrastructures [120]. These vehicles resemble taxis in terms of their mobility and expandability [120]. The concept revolves around using these charging vehicles to balance the charging demand, especially during peak hours, and to respond to unexpected charging needs [120].

The core of this research lies in developing a novel, data-driven methodology for scheduling mobile charging vehicles. Utilizing an extensive dataset from Beijing's charging piles and a dedicated mobile app, the study innovates in estimating unmet charging demands. This estimation is fine-tuned with real-world charging records, incorporating temporal patterns and user preferences. The urban area within Beijing's Sixth Ring Road is divided into grids, mapping out the charging demand distribution and facilitating the strategic deployment of these vehicles [120].

Three distinct scheduling strategies are put to the test: a greedy algorithm based solely on demand, a modified version of this algorithm that also considers the scheduling distance, and a comprehensive global optimization algorithm that integrates both demand and distance factors. The evaluation of these strategies reveals that while the greedy algorithm based on demand shows promise, incorporating scheduling distance results in a more balanced and effective approach. However, the global optimization strategy, despite its thoroughness, is computationally demanding and less suited for real-time applications [120].

The study reveals that mobile charging vehicles, with their superior mobility and adaptability, can effectively alleviate the load on fixed charging stations and reduce waiting times for EV users. Furthermore, the frequent deployment locations of these vehicles provide valuable insights for future charging station construction, suggesting potential sites and helping to estimate the necessary scale of these stations [120].

2.4. Benefits of Mobile Charging Systems

Apart from the introduced benefits of each discussed type of mobile system in Section 2.2, their applications have various effects from different perspectives. In this section, first, the challenges associated with today's charging methodology are emphasized to answer Research Sub-Question 1. Then, the potential benefits of mobile applications are evaluated from different points of view, to answer Research Sub-Question 1 fully.

Mobile charging systems aim to address various setbacks observed in daily charging experiences with regular charging poles, thereby enhancing the overall EV driving experience. Moreover, the benefits of such systems can be analysed from three different stakeholders' perspectives. They can serve to alleviate the adverse impacts regular charging poles exert on the power grid from the public perspective and attract investor interest in the system, also yielding additional advantageous outcomes on the EV owners' end [4].

2.4.1. EV Owners' Perspective

As mentioned, range anxiety, charging availability, and charging time stand as pivotal factors influencing the EV driving experience according to the users [3], [4]. Mobile charging systems can emerge as a remarkable choice to address these concerns raised on the drivers' end.

The restricted range of EVs presents a considerable barrier to their widespread adoption. Especially for drivers undertaking long-distance journeys, this challenge is often referred to as range anxiety. One potential solution involves strengthening the charging network to improve the availability of charging stations for EVs [4]. However, this strategy requires significant financial investment as further elaborated in Section 4.4.1. In contrast, mobile charging systems offer a promising solution to mitigate EV owners' range anxiety by providing supplementary charging alternatives that can be easily deployed, thereby diminishing the dependence on extensive charging pole infrastructures [4].

The availability of charging poses a significant challenge in the widespread adoption of EVs [180]. Fixed charging systems often encounter a limited number of charging outlets and may face difficulties in accommodating sudden increases in demand for charging [29]. Additionally, public charging stations, in accessible areas, encounter issues such as prolonged station occupancy beyond the necessary EV charging time [191]. Furthermore, the occupation of charging poles by internal combustion vehicles poses an additional concern, blocking EV owners from access to charging facilities for extended periods [156]. In numerous urban settings where household garages are scarce, outdoor charging becomes imperative [158]. At this point, mobile charging services such as robot-like systems can provide a viable solution by delivering charging services at convenient times and locations for EV users, featuring fewer site limitations and the flexibility to adapt to changing demand [120], [4].

The charging duration involves several elements, such as the time taken to reach charging stations, waiting periods in queues, and the actual charging time [131]. While home chargers address time constraints for many EV owners, the expansion of public charging remains essential to accommodate the growing EV market [169]. Generally, EV charging is slower compared to refuelling internal combustion vehicles, although fast charging stands out as an exception. However, the proportion of public charging stations equipped with fast charging technology remains relatively low [4]. Mobile charging systems present a solution by offering quicker charging options, especially when they support DC charging, and potentially saving time through convenient charging locations and eliminating queues, thereby streamlining the overall charging process for EV owners [131], [38], [4]. Especially, when the offered service is provided with robot-like units, the convenience could be enhanced due to the possibility of user-integrated service determining the desired SoC level within the connection time. Finally, offering a potential solution to cable handling, these systems can also mitigate the safety and ergonomic concerns raised as a consequence of high-power charging applications [92]. As the cables become heavier and stiffer to support higher power flow to reduce the charging duration, a significant barrier against the faster charging methodologies can be eliminated since the connection will no longer be established by human intervention as demonstrated in battery-less and robot-like types [92].

2.4.2. Grid Perspective

As the number of EVs on the roads continues to grow, the demand for charging will naturally increase. However, this upsurge in charging needs often coincides with peak periods in the power network, resulting in various technical challenges in grid management and more costly charging [160], [4]. The impact on the power grid varies significantly depending on the charging speed. For instance, a 10-minute fast charge for an EV can consume as much power as 140 family homes [40], [4]. Furthermore, widespread deployment of Level 1 or Level 2 charging stations in residential areas significantly boosts electricity consumption and introduces detrimental peaks to the existing distribution grid [179], [4].

In terms of slow charging, the charging stations which are commonly found in workplace settings, lead to peak power demand coinciding with employees' arrival and return after lunch [27], [4]. As a result, areas with high concentrations of EVs encounter a notable surge in charging demands at particular times of the day, placing pressure on the power grid. At this point, charging poles exhibit limited charging flexibility. Conversely, mobile charging systems equipped with battery units can store and preserve energy during off-peak periods, providing charging services that align with real-time energy demand [131], [198], [194], [4].

Even though it is a remarkable solution to reduce charging times, fast charging, characterized by its high demand, has the potential to cause significant voltage drops in the network, jeopardizing system stability [1], [4]. Proper scheduling of EV charging processes becomes imperative to mitigate the risk of grid failure when multiple EVs are charged simultaneously [170], [112], [4]. With the increasing penetration of EVs and the growing number of DC fast charging stations connecting to the power grid, substantial investments are necessary to adapt existing infrastructure. For instance, transformers in the US are typically designed to serve 3–5 households. However, if every home has two EVs, these

transformers must suddenly meet the electricity needs equivalent to 9–15 households, leading to rapid failures [40], [125], [4]. Consequently, a large number of charging poles may strain the current power grid beyond capacity [120]. In contrast, mobile charging systems can operate independently of nearby grid infrastructure for EV charging if they are equipped with storage systems, while still having the potential to offer comparable charging powers [120]. The ability to store electricity during off-peak periods can alleviate network stress, potentially minimizing the need for extensive infrastructure upgrades due to the decoupling of charging demand from the electricity network [160], [194], [159], [4]. Furthermore, mobile charging with batteries can improve power quality by reducing voltage drops and decrease pollution levels by offering a better integration possibility of renewable generation [160], [4]. These systems can act as a buffer to store the abundant renewable energy to be used in case of a deficit [41].

2.4.3. Investors' Perspective

Mobile charging systems hold the potential to improve the utilization rate of charging services, thus appearing as a remarkable investment option for investors to establish charging stations [4].

One of the major challenges encountered on the investor ground can be associated with the utilization rate of the charging stations as mentioned in Section 1. This higher utilization rate thanks to the optimal placement and sizing of the mobile charging systems could address this significant setback and therefore attract more capital flow toward the charging services. As a consequence of the higher rates, the system has the potential to sustain its profitability without relying on subsidies. This advantage can not only be categorized as a benefit solely for the investors but also it is a significant metric for the public allowing taxpayer money to be used for other welfare sources.

The dilemma of investing in charging infrastructure versus the widespread adoption of EVs presents a significant challenge. Determining whether to develop an extensive network of charging facilities to drive electric vehicle adoption or wait for increased EV adoption before expanding infrastructure is a complex decision [198], [4]. Given the slower rate of EV adoption compared to internal combustion engine vehicles, installing fast charging stations everywhere may not be economically viable [166], [4]. Especially, considering the investment cost and public space requirement of such stations, as argued in detail in Section 4.4.1, this investment decision becomes even more critical. In this context, mobile charging systems emerge as a pivotal solution due to their easier and more flexible deployment. By leveraging mobile systems, investors can potentially limit the amount of money they need to invest in the system, obtaining considerable returns within the product life of the system, as well. Especially, compared to DC charging systems, which are an important part of the expanding infrastructure, mobile charging systems can appear as a competitive solution to obtain higher returns on investment [37], [111]. Furthermore, the mobile systems allow the investors to redeploy the purchased system to another location more easily. The financial analysis of the system and comparison to the charging poles are discussed in detail in Section 4.4.2.

2.5. Configuration Evaluation

In accordance with the mentioned advantages and disadvantages of different mobile charging system configurations, it is essential to reflect on these factors to develop a system which is fit for purpose. As the main setting of this thesis is the urban space where private, public and workspace charging demands are accommodated, the suitability of different mobile charging systems has to be analysed. Among 4 different types of systems introduced in Section 2.2, the necessity of implementing a battery energy storage system becomes evident in order to effectively reduce the peak charging demand on the grid, by decoupling these operations from the electricity network. This way can also facilitate a better integration of renewable generation by offering the potential to store excess energy. At this point, large-scale battery-integrated systems might not be an adequate choice given the setting requirements. These types of systems are not very scalable and integratable, due to the limitations in the service area. Furthermore, as the smaller-scale systems falling under this category such as vans are mostly used for emergency charging services, they are not found as an adequate configuration for serving in relatively small neighbourhoods or parking places. Due to the inconvenience in mobile applications associated with the battery size, and weight together with the related scalability and acceptance issues, battery swapping systems may not also be an adequate choice. Lastly, robot-like systems with integrated batteries combine the introduced advantages and pave the way for an easily deployable and convenient charging service. As these systems usually employ relatively smaller batteries than large-scale config-

urations, they can potentially perform better in the urban setting. It is also important to note that they require less space and could exhibit more efficient transportation by employing autonomous robots. In addition, it is still possible to offer fast charging with these systems to address some of the mentioned challenges drivers face today by charging the vehicles up to a desired level in a given time. Last but not least, this configuration allows energy arbitrage due to the easy establishment of grid connection regarding the service distances and flexibility, which is more difficult to achieve with swapping stations and battery vans. Consequently, robot-like mobile charging systems are concluded as an advantageous configuration to hinder the issues from the driver's perspective, while not sacrificing the other benefits that the use of mobile charging systems can bring along, in the urban setting. In this way, Research Sub-Question 2 can be answered generally and the rest of the study and calculations focus on robot-like mobile charging systems with batteries considering different layouts.

3

Sampling Charging Operations

This section introduces the random sampling algorithm developed to simulate the charging tasks that will be fulfilled by the mobile charging system under consideration to answer Research Sub-Question 3.

A random sampling algorithm is developed to create synthetic and realistic charging profiles taking place at a designated parking area. The main objective of this algorithm is to represent charging operations in matrix format, expressing the charging power drawn from a regular charging station dependent on the time of the day. Operation logic further relies on sampling the EV models getting connected to the grid with their battery capacities, and the maximum charging power they support to correct the output data, accordingly.

One of the most important factors the developed algorithm takes into account is the type of charging profile. It can easily be predicted that the connection time, the power drawn from the grid, and the timing of the charging process primarily depend on the use of charging space. At this point, charging stations can be sorted into 3 groups, such as private, public, and workspace charging stations.

Private charging stations typically refer to those purchased by individuals or private investors, allowing car owners to regularly charge their EVs at residential locations. This could be done via a direct connection to the residential infrastructure or a wall box.

Secondly, public charging stations refer to the widely available charging poles located in public spaces, accessible to all car owners. Those are generally offered in designated parking lots on the streets or contained parking places and drivers are free to utilize the charging station at any available time at the expense of paying the surcharges.

Finally, workspace charging stations consist of the charging poles that are located in the parking places daily commuters use to travel to the offices. Even though its load profile is similar to public charging, workspace use mainly differs by the charging duration and time schedule influenced by the work hours. At this point, it is important to keep in mind business hours generally start at 8:30 in the morning and last at 17:30. These starting and ending times mainly impact the connection times observed at workspace charging stations since the main use of such is to benefit from the period where the car is stationary by charging the car to be ready to travel by the end of working hours.

3.1. Public and Workspace Demand Estimation

The algorithm is designed such that it can create the charging data tailored for any considered number of EVs and percentage of charging type, as well as the type of the day such as a typical weekday or a weekend. At this point, it is aimed to realize a typical weekday in the parking place that is mostly used by workspace chargers as well as some public customers. It is further assumed that each driver using the parking place utilizes the charging service once a week, based on a survey of EV drivers' charging behaviour in the Netherlands, which indicates an average of four monthly charges at the workplace and public charging stations [156]. This results in 55 charging operations on a weekday when a charging place with 275 EV capacity is considered, with the majority of them being workspace charging.

First, the percentage distribution of charging operations in the Netherlands is derived to create a realistic sample out of these numbers and percentages. Data in Figure 3.1 shows the percentage of

EVs arriving at the charging stations on a typical weekday, grouped under the Private, Public, and Workplace categories.

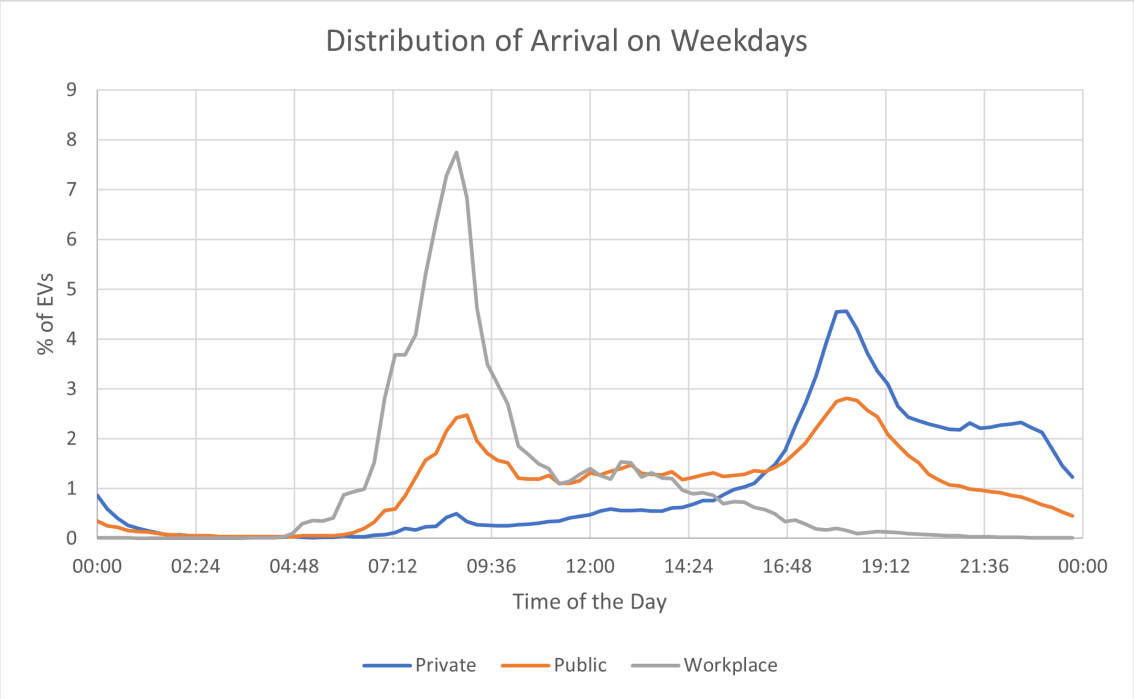

Figure 3.1: Percentage of EVs Arriving at the Charging Station in the Netherlands as a Function of Time of the Day

As Figure 3.1 shows, workplace charging demand peaks at 8:45, around the typical starting time of working shifts while reaching the bare minimum by 18:00. Meanwhile, public charging peaks twice in a day at 09:00 and 18:15, coinciding with workplace and private peaks.

Next, the percentages of EVs sorted by time are converted into integer number of EVs. In this case, this calculated number is expressed as a function of the percentage of the EVs getting charged at the timestep and the total number of EVs considered. In simple words, a certain percentage of the public and workspace chargers will be demanding energy. As this percentage differs as a function of time, the number of charging operations taking place changes accordingly. Therefore, this step reflects the effect of arrival time on the overall charging demand. The maximum number of EVs arriving at the same timestep describes the number of rows of the matrix, and the number of charging poles needed, to be used during samples.

Furthermore, the algorithm takes the cumulative energy demand distribution data to create energy demand, charging power and connection time matrices. This data is made up of 1% steps, expressing the probability of the EVs demanding at least a certain amount of energy. This cumulative distribution is plotted in Figure 3.2.

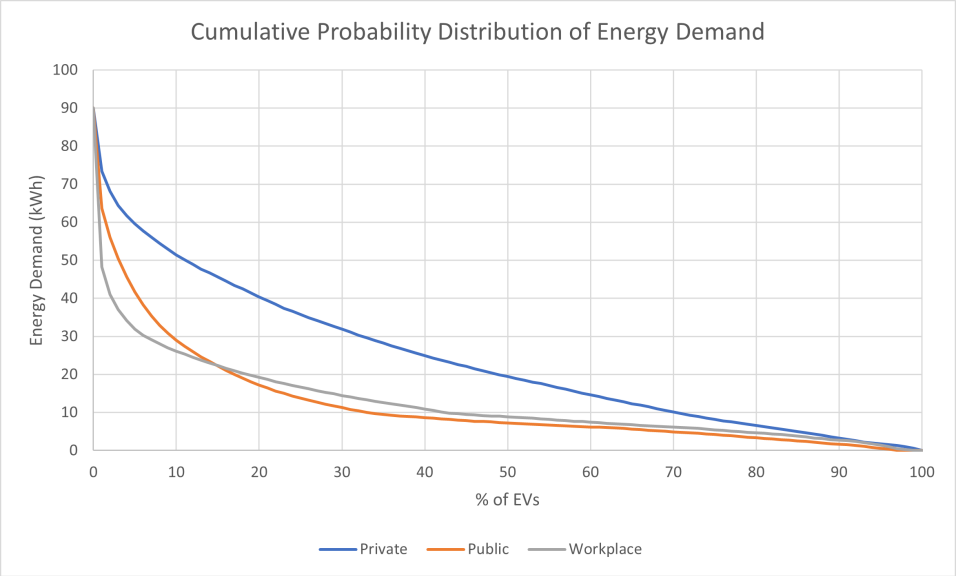

Figure 3.2: Cumulative Probability Distribution of Energy Demand Associated with the Charging Operations

The dataset plotted in Figure 3.2 is interpreted such that 100% of EVs, demand 0 kWh of energy, while 99% of them demand 0.6 kWh and 98% demand 1.2 kWh. The amount of energy demanded increases as the percentage decreases as fewer drivers charge from 0% SoC to 100% SoC.

The same method of cumulative distribution is also applied to the connection duration data, which is plotted in Figure 3.3. These data show how the connection time is distributed among the charging operations taking place.

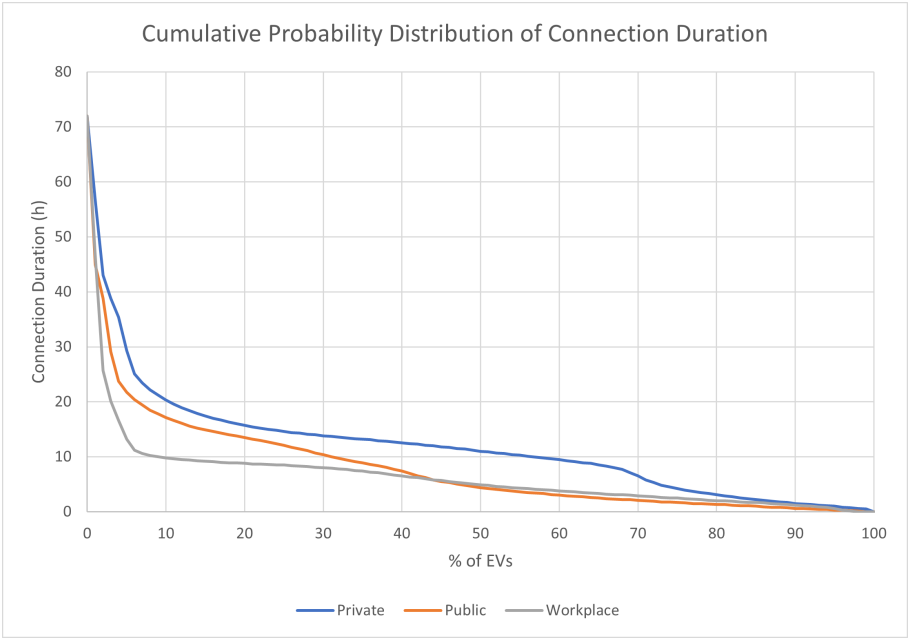

Figure 3.3: Cumulative Probability Distribution of Connection Duration Associated with the Charging Operations

As shown in Figure 3.3, public and workplace charging operations are mainly accumulated in the charging times under around 5 hours, as this number is more than 10 hours for private charging. This is fundamentally due to the traditional use of private charging services, in which the driver generally starts the connection in the evening and keeps the car connected until the next day or the next instance of travelling.

Finally, the same cumulative probability distribution approach is also followed in charging power data. However, in this case, since it is not possible to obtain private charging data due to data privacy reasons, this data set is only derived by using public charging services. Charging power data is plotted in Figure 3.4.

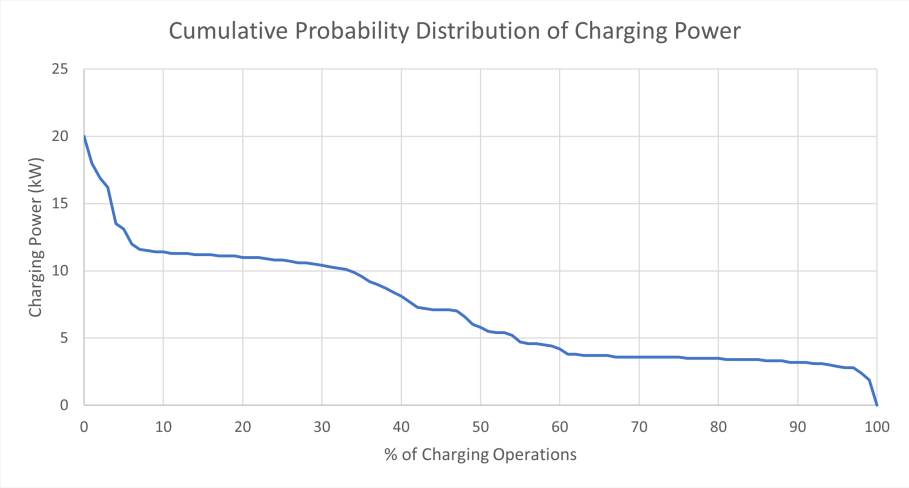

Figure 3.4: Cumulative Probability Distribution of Charging Power Associated with the Charging Operations

As the charging power values offered in most of the charging stations equipped with AC charging are certain and intermittent such as 3.7, 7.4 and 11 kW, these values described in the plot are further normalized to these values, whichever is the closest.

After the data sets described above are imported, they are further processed to form the matrix set to be used in the sampling. These matrices are constructed by the energy demand, charging power and connection time values randomly selected among the distributed values with respect to their percentages. It means it is more likely to find the charging duration, power and energy demand values corresponding to higher probability in the matrices, compared to less probable instances. These matrices are then shuffled to mimic the randomness of the reality. Lastly, as the use of DC fast charging infrastructure is announced as 8% of the charging operations in the National Survey, this percentage of the charging operations is randomly replaced with DC charging operations [156]. This replacement is applied in only public and workspace loads as fast charging is not a solution applied in private data due to its high cost and unsuitability in residential electricity infrastructure. Also, it is important to note that the power drawn from the grid significantly changes with the SoC of the EV. Consequently, it is advisable to disconnect the charger when the EV battery reaches approximately 80% SoC [4]. Beyond this threshold, it is reported that the charging rate diminishes significantly, and filling the last 20% of the charge may take nearly as long as reaching 80% initially. As this behaviour also matches with the charging curves of the vehicles under consideration given in Table 3.1, these charging operations are also corrected so that the DC operations abide by this charging behaviour and maximum power values depending on their SoC values.

In the next step, these charging operations that are chosen among the created matrices are matched with EV Models. At this point, the most popular 10 EV Models are taken into consideration [156]. These models and their specifications are stated in Table 3.1.

EV Model	Total Number of Vehicles	Share (%)	Battery Capacity (kWh)	Maximum Charging Power (kW)
Tesla Model 3	42618	0.25610	57.5	11
Kia Niro	19815	0.11907	64.8	11
Volkswagen ID3	16802	0.10097	58.0	11
Hyundai Kona	16688	0.10028	39.2	11
Renault Zoe	13195	0.07929	52.0	22
Skoda Enyaq	12616	0.07581	58.0	11
Nissan Leaf	12193	0.07327	39.0	6.6
Audi eTron	11567	0.06951	85.0	22
Tesla Model S	10899	0.06549	95.0	11
Volkswagen Golf	10019	0.06021	32.0	7.4

Table 3.1: The most popular EVs in the Netherlands and their specifications

Furthermore, taking the shares of each EV Model into account, the number of each EV model in the scenario studied is calculated by multiplying these numbers by the total number of cars.

Finally, charging power and energy demand values of individual operations are sampled from the created matrices uniformly. As soon as these operations are matched with the EV Models, a set of corrections are applied accordingly to keep the charging power less than the available maximum charging power, keep the energy demand lower than the capacity, and keep the connection time longer than or equal to the charging duration. Finally, in case the operation is sampled as a DC Fast Charging, corresponding power values are also corrected by taking the charging curves of individual vehicles into account. In the end, sampled 55 operations are allocated to 16 charging stations in 1 minute-long time steps. Accordingly, the total daily charging power in the studied scenario is plotted in Figure 3.5.

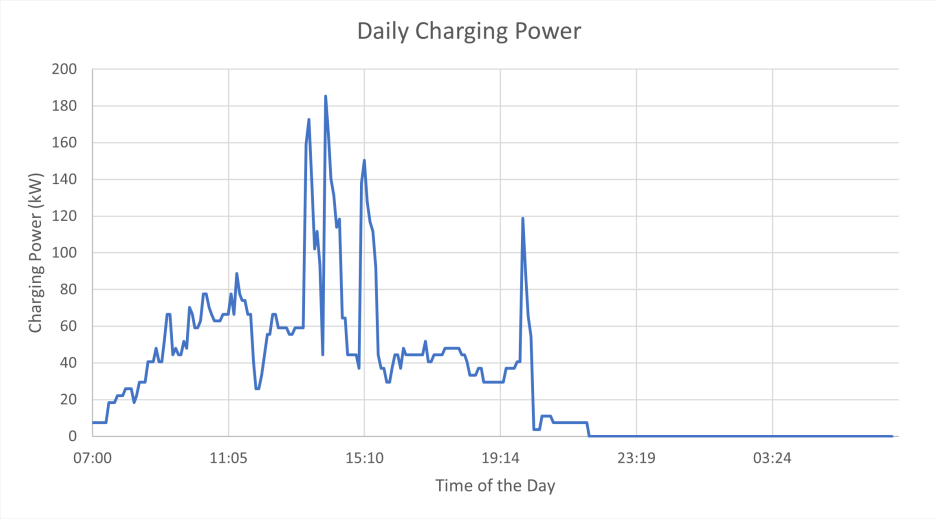

Figure 3.5: Daily Charging Power in the Studied Scenario

In detail, this total demand shown in Figure 3.5 consists of the summation of power values flowing from the charging stations to the EVs. When these charging operations are represented individually, the charging power for each charging operation can be seen. Figure 3.6 shows this representation in the form of instantaneous power drawn from each charging station. Charging stations are differentiated and numbered in the plot by using the abbreviation, CS. Research Sub-Question 3 can be answered in this way.

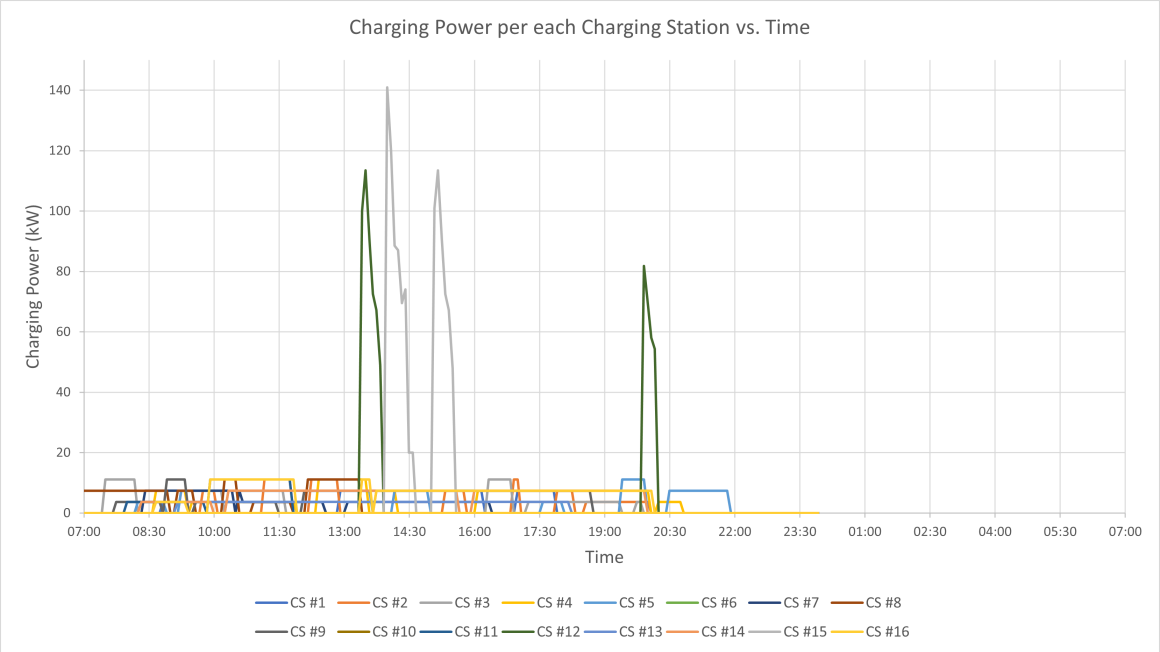

Figure 3.6: Charging Power Instantaneously Drawn from each Charging Station in the Studied Scenario

3.2. Private Charging Demand Estimation

The system's performance under private charging applications is also tested. To achieve this, the same demand estimation algorithm is run, only considering the private load for the same number of EVs. It is expected that the demand profile will exhibit a different shape compared to the public and workspace load due to the difference in the arrival times shown in Figure 3.1. Regarding this distribution, it is expected to see a gradual increase in demand around 4 pm, to reach its peak value later on as a consequence of the accumulation of EVs getting charged. It is also important to note that, as the energy demand corresponding to the private load is higher than that of workplace and public charging, as shown in Figure 3.2, higher total energy demand is anticipated in this scenario for the given 55 EVs. Obtained private load charging power for a typical weekday is shown in Figure 3.7.

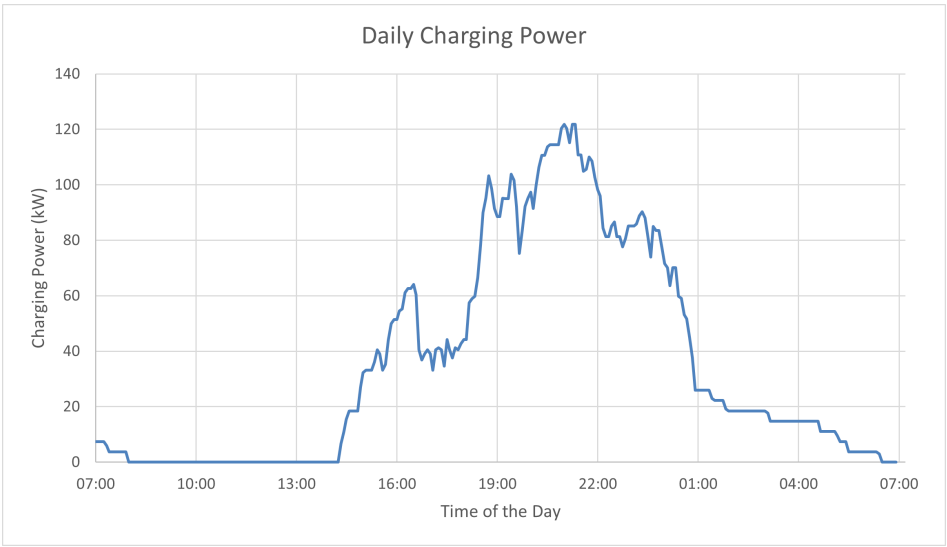

Figure 3.7: Daily Charging Power Plot in the Studied Private Charging Scenario

According to the plot given in Figure 3.7, the peak load is observed around 8 pm, following an upward trend starting in the afternoon. Furthermore, the total energy sold throughout the day is around

840 kWh, which is higher than that of public and workspace charging with around 750 kWh, as expected. Compared to the public and workspace scenario, the peak power value is around 34% lower than this scenario due to the lack of DC charging operations in the private case. As all of the charging operations are fulfilled by 3.7, 7.4 or 11 kW in AC charging, the peak power drawn from the grid is more limited compared to the first case. However, it is also important to note that this lower power results in a higher occupation rate of charging stations, especially when combined with the connection time distribution shown in Figure 3.3. Therefore, in this scenario, a considerably higher number of charging stations have to be installed to fulfil the demand, which is 28. The system's performance under these demand scenarios is further investigated in the following Sections.

4

System Sizing

This section discusses the methodology developed to design a framework to answer Research Sub-Question 4. In accordance, an effective sizing strategy to minimize the investment cost of the system while not compromising performance is proposed. According to the results obtained by employing the methodology, the utilization of different numbers of units and battery capacities are simulated under different scenarios to develop a reasonable sizing strategy.

The main objectives of the problem are to decide on the most feasible number of robots, battery capacity, and the best action sequence. These actions can be described as the activities which robots and batteries are free to do at any time under certain conditions, namely, charging an EV, travelling, or establishing a connection with the grid to undergo an energy exchange. Considering the complexity of the system as lots of different activities are involved and it is given a great degree of freedom to act, different challenges come into play. These challenges can be categorised into two different groups. The first one regards the computational difficulties which depend greatly on the type of the problem, dimensions and solver capabilities. Considering the variables and parameters affecting the final result, the problem can originally be classified as highly non-linear and non-convex. These types of problems result in lots of complications. Due to their nature and the solver algorithms used to solve such problems, they are computationally very expensive, costing lots of time and resources heavily dependent on the complexity and dimensions of the problem. Furthermore, the algorithms often used can not always guarantee a global solution, requiring additional effort to verify global optimality and rule out infeasibility.

At first, a nonlinear version of the problem is studied. The first challenge observed is due to the computational resource requirements. As there are some decision variables indexed by the number of daily charging operations, it is noted that the memory requirement of the solver significantly and exponentially increases by the number of EVs considered in the scenario as shown in Figure 4.1. Consequently, running the non-linear simulation in a local environment is found impractical due to the required memory exceeding available resources for the desired number of operations. Therefore, the simulation is run on a high-memory remote server which can facilitate the use of the desired number of daily charging operations.

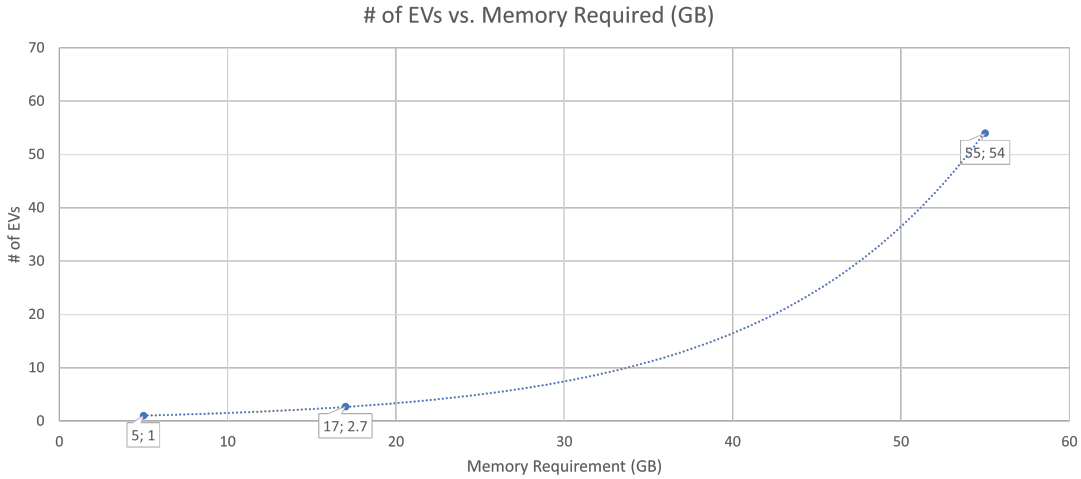

Figure 4.1: Resource Requirement of the Nonlinear Problem depending on the indexed number of charging operations

Even when the server used provides sufficient memory for the solver to return a solution, a verification problem arises. As the solvers utilized are not able to claim global optimality unless they are global solvers, the acquired solutions can be misleading in the decision process. It is sometimes observed that solutions bear unexplainable results highly deviating from what is reasonably expected, pointing out the probability of the model getting stuck at a local optimum point. This evidence significantly undermines the reliability of the resulting data, impeding the ability to draw conclusions from interpreting the output. Furthermore, when a global solver which can potentially return better results is used the solution times increase substantially, increasing the computational cost of the problem.

Furthermore, heuristic approaches are also considered as another method used in the literature to solve complex optimization problems. These approaches, depending on their application strategies, facilitate the use of more intricate objectives and constraints, whether they are nonlinear or non-convex, which cannot be addressed by mathematical formulations [128]. However, the main drawback of this method is again it can not guarantee the global optimality of the solution returned. Furthermore, it is also observed that the final solution obtained by this method differs for various tuning parameters such as the weights attached to the terms on the objective function [128]. Therefore, it can be concluded that using heuristic methods is not an adequate framework to achieve an absolutely truthful solution.

As a result, the decision is made to linearize the problem by eliminating the non-convex and nonlinear relations. This is achieved by incorporating techniques such as auxiliary variables and methods documented in the literature. Although these methods increase the number of constraints and variables, the reduced complexity paves the way to obtain solutions proving global optimality.

Apart from the computational challenges described, intellectual difficulties are often a part of the complex optimization problems where lots of different parameters have to be taken into consideration, affecting the final decision. As the primary aim of the decision is to find the best size and configuration of the system, there are lots of different physical and financial parameters affecting the result as well as qualitative aspects associated with the stakeholders and impacting them negatively or positively. The physical parameters can be summarised as the number of active batteries involved in the system, their respective battery capacities, the degradation observed on Li-ion material, number of vehicles to serve in a day while the financial parameters can be listed as the total amount of investment in the system, the cost of buying electricity from the grid, the revenue earned by selling energy either to the grid or a vehicle. On the other hand, the qualitative aspects are mostly related to the overall welfare and the attractiveness of the solution on all grounds such as the public and the investor such as convenience, affordability and competitiveness. Another example of this can be the grid capacity utilized. A high grid capacity requires more investment in the system due to the realisation of high power flow between the system and the grid. Furthermore, in case of grid congestion, this capacity allows more energy transfer from the system to the grid as it has a direct effect on the electricity price. A higher price will incentivise a positive flow from the batteries to the grid as the transaction becomes more profitable for the investors and beneficial for the public. On the other hand, if this congestion occurs at a moment when the system has to charge itself to fulfil the upcoming charging demand, this will further increase the

difficulty of local grid management. Since an extra energy demand occurs at a moment of scarcity, the resulting scenario will be unfavourable for the public and investors. Furthermore, a lower grid capacity facilitates more effective decoupling of charging demand from the demand on the grid, offering a high power fast charging by drawing less peak power from the grid. For example, even if the instantaneous charging power reaches high ratings such as 100s of kW at its peak time, its reflection on the grid will be limited by 10s of kW, as the exchange power is capped by the capacity. This results in great benefits for the grid, offering significant advantages to the public such as peak reduction. On the other hand, this grid capacity also limits the energy intake of the system at a moment, causing the system to not fully benefit from the low electricity price moments, decreasing the overall profits of the system.

These value and interest conflicts significantly increase the complexity of decision-making, highlighting the need for an alternative method. This method should set the background to analyse the performance of the system in different scenarios and discuss the effects of upcoming results from different perspectives. Therefore, the system is simulated by using 3 different electricity price scenarios from different days in the Netherlands and with 2 different grid capacities such as 50 kW and 100 kW. Both of the capacity values are lower than the peak power values observed throughout the day as shown in Figures 3.5 and 3.7 previously, hence reducing the peak power demand from the grid. Thus, both scenarios are more advantageous than using regular charging poles from the grid's perspective, even though the scale of benefits differs for each scenario.

Another challenge associated with the sizing problem is to derive an objective function representing a numerical transformation of reality. The objective of the decision is to find the most feasible sizing of the system and set a basis to discuss the effects of different parameters such as grid capacity. This feasibility includes the daily revenue, lifetime of the system and the cost of investment to realise such. However, these terms naturally imply an unbalance in terms of monetary value. In detail, the daily revenue of the system is in the scale of hundreds of euros whereas the investment cost of the system is on the order of hundreds of thousands. When these unbalanced terms are introduced in the objective function, the simulation will be heavily biased by the higher costs associated, and therefore return the bare minimum size of the system, the source of the heaviest penalty by far. However, this is not the desired output since a minimised size could bring along inefficient use of the bought material. This inefficient usage can lead to faster degradation and, consequently, a shorter product lifespan. Additionally, it may result in sub-optimal energy exchanges between the grid and the batteries such as buying at high prices and selling at low prices. Thus, scaling becomes necessary to keep every term close to each other in terms of numbers. However, this scale, whether it's an arbitrary weight without substantial real-world relevance or a temporal normalization, such as assuming a specific system lifetime to calculate daily investment cost, significantly impacts the accuracy with which real-world conditions are mathematically represented, leading to a more unrealistic approach. As a result, the simulation is decided to run for each fixed number of units and battery capacity. Even if this methodology significantly increases the number of runs, it prevents the unreasonable outputs that can potentially be returned by the simulation, bringing along the most effective way of utilising the tools. All in all, the objective of the simulation is to find the most profitable way of using the given resources for the given demand scenario, also considering the capacity fade realised over time. It is also important to note that the simulation is run for a day due to the computational limitations. Therefore, the solution returns the optimal use of the resources under the given circumstances for a day. Subsequently, the results are further processed to determine the optimal utilization of the units over their lifetime.

Another reason making this approach inevitable is due to the nature of investment cost calculation. As this cost is a function of the number of units and their battery capacity, this calculation requires the multiplication of two decision variables in the system. This causes the problem to become non-linear hence bringing along the technical challenges mentioned. Therefore, the introduced framework also prevents this situation from occurring, avoiding the non-linearity.

The energy transaction scheme implemented in the system allows a bidirectional flow between the batteries used for charging EVs and the grid. In this case, the system is expected to sell energy to the grid whenever it is profitable and there is time and energy available, pointing out peak demand hours throughout the day. In detail, the price offered by the grid acts as a major factor determining when to sell and buy energy. Therefore, the price gap observed throughout the day also impacts the feasibility of energy arbitrage. For example, if the difference between the highest and lowest prices fails to offset the cost of degradation, then arbitrage activity is not expected. Therefore, it can be concluded that the flow between the set of batteries and the grid is primarily dependent on the energy prices and incentivized

accordingly. Dutch intraday electricity market prices on different days are used to implement the price-incentivised decision-making in the system [54]. Price data obtained on a Winter day are plotted in Figure 4.2.

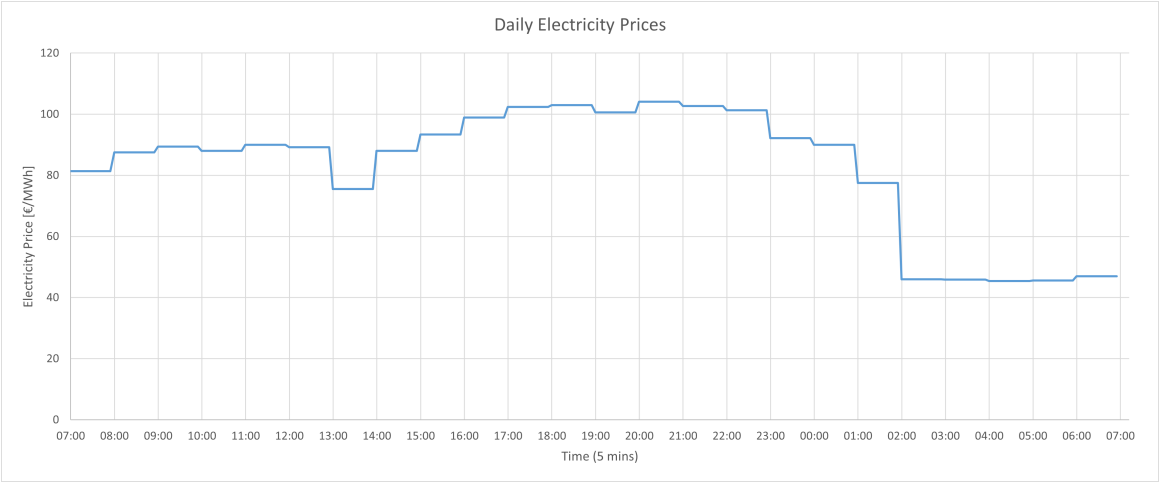

Figure 4.2: Daily Electricity Prices in the Netherlands on Dec 09, 2023 [54]

Furthermore, to analyse the system's performance in different conditions, analyses are repeated with different price variations. As shown in Figure 4.3, electricity wholesale market prices in the Netherlands have shown considerable volatility. The average price reached its peak in August while exhibiting a substantial decrease later on. Hence, the system's performance is also investigated by taking the average daily prices in August, questioning if it sustains profitability with extremely high prices for verification purposes.

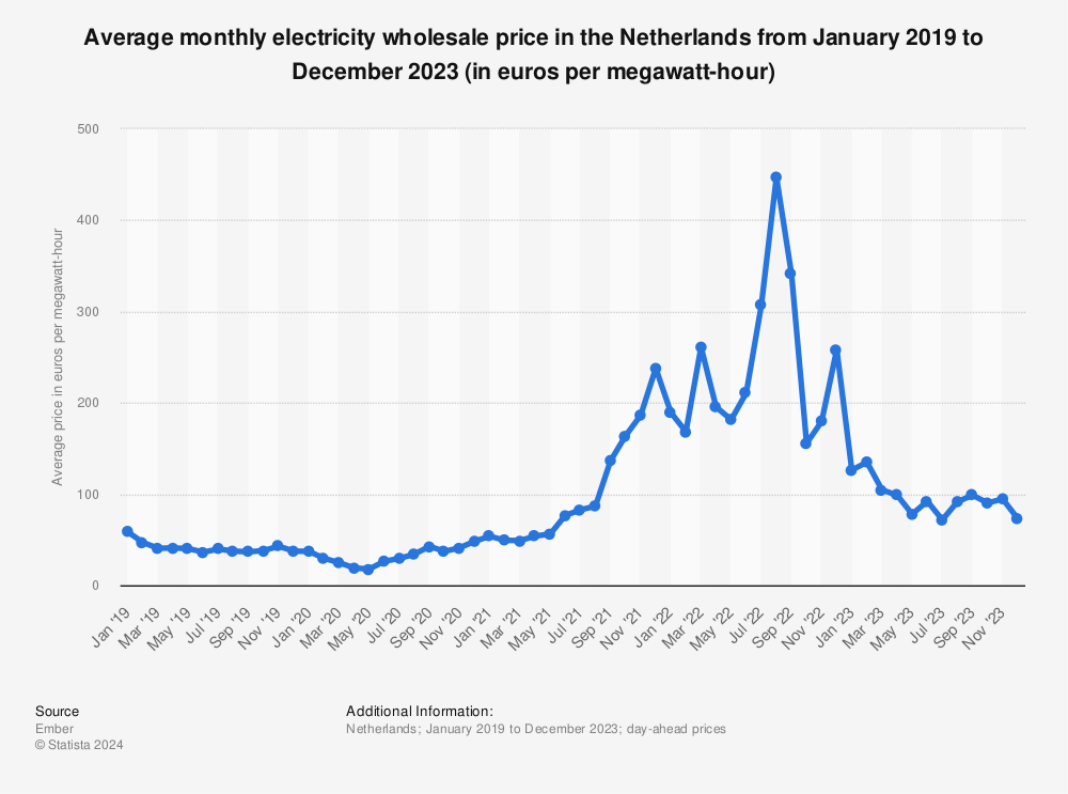

Figure 4.3: Average Monthly Electricity Wholesale Price in the Netherlands from January 2019 to December 2023 [176]

As a consequence, the price data in August is also gathered and averaged to derive the following daily price curve shown in Figure 4.4. This price set has a significantly higher average price, affecting the cost of buying energy from the grid. Moreover, the data has an adequate daily price difference, allowing a great possibility to sell energy to the grid, encouraged by the buy low and sell high principle.

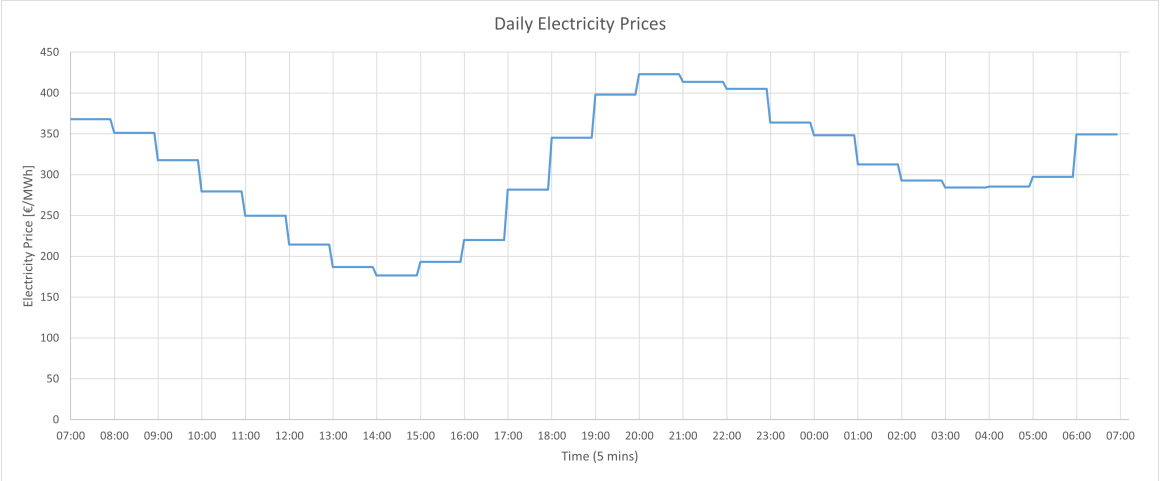

Figure 4.4: Average Daily Electricity Prices in the Netherlands in August [54]

Lastly, as the contribution of renewable energy sources such as solar and wind energy increases year by year in the Netherlands, the occurrence of negative prices has also increased. Due to the unpredictable and uncontrollable nature of renewable sources, electricity prices can drop under zero prices due to excess generation. In 2023, 212 hours of negative prices are recorded and further growth

of these instances is predicted for 2024 [35]. Accordingly, a price data set recorded on July 16 is also gathered to be used as shown in Figure 4.5. In this study, negative instances are set to zero, as the system is not acting directly on the wholesale market but using the same prices. Again, these prices also have enough price gaps to allow energy sales from the batteries to the grid, according to the energy arbitrage principle.

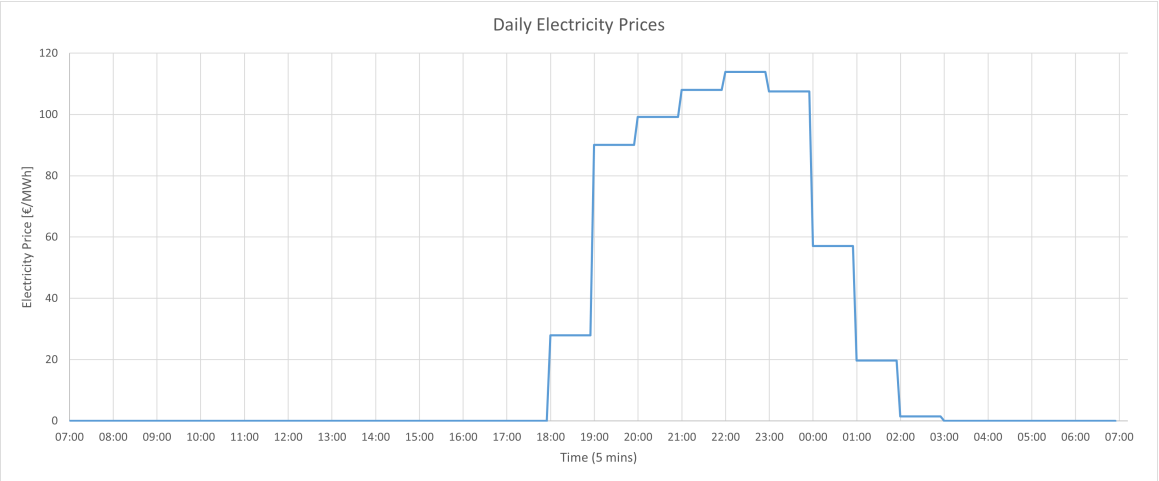

Figure 4.5: Daily Electricity Prices in the Netherlands on July 16, 2023 [54]

According to the prices plotted in Figure 4.2, the lowest prices are observed after 02:00 in the night while the price asked is relatively higher during the rest of the day. This lowest price period points out a low demand, compared to the rest of the day, hence has a great potential to offer a charging opportunity to the batteries. Because the batteries have to get charged at some point in the day, having these charging sessions during peak hours can potentially lead to local congestion, posing an extra demand the grid should supply. Especially, if such systems become widely used such that different parking places are powered by mobile systems, the magnitude of this impact can be further amplified. On the other hand, charging at off-peak hours is both advantageous for the grid and the investor. Mobile EV chargers can fulfil the charging tasks without relying on the grid at high demand hours, decoupling the energy demand from EV charging activities from the grid. Therefore, even if there is a significant charging demand at those hours, the load is not reflected on the grid, reducing peak demand, since the energy is transferred via batteries. Meanwhile, investors can greatly benefit from energy arbitrage as a consequence of the system buying at low prices, and selling at higher, while the local grid can also benefit from extra small-scale energy supplied by the batteries. Especially, in case the system is charged with renewable energy, it can act as a buffer to store the abundant generation at low demand hours to supply it back when it is needed, bringing along an efficient use and enhanced integration of renewable electricity [41].

4.1. Lithium Ion Battery Cost

To make a realistic sizing decision and practical business assessment, it is vital to address the costs associated with the battery energy storage system. As the battery is the main part of the system, it also has a significant effect on the investment cost as discussed further in Section 4.4.1. It is possible to express the effect of increasing the battery capacity on its monetary value in terms of the economies-of-scale principle [124]. Furthermore, this approach makes it also possible to define a monetary value for battery degradation, as this phenomenon implies the loss of bought capacity. Therefore, battery cost is an essential term to be taken into consideration in the optimization problem, as this unit price is pivotal in determining the investment cost and the monetary value of battery degradation.

In the literature, lithium-ion battery costs are often indicated as a constant $/kWh value. In this approach, this cost per unit capacity generally shows no difference as the capacity increases. On the other hand, it is also found that this is often not the case, and a certain discount factor can be applied when larger units are ordered from a manufacturer due to economies of scale [124]. To come up with a

realistic assumption, a market search is conducted to reproduce an overall price function. According to market research, the relationship between price and battery capacity is studied to test this hypothesis. The options found along with their capacities and prices are plotted in Figure 4.6 and fitted linearly. It is further acknowledged that the cost per kWh varies with the battery capacity, Q, and the unit cost gets smaller as the battery capacity increases. As a consequence, the cost function, C_{battery}, is obtained to be used in the degradation and investment cost calculations. This function can also be seen in Equation 4.1.

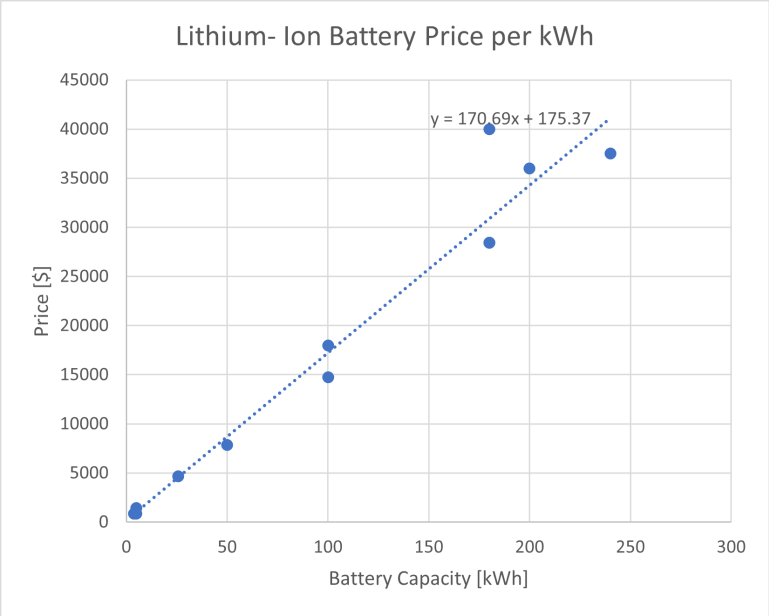

Figure 4.6: Lithium- Ion Battery Price per kWh of Capacity

$$C_{\text{battery}}(Q) = 170.69 \cdot Q + 175.37 \tag{4.1}$$

Furthermore, it is also important to note that Li-ion batteries have a developing second-life market, which is beneficial for the global economy. This second-life market emerges primarily as a consequence of the increasing EV penetration rate [52]. Considerable capacity fading occurs over time when EVs are driven. As more and more EVs are sold and used, the number of batteries whose capacity is lost up to a certain percentage increases, acting as a driving factor for the second-life market to facilitate a better and circular use of them. When this capacity loss reaches the end-of-life point and the battery can not fulfil the performance requirements, the batteries are retired and primarily end up in 3 different situations. They can be disposed of and no longer serve a purpose, recycled to extract precious materials used in components such as Cobalt and Nickel or repurposed to contribute to the economy [52].

Various studies in the literature have focused on how to use repurposed batteries in applications where they can significantly contribute to the public and the economy. For example, there are some studies analysing the use of retired Li-ion batteries in centralized renewable energy power stations for promoting emission-free energy sources' integration, smoothing control and decreasing service disruptions [85], [10], [110], [161]. As retired batteries can be repurposed to be a part of the energy generation side, there are also some studies analysing the use of them in grid management side. In such studies, it is shown that retired batteries can significantly contribute to easing grid congestion, provide auxiliary assistance to the network, and postpone the need for expanding power transmission and distribution capacity [139], [115], [73]. Lastly, some studies also proposed the use of such batteries in uninterrupted power supplies, residential energy storage systems and reserve storage systems [23], [91], [204], [44].

A practical example of the use of second-life applications of Li-ion batteries is a 2.8 MWh battery storage system installed in Johan Cruijff Arena in Amsterdam [107]. It is important to note that the entire storage system consists of 148 EV batteries, of which 40% of them are retired [201]. In this way, the installed storage brings along lots of potential benefits such as enhancing the renewable generation

integration to the grid, acting as a backup source, supporting the grid by acting as a frequency containment reserve, and peak load reduction [201]. In addition, the system size allows for serving 7000 households in Amsterdam in one hour and a potential CO_2 emission reduction of 116,683 tons [107].

Because of the swift growth in EVs witnessed in recent times, and an even more accelerated anticipated expansion over the coming decade according to certain projections, the supply of second-life batteries for stationary purposes is estimated to surpass 200 gigawatt-hours annually by 2030 [52]. This sector is expected to represent a market valued at over $30 billion on a global scale by 2030, emphasizing how the second life market will be an essential part of the economy [52].

Finally, there are many studies in the literature projecting the costs and evaluating qualification criteria for the batteries in retired status. For example, a SoH level of 70-80 % is marked as the end-of-life condition and the batteries are repurposed after reaching this point [87]. Furthermore, various studies realize a second-life battery price between 44-300 $/kWh range while most of them concur on a price lower than 100 $/kWh [87], [86]. Moreover, some studies also consider regional price differences and a second life price range of 19-72 $/kWh which European prices are closer to the higher end [32]. National Renewable Energy Laboratory highlights an end-of-life point of 70% of the initial capacity and remarks a second-life battery salvage value range of 72-131 $/kWh with 72% health factor [139]. Lastly, some reports evaluating the second-life market underscore a second-life price range between 30-70% of the new battery price in 2025 considering the market price is primarily governed by the new battery market and subsequent price per kWh [52]. As a result, 70% SoH can be taken as the end-of-life point with 70$/kWh sale price. This value points a close value to the reported prices while it is equal to almost 40% of the new battery price considered, staying within the price range reported [52]. The reasoning and verification to show that this selected point can maintain effective use of the invested battery material is further elaborated in Section 4.3.3.

4.2. Optimization Problem

An optimization problem is formulated to simulate the mobile charging system to evaluate its performance and interactions with the EVs and the grid under different conditions. The main objective of the formulation is to establish a realistic simulation to discuss the effects of different system parameters to size the system critically.

Some constant values are used in the formulation to be able to represent the operation realistically. These values are given in Table 4.1. At this point, charging efficiency regarding the energy transfer between the batteries and EVs is denoted by η_{B2V}, charging and discharging efficiency taking place between the grid and batteries are denoted by η_{G2B} and η_{B2G}, respectively. Powertrain efficiency is denoted by η_{M}, meanwhile, the duration of a timestep is denoted by Δt as 5 minutes sensitivity is used in the optimization problem. Grid capacity is expressed as GC, while the maximum power rating of batteries is $P_{\text{B}_{\text{MAX}}}$. It is important to note that this value is derived by averaging the maximum charging power values from the charging curves of the 10 most popular EV models in the Netherlands, which vary depending on their SoC. This makes it possible to generalize the model over different EV models and SoC conditions observed in the arrival. These models are given in Table 3.1, in the previous section. Furthermore, Q stands for individual battery capacity values and $Price_{\text{G}}$ is the daily electricity prices requested by the grid as shown in Figure 4.2, 4.5 and 4.4. The price offered for charging EVs is denoted by $Price_{\text{C}}$, and the reason behind this value is further described in Section 4.4.2. The degradation of the battery per kWh of charged and discharged is expressed as L, and it is a function of Li-ion battery price and linear degradation as explained in Equation 4.25 later. Lastly, $P_{\text{M}_{\text{avg}}}$ stands for the average power consumption per driving cycle as explained in Equation 5.14.

Table 4.1: Constant Parameters

Parameter	Value
η_{B2V}	0.95
η_{G2B}	0.95
η_{B2G}	0.95
η_{M}	0.9
Δt	$\frac{5}{60}$
GC	50/100 kW
$P_{\text{B}_{\text{MAX}}}$	85.7 kW
Q	70-400 kWh
$Price_{\text{G}}$	See 4.2/4.5 /4.4
$Price_{\text{C}}$	0.65 €/kWh
L	See 4.25
$P_{\text{M}_{\text{avg}}}$	See 5.14

Objective Function

The objective function regards the maximization of the total daily profit associated with the energy exchange between the grid and the battery and the charging operations while also considering the battery degradation. In this regard, R_{B2V} denotes the revenues earned by charging EVs, while R_{B2G} expresses the revenues earned by energy sales to the grid. Next, C_{G2B} denotes the cost of buying electricity from the grid while C_{D} is the monetary cost of battery degradation, expressing the cost of loss material.

The summation $\sum_{r=1}^{R}$ iterates over the set of battery units, while $\sum_{t=1}^{T}$ iterates over the time steps discretizing a day into intervals of 5 minutes. $P_{\text{B2V}_{\text{r,t}}}$ denotes the power supplied from battery unit r to an EV at time step t. The variables r and t are constrained to the set of units and time steps, respectively. On the other hand, $P_{\text{B2G}_{\text{r,t}}}$ denotes the power supplied from battery unit r to the grid at time step t, while $P_{\text{G2B}_{\text{r,t}}}$ expresses the power flowing from the grid to battery unit r.

$$\max(R_{\text{B2V}} + R_{\text{B2G}} - C_{\text{G2B}} - C_{\text{D}}) \tag{4.2}$$

Where:

$$R_{\text{B2V}} = \sum_{r=1}^{R}\sum_{t=1}^{T} P_{\text{B2V}_{\text{r,t}}} \times \Delta t \times Price_{\text{C}} \quad \text{where r} \in \text{Units}, \quad \text{T} \in \text{Timesteps} \tag{4.3}$$

$$R_{\text{B2G}} = \sum_{r=1}^{R}\sum_{t=1}^{T} P_{\text{B2G}_{\text{r,t}}} \times \Delta t \times Price_{\text{G}} \quad \text{where r} \in \text{Units}, \quad \text{t} \in \text{Timesteps} \tag{4.4}$$

$$C_{\text{G2B}} = \sum_{r=1}^{R}\sum_{t=1}^{T} P_{\text{G2B}_{\text{r,t}}} \times \Delta t \times Price_{\text{G}} \quad \text{where r} \in \text{Units}, \quad \text{t} \in \text{Timesteps} \tag{4.5}$$

$$C_{\text{D}} = \sum_{r=1}^{R}\sum_{t=1}^{T} [P_{\text{B2V}_{\text{r,t}}} + P_{\text{B2G}_{\text{r,t}}} + P_{\text{G2B}_{\text{r,t}}}] \times \Delta t \times L \quad \text{where r} \in \text{Units}, \quad \text{t} \in \text{Timesteps} \tag{4.6}$$

Constraints

The following constraints are defined to simulate the system. Constraints are aimed at transforming real-world phenomena into mathematical formulations, enabling comprehensive understanding and accurate predictions of system behaviour. Hence, they indicate equations of energy transfer and consumption as well as basic logical expressions to transcribe reality.

1. In the system, the robot has 4 degrees of freedom, meaning it can charge an EV, get charged from the grid, sell energy to the grid, and travel either from hub to EV, EV to EV, or EV to the hub. At this point, the following constraint is defined to ensure each unit is only allowed to do one of the listed activities at a time. When the unit is active, it is free to do one of those 4 activities

at any time, or none of them if its contribution is not necessary to fulfill the demand. In this constraint, explained degrees of freedom are introduced. The battery can conduct a charging operation indexed by o, and it is controlled by binary variable $B2V_{r,t,o}$. It can also charge itself from the grid, denoted by $G2B_{r,t}$, sell energy to the grid $B2G_{r,t}$, travel $T_{r,t}$ or do nothing at a timestep. When the unit does any of these activities, corresponding binary variables become 1 at that timestep, while it is 0 otherwise. Furthermore, the unit can only fulfil one assigned charging operation at a timestep. Hence, the sum of $B2V_{r,t,o}$ over all indexed charging operations can either take 1 or 0 at a timestep. This logic is shown in the following equation:

$$\sum_{o=1}^{O} B2V_{\mathrm{r,t,o}} + G2B_{\mathrm{r,t}} + B2G_{\mathrm{r,t}} + T_{\mathrm{r,t}} \leq 1 \quad \forall r \in R, \quad \forall t \in T, \quad \text{where o} \in \mathrm{O} \tag{4.7}$$

2. This constraint defines the SoC evolution of the batteries. The battery's SoC is increased by energy intake from the grid, denoted by $P_{\mathrm{G2B_{r,t}}} \times \Delta t$, decreased by any means of discharge, $P_{\mathrm{B2G_{r,t}}} \times \Delta t$, $P_{\mathrm{B2V_{r,t}}} \times \Delta t$ and travel, $P_{\mathrm{M_{r,t}}} \times \Delta t$. The endpoint of this discharge can be the grid, motor or an EV. Also, the effect of this charge and discharge is a function of the battery capacity, Q and constant efficiency values, η_{G2B}, η_{M}:

$$\begin{aligned} SoC_{\mathrm{r,t+1}} = SoC_{\mathrm{r,t}} + \frac{P_{\mathrm{G2B_{r,t}}} \times \Delta t}{Q} \times \eta_{G2B} - \frac{P_{\mathrm{B2G_{r,t}}} \times \Delta t}{Q \times \eta_{\mathrm{G2B}}} \\ - \frac{P_{\mathrm{B2V_{r,t}}} \times \Delta t}{Q \times \eta_{\mathrm{B2V}}} - \frac{P_{\mathrm{M_{r,t}}} \times \Delta t}{Q \times \eta_{\mathrm{M}}} \quad \forall r \in R, \forall t \in T \end{aligned} \tag{4.8}$$

3. The constraint defines the power required by the powertrain as a result of travelling activities in a way that the power drawn by the motor, $P_{\mathrm{M_{r,t}}}$ is equal to the average power demand of the powertrain during a driving cycle, $P_{\mathrm{M_{avg}}}$ when the battery is on travel, and 0 otherwise. The calculation method of this average power is further elaborated in Section 5:

$$P_{\mathrm{M_{r,t}}} = P_{\mathrm{M_{avg}}} \times T_{\mathrm{r,t}} \quad \forall r \in R, \forall t \in T \tag{4.9}$$

4. The set of constraints introduces the travelling logic implemented in the system, controlled by binary variable, $T_{\mathrm{r,t}}$. The battery should be identified as travelling one timestep right before a charging operation starts as well as one timestep right after the charging session ends:

$$T_{\mathrm{r,t+1}} \geq \sum_{\mathrm{o}=1}^{\mathrm{O}} B2V_{\mathrm{r,t,o}} - \sum_{\mathrm{o}=1}^{\mathrm{O}} B2V_{\mathrm{r,t+1,o}} \quad \forall r \in R, \quad \forall t \in T, \quad \text{where o} \in \mathrm{O} \tag{4.10}$$

$$T_{\mathrm{r,t-1}} \geq \sum_{\mathrm{o}=1}^{\mathrm{O}} B2V_{\mathrm{r,t,o}} - \sum_{\mathrm{o}=1}^{\mathrm{O}} B2V_{\mathrm{r,t-1,o}} \quad \forall r \in R, \quad \forall t \in T, \quad \text{where o} \in \mathrm{O} \tag{4.11}$$

5. This constraint enforces the battery to not do two different charging operations consecutively since there is a necessity for travel. Although Equations 4.10 and 4.11 are employed to implement the travelling logic, the sum of binary variables used to monitor the charging condition in these constraints only takes 1 when there is any charging operation taking place at that time step. Therefore, these variables take a positive value regardless of which charging operation is being fulfilled. This points out the necessity of developing the travelling logic by also checking which operations are being conducted at consecutive timesteps. Consequently, when the battery is away from the hub, there must be at least one timestep of travel activity between two different charging operations, $o1$ and $o2$:

$$B2V_{\mathrm{r,t,o1}} + B2V_{\mathrm{r,t+1,o2}} \leq 1 \quad \forall r \in R, \quad \forall t \in T, \quad \forall o1 \in O, \quad \forall o2 \in O, \quad \text{where o1} \neq \text{o2} \tag{4.12}$$

6. The following set of constraints defines the grid capacity behaviour. According to the implemented logic, the net power drawn from the grid, as well as fed to the grid, should be smaller or equal to the grid capacity, denoted by GC:

$$\sum_{\mathrm{r}=1}^{\mathrm{R}} \left(P_{\mathrm{G2B_{r,t}}} - P_{\mathrm{B2G_{r,t}}}\right) \leq \mathrm{GC} \quad \forall t \in T, \quad \text{where r} \in \text{Units} \tag{4.13}$$

$$\sum_{\mathsf{r}=1}^{\mathsf{R}} \left(P_{\mathsf{G2B}_{\mathsf{r,t}}} - P_{\mathsf{B2G}_{\mathsf{r,t}}}\right) \geq -\mathsf{GC} \quad \forall t \in T, \quad \text{where r} \in \text{Units} \tag{4.14}$$

7. This set of constraints defines the maximum power that an individual robot can feed or draw, denoted by $P_{\mathsf{B}_{\mathsf{MAX}}}$. If the binary variables regulating the power flow between the grid and the batteries are active, meaning $G2B_{\mathsf{r,t}}$ and $B2G_{\mathsf{r,t}}$ are 1, the instantaneous power value should be smaller or equal to the maximum power rating. These binary variables only take 1, when a connection between the individual batteries and the grid is established. This can only happen when the unit is not charging an EV or travelling as this logic is defined by Equation 4.7. Otherwise, it is 0 since there is no exchange:

$$P_{\mathsf{G2B}_{\mathsf{r,t}}} \leq P_{\mathsf{B}_{\mathsf{MAX}}} \times G2B_{\mathsf{r,t}} \quad \forall r \in R, \quad \forall t \in T \tag{4.15}$$

$$P_{\mathsf{B2G}_{\mathsf{r,t}}} \leq P_{\mathsf{B}_{\mathsf{MAX}}} \times B2G_{\mathsf{r,t}} \quad \forall r \in R, \quad \forall t \in T \tag{4.16}$$

8. A battery can only charge one vehicle at a time. When it conducts a charging operation indexed by o, the binary variable corresponding to this operation, $B2V_{\mathsf{r,t,o}}$ takes 1, while that of other operations must be 0. It can not be used to charge more than one vehicle at a certain timestep:

$$\sum_{\mathsf{o}=1}^{\mathsf{O}} B2V_{\mathsf{r,t,o}} \leq 1 \quad \forall r \in R, \quad \forall t \in T, \quad \text{where o} \in \mathsf{O} \tag{4.17}$$

9. To set a noncollaboratory charging scheme, the following constraints are defined. According to the rule, there is an assignment logic such that every charging operation must be assigned to a robot. However, this assignment, denoted by $A_{\mathsf{r,o}}$ cannot be any other value than 1, since no more than 1 battery can be used to charge a certain EV:

$$\sum_{\mathsf{r}=1}^{\mathsf{R}} A_{\mathsf{r,o}} = 1 \quad \forall o \in O, \quad \text{where r} \in \mathsf{R} \tag{4.18}$$

10. The following constraint is defined to combine the assignment logic with charging power. The binary variable regulating the power flow value between a battery and an EV within the connection time can be nonzero if and only if that operation is assigned to this battery. If the operation is not assigned and hence being conducted by another unit, then there must be no power flowing from that battery to the corresponding EV:

$$\sum_{t=Start_{\mathsf{o}}}^{End_{\mathsf{o}}} B2V_{\mathsf{r,t,o}} \geq A_{\mathsf{r,o}} \quad \forall r \in R, \quad \forall t \in T, \quad \text{where o} \in \mathsf{O}, \quad Start_{\mathsf{o}}, End_{\mathsf{o}} \in \mathsf{T} \tag{4.19}$$

11. To keep the energy flow between the individual batteries and vehicles regulated, the following set of constraints are implemented. This definition aims to ensure the power flow between the battery and the EVs can be monitored in a separate approach allowing observation of every single charging operation. Since the batteries are not allowed to collaborate on a charging task, there exists a requirement to define charging power indexed by battery units, time and charging operation. The main objective is to ensure that the power flow is regulated by the binary variable $B2V_{\mathsf{r,t,o}}$ and specified for each charging operation to set the non-collaboratory changing scheme and fulfilment of charging demand. In this case, this power value has to be equal to zero when a battery is not conducting some certain charging operation at a certain time, or that operation is assigned to another battery. However, this approach brings along the necessity of multiplication of two decision variables, the power value and the binary variable regulating it, changing the nature of the problem and making it non-convex. At this point, the following constraints are defined to avoid this change, inspired by the method McCormick Envelopes [126]. The method exemplifies a technique to relax non-convex problems to address the related issues and linearise

the optimization problems by the use of auxiliary variables, such as $P_{\mathsf{x_{r,t,o}}}$. In this case, this auxiliary variable represents the power flow between the batteries and EVs, distinguished for each charging operation:

$$P_{\mathsf{x_{r,t,o}}} \leq P_{\mathsf{B_{MAX}}} \times B2V_{\mathsf{r,t,o}} \quad \forall r \in R, \quad \forall t \in T, \quad \forall o \in O \tag{4.20}$$

$$\sum_{\mathsf{o}=1}^{O} P_{\mathsf{x_{r,t,o}}} = P_{\mathsf{B2V_{r,t}}} \quad \forall r \in R, \quad \forall t \in T, \quad \text{where o} \in \mathsf{O} \tag{4.21}$$

$$P_{\mathsf{x_{r,t,o}}} \geq P_{\mathsf{B2V_{r,t}}} - P_{\mathsf{B_{MAX}}} \times (1 - B2V_{\mathsf{r,t,o}}) \quad \forall r \in R, \quad \forall t \in T, \quad \forall o \in O \tag{4.22}$$

12. Combined with the other three constraints above, this one ensures that the charging demand of individual EVs, dependent on how much energy they desire, E_{o}, should be fulfilled within the connection time defined by the start of the period, $Start_{\mathsf{o}}$, and the end, End_{o}. Therefore, this logic ensures the system will charge every vehicle in the system up to the desired SoC and the duration of the operation is smaller or equal to the time the EV is stationary in the parking lot:

$$\sum_{t=Start_{\mathsf{o}}}^{End_{\mathsf{o}}} P_{\mathsf{x_{r,t,o}}} \times \Delta t = E_{\mathsf{o}} \quad \forall r \in R, \quad \forall t \in T, \quad \forall o \in O, \quad \text{where } Start_{\mathsf{o}}, End_{\mathsf{o}} \in \mathsf{T} \tag{4.23}$$

13. This constraint forces the power flow value between the battery and an EV corresponding to a battery at a time step to be zero if it is not conducting a charging operation. This value can be non-zero if and only if the battery charges an EV and must be smaller than the maximum power rating:

$$P_{\mathsf{B2V_{r,t}}} \leq P_{\mathsf{B_{MAX}}} \times \sum_{\mathsf{o}=1}^{\mathsf{O}} B2V_{\mathsf{r,t,o}} \quad \forall r \in R, \quad \forall t \in T, \quad \text{where o} \in \mathsf{O} \tag{4.24}$$

4.3. Results and Discussion under Public and Workspace Charging Load

Complex systems have a wide range of stakeholders and factors involved. These stakeholders can often have conflicting interests requiring critical thinking in decision-making processes. To study the problem in detail, results are comprehensively analysed regarding the interests of these stakeholders.

In this particular system, various stakeholders can be listed. First, the public is the most important side. Mainly, the community can be categorized as the client, getting the service from the system. Thus, the overall convenience of the system is the key issue. The system should address the requirements of the drivers inclusively and the challenges they face. Therefore, the parameters and takeaways found in the study should act as a solution to the difficulties of regular charging operations that take place today. To accomplish this, the design outputs must offer an accessible and sufficient charging experience where the charging task is fulfilled within a given time and up to a desired level. The decided number of units and battery capacities must facilitate the satisfaction of the charging process. Therefore, the search space of the solution starts from the minimum battery capacity that can fulfil all charging tasks in the studied scenario, which is 70 kWh for the public and workspace demand and 120 kWh for the private demand. The considered number of units ranges from 3. The main reason behind it is attributed to the occurrence of fast degradation and the large size of batteries required below this number and resulting incompetence.

Meanwhile, the investor ground can be categorized as another stakeholder. In this case, the required investment to fulfil these requirements is also a key aspect. This issue has many sides such as the investors themselves and the government as well as the public. For the investor, the system should be financially viable, ensuring a notable turnover. To address this, daily profits of the system are investigated as well as discussing the effect of different parameters on these numbers. Processing the output values further, a total investment cost is calculated and the system's financial performance is analysed. Furthermore, the monetary return of this investment can not be classified as sole profits. Because some investments in the charging infrastructure face continuous subsidies from governmental institutions, using an optimized system tailored to addressing the charging demand becomes more important to ensure the self-sufficiency of the system. As today's ambitious expansion in charging

infrastructure highlights the risk of low utilization rate and therefore inevitable subsidy schemes, an optimally sized system can potentially alleviate the financial burden of the investments on the public [187]. Consequently, the investment cost of the system is compared to the systems made up of charging poles. In addition, it should also be remembered that as the system has significant benefits for the grid such as peak reduction, the consequences of this investment again affect the public. Therefore, the advantages and disadvantages of using higher grid capacity are also discussed, paying attention to this motivation.

4.3.1. Effect of Energy Arbitrage

Bidirectional energy flow between the grid and the batteries can be categorized as V2G. This flow consists of batteries buying energy from the grid to charge themselves for either fulfilling the demand or profiting off the energy arbitrage.

The overall daily profit of the system regarding the energy arbitrage is mainly dependent on various factors. First, there must be enough price gaps to facilitate energy arbitrage. In this case, there are two costs associated with purchasing energy from the grid. One of them is the transaction cost mainly defined by the instantaneous electricity price asked by the grid, while the other is the degradation cost. Since there is a capacity loss associated with any amount of energy the battery is charged with or discharges, the total cost of the purchase is in fact higher than what is paid to the grid. Another factor is the selling price. The selling price must be high enough to compensate for the cost of purchasing and the loss of battery capacity. Lastly, there must be enough grid capacity to pave the way for buying at low prices and selling at high prices.

The price gap mainly differs daily and seasonally. For the three scenarios analysed, daily price gaps are shown in Table 4.2

Table 4.2: Scenarios and Daily Price Gaps (€/kWh)

Scenario	Maximum Price Gap (€/kWh)
Winter Scenario	0.056
Summer Scenario	0.11
Extreme Scenario	0.24

As shown in Table 4.2, the winter scenario has the lowest price gaps due to the relatively low energy generation of renewable sources. It can be concluded that this small price gap is not enough to profit notably from energy arbitrage. The effect of renewable sources appears more remarkably in the summer scenario due to the negative prices. As the price is determined by an auction, balancing the supply and demand, these negative prices are an indicator of either a significant drop in demand or a sharp increase in supply [173]. In this case, due to the abundance of renewable electricity generation, and the ramping duration of fossil fuel generators, a surplus of production takes place. Often, it becomes more costly to shut down the generation than to sell it for a negative price and this causes the negative prices to occur [173]. As stated, in this study, negative prices are set to zero. At this point, the emerging price gap can give the system great potential to do energy arbitrage. Furthermore, as this transaction is mainly dependent on the daily price gap, the demand from the battery side is price-driven, hence increasing by the surplus and decreasing by the deficit. This reveals another advantage of the system. A portion of this surplus of energy can be stored and utilized later on to support the grid, in case it is needed. In this way, in case this price drop is sourced by emission-free generation, renewable electricity can be utilized and integrated more effectively. The effect of electricity prices becomes much clearer when the total exchange power between the system and the grid is investigated. For example, when 3 units with 270 kWh battery capacity and 50 kW grid capacity are utilized, consequent exchange power is plotted in Figure 4.7.

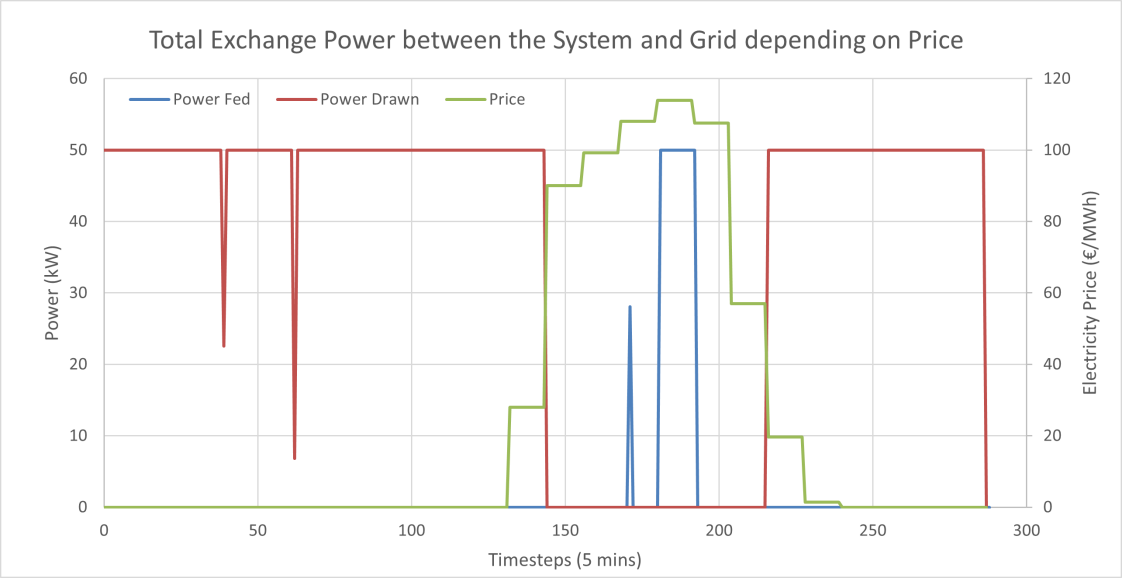

Figure 4.7: Total Exchange Power between the System and Grid when 3 Units with 270 kWh Battery Capacity and 50 kW Grid Capacity is Used

Figure 4.7 reveals the effect of overgeneration and resulting prices on the exchange between the system and the grid. As shown in the figure, the system tries to take full advantage of zero prices by charging itself whenever there is availability. As the electricity price increases later in the day, the direction of this flow changes so that the system sells the purchased and stored energy back to the grid when the demand is higher. As the amount of energy available for sale is finite and constrained by both the battery and grid capacities, it only exhibits a positive flow from the system to the grid during the two highest price periods, aimed at maximizing profits. It is also important to note that the system avoids selling energy excessively, even though the price is non-zero in some instances. The effect of battery degradation becomes evident at this point. Since the earned profit is not enough to compensate for the degradation cost, the system strategically limits energy sales to mitigate battery wear and maintain its longevity. As a result, it balances profit generation with the need to preserve the battery's state of health and optimize long-term performance.

4.3.2. Number of Units and Battery Size

The total energy displaced by the system is directly proportional to the number of batteries and the battery capacity. However, for a constant displacement, these two variables exhibit an inverse relation. The same amount of energy can either be stored in a system with a higher battery capacity but less number of units or with a lower battery capacity but a high number of units. Having a higher number of units can increase the number of operations that can take place at the same time. These operations can be charging EVs as well as feeding energy to the grid or purchasing energy.

For a given total energy capacity, having more units with smaller capacities gives the system more flexibility. For example, in a system with 1000 kWh total capacity, divided into 10 batteries of 100 kWh, a charging task can be fulfilled by allocating only 10% of the total capacity to a specific job, while keeping the rest engaged in a transaction with the grid, either feeding or drawing energy for profits. At a low price period, an available extra unit might take full advantage of the cheap electricity, while the other units are fulfilling the charging demand. However, one should not forget the sustainability of the system while making this decision. Considering a long period where the system will be serving the public, this configuration significantly increases the number of cycles each battery undergoes. This increase brings about a fast degradation and hence replacement, shortening the service life of the product, requiring continuous spending and investment. Furthermore, the investment cost of the system is highly dependent on the number of units, either the batteries or robots, as the costs of the equipment can not be underestimated. Consequently, more units bring along more onboard components such as chargers, robotic arms and motors and cause the cost of investment to increase substantially. Also, considering that larger batteries are cheaper per kWh as explained in Section 4.1, fewer units could

minimize the cost of investment. The effect of increasing the number of units and battery capacity is further discussed in the following sections.

Effect on Grid Interaction

To address the effect of battery capacity on the system's performance, various sizes are evaluated. Increasing the battery capacity paves the way for a more flexible operation scheme where the battery undergoes less urgent charging stops to satisfy the charging demand. As the primary revenue source and the fundamental duty of the system is charging the EVs, the batteries should always be at the adequate SoC level to charge the vehicles up to the desired state, within the connection time. Therefore, after a charging operation, the battery can either do sequential charging by directly travelling to the next customer and initiating the operation, or postpone the starting time for a few time steps to get itself charged from the grid. As the capacity of a battery increases, it can act more efficiently by taking the charging break only if the electricity price is at a good level to buy or sell. The main reason is the low SoC of the battery becomes a less frequent issue and hence it does not have to undergo urgent charging breaks.

Secondly, as the total stored energy in the system increases, when there is an adequate price gap, the system starts selling more energy to the grid, improving the daily revenue. However, this occurs up to a certain point. After that point, further increasing the battery capacity does not improve the sales to the grid because grid capacity starts to become an issue. In a system where the maximum useful energy to be sold to the grid is restricted by the capacity and the electricity prices, there is a maximum amount of energy exchange level that can be reached in a day. As a result, after reaching this level, an increase in size no longer has a significant impact on the amount of energy sold to the grid. This effect is demonstrated on the Figure 4.8

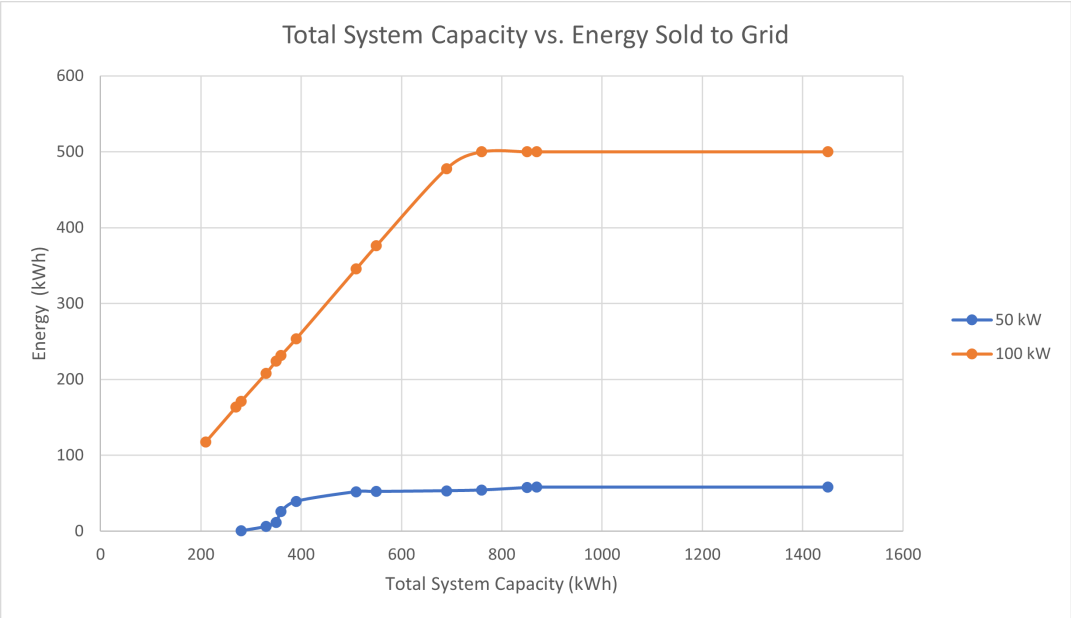

Figure 4.8: Total Energy Capacity of the System vs. the Amount of Energy Sold to the Grid in the Summer Scenario

As shown in Figure 4.8, in the 50 kW grid capacity scenario, the total amount of energy sold to the grid exhibits a direct proportion to the total system capacity until it reaches a plateau. At that point, the sales become limited by the grid capacity. Therefore, a higher grid capacity of 100 kW provides the system with a higher rate of energy arbitrage, with a maximum of 500 kWh, while this value is capped at around 58 kWh for the lower grid capacity scenario. This substantial difference is not only due to the more capacity the system can benefit during peak hours but also the amount of energy that can be bought at off-peak instances. When the energy capacity allocated for the system is limited by the grid capacity, this could be barely enough to compensate for the energy sold to the EVs, as is the case for some configurations in the 50 kW scenario. However, when the system is provided with more flexibility, it can engage in more arbitrage, since the sold energy can be compensated due to the higher grid

capacity.

As a result, with a higher grid capacity, the batteries can be charged and discharged more effectively, resulting in the system storing an adequate level of energy and feeding it back to the grid during the peak demand hours. This feed brings along benefits for the grid as the system can act as an energy source to support the grid, especially in instances where local congestion takes place. Once more, when renewable electricity is abundant, the system paves the way for enhanced integration, acting as an energy buffer.

On the other hand, this higher grid capacity also causes the system to rely on the grid more. As the system is free to draw higher power, it also acts like another source that has to be fed by the generated electricity. This reliance on the grid becomes much clearer when the amount of energy bought from the grid is compared as shown in Figure 4.9. At their peak values, higher grid capacity results in an overreliance on the grid by 490 kWh more energy purchased.

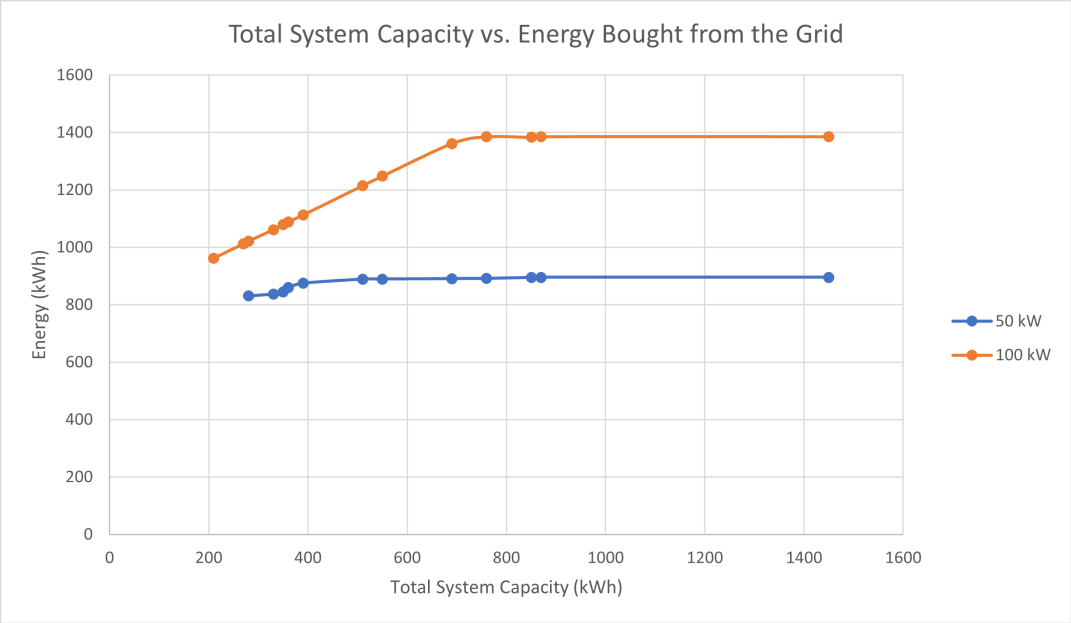

Figure 4.9: Total Energy Capacity of the System vs. the Amount of Energy Bought from the Grid in the Summer Scenario

Even if transactions between the grid and the batteries are mainly controlled by price incentives, and hence the system will avoid buying at the peak demand hours as much as possible, this conflicts with another objective of the mobile charging concept, which is the reduction in peak demand. As the EV charging power is decoupled from the grid, a system with a higher grid capacity has a limited ability of peak power reduction. In this case, 100 kW grid capacity only manages to reduce the peak demand by around 45.9% while 50 kW reduces it by almost 73%. Therefore, using a 50 kW grid capacity reveals more significant benefits in terms of peak demand reduction.

Furthermore, it is also important to note that the excessive use of battery through more charge and discharge cycles have also a considerable effect on the capacity loss. Therefore, heavy use of the batteries exhibited with 100 kW grid capacity also brings notable reductions in the cycle life of the batteries as discussed in detail in Section 4.3.2.

Effect on Daily Profits

Battery capacity and the number of units in the system have a critical effect on the daily profits that can be realised as a consequence of providing charging services to EVs and energy arbitrage. Some factors directly influence the financial benefits of the system. Generally, more battery capacity and more number of units allow the system to act more flexibly and take full advantage of price opportunities observed throughout the day. For example, as the total energy stored is limited by the total capacity of the system, batteries are mainly used to satisfy the charging demand. Therefore, the instances where the batteries buy the energy from the grid are mainly determined by the charging demand. At this point, sometimes the energy could be purchased just to store enough energy to charge the upcoming vehicles,

not because it is very cheap, since the charging demand must be fulfilled under any conditions. This results in a high cost of buying electricity and hence lower profits. As the total capacity of the system increases, the system gains enough flexibility to take full advantage of the low prices. As a result, the average cost of purchasing decreases, improving the profitability of the system in a day. This is shown in Figure 4.10. When the individual battery capacity increases up to 150 kWh with 50 kW grid capacity, then the over-sizing no more influences the daily profits significantly and the earnings reach the plateau of around €425. The main reason behind this is that, after a certain point, the system can take advantage of the cheapest electricity prices with the given grid capacity. After that point, increasing the system capacity no longer improves profitability, since the purchased energy is mainly restricted by the grid capacity.

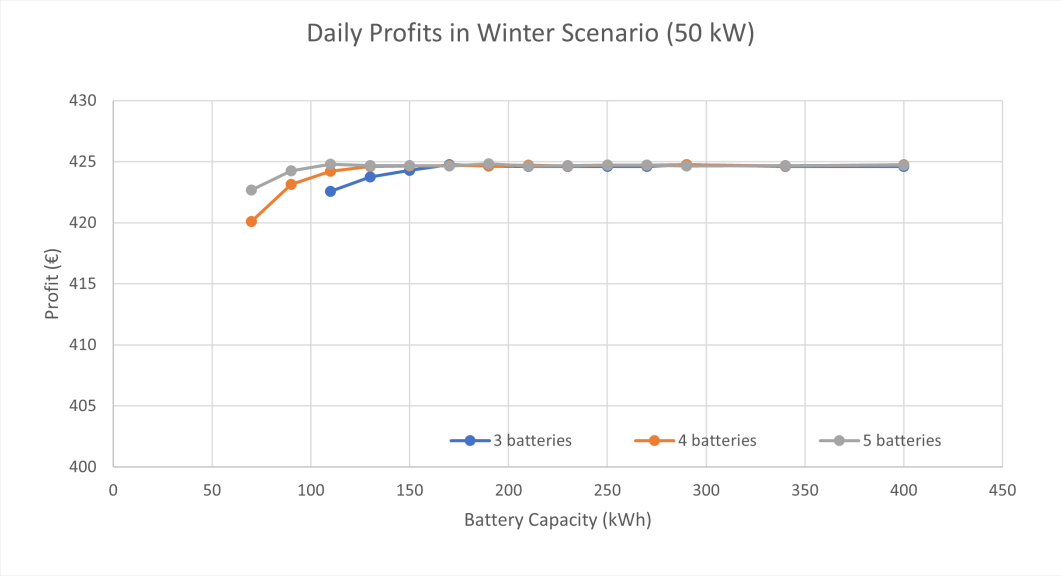

Figure 4.10: Daily Profits Earned in the Winter Scenario Depending on the Number of Batteries and the Battery Capacity with 50 kW Grid Capacity

Daily profits can be further improved by increasing the grid capacity. This increase allows the system to benefit from cheap electricity prices more. As a consequence, the batteries can get charged up with cheaper electricity, bringing along a lower cost of purchasing energy from the grid. Once more, after a certain point, further increasing the size does not increase the profits as the energy that can be bought is primarily limited by the grid capacity. After 250 kWh of battery capacity, the system takes full advantage of the low-price instances up to the margin it is allowed. Hence, the profits reach their maximum limit and reach a plateau of around €437.5. This point can be reached with less individual battery capacity when more units are utilized as can be seen in Figure 4.11. For example, when 5 battery units are utilized, the system reaches the profit plateau of around 170 kWh of battery capacity.

Furthermore, it is important to note that this increase in grid capacity improves the maximum daily profit of the system by almost 3% in the Winter Scenario.

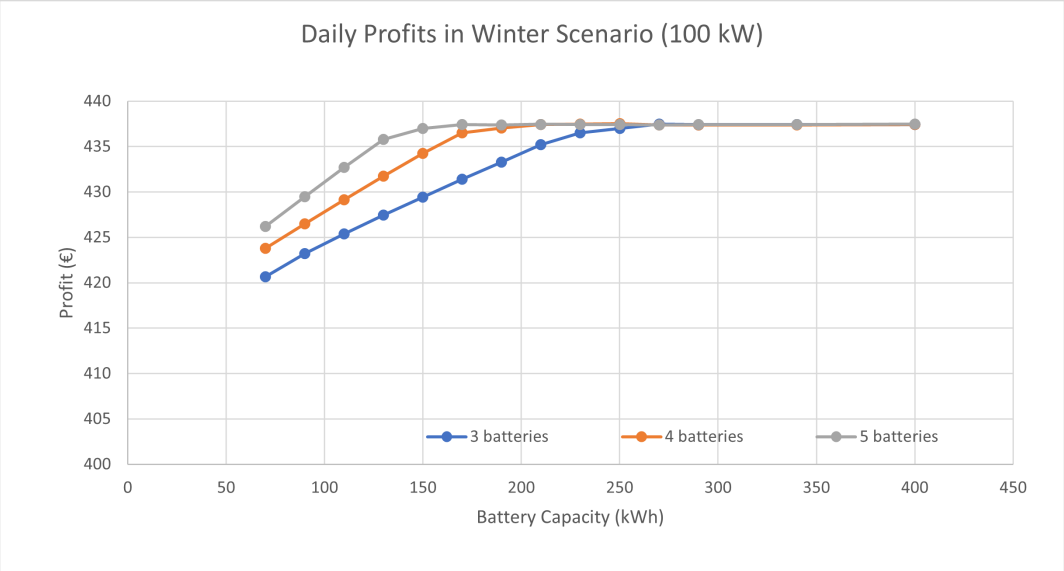

Figure 4.11: Daily Profits Earned in the Winter Scenario Depending on the Number of Batteries and the Battery Capacity with 100 kW Grid Capacity

As mentioned, another important factor influencing the daily profitability of the system is electricity prices. Costs can be reduced by buying at a cheaper rate as well as profits can be improved by engaging in more energy arbitrage. At this point, the Summer Scenario underscores how both factors can enhance the cash inflow of the system. Unlike the Winter Scenario, the system can notably profit from energy arbitrage, due to the higher price gap observed as a consequence of the zero prices. Furthermore, the average daily price observed throughout the day is lower compared to the Winter Scenario. As a consequence of both factors, the system can return a profit of around €490 even with a grid capacity of 50 kW as can be seen in Figure 4.12. Compared to the Winter Scenario with the same grid capacity, this means around 15.3% improvement in daily profitability.

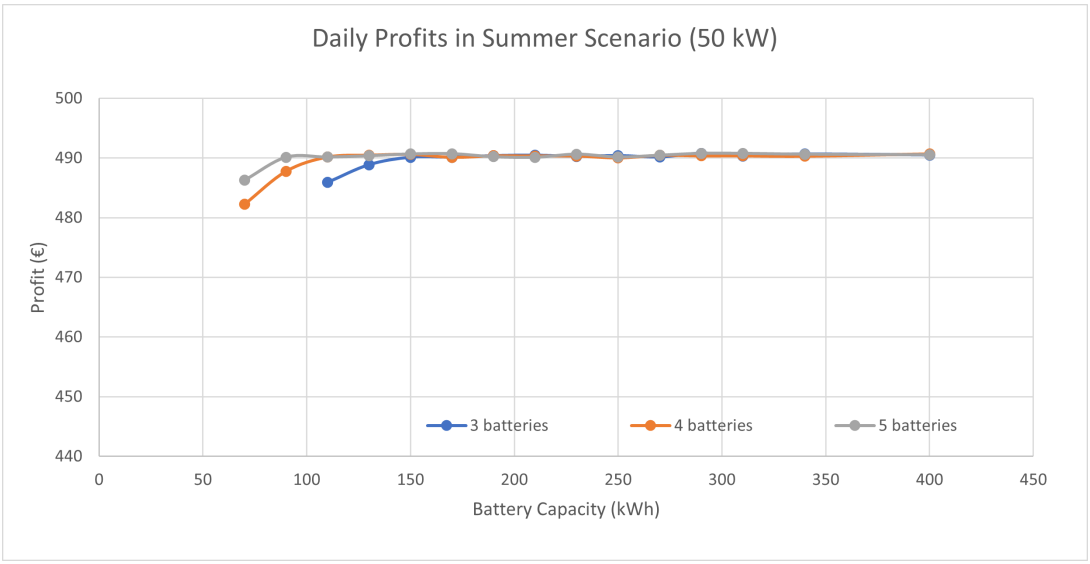

Figure 4.12: Daily Profits Earned in the Summer Scenario Depending on the Number of Batteries and the Battery Capacity with 50 kW Grid Capacity

Moreover, the effect of increasing the grid capacity becomes much more evident in the Summer Scenario. Primarily, higher grid capacity allows the system to sell much higher amount of energy to the grid, and take more advantage of cheap electricity prices triggered by the abundance of renewable generation. As can be shown in Figure 4.13, this brings along a considerably higher maximum daily

profit of around €538. Compared to the 50 kW grid capacity case, this means a 9.7% profitability improvement. Furthermore, when compared to the Winter Scenario with the same grid capacity, it can be concluded that energy arbitrage and the presence of renewable generation can bring along a potential improvement of profitability of around 22.97%.

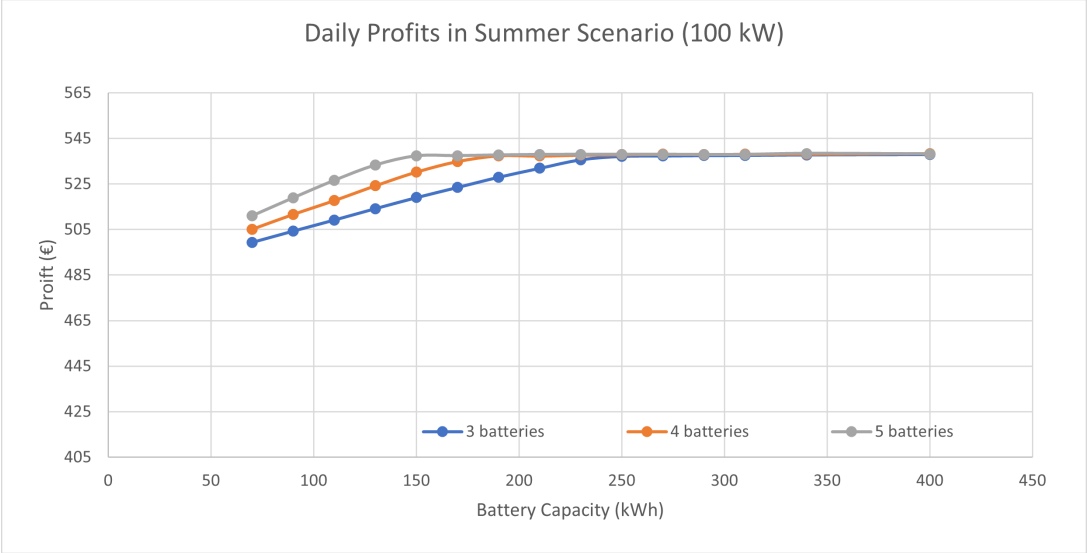

Figure 4.13: Daily Profits Earned in the Summer Scenario Depending on the Number of Batteries and the Battery Capacity with 100 kW Grid Capacity

Effect on Public Space Use

As the system can potentially be deployed to serve the EVs in a public place, the space it occupies has to be analysed and taken into consideration. The occupation of space is mainly due to the area that the units and components take up. The unit's size is mainly determined by the storage capacity as it occupies a significant space due to the Li-ion battery's energy density. Furthermore, as the units will be getting charged from the grid at the hub, the volume of the batteries also affects the size of the hub that will be designated for the service. Lastly, the number of units also proportionally contributes to the area requirement as the total area of the hub should provide a secure space for each unit.

To calculate how much area is required for the system, the volumetric energy density of $LiFePO_4$ batteries is researched. According to the thermodynamics analyses conducted on this type of battery, the theoretical volumetric energy density is calculated as 2107.0 Wh/L [202]. However, it is important to note that there are lots of other components involved in a typical battery pack such as BMS, cooling components and casing, therefore reducing this volumetric density. At this point, it is important to refer to practical packing densities instead of theoretically calculated values to realistically estimate the area required for the system.

In a study focusing on different $LiFePO_4$ batteries used by car manufacturers, the average volumetric pack density of such batteries is reported as 243 Wh/L [164]. Following this, the volume of the battery pack can be calculated as 0.288 m^3 for a 70 kWh battery, while it is 1.646 m^3 for a 400 kWh battery.

At this point, the area requirement is directly proportional to the total overall capacity of the system. On the other hand, more system capacity brings along higher profits due to the flexibility of sales and transactions between the system and the grid. These two factors conflict with each other due to the various interests of different stakeholders.

The total area occupied by the system can be calculated by using the volumetric energy density mentioned, and the dimensions of similar products in the market. A mobile autonomous charging robot with similar specifications has dimensions as 1850 mm length, 950 mm width and 1500 mm height [122]. Using the battery energy density mentioned, it can be calculated that these dimensions allow the placement of a $LiFePO_4$ battery around 640 kWh capacity. Therefore, even in the case with the highest battery capacity considered, 400 kWh, there will be almost 1 m^3 of empty packaging volume, allowing the placement of other components of the system. Taking the length and the width of the

robot as the base, the total area occupied by the units for different battery capacities and the number of batteries can be calculated as 5.27 m^2 for 3 units, 7 m^2 for 4 units and 8.75 m^2 for 5 units.

These values determine the minimum area of the hub and it has to be large enough to accommodate these units while they are not charging EVs. Furthermore, a certain area will be assigned for the charging equipment installed in the hub. As the task fulfilled by this charger is the same as what a typical charging pole does, the land use of this charger can be taken as the same as what is required for a regular EV charging station. Considering the reported land use of 20 m^2 per charging station, and the total area occupied by the units is comparable to that of an EV, the total land use can be taken as the summation of land utilization of a charging station [209]. Therefore, it can be concluded that the hub occupies approximately the area of one charging pole, while a system made up of regular charging poles takes up multiple times larger space, directly proportional to the number of stations. Consequently, the use of a mobile system can also bring along a significant reduction in space use while fulfilling the same charging tasks done by the traditional system.

Effect on Product Life

Product life can be described as the duration it takes to reach the end-of-life point of a critical component in the system. In this case, this duration is mainly described by the capacity fade of the Li-ion battery utilized. The batteries implemented in the system undergo several different cycles while they get charged and discharged throughout the day. Different system parameters have considerable effects on the product life. These parameters can be listed as the number of batteries utilized and the capacity of each battery. They have a direct effect on the total number of cycles the batteries undergo daily, hence have a significant influence on the product life. On the other hand, some parameters have indirect effects on the product life. These parameters can be listed as daily electricity prices and grid capacity. Fundamentally, the combination of these determines the availability of energy arbitrage. Even if these factors do not directly affect the degradation dynamics, they primarily determine how much energy will be exchanged in a day. Therefore, as the price gap and the grid capacity allow more energy arbitrage, the battery material becomes utilized more during the day.

The main factor defining the battery life is how much it is used throughout the day by any means such as getting charged and discharged. Therefore, in a scenario where the price gap is suitable for energy arbitrage, it is expected to see a lower product life due to the higher number of cycles. Otherwise, when the batteries are solely used for charging EVs, the product sustains a longer service life. In this case, grid capacity does not show a significant influence on the service life when it does not effectively limit the amount of energy that can be sold. For example, in the Winter Scenario where the price gap does not give a suitable position for energy arbitrage, the service life changes between 1 and 6 years when 70% capacity retention is marked as the end-of-life point as mentioned in Section 4.1. The use of this point is further elaborated in Section 4.3.3. Battery life plot depending on the battery capacity for different numbers of batteries is plotted in Figure 4.14.

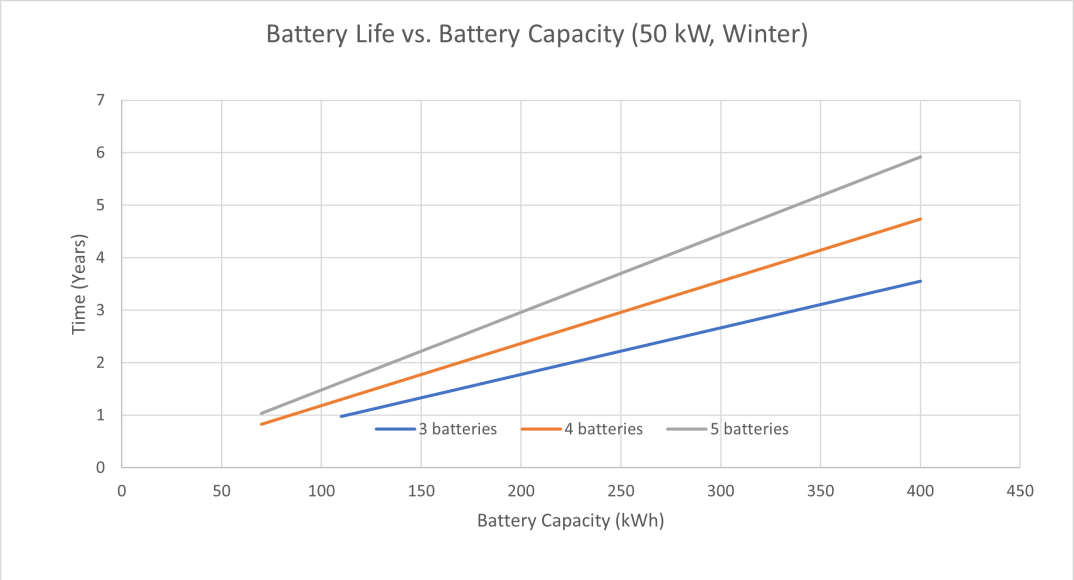

Figure 4.14: Battery Life in the Winter Scenario Depending on the Number of Batteries and the Battery Capacity with 50 kW Grid Capacity

As shown in Figure 4.14, there is a direct correlation between the service life and the battery capacity. A higher capacity brings along less cycling and more material to be degraded, therefore a longer service life. Not surprisingly, implementing more batteries in the system allows the load to be shared among different units and further increases the product life. As mentioned, due to the lack of profitable buy and sell positions, no effective energy arbitrage is observed in this price scenario. Therefore, further increasing the grid capacity does not exhibit a considerable influence on the service life. For comparison, the battery life plot with 100 kW grid capacity is shown in Figure 4.15.

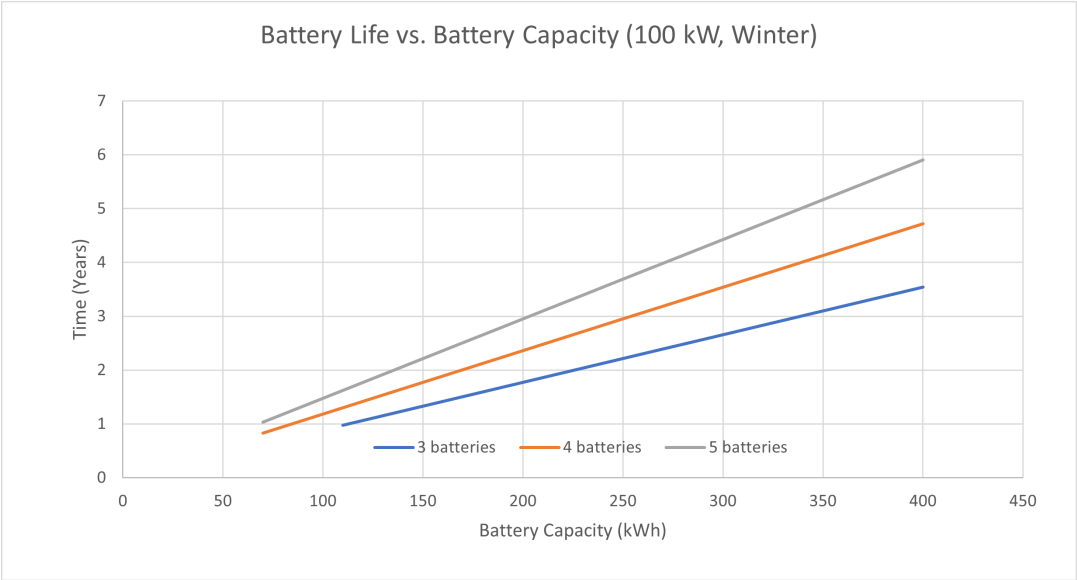

Figure 4.15: Battery Life in the Winter Scenario Depending on the Number of Batteries and the Battery Capacity with 100 kW Grid Capacity

As shown in Figure 4.14 and 4.15, increasing the grid capacity does not affect the service life considerably since the batteries are only used for charging EVs in the Winter Scenario. Therefore, it can be concluded that the service life of the batteries changes between around 1 and 6 years when they are only used for EV charging. The higher end of this interval is reached by using 5 batteries in the system with a large size of 400 kWh. Even if this decision seems like the best one to sustain a

higher battery life, it is also important to note the costs associated with the size of the system, as well as the public space occupation.

On the other hand, the summer prices allow the system to engage in energy arbitrage due to the presence of zero prices. In this case, as the battery goes under more cycles, more capacity loss occurs over time. This is simply because batteries are not only used for charging EVs but also to sell electricity to the grid during peak demand hours to yield more. When the battery is also used in this way to increase daily profits, a shorter battery life is experienced. A corresponding plot for the Summer Scenario with 50 kW grid capacity is found in Figure 4.16.

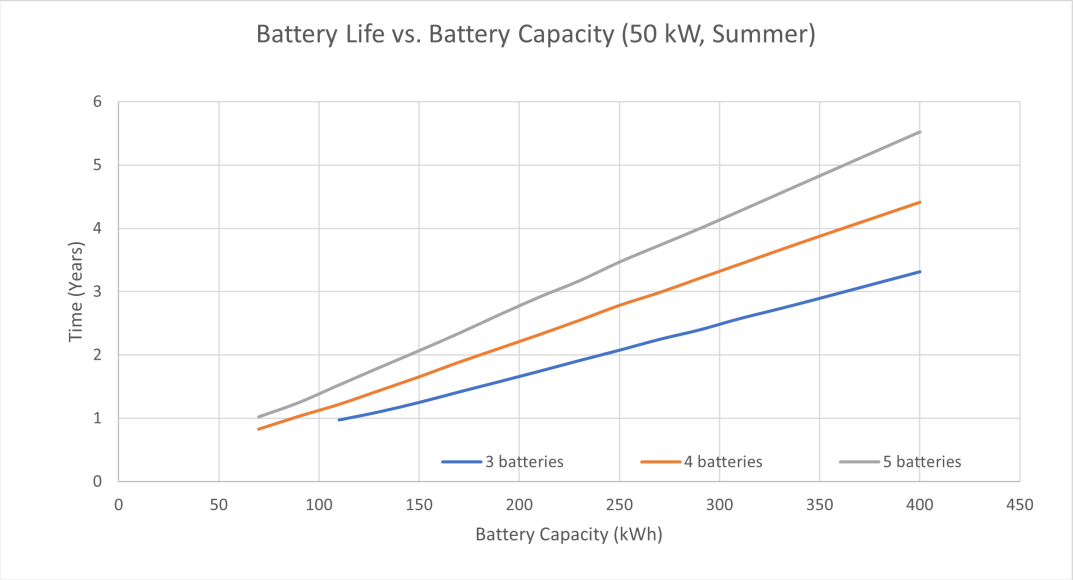

Figure 4.16: Battery Life in the Summer Scenario Depending on the Number of Batteries and the Battery Capacity with 50 kW Grid Capacity

As shown in Figure 4.16, a slightly shorter battery life is exhibited in this case. It is important to note that, the exchange between the grid and the system is primarily limited by the grid capacity in this scenario. Therefore, it is expected to see even shorter product life when the system is allowed to demand from or feed to the grid more. Even if it increases the daily profits, this brings along a significant reduction in the years the system retains an adequate SoH. For example, battery life corresponding to the Summer Scenario with 100 kW grid capacity is plotted in Figure 4.17.

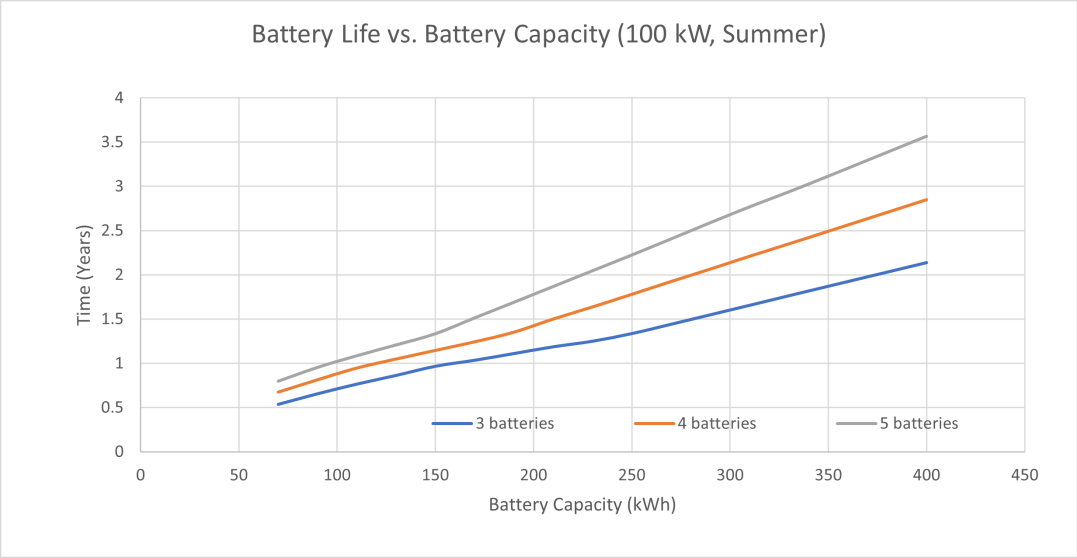

Figure 4.17: Battery Life in the Summer Scenario Depending on the Number of Batteries and the Battery Capacity with 100 kW Grid Capacity

As shown in Figure 4.17, this case presents the shortest battery life due to the large amount of daily energy exchange between the system and the grid. At first glance, this enhanced exchange can be very advantageous in terms of cash inflow, as the daily profit reaches up to around €538 as can be seen from the previously shown plot in Figure 4.13. However, using the battery material at this high rate also causes a significant reduction in the period in which the units can be used seamlessly. As a consequence, even with the maximum system size of 5 batteries with 400 kWh capacity, the units can maintain an adequate SoH for around 3.5 years. This duration is remarkably shorter when compared to the scenarios where the units are mostly used for charging EVs, with limited engagement in energy arbitrage.

4.3.3. Battery Degradation

To address the costs and benefits associated with energy trade activities between a battery and the grid, it is essential to analyse how much the arbitrage damages the storage material. Due to the nature, materials and chemistry of Li-ion batteries, a considerable loss in the overall capacity is observed over time. This loss is affected by lots of different parameters such as the C-rate, temperature conditions, and DoD of the battery. Furthermore, the purchase price of the batteries and the daily energy prices also significantly influence the feasibility of energy arbitrage, as the overall profitability depends on comparing the daily price difference with the monetary expression of battery degradation. When factoring in the cost of battery degradation from discharging and then charging later to compensate for the sold energy, if this cost exceeds the price difference between buying and selling energy throughout the day, energy arbitrage becomes a viable option. This ultimately boosts the system's daily profit. Otherwise, the system sacrifices a certain amount of capacity per transaction, which is meant to be bought to profit, at the expense of a return, which is not enough to compensate for the ageing.

Linear Degradation Model

As mentioned, Li-ion battery degradation is dependent on different factors. These factors result in primarily three different modes of degradation in terms of material loss. First, lithium ions can be lost over time due to the parasitic reactions as a consequence of solid electrolyte interphase growth, planing or decomposition. As those ions are lost over the composition of the mentioned structures, they will no longer be available to cycle, resulting in a reduction in the battery capacity [20]. Furthermore, a portion of active material used in the composition of anode and cathode can also be faded over time. Particle cracking and decline in electrical contact can be listed among the primary causes of this phenomenon [20].

As these loss mechanisms exhibit highly nonlinear and multidimensional behaviour, affected by many different conditions, there is extensive research in the literature, deriving degradation models,

testing batteries and analysing how much capacity is lost over time [74], [148], [22], [79]. These studies and their findings under different C-Rate conditions are given in Table 4.3.

Study	C-Rate	Capacity Loss (kWh/kWh)
[74]	0.08C	0.00015
[148]	0.45C	0.000134
[22]	1C , 3C	0.0002 , 0.00023
[79]	4C , 0.5C	0.00013 , 0.0001

Table 4.3: Summary of Battery Studies

In the designed system, the battery undergoes two different charging and discharging operations, exhibiting different maximum power ratings and C-rates. One regards the exchange between the battery and the grid, while the other considers the charging operation of EVs. Comparing these two different operation modes, the maximum power is observed while the battery is used for charging an EV, with a maximum of 175 kW of power. Because this power is drawn by one of the popular models like the Tesla Model 3, the probability and frequency of achieving this high C-rate further increase [72]. On the other hand, it is also important to note that this power rating is observed only for a short amount of period. Figure 4.18 shows the charging profile for the corresponding model. The profile demonstrates this high charging power is only drawn at SoC levels around 10% and gradually drops as the EV gets further charged.

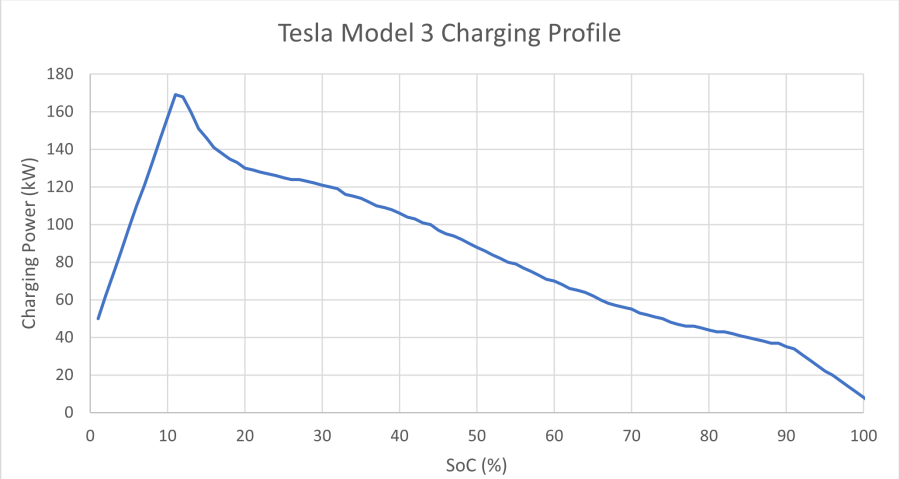

Figure 4.18: Tesla Model 3 Charging Profile
[72]

According to the results, this discharging power requires the battery to operate at a maximum C-rate between 1 and 0.5, when a battery capacity between 175 and 350 kWh is used to maximise the profits while also considering the investment cost. Assuming an ideal temperature management system will be implemented in the system, these rates correspond to a degradation value larger than 0.00015 kWh/kWh and lower than 0.0002 kWh/kWh, according to the results given in Table 4.3. Even if this C-rate will not be observed continuously throughout the battery's operational life, the frequency of this discharge rate primarily depends on how frequently EV models with relatively higher power utilize the charging service. As a consequence, a degradation rate of 0.000175 kWh, per charged and discharged kWh of energy is assumed in the study.

Following this degradation rate, the cost of capacity loss to be used in the optimization problem can be represented as a function of battery price when combined with the price function given in Equation 4.1. The resulting function is shown in Equation 4.25.

$$L(Q) = 0.000175 \cdot \frac{(170.69 \cdot Q + 175.37)}{Q} \$/kWh \tag{4.25}$$

Empirical Degradation Model

As introduced, battery degradation can be represented as a function of various factors such as the C-rate, thermal maintenance and cycling behaviour. In fact, it is difficult to express the rate of capacity fading with simple equations. There is extensive research going on to test the batteries under different conditions and reproduce representative equations to model the loss mechanisms. As a linear approximation of capacity loss is a simplified approach and the degradation is often far from exhibiting linear behaviour, the accuracy of this approximation has to be investigated to verify the trustability of the results.

To achieve the verification, an empirical battery model is taken into consideration and the results of both estimations are compared. The empirical model identifies two different ageing mechanisms such as cycling and calendar aging. Cycling ageing regards the loss of capacity while the battery is getting charged and discharged while calendar ageing considers the capacity fading during the idle operation where the battery stores the energy without any exchange [177], [178]. An extensive study develops an empirical model whose accuracy is also tested and verified. The empirical equation developed by the mentioned study to calculate calendar ageing, C_{cal}, is given in Equation 4.26 while cycling ageing, C_{cyc}, is given in Equation 4.27 [178].

$$C_{\text{cal}} = 0.1723 \cdot e^{0.007388 \cdot \text{SoC}} \cdot t^{0.8} \tag{4.26}$$

$$C_{\text{cyc}} = 0.021 \cdot e^{-0.01943 \cdot \text{SoC}_{\text{avg}}} \cdot \text{cd}^{0.7612} \cdot \text{nc}^{0.5} \tag{4.27}$$

In Equation 4.26, SoC represents the level where the constant idling is observed while t is the duration. On the other hand, in Equation 4.27, SoC_{avg} represents the average SoC of the battery cycle, while nc is the number of cycles and cd denotes the depth of the corresponding cycle.

Furthermore, calendar ageing calculation is neglected in the calculations. There are two reasons for that. First, calendar ageing becomes significant for systems where the idling periods are much more frequent than charging or discharging periods while it is not the case for the studied charging system [108]. Second, the time unit in Equation 4.26 is months while the idling behaviour only occurs in the scale of minutes in the system. In addition, the linear degradation models consider tests where the battery is exposed to charging and discharging cycles under a constant C-rate. Therefore, calendar ageing is not also relevant for these models. Combining all of these, calendar ageing is found negligible and therefore excluded from the battery life calculations. Moreover, to calculate the capacity fading related to cycling, the output SoC curve of the batteries, taken from the optimization model is plugged into the equations, to check if the linear and empirical models return similar results. The degradation of battery cycling capacity arises from numerous cycles, each presenting varied characteristics in terms of cd and SoC_{avg}. To plug in the required terms indicated in the equations, and express the SoC behaviour in terms of cycles, Rainflow Counting Algorithm is used. The Rainflow Counting Algorithm operates by analyzing the state of charge (SoC) profile of the battery. It begins by detecting all the local extreme points within the profile, then proceeds to establish the cycle depth and average state of charge [167]. The algorithm exemplifies its functionality by extracting local extreme points from the SoC profile, which are subsequently utilized to identify either full or half cycles [167]. Battery degradation can be conceptualized as a material fatigue phenomenon rooted in stress cycles. Therefore, the rainflow algorithm stands out as a widely used method for identifying cycles within material fatigue processes and has seen widespread application in assessing battery degradation [167]. To calculate the terms to plug into the empirical equations, a PyPi package named Rainflow 3.2.0 is utilized [154].

To compare the results obtained from two estimation methods, SoC data of different scenarios is tested for comparison. For example, SoC data corresponding to 3 batteries with 210 kWh capacity and 50 kW grid capacity on a summer day is shown in Figure 4.19

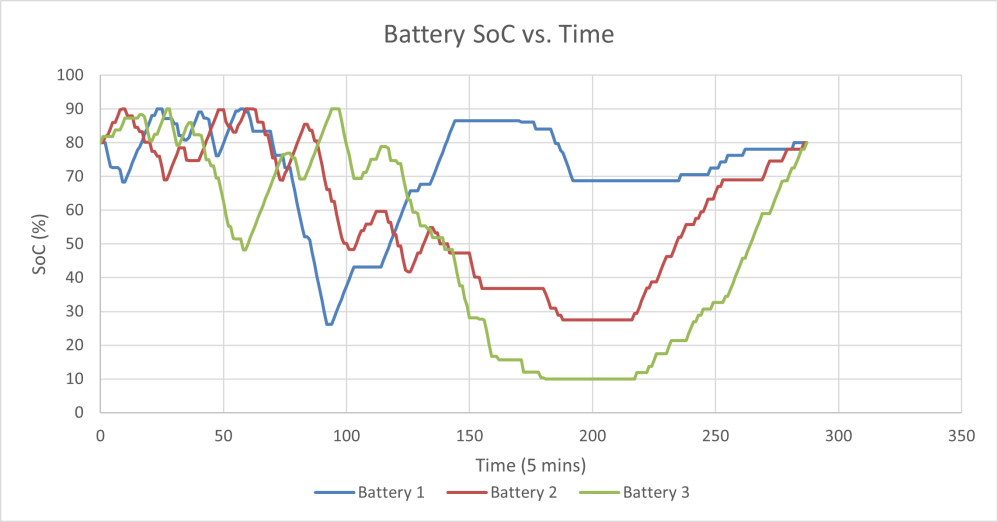

Figure 4.19: State of Charge Data Corresponding to the Scenario with 3 Batteries, 210 kWh capacity and 50 kW Grid Capacity in Summer

End of life point of the battery is mainly determined by the period it takes to retire the equipment. 70% of SoH can be accepted as the end-of-life point as this is often expressed as the lowest limit of acceptance in the second life market in the literature [87], [24], [149]. It is also advantageous for the business to keep using the purchased material as much as possible to postpone the replacement process. Furthermore, regarding the fact that the batteries are cycled with an 80% DoD to limit the fast degradation, 20% of the original capacity becomes unused. Moreover, as the system's overall size increases, it is observed that some batteries do not even use the entire 80%, as shown by the cycling behaviour of Battery #1 and #2 in Figure 4.19, using almost 60% DoD. As a consequence of this limited use of battery material, it can be concluded that a 30% fade in the overall capacity can still sustain the same charging and discharging sequence and hence the same amount of profits. Lastly, this argument can also be verified by choosing a size of at least 30% larger than the point where the daily profits reach the plateau as shown in Figures 4.10, 4.11, 4.12 and 4.13. This selection ensures even if the batteries lose 30% of their initial capacities, they can still return the maximum amount of profits which can be achieved in a day under given conditions.

When 70% capacity retention is marked as the end-of-life point, overall product life under both estimations is calculated. It is also important to note that the degradation rates are averaged bearing in mind that the batteries can switch the tasks in a daily sequence. For example, the cycles that Battery #1 undergoes in a day can be handed over to Battery #2 the day after. In this way, a homogeneous degradation can be realised within the batteries, preventing a situation where one battery is heavily used while others still sustain relatively higher SoH. As a result, the linear model returns 1.74 years of product life until the point the batteries lose 30% of their capacities, while the empirical model returns it as 1.71. When the results obtained from the two models are compared, the relative difference is found to be 1.75%. Therefore, it can be concluded that the simplification by using linear estimation does not influence the result considerably.

4.4. Comparative Financial Assessment

The results obtained from the optimization model should be processed further in order to assess the mobile system's financial performance and compare it to that of regular charging poles. This gives valuable insights into how attractive the solution is from the investors' perspective as well as how to choose an effective system size. The costs associated with the individual systems are calculated and compared, while also evaluating how much return can the systems yield. As a consequence, an evaluation metric is utilized to highlight an ideal system size and configuration. This metric considers the total amount of profits, investment costs, and the period it takes to earn that yield. As the total profits the system can return are mainly dependent on the battery life, this metric inherently considers the degradation, as well.

4.4.1. Investment Cost

The amount of money that has to be invested in the system plays a critical role in attracting capital as well as in setting a financially feasible and competitive investment plan compared to the charging poles. As the considered mobile charging system can be developed in two different system configurations, consisting of built-in or switchable batteries, the investment cost differs for each layout. To calculate a realistic investment cost, the main components of the individual configurations have to be investigated, as they have a direct effect on the amount of money that has to be invested.

Built-in Battery Configuration

Built-in battery configuration requires a heavy-duty robotic platform to carry onboard equipment. These platforms support flexibility as they accommodate integrated sensors for autonomous operation, as well as chassis and wheels suitable for heavy loads. Furthermore, a battery to fulfil the tasks is necessary. To facilitate the desired operation, a DC/AC converter should be implemented to drive the motor as well as a state-of-the-art charger which is primarily a DC/DC converter to charge the vehicles with high power. Lastly, a robotic arm is necessary to realise the docking to the EV inlet, or the bridge connector that can be located in the pavement. The general layout of the introduced configuration is shown in Figure 4.20.

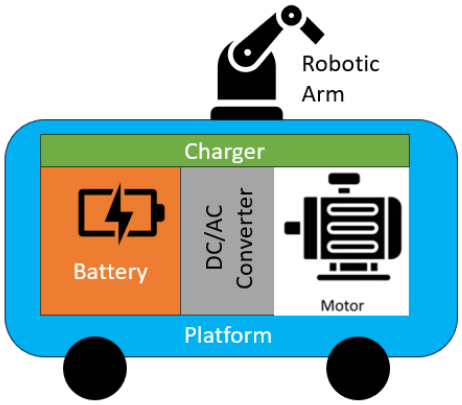

Figure 4.20: General Layout of the Built-in Battery Configuration

Switchable Battery Configuration

Switchable battery configuration consists of two separate platforms, one for carrying the battery on board and another for mobilizing it. The first one is almost the same as the one introduced in Built-in Configuration, except for the absence of the motor, DC/AC converter and robotic arm. These components are parts of the carrier robot as it is responsible for towing the battery platform to the designated parking lot or the hub. To realise the stand-alone operation of the carrier robot, a small battery has to be installed, while the energy required for the travel can be sourced by the larger battery in other cases. The general layout of this configuration is illustrated in Figure 2.14.

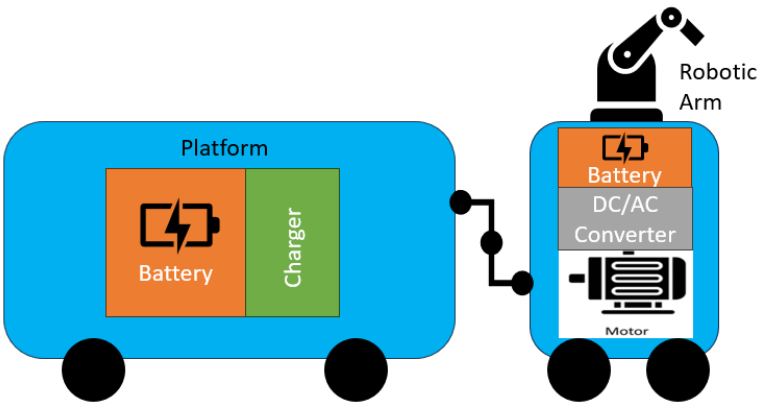

Figure 4.21: General Layout of the Switchable Battery Configuration

Another alternative docking mechanism can also be realised by using a much larger carrier robot platform and attaching or detaching the main battery on it as introduced in Section 2.2 and shown in Figure 2.14 [16]. This requires the batteries to be stored on shelves or designated spaces in the hub. However in this case an autonomous robotic mechanism is required to detach the battery from the robot and lift it to the charging port in the hub. Considering how heavy the batteries are an advanced mechanism which can control heavy loads precisely is necessary. Consequently, this further increases the money that has to be invested in the system. On the other hand, a quick-release mechanism can do the task requiring a much lower investment, acting as a dock to couple the carrier and the main battery while still facilitating the use of large batteries. In this way, the down times can also be minimised due to the easiness of the switching operation. For these reasons, a switchable configuration where this quick-release mechanism is studied instead of the one with battery shelves.

Total Cost of Mobile Charging System

The total cost of the system differs for each configuration as the number of units and components vary for the built-in and switchable battery layouts. As a consequence of market research, the prices of the components with the required specifications are found. They are listed in the following Bill of Materials Table 4.4. $LiFePO_4$ battery prices differ for battery capacity and therefore can be derived depending on battery capacity using the price function in Equation 4.1.

Table 4.4: Bill of Materials for Built-in and Switchable Battery Configurations

Built-in Battery Configuration		
Unit Type	**Component Name**	**Cost**
Main Unit	$LiFePO_4$ Battery	See 4.6
	DC/AC Converter	$321
	Motor	$200
	Heavy Duty Robot Platform	$10,000
	Robotic Arm	$30,000
	Onboard Charger	$11,600
Switchable Battery Configuration		
Unit Type	**Component Name**	**Cost**
Battery Unit	$LiFePO_4$ Battery	See 4.6
	Heavy Duty Robot Platform	$10,000
	Onboard Charger	$11,600
Carrier Unit	$LiFePO_4$ Battery (10 kWh)	$1,882
	Lighter Duty Robot Platform	$3,500
	Motor	$200
	DC/AC Converter	$321
	Robotic Arm	$30,000

Following the costs given in Table 4.4, the total cost function for each system is derived as a function

of the battery capacity, Q, and the number of units, N. For built-in configuration, the total cost of the system can be calculated as shown in Equation 4.28.

$$C_{built-in}(Q, N) = (52,121 + 170.69 \cdot Q + 175.37) \cdot N \tag{4.28}$$

On the other hand, the total cost function for the switchable configuration can be expressed as a function of the battery capacity, Q, the number of battery units, N_b and carrier units, N_c. The function is shown in Equation 4.29

$$C_{switchable}(Q, N_c, N_b) = (35,903 \cdot N_c) + (21,600 + 170.69 \cdot Q + 175.37) \cdot N_b \tag{4.29}$$

To verify the accuracy of price estimation, some example pricing approaches followed in the literature are evaluated. In particular, it is found that when a built-in configuration is used, some studies point out an investment cost of $55,000, excluding the battery cost [111]. Meanwhile, the pricing scheme in Table 4.4 and the consequent cost function in Equation 4.28 calculate an investment cost of $52,121. Furthermore, the same study estimates a full unit cost of $100,000 for 225 kWh storage, while the cost function calculates it as $90,701 [111]. As a result, it can be concluded that the cost function returns close values when compared to the values in the literature, but this cost is lower. At this point, it is expected because the study was conducted in 2019, hence regards higher component costs. Fundamentally, this difference is a result of economies of scale, due to the increase in supply and demand for batteries and semiconductor materials, triggering a price drop over the years. It is also important to note that the same study does not take into account the difference in price per kWh with increasing capacity and rather accepts a constant cost, which does not change with the capacity.

Moreover, additional costs are also associated with the equipment utilized in the hub, allowing the bidirectional flow of energy. In this case, it is necessary to use a conversion topology functioning bidirectionally to charge the batteries and feed the energy back to the grid when required. As a consequence of market research, it is found that bidirectional EV fast chargers allowing V2G functionality can be used for the task. These chargers couple with the grid to be fed by AC from the network side and carry out a rectification process to charge the EV with DC electricity. In case an opposite flow takes place, the implemented topology converts DC to AC to sell to the grid. Furthermore, this kind of converter also includes galvanic isolation to ensure safety. It is further reported that these converters can be used as aggregates in parallel to build up higher power varying between 5 kW and 200 kW. Following this, the hardware cost associated with the battery chargers can be calculated as $11,925 for 50 kW and $23,850 for 100 kW configurations. It is also important to note that 100 kW infrastructure may also require additional costs due to the necessity of a more advanced transformer as mentioned in Section 4.4.1. Installation costs are also a part of the investment scheme. However, as the operation taking place in the hub is similar to what happens in a regular charging station, installation costs associated with charging poles can be taken as a reference to estimate the installation cost of the hub. As Level 2 charging infrastructure mainly covers power ratings up to around 20 kW, the installation cost of 50 kW infrastructure can be considered higher than what is required for this type of station [83]. Furthermore, as this power rating is close to what is offered by Level 1 DC charging infrastructure in SAE Standard, the cost value can be taken as an expenditure close to the lower limit of the intervals introduced in Section 4.4.1, $10,000 [140], [83]. When this value is taken, it is concluded that the total cost associated with the charging system in the hub falls within the cost intervals reported in the literature [140], [39]. This installation cost can be taken as $37,500 for 100 kW grid capacity, as the rating falls within what is provided by the DC fast charging stations. It is important to note that this value is the average installation cost value used for DC charging poles in Section 4.4.1. Following the costs given, the sum of hardware and installation costs can be calculated for 50 kW and 100 kW grid capacity as $21,925 and $61,350, respectively.

Total Cost of Regular Charging Poles

To compare the investment costs related to the mobile charging system with charging poles, different price data are analysed. It is further acknowledged that the costs associated with instalment of a charging pole mainly consist of equipment costs, installation costs and area costs. A study assumes a fast charging station cost of $163,000, with a land use cost of $407\$/\text{m}^2$. Furthermore, it is reported that installing the charging station requires 20 m^2 land area, and purchasing the parking lot costs $23,500. The study further emphasizes a distribution line cost of 120 $/(kVA km), and a substation expansion cost of 788 $/kVA [209].

Furthermore, another study underscores a DC charger hardware cost of $32,023 and an AC charger cost of $6,404–9,607, considering only the equipment costs [184].

Another study presents an acquisition cost for the EV charging station of a minimum of $14,000 and a maximum of $91,000 with an average of $52,500 for DC fast chargers [39].

In addition, the International Council On Clean Transportation calculates the costs associated with installing charging stations in the United States. The hardware costs stated in the report differ for charging station type. In detail, it highlights $3,127 for an AC Level 2 charging station, $28,401 for a 50 kW and $75,000 for a 150 kW DC charging station. Furthermore, it announces an average of $3,492 of the installation cost for Level 2 charging stations, $45,506 for 50 kW and $47,781 for 150 kW DC charging stations [141].

Lastly, the U.S. Department of Energy remarks a hardware cost between $400 and $6,500 for Level 2 AC chargers and $10,000 to $40,000 for DC fast chargers. The report further mentions installment costs between $600 - $12,700 for Level 2 chargers, and $4,000-51,000 for DC fast chargers [140].

To verify the findings, market research is also conducted. As a result, it is concluded that hardware costs are between $1,950 and $3,000 for a Level 2 charger and $40,000 and $100,000 for a DC fast charger. Additionally, around $6,000 installation costs for Level 2 and $15,000 to $60,000 can be reported for fast chargers, depending on the transformer requirement. As a consequence, costs associated with AC and DC charging stations, C_{AC} and C_{DC}, in terms of hardware costs, C_H, and instalment costs C_I, can be calculated as shown in Equation 4.30 and 4.31 as a function of the number of stations, N_{AC} and N_{DC}, by taking the average values.

$$C_{AC}(N_{AC}) = (C_{H_{AC}} + C_{I_{AC}}) \cdot N_{AC} = 8475 \cdot N_{AC} \tag{4.30}$$

$$C_{DC}(N_{DC}) = (C_{H_{DC}} + C_{I_{DC}}) \cdot N_{DC} = 107500 \cdot N_{DC} \tag{4.31}$$

4.4.2. Profitability Analysis

This section analyses the profitability of systems made up of mobile charging robots and regular charging poles to assess the financial viability of the system. It mainly evaluates the system by using financial metrics to question its attractiveness from the investors' perspective.

Profits of the Charging Poles

Regular charging poles act as a bridge between EVs and the grid, buying the energy instantaneously from the grid to sell it to drivers. In this case, as they lack an effective storage system which can be charged up with cheap electricity during low demand to reduce the purchase costs, its profitability per transaction also depends on the arrival time of a vehicle. If it conducts a charging operation at peak demand hours when the electricity prices are much higher, then the system earns less from a charging process. Therefore, the daily profit of the system is mainly the charging revenues subtracted from the purchase costs. In this case, the system's profits, revenues and costs corresponding to different price scenarios are given in Table 4.5. In detail, it is found that the current rates offered for AC and DC charging in the Netherlands are 0.4 €/kWh and 0.69 €/kWh according to two popular service providers, respectively [193],[75]. When these rates and given electricity prices in each different scenario are applied to the charging load data, the profitability of the system is calculated and shown in Table 4.5.

Table 4.5: Comparison and Breakdown of Charging Station Revenues

Scenario	Revenue of Charging (€)	Cost of Electricity (€)	Daily Profit (€)	Yearly Profit (€)
Winter	345.18	67.99	277.19	101,174.35
Summer	345.18	7.8	337.38	123,143.7
Extreme	345.18	192.99	152.19	55,549.35

Profits of the Mobile System

When a mobile charging system is offered to the drivers, it is assumed that the pricing of the service should not be as low as a standard AC charging rate due to improved convenience, higher investment in the system and faster charging. However, to realise a competitive business, the system could offer the service for a cheaper rate than some of the comparable services, such as DC charging, to attract

customers. Therefore, asking for a rate of 0.65€/kWh could pull the drivers who generally use AC charging outside due to the ease of use and convenience of the system and DC chargers as a consequence of the possibility of achieving the same charging speed in a more user-friendly and cheaper way. It is important to note that this rate is also equal to the price asked by one of the largest charging network operators in Europe, and 13.3% cheaper than the average cost of DC recharging in the Netherlands announced by European Alternative Fuels Observatory [11], [55]. In this case, revenues coming from charging EVs, and selling electricity to the grid as well as the cost of purchasing electricity from the grid are shown in Table 4.6 for each electricity price and grid capacity scenario.

Table 4.6: Comparison and Breakdown of Mobile System Revenues for Different Grid Capacities

Scenario	50 kW Grid Capacity			100 kW Grid Capacity		
	Revenue of Charging (€)	Revenue of Energy Arbitrage (€)	Cost of Electricity (€)	Revenue of Charging (€)	Revenue of Energy Arbitrage	Cost of Electricity (€)
Winter	486.67	0.19	62.25	486.67	0.39	49.65
Summer	486.67	6.25	2.45	486.67	51.86	0.86
Extreme	486.67	1.45	225.3	486.67	130.69	290.35

According to the results shown in Table 4.6, it can be concluded that the cost of purchasing electricity is the lowest in the Summer Scenario, due to the abundance of cheap electricity. Furthermore, it can be noted that this cost is reduced even further when a higher grid capacity of 100 kW is used due to the increased flexibility of buying. Similarly, the effect of flexibility is also evident in the revenue values earned by energy arbitrage. As the system is allowed to buy cheap and sell expensive energy, the return of energy arbitrage increases significantly. Especially in the Summer Scenario, where the price gap exhibits lots of profitable positions for energy arbitrage, the system can return 7.29 times more revenue only regarding the sales to the grid. However, it is also important to remember that it only improves the daily profit by 9.7% as the main revenue source of the system is charging EVs, as discussed in Section 4.3.2. Processing the revenue and cost values shown in Table 4.6, daily and yearly profits of the scenarios can be calculated. Results are shown in Table 4.7.

Table 4.7: Comparison and Breakdown of Mobile System Profits for Different Grid Capacities

Scenario	50 kW Grid Capacity		100 kW Grid Capacity	
	Daily Profit (€)	Yearly Profit (€)	Daily Profit (€)	Yearly Profit (€)
Winter	424.61	154,982.65	437.41	159,654.65
Summer	490.47	179,021.55	537.67	196,249.55
Extreme	262.82	95,929.3	327.01	119,358.65

As can be seen in Table 4.7, mobile charging systems can yield significant profits. Especially compared to the profits earned by regular charging poles, listed in Table 4.5, yearly profit improvement of 45.4%-59.36% in Summer, 53.2%-57.8% in Winter can be achieved depending on the grid capacity the system is allowed to benefit from. Lastly, despite expensive electricity prices, the system can still obtain higher profits compared to the charging poles in the extreme scenario. In this scenario, profits are lowest because of higher average electricity prices and more frequent overlaps between costly price periods and times when the system charges for the next day's operation. However, the mobile system's advantage in daily profits can be maintained, even with significantly higher electricity prices and volatility.

4.4.3. Investment Decision

When the results of both systems are evaluated, an investment decision can be made. This conclusion should consider how much profit the system can make in each scenario, the amount of money that has to be invested in the system to realise this profit, and how many years the system will sustain this return before the batteries reach their end-of-life points. Regarding those parameters, various financial

evaluation metrics can judge the system's performance, such as Net Present Value and Return on Investment. However, when these parameters are used, it is concluded that the final result will be very biased on the product life. As the life of the batteries continuously increases as the system's size increases, as shown in Figures 4.14, 4.15, 4.16, 4.17, the net present value and return on investment values also continuously increase because the batteries have more years ahead to sustain profits. However, it is also observed that, after a certain point, increasing the size of the system does not improve the daily profits. Therefore, after that point, further increasing the capacity is oversizing the system only to increase the battery life. At first glance, this looks like an advantageous way to deploy a system to realise the longest amount of time horizon to return steady profits. However, a critical point emerges related to this decision. First, it should be noted that oversizing the system brings about a much higher initial investment. This higher investment results in a long-living system with solid profits, therefore increasing the total amount of money that will be earned until the batteries wear out. On the other hand, it also results in a longer investment horizon, decreasing the return on investment per year. Therefore, not only the total amount of profits and investment costs but also the period it takes to earn the invested amount has to be taken into consideration. In this case, the period can be taken as a fixed period, such as a year, to evaluate the portion of the investment the system will return in that time. This way helps investors compare the efficiency of different investments and understand how quickly they are earning returns relative to the time invested.

The investment cost of the system consisting of regular charging poles can be calculated by the cost function given in Equation 4.30 and 4.31. Utilizing the functions, for a system consisting of 14 AC charging poles and 2 DC charging poles, the total investment cost can be calculated as $333,650, considering the hardware and installation costs.

For the mobile system with built-in batteries, the calculation of the investment cost is also straightforward by using the cost function given in Equation 4.28. In this case, the number of units is the number of robots with installed batteries. However, this investment cost can be further reduced by realising a switchable system. In this case, the number of battery units is the same as that input for the built-in system. However, the number of carrier units can be less than the number of battery units. As the carrier units are only used to pick up the batteries when they are in a stationary position and take them to the next duty location, the number of carriers should not necessarily be equal to the number of batteries. In fact, it might be possible to manage 3 batteries with only 2 carrier units, which could bring a significant reduction in the investment cost while the system can maintain the same amount of profits. At this time, the question becomes how many batteries travel around the parking place at a time. After this, when one carrier unit per battery is implemented in the system, how effectively will robots be used? If the frequency of the instances where all of the batteries are travelling is rather low, that points out an ineffective use of robots and an overbought number of carrier units. Therefore, the number of robots can be further reduced to decrease the total investment in the system with minimal or no reduction in daily profits.

In order to address this question, travelling times in every scenario are evaluated. The objective of the evaluation is to analyze the circulation patterns of battery units in the system with different numbers of batteries utilized and to understand how frequently different numbers of battery units are simultaneously circulating within the system.

In this case, when 3 batteries are implemented in the system, it is found that for almost 75% of the time, the batteries are in a stationary position, either at the hub or the parking lot. Furthermore, for almost 20% of the time, only one battery travels around the designated area while, for 4.63% of the time, two of them travel at the same time. These frequencies are plotted in Figure 4.22.

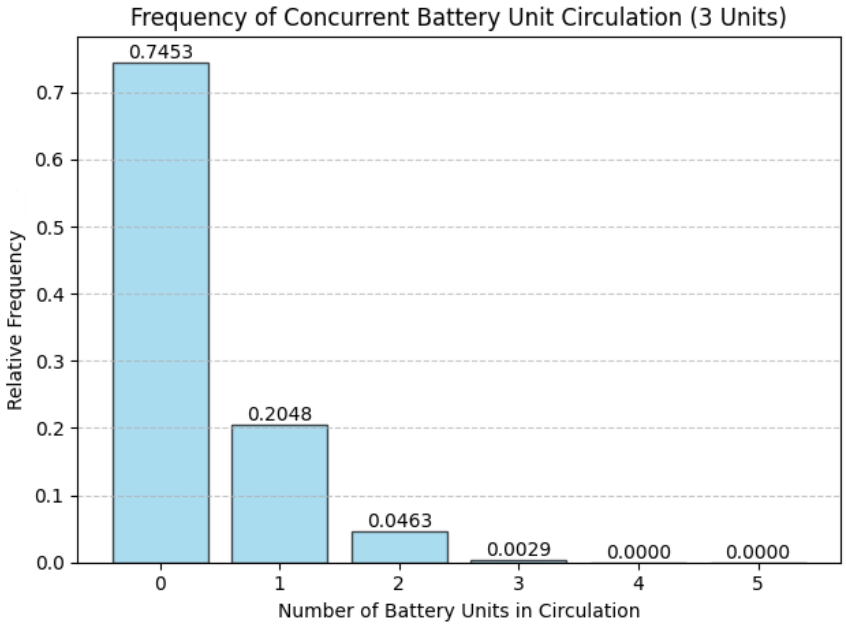

Figure 4.22: Relative Frequency of Simultaneously Travelling Batteries in the System with 3 Batteries

According to the plot in Figure 4.22, when 3 batteries are implemented in the system, having 2 carrier units instead of 3 can still meet 99.64% of the travel requirements. Furthermore, this percentage is even lower when considering that the analysis realizes 5 minutes of time steps and in fact, it takes less amount of time for the robot to complete the driving cycle. Therefore, it can be concluded that the number of carrier units can be reduced to 2 to further minimize the investment costs without any significant service disruption. In this way, the system can maintain the same amount of profits with more efficient use of the invested units.

Moreover, the frequency of travel values corresponding to the scenario with 4 robots is shown in Figure 4.23.

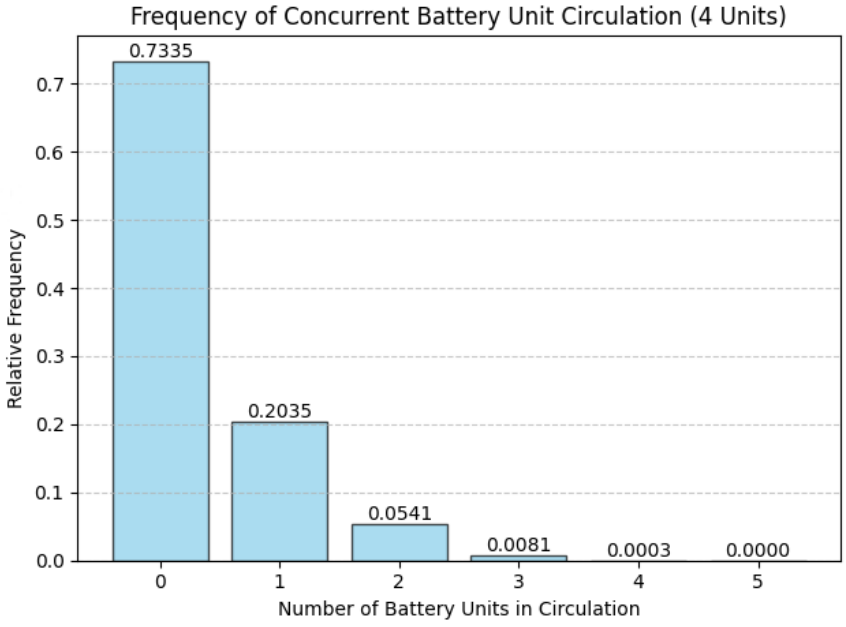

Figure 4.23: Relative Frequency of Simultaneously Travelling Batteries in the System with 4 Batteries

As shown in Figure 4.23, implementing 3 carrier units to support the travel requirements of 4 batteries can fulfil 99.9% of the batteries in circulation. Again, the effect of the service disruption will be even less in reality due to the sensitivity of the model. Therefore, it can be concluded that 3 carrier robots can support the convenience of the system with minimal service disruptions and bring about lower investment costs.

Lastly, the frequency of concurrent travels for the system with 5 batteries is plotted in Figure 4.24.

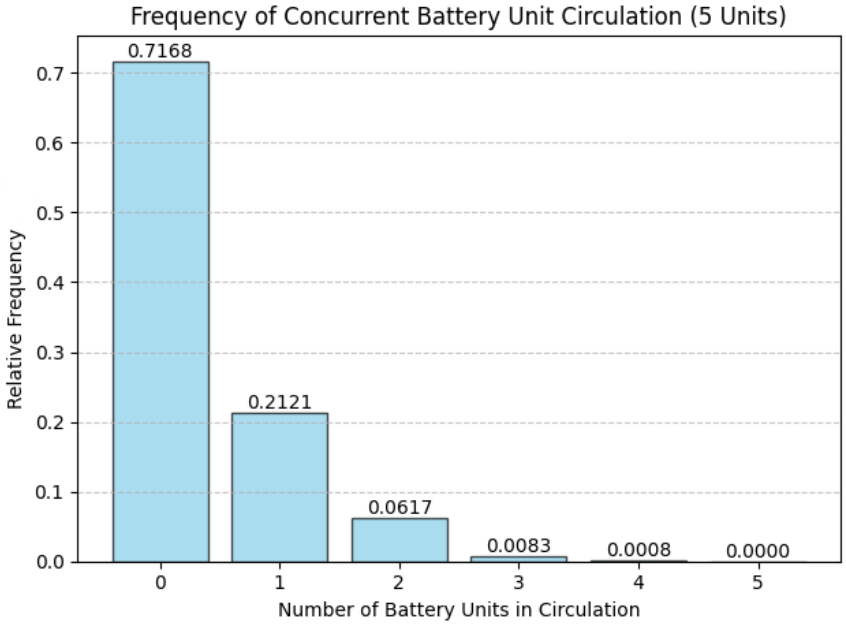

Figure 4.24: Relative Frequency of Simultaneously Travelling Batteries in the System with 5 Batteries

According to the plot in Figure 4.24, having 3 carrier robots in the system can fulfil 99.9% of the travelling requirements, supporting the batteries in the instances where they are required to travel around the parking facility. Furthermore, it would be an ineffective use of investment to buy 5 robots as the frequency of instances where 5 of the batteries are in circulation is 0. This would cause the fifth robot implemented in the system to be non-used even if it is implemented, bringing along a very inefficient valuation of investment and public space.

All in all, it can be concluded that 2 carrier robots are sufficient for a scenario with 3 batteries, while 3 robots are needed for scenarios with 4 and 5 batteries. In this way, an effective reduction in the investment requirements and public use can be carried out. It can also be noted that the formulated optimization problem returns a scenario which aims to maximize the daily return of the system, without paying attention to how many concurrent travels are taking place. Therefore, these numbers can even be minimized further in sub-optimal solutions which can sacrifice a small portion of profits to reduce the number of batteries in circulation at the same time to decrease the investment costs.

Taking this analysis into account, the total amount of initial investment required for the realisation of the mobile system for each configuration can be calculated and plotted as a function of the battery capacity for each different configuration in Figure 4.25. As different hardware and installation costs are associated with various grid capacity values, the initial investment costs are also distinguished for 50 and 100 kW configurations.

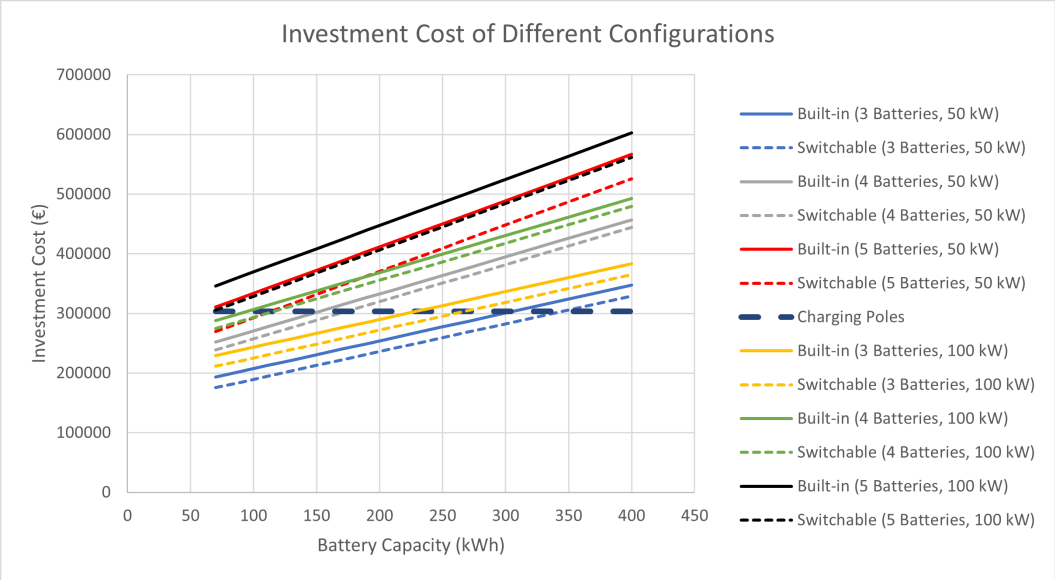

Figure 4.25: Initial Investment Cost Associated with Different Configurations as a Function of Battery Capacity

As shown in Figure 4.25, the reduction in initial investment cost due to the use of a switchable system is evident. In particular, this reduction becomes much more clear with respect to a larger number of battery units. Decoupling the travel freedom of the robot from the main unit, this configuration significantly decreases the hardware costs, revealing an attractive solution for investors. Furthermore, it can also be observed that for some different combinations of unit numbers and battery capacity, the resulting initial investment cost corresponding to the mobile charging system can outperform regular charging pole systems. For example, using 3 built-in or switchable batteries with 50 or 100 kW grid capacity can set a more attractive solution in terms of initial investment. However, this cost can also be reduced further by employing lower grid capacity and switchable configuration as this combination requires the least amount of investment.

To distinguish the most efficient sizing, yearly return on investment (ROI) values are calculated for each number of battery units considered and individual battery capacities considering a switchable configuration due to their lower initial investment costs. This calculation process is repeated over different price and grid capacity scenarios. For each price scenario, it is assumed that the system will sustain earning the same amount of daily profits until it reaches the end-of-life point presented in Section 4.3.2. As soon as it reaches the minimum capacity retention, it is further assumed that the battery units will be sold at the second life market for the price mentioned in Section 4.1. As a consequence, obtained yearly ROI plots are given in Figures 4.26, 4.27, 4.28, 4.29.

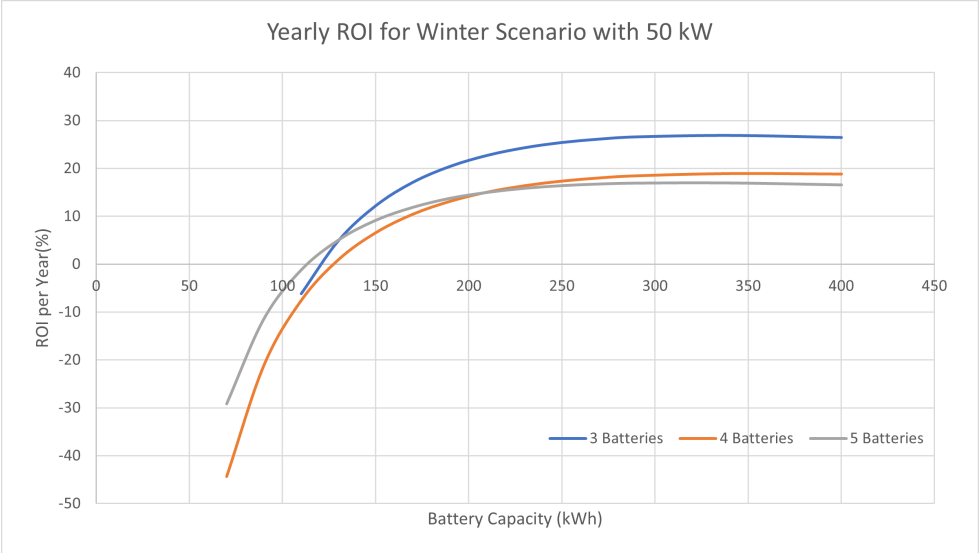

Figure 4.26: Yearly Return on Investment Plot of Switchable Configuration varying with Different Number of Units and Battery Capacities in Winter Scenario with 50 kW Grid Capacity

As shown in Figure 4.26, the highest yearly ROI is reached with 3 batteries installed, due to the reduction in the initial investments. Yearly ROI reaches 26.2% when 270 kWh battery capacity is used and after that point, further increasing the capacity only brings along around 0.7% improvement. In addition, this improvement is realised when the capacity is increased further by 70 kWh, just before a slightly decreasing trend starts due to overinvestment.

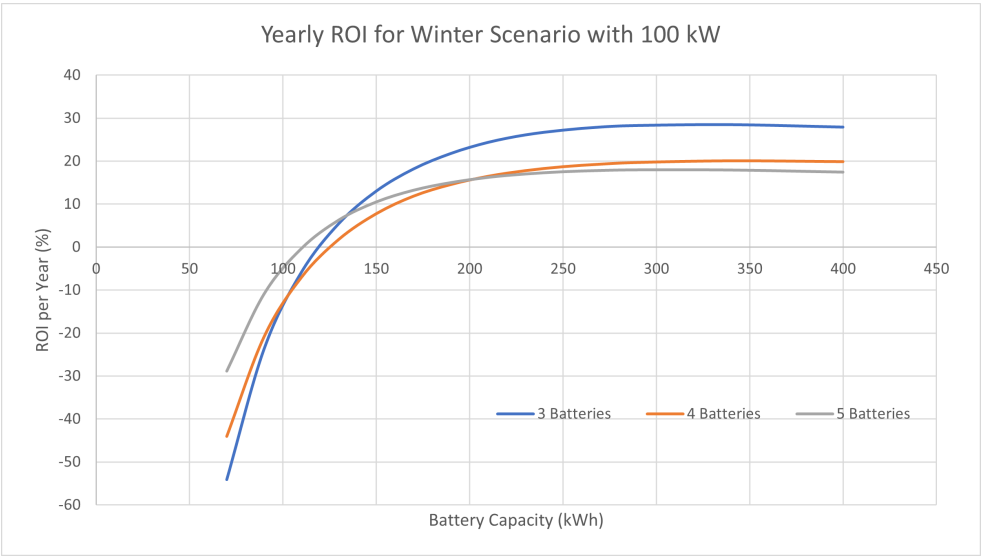

Figure 4.27: Yearly Return on Investment Plot of Switchable Configuration varying with Different Number of Units and Battery Capacities in Winter Scenario with 100 kW Grid Capacity

Furthermore, as it is shown in Figure 4.27, a slightly higher ROI of around 28% can be achieved around 270 kWh, when the grid capacity increases up to 100 kW. This slight improvement is due to the more flexible purchases and related lower cost of purchasing electricity. After this point, further oversizing the capacity by 70 kWh only improves yearly ROI by 0.5% before it starts dropping.

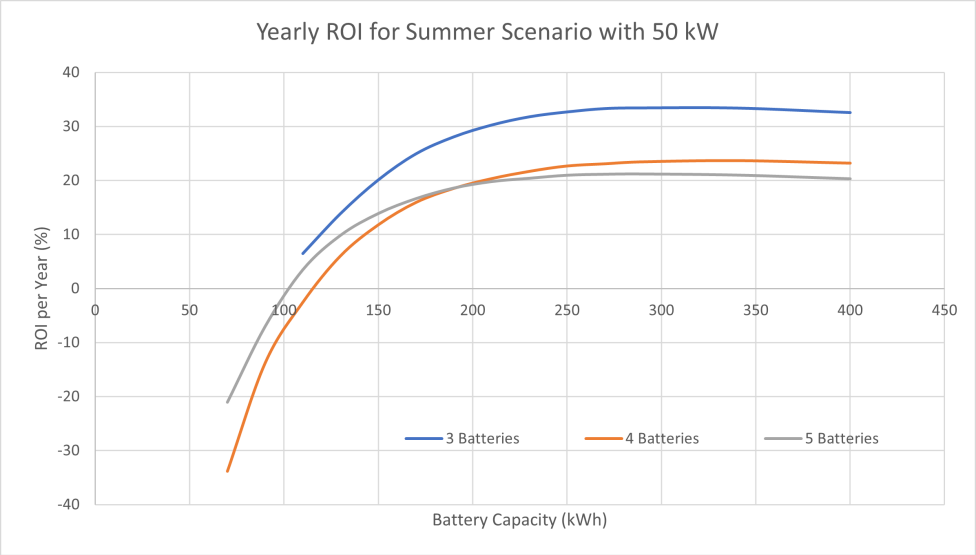

Figure 4.28: Yearly Return on Investment Plot of Switchable Configuration varying with Different Number of Units and Battery Capacities in Summer Scenario with 50 kW Grid Capacity

On the other hand, zero prices observed in Summer can further improve the financial performance of the system, as can be seen in Figure 4.28. In this Summer Scenario with 50 kW grid capacity, 3 batteries with 270 kWh capacity can make the system achieve a yearly ROI of around 33.3%. Further increasing the capacity by 20 kWh increases this number by only 0.12%, followed by a decreasing trend.

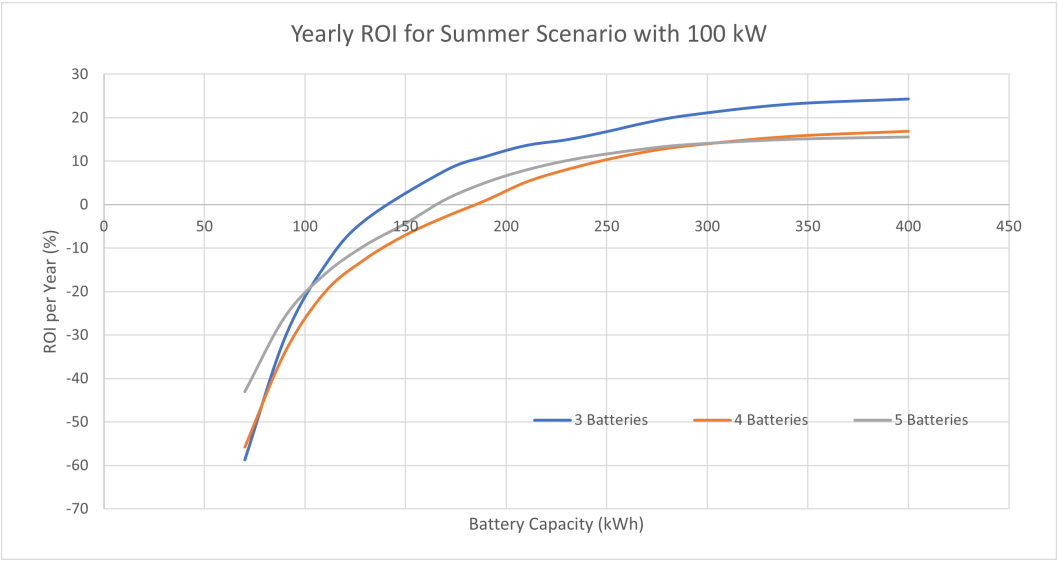

Figure 4.29: Yearly Return on Investment Plot of Switchable Configuration varying with Different Number of Units and Battery Capacities in Summer Scenario with 100 kW Grid Capacity

Lastly, the system can achieve a maximum annual ROI of 24.36% when 3 batteries are equipped in Summer and grid capacity is 100 kW. In detail, this value is the smallest when compared to the other peak values obtained in the other scenarios. On the other hand, this scenario is the one returning the highest amount of daily profits due to the excessive rate of energy arbitrage. The primary reason behind this finding is that even in the best-case scenario, the system buys energy at the cheapest price to be sold at the peak price in Summer, the maximum profit that can be earned is around 0.11€/kWh, without considering battery degradation. However, when the same amount of energy is purely used for charging EVs at a rate of 0.65€/kWh, this transaction becomes more profitable for the system. By

discharging the same amount of energy, batteries lose a portion of their capacity at the expense of making profits. When this portion of the capacity is only or mostly sacrificed for earning 0.65€/kWh throughout the battery's product life, then the system yields more returns bringing along a higher yearly ROI. Therefore, a lower value of ROI is achieved when the battery is used more for energy arbitrage, which is less profitable than charging EVs in a broader perspective. Even if this conclusion points out that energy arbitrage may not be very beneficial in terms of profits, it is also important to note its advantages to the grid. In addition, it is another source of profit which is increasing the daily profits, and hence decreasing the payback period of the system, even though in a longer time horizon, it causes the precious capacity of the batteries which can possibly serve EVs to fade.

Analysing the system's profits, investment costs and lifetime values, a decision can be made to highlight an effectively sized mobile system. First, the advantages and disadvantages associated with the grid capacity can be interpreted by evaluating the data presented. It can be concluded that the profits can only increase by 9.7% in Summer and 3% in Winter when 100 kW grid capacity is used at the expense of sacrificing peak reduction, as shown in Section 4.3.2. Furthermore, the system will live and operate for a shorter amount of time due to more energy arbitrage as explained in Section 4.3.2. Moreover, in the long term, it is shown that using the battery material heavily for grid arbitrage is not a good financial strategy instead of keeping it for the charging operations. That is why the yearly ROI of the system with 100 kW grid capacity is the lowest in Summer, while the improvement is limited by 1.6% in Winter due to the lack of energy arbitrage. With a smaller grid capacity, the system can sustain a longer product life by around 52% on average, effectively reducing peak demand by 73% by sacrificing only a small portion of its daily profits. Lastly, it is also important to note that the grid capacity significantly affects the cost of installing the required hub to accommodate the mobile units, as explained in Section 4.4.1. It can be noted that higher grid capacity results in a 2.88 times higher spending on the hub instalment, primarily due to increased hardware and installation costs. In light of these results, the advantages of higher grid capacity, which are only observed as a slight increase in daily profits, do not outweigh the associated disadvantages. Therefore, using a 50 kW grid capacity can be highlighted as a better strategy.

Next, a switchable configuration of the mobile system made up of 3 battery units, which are smaller than 344.8 kWh each, can appear as a more attractive solution in terms of initial investment, as shown in Figure 4.25. For example, compared to a mobile system with 270 kWh of battery capacity, regular charging poles require almost 13% more initial investment to fulfil the same charging operations. The same figure also demonstrates how the costs can be minimised by employing a switchable configuration. Therefore, choosing a switchable system size smaller than 344.8 kWh can demonstrate a more attractive solution for the investors. Furthermore, as a consequence of the yearly ROI analysis shown in Figures 4.26, 4.27, 4.28, 4.29, it is also noted that increasing the battery capacity further than 270 kWh has only limited improvement on the financial performance while increasing the initial investment costs and size of the system notable. Therefore, oversizing the system to obtain a slightly higher yearly ROI could cause this leverage of initial cost to fade away. On the other hand, choosing the maximum yearly ROI point of 340 kWh can bring along longer service life, by 25.56% on average. As a consequence, the system can yield more returns until the batteries reach the end-of-life point. Financial performance parameters of the system with these two configurations, including also the costs associated with the hub, are shown in Table 4.8 for comparison to regular charging poles. At this point, the service life of the charging poles is taken as 10 years [111]. Furthermore, a yearly operation and maintenance cost of $400 per charger is applied as reported by Alternative Fuels Data Center [188]. This yearly maintenance cost is also considered in the mobile system as it is required for the charger in the hub [188].

Mobile System with Switchable Batteries					
Scenario	**Capacity (kWh)**	**Product Life (Year)**	**Total Investment (€)**	**Revenue Earned until End-of-Life (€)**	**Profit Earned until End-of-Life (€)**
Winter	270	2.398	271,430.46	407,791.58	136,361.13
Winter	340	3.02	304,275.41	513,409.96	209,134.55
Summer	270	2.247	271,375.52	438,149.33	166,773.81
Summer	340	2.81	304,200.58	549,366.63	245,166.05
Charging Poles					
Winter	-	10	361,861.5	1,011,743.5	649,882
Summer	-	10	361,861.5	1,231,437	869,575.5

Table 4.8: Comparison of Costs and Profits of Mobile Systems and Regular Charging Poles

As shown in Table 4.8, the mobile system has a considerably shorter period of service life when compared to the charging poles due to capacity loss, even though the initial investment cost could be reduced. This shorter life causes the total revenues to be less as it limits the number of years that relatively higher daily profits are sustained. On the other hand, even though charging poles can yield higher revenue and profits, those returns are obtained at the end of a long period such as 10 years. This also brings along an investment risk. As the lifetime of the charging poles is taken as 10 years, a significant amount of money is invested, expecting that this trend will sustain throughout this long period. Meanwhile, a disruptive technology or event might develop, reducing the interest in such systems or increasing the associated costs. When the mobile system is used, the investors have the opportunity to revise the investment decision due to the reinvestment period of batteries in 2-3 years, while acquiring almost the same or higher yearly profits they earn by charging poles. In this way, the investors are also provided with the flexibility of redeployment to another location much more easily since the only stationary part is the charger installed in the hub. Also, they are given the opportunity to decide to no longer invest in the system after this short amount of time. Otherwise, the investment is locked for 10 years while expecting that it will sustain the same profitability and the purchased system can not be redeployed easily.

It is important to note that the expenditures related to the hub are one-time costs that have to be invested. Therefore, it can be said that the system requires a reinvestment period due to the replacement of batteries. In this case, this replacement cost only considers the batteries hence much lower than the initial investment, since other equipment such as the motor and chargers can be used for a longer time. In this case, the replacement cost is equal to €126,294.36 for a 270 kWh system and €158,913.22 for 340 kWh. The total amount of money invested in the system, resulting cumulative service life and total cumulative returns at the end of each re-investment period are given in Tables 4.9, 4.10 and 4.11. This reinvestment considers the repurchase of the batteries to replace the old ones at the end of their service life after they are sold in the second-life market. Therefore, as a consequence of the reinvestment, the total service life proportionally increases.

Mobile System with Switchable Batteries					
Scenario	**Capacity (kWh)**	**Service Life (Years)**	**Total Investment (€)**	**Total Revenue (€)**	**Total Profit (€)**
Winter	270	4.80	398,597.70	815,583.17	416,985.47
Winter	340	6.04	464,287.61	1,026,819.92	562,532.31
Summer	270	4.49	398,487.83	876,298.65	477,810.83
Summer	340	5.63	464,137.95	1,098,733.25	634,595.30

Table 4.9: Summary of Investment and Returns by the End of Reinvestment Period 1

Mobile System with Switchable Batteries					
Scenario	**Capacity (kWh)**	**Service Life (Years)**	**Total Investment (€)**	**Total Revenue (€)**	**Total Profit (€)**
Winter	270	7.19	525,764.95	1,223,374.76	697,609.81
Winter	340	9.06	624,299.81	1,540,229.88	915,930.07
Summer	270	6.74	525,600.14	1,314,447.98	788,847.84
Summer	340	8.44	624,075.32	1,648,099.88	1,024,024.56

Table 4.10: Summary of Investment and Returns by the End of Reinvestment Period 2

Mobile System with Switchable Batteries					
Scenario	**Capacity (kWh)**	**Service Life (Years)**	**Total Investment (€)**	**Total Revenue (€)**	**Total Profit (€)**
Winter	270	9.59	652,932.19	1,631,166.34	978,234.15
Winter	340	12.07	784,312.01	2,053,639.84	1,269,327.83
Summer	270	8.99	652,712.44	1,752,597.31	1,099,884.86
Summer	340	11.25	784,012.68	2,197,466.5	1,413,453.82

Table 4.11: Summary of Investment and Returns by the End of Reinvestment Period 3

In accordance with the results given in Tables 4.9, 4.10 and 4.11, lifetime of the mobile system can be increased up to a comparable level to the regular charging poles as a consequence of battery replacements. Especially, at the end of the second and third reinvestment periods, this period appears very close to the charging poles, revealing around 7 to 12 years of operation. As shown in the table, even though the mobile system requires more total amount of investment to achieve a comparable operation period, it can also return notably higher profits than what is acquired by the charging poles. For example, a 270 kWh system requires 1.8 times higher investment while returning 1.51 to 1.26 times higher profits in the third round of reinvestment. Furthermore, these higher profits are achieved in a shorter period, when compared to the charging poles, highlighting that the mobile system can return more profits per year. Therefore, in terms of yearly return, the mobile system appears as a better choice than the regular charging poles, while it requires more investment over the course of years. On the other hand, further oversizing the capacity up to 340 kWh, very close operation durations can be achieved at the end of the second reinvestment. In this case, by investing 1.73 times higher, the investors can earn 1.41 to 1.18 times higher profits than regular charging poles, in a shorter amount of time. These numbers are further improved by the third reinvestment. However, it is important to note that this results in very high operation period values such as 11 to 12 years, which again might bring along investment risks due to uncertainties.

All in all, the 270 kWh system can give investors more flexibility. With the help of this, the total cost of investment is paid in four instalments which are the decision periods of investment. As a consequence of the varying parameters, the investors are given the choice of not reinvesting or redeployment, while obtaining almost 40.7 to 57% higher yearly profits compared to the charging poles, depending on the scenario. This number can be improved slightly up to 44.5 to 61.82% when 340 kWh batteries are used, regarding the end of the third investment round. However, in terms of yearly profits, this configuration only brings along an average yearly profit improvement of 2.85%, compared to the 270 kWh configuration. Meanwhile, using that configuration requires around 20% more investment considering the end of the third investment round, even though realising more operation life. Therefore, for investors looking for a more compact system with less investment cost per round while still not compromising the maximum yearly returns significantly, the 270 kWh system appears as a remarkable choice. On the other hand, if the service area is suitable for larger units, and the investors are looking to maximize the yearly return at all costs, the 340 kWh system can appear as the best choice.

4.5. System's Performance Under Private Charging Load

The analysis is also repeated to assess the system’s performance under private charging demand. In particular, this charging demand mainly represents the people who can not access a private home charger and hence need to charge their vehicles using the public infrastructure. Therefore, the demand

schedule typically corresponds to private charging demand as this load demonstrates the use of the service located at residential locations. To achieve this, the demand data obtained by the sampling algorithm is used. This charging demand is presented in Figure 3.7, in Section 3.2. As this charging demand has a different peak value, total energy demand and different arrival times, its performance is investigated to reveal the effect of these factors in the final solution.

As the system's performance is analysed with two different grid capacity values, 50 and 100 kW, peak demand reduction performance also differs accordingly. In this case, using 50 kW capacity can bring along around 59% peak reduction, while it is around 18% with 100 kW capacity. These numbers are higher for public and workspace demand scenarios due to the presence of DC charging operations contributing to peak demand.

4.5.1. Profitability Analysis

For this particular scenario, again the effect of system size on the daily profits is investigated. To achieve this goal, daily profits that can be earned in a day when different numbers of units and battery capacities are used are simulated. As it is done in the public and workspace demand scenario, the analysis is repeated for different grid capacities to see how much the system can benefit from more flexibility.

Daily profits of the system in the Winter Scenario with 50 kW grid capacity are given in Figure 4.30. According to the results, oversizing the system can improve profits by approximately 0.4%. Especially, after 210 kWh battery capacity, the profit values do not vary considerably, and stay constant around €473.6.

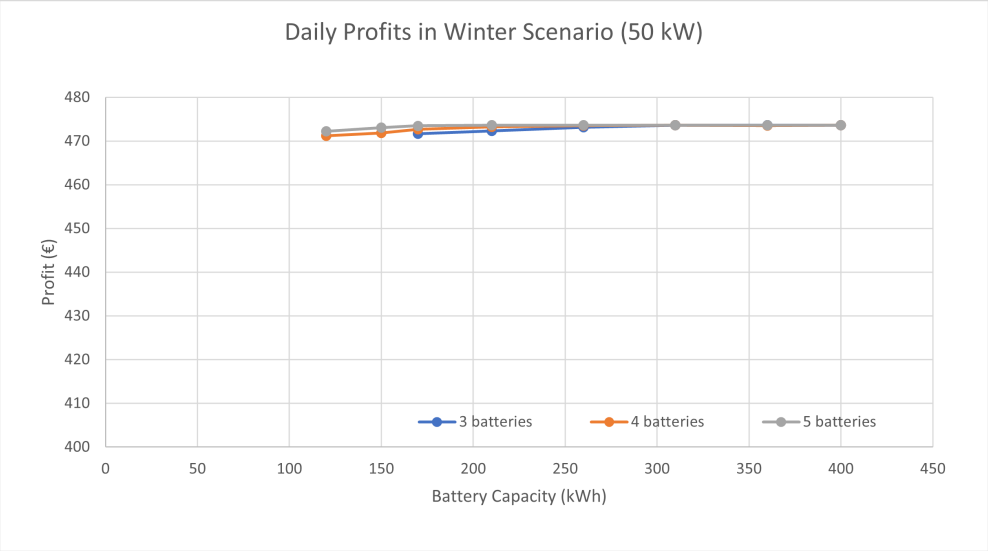

Figure 4.30: Daily Profits Plot in Winter Scenario with 50 kW Grid Capacity under Private Charging Load

On the other hand, when a higher grid capacity of up to 100 kW is used, oversizing the system affects the maximum profits by only around 2.9%. Profit values are capped at around €487.3 in this scenario, and increasing the battery size beyond 260 kWh has a limited effect on the return. The profit values are plotted in Figure 4.31.

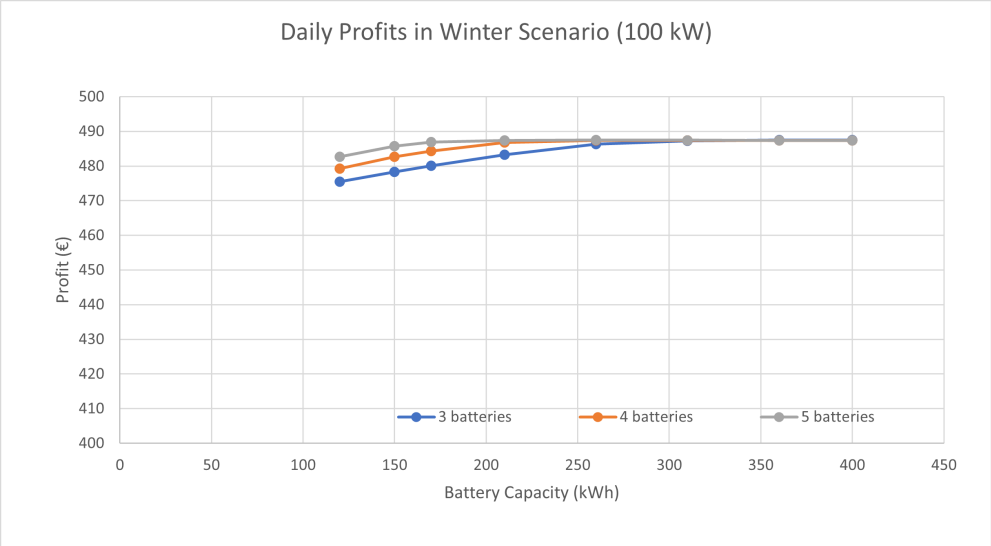

Figure 4.31: Daily Profits Plot in Winter Scenario with 100 kW Grid Capacity under Private Charging Load

As expected, the Summer Scenario yields more due to the cheaper prices and the presence of free electricity. In this case, the profit of the system is capped at around €540, when 50 kW grid capacity is used. This brings along an improvement of 14.22% when compared to the Winter Scenario with the same grid capacity. This maximum profit value is achieved at a battery capacity value of 170 kWh with 5 batteries, 210 kWh with 4 batteries or 310 kWh with 3 batteries. The daily profit plot corresponding to this scenario is given in Figure 4.32.

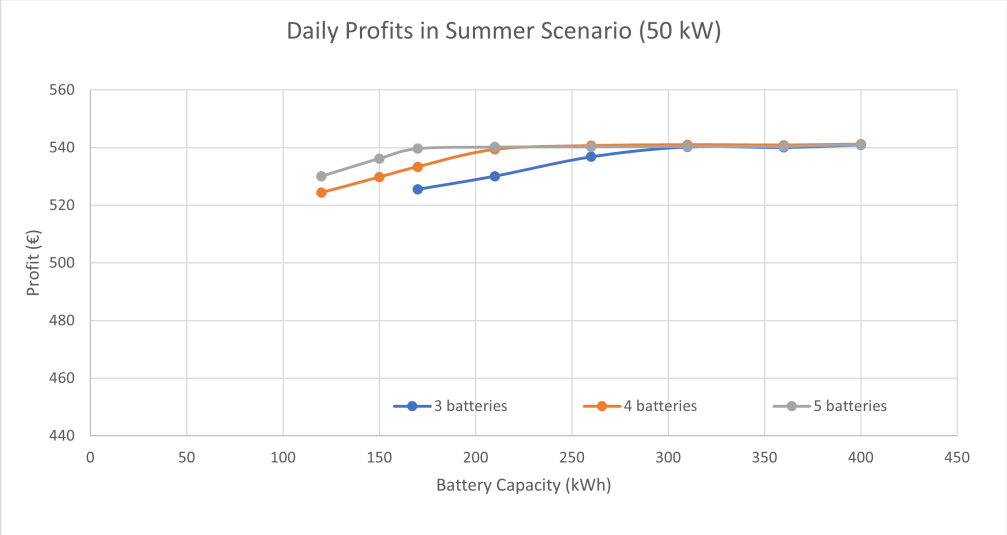

Figure 4.32: Daily Profits Plot in Summer Scenario with 50 kW Grid Capacity under Private Charging Load

Lastly, further increasing the grid capacity up to 100 kW yields a much higher amount of profits. This value is capped at around €596.2, as shown in Figure 4.33. This value expresses a 10.2% improvement in profits when compared to the scenario with 50 kW. However, this value can only be achieved when 5 units are implemented with more than 360 kWh capacity. It can be observed that the configurations with 3 and 4 units can not effectively reach this value and the capacity has to be increased further beyond 400 kWh to yield the maximum profit that can be returned. Therefore, the system has to be further oversized to take full advantage of the cheap electricity, while the scenarios under public and workspace load can efficiently realise the maximum amount of profits. The main reason behind this oversizing requirement is due to the significant overlap of charging operations with the peak demand hours where the electricity price exhibits a good possibility of energy arbitrage. At this point, the system

requires more battery and grid capacity to store cheap electricity to charge the EVs while selling a portion of it back to the grid. It is also important to note that overall charging demand is higher in this scenario. Hence, the system can use higher-capacity batteries more effectively when it is given more availability to exchange with the grid. However, it is important to note that this capacity can also bring along mobility challenges due to the mass and volume of the Li-ion batteries.

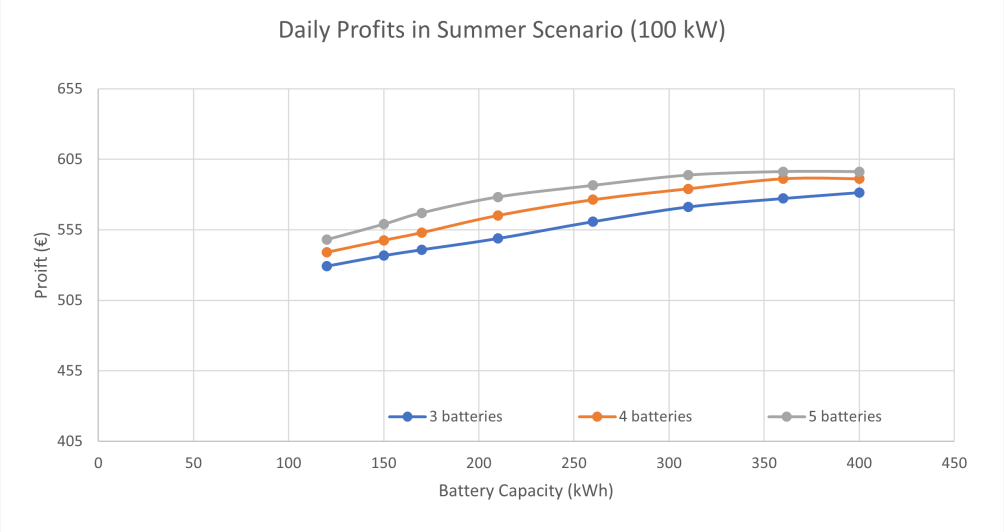

Figure 4.33: Daily Profits Plot in Summer Scenario with 100 kW Grid Capacity under Private Charging Load

4.5.2. Life Expectancy Analysis

Product life values of the batteries are calculated under private charging load by using the same degradation model introduced in Section 4.3.3. Considering the fact that the batteries discharge approximately 12% more energy to the EVs, it is expected to observe a slightly shorter period of life until the SoH of the batteries reach their end-of-life points, compared to the public and workspace demand scenario. The effect of this utilization is even amplified when more energy discharge brings along more charging to keep the SoC of the batteries at an adequate level for the day after. Therefore, this more energy input and output causes a slightly faster degradation.

In the Winter Scenario with 50 kW grid capacity, product life differs between 5.28 and 1.27 years, as shown in Figure 4.34. As expected, the maximum life expectancy is slightly lower than what is observed under public and workspace load, due to more utilization of batteries. This reduction can be calculated as almost 12%.

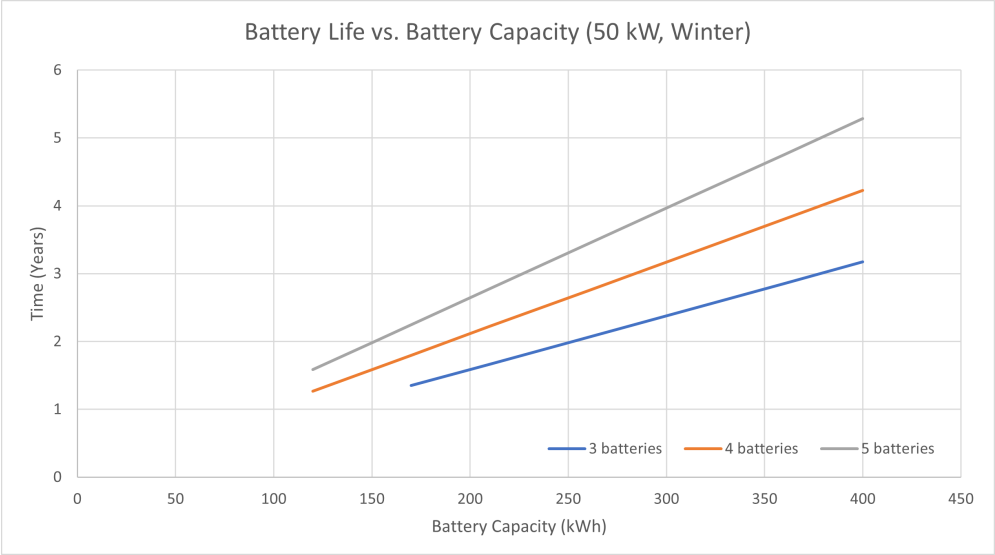

Figure 4.34: Product Life Plot in the Studied Private Charging Scenario in Winter with 50 kW Grid Capacity

As observed under public and workspace load, increasing the grid capacity up to 100 kW in the Winter Scenario does not affect the product life by a notable margin, as shown in Figure 4.35. This invariance can be attributed to the lack of effective energy arbitrage positions as explained in the previous section.

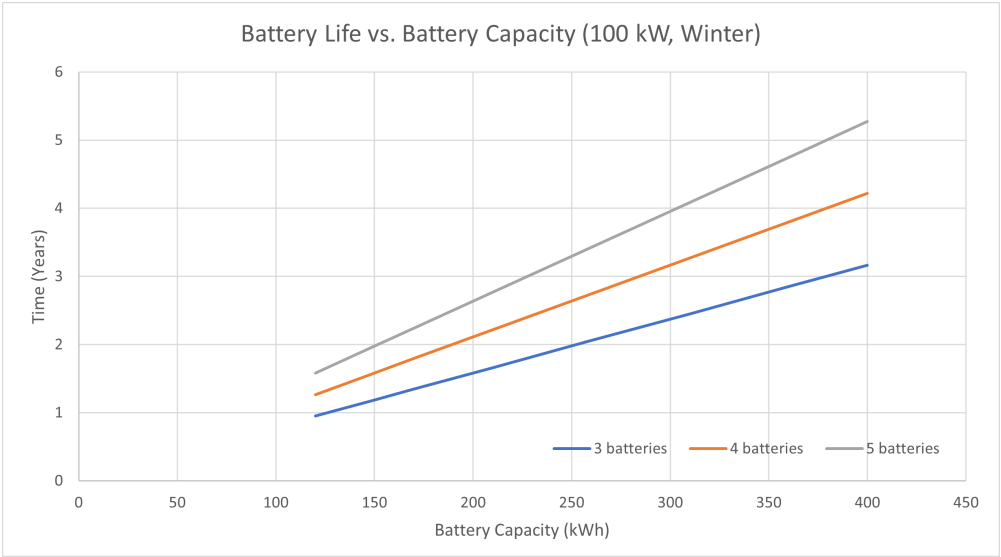

Figure 4.35: Product Life Plot in the Studied Private Charging Scenario in Winter with 100 kW Grid Capacity

On the other hand, in the Summer Scenario, the life expectancy outcome is comparable to the results obtained under public and workspace load, as shown in Figure 4.36. Again, the maximum product life value is slightly less than that of public and workspace load. When compared to the Winter Scenario with 50 kW, it can be observed that the maximum product life values are almost the same. The main reason behind this is again due to the timing of the arrival times. In private load, the arrival times of EVs coincide with the peak demand hours where higher prices are observed. In this case, due to the occupation of battery units with charging tasks, energy arbitrage observed is very limited. Furthermore, limited grid capacity also does not allow the batteries to store extra energy to be sold to the grid. Therefore, this capacity is mainly used for charging in this case.

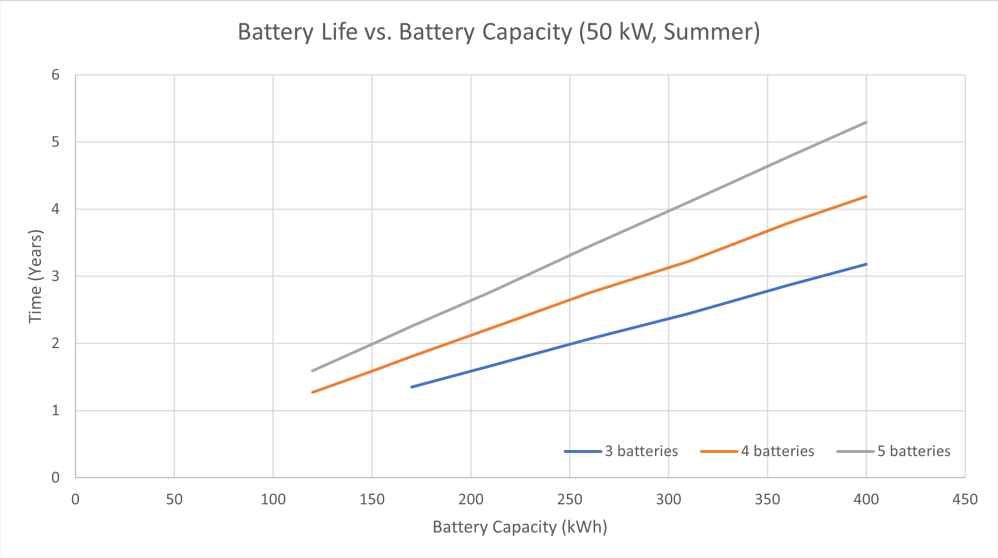

Figure 4.36: Product Life Plot in the Studied Private Charging Scenario in Summer with 50 kW Grid Capacity

Further increasing the grid capacity results in more effective energy arbitrage as the batteries are allowed to purchase more when prices are zero. In this case, the effect of energy arbitrage becomes evident from the product life plot shown in Figure 4.37, with 100 kW grid capacity. As a result, almost 35.5% reduction in the maximum life expectancy is attained due to the heavier use of batteries.

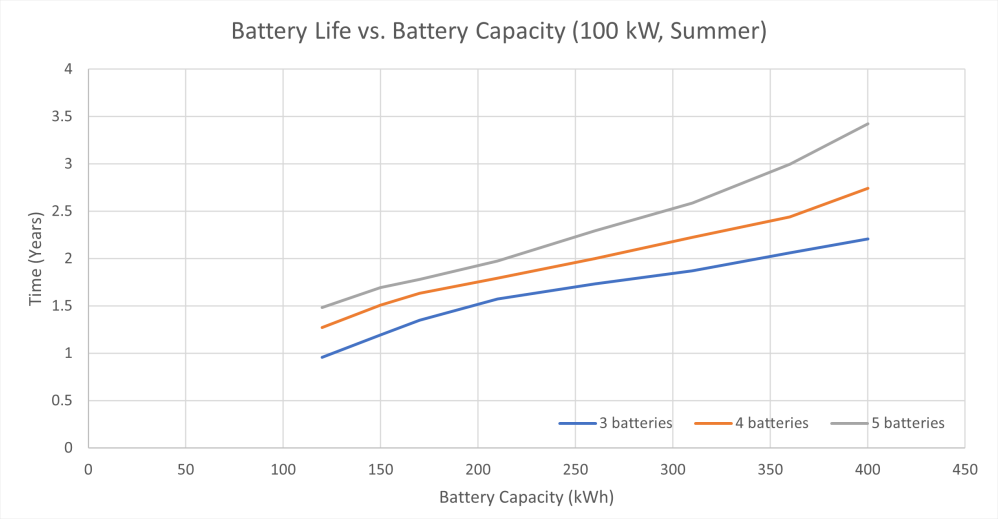

Figure 4.37: Product Life Plot in the Studied Private Charging Scenario in Summer with 100 kW Grid Capacity

4.5.3. Financial Evaluation and Comparison

Financial evaluation should consider the overall profits that will be earned, the amount of time in which those profits will be sustained and the required investment, as well as how quickly the costs will be earned back. To achieve this comprehensive analysis, ROI per year is used as an evaluation metric for the switchable configuration again. The analysis is repeated for different numbers of units, battery capacities and scenarios.

First, in the Winter Scenario with 50 kW grid capacity, the configuration made up of 3 battery units notably overperforms due to the lower investment costs associated as shown in Figure 4.38. A maximum ROI per year of 28.7% is achieved around 260 kWh battery capacity and beyond this point, further oversizing the system does not contribute by a significant margin as also shown by the plateau that the daily profits reach in Figure 4.30. Following this, increasing the capacity by 50 kWh results in only

1.2% improvement. Therefore, it can be seen that the switchable configuration with 3 battery units can return almost 30% of the initial investment per year.

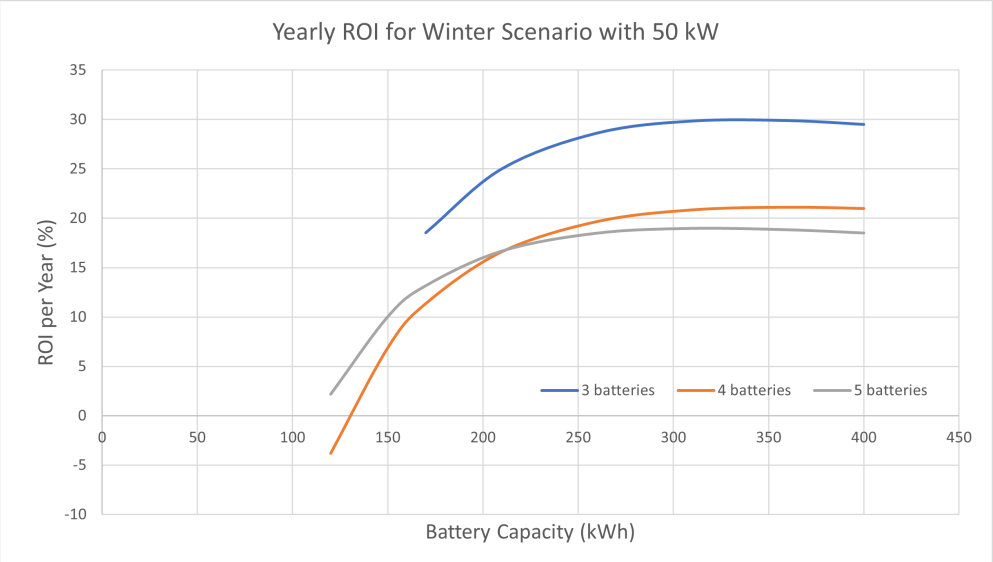

Figure 4.38: Yearly Return on Investment Plot of Switchable Configuration varying with Different Number of Units and Battery Capacities in Winter Scenario with 50 kW Grid Capacity under Private Charging Load

When the grid capacity is further increased, the daily profit the system returns also increases by a margin as stated in Section 4.5.1. The effect of this improvement becomes evident as the maximum ROI also increases by almost 5.66% when 100 kW of grid capacity is utilized due to the reduced electricity costs, as shown in Figure 4.39. Again, the maximum value is obtained when 3 batteries are used. After 260 kWh of capacity, improvement of ROI becomes very limited and a gradual decrease follows after it reaches the peak value of 31.6% at around 310 kWh, as the system reaches the maximum profit value that can be earned shown in 4.31.

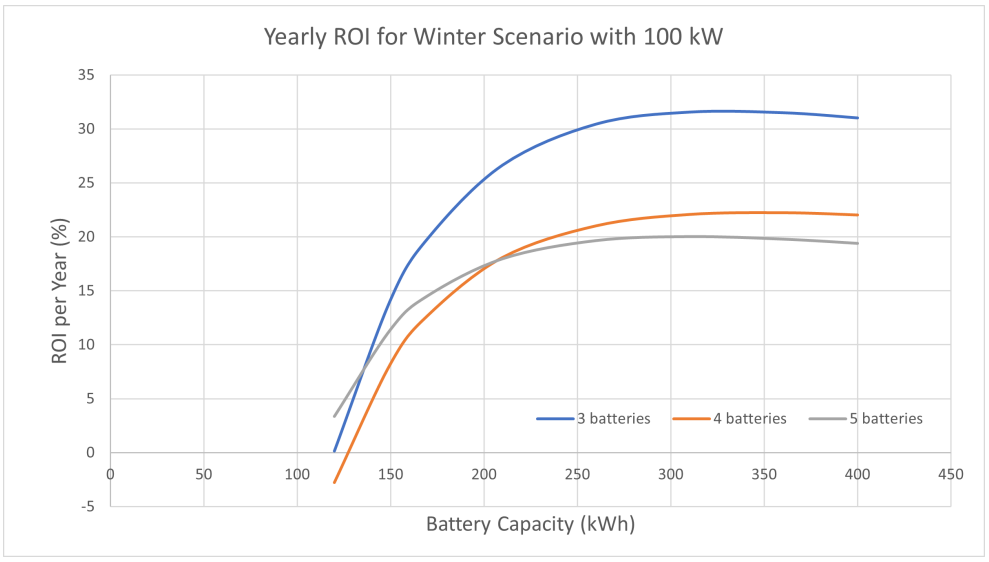

Figure 4.39: Yearly Return on Investment Plot of Switchable Configuration varying with Different Number of Units and Battery Capacities in Winter Scenario with 100 kW Grid Capacity under Private Charging Load

In the Summer Scenario, the system can yield more return due to the cheaper energy prices. At this point, a maximum ROI of 38.5% can be attained per year, when 50 kW of grid capacity is used, as shown in Figure 4.40. This brings along 28.3% of improvement, compared to the Winter Scenario

with the same grid capacity. The maximum value is obtained with 3 battery units and around 310 kWh, following the profit plateau shown in Figure 4.32, and again after 260 kWh, oversizing the system brings along very limited improvement around 0.46%.

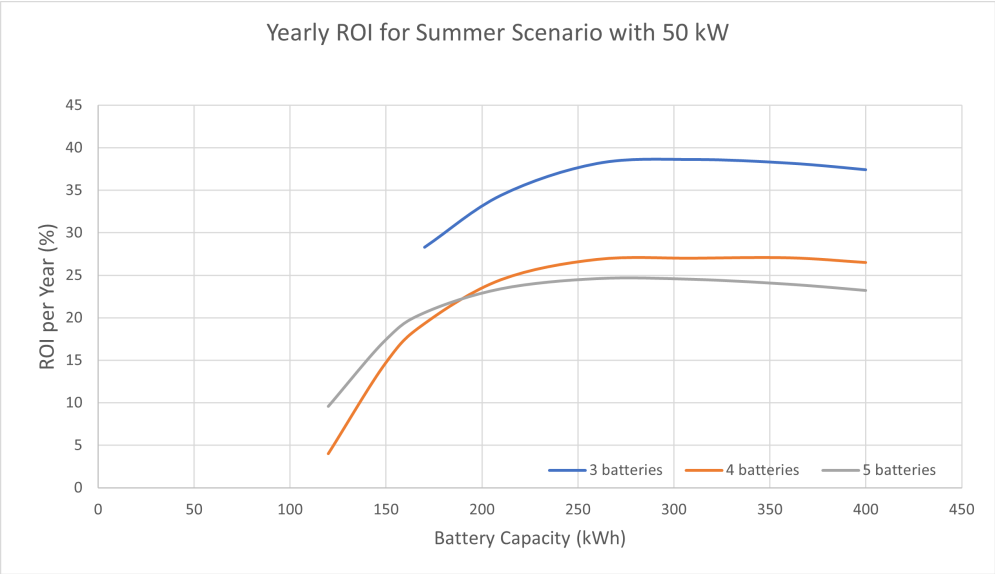

Figure 4.40: Yearly Return on Investment Plot of Switchable Configuration varying with Different Number of Units and Battery Capacities in Summer Scenario with 50 kW Grid Capacity under Private Charging Load

Finally, when grid capacity is further increased up to 100 kW, the system starts doing more energy arbitrage. Even if this increases the daily profits of the system by a significant margin as stated in Section 4.5.1, it affects the ROI obtained per year negatively. As this was the case under public and workspace load, doing more energy arbitrage in fact causes the battery material to fade at the expense of earning less money, compared to charging an EV. Since the profit of charging an EV is much higher than what can be earned by energy arbitrage, a system which keeps its battery material to only charge EVs and hence profit more can yield better ROI per year. This becomes more evident when the results with 50 kW are compared. In this case, the system has a maximum ROI per year of around 34.5%, which is almost 10.4% lower, as shown in Figure 4.41. Furthermore, this value is observed around 210 kWh of battery capacity. In addition, the effect of energy arbitrage becomes more clear corresponding to 3 batteries. After reaching a capacity of 210 kWh, the system begins to take advantage of the extra storage by heavily engaging in energy arbitrage. Up until that point, the system utilizes a significant portion of the energy to only charge EVs. As energy arbitrage becomes more prevalent, the yearly return on investment of the system begins to exhibit a downward trend. This trend is attributed to accelerated ageing, as highlighted by the inflection point of the corresponding product life curve shown in Figure 4.37. When the slight improvement in profitability is not enough to compensate for this fast degradation, the system yields less returns, due to the limited operational life.

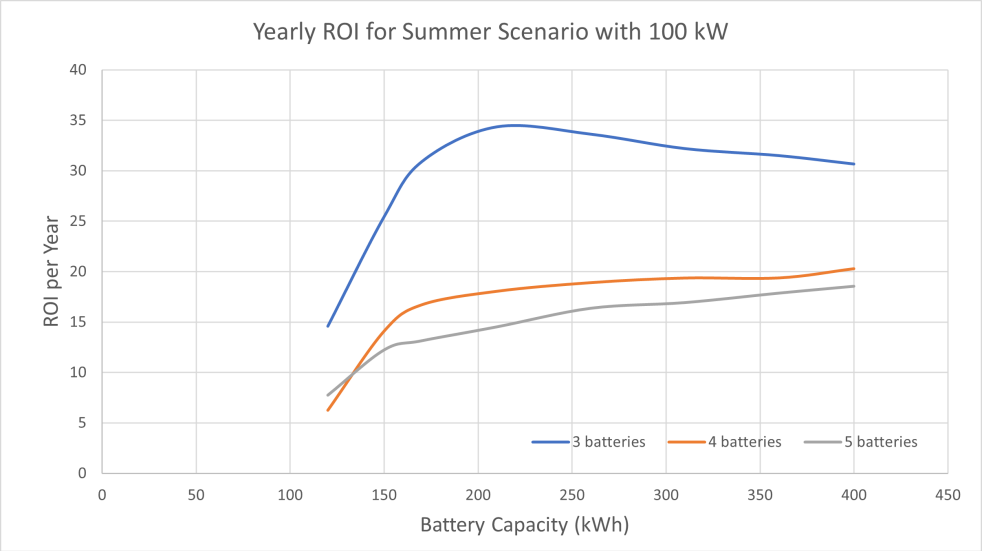

Figure 4.41: Yearly Return on Investment Plot of Switchable Configuration varying with Different Number of Units and Battery Capacities in Summer Scenario with 100 kW Grid Capacity under Private Charging Load

All in all, it can be concluded that in a battery capacity range of around 310 kWh, the system can maximise its financial performance and after 260 kWh, the effect of battery capacity on yearly ROI becomes minimal. The use of 3 battery units can significantly reduce the amount of investment in the system and hence yield a better return on this amount per year, exhibiting a more efficient investment scheme. Furthermore, increasing the grid capacity up to 100 kW does not strongly improve this performance while it compromises the peak power reduction by a large margin. Therefore, 50 kW grid capacity results in more profitable and efficient use of the bought material. Furthermore, more investment is required to build the necessary high-power charging equipment. Considering these disadvantages, only a 5.66% improvement in ROI per year obtained in Winter does not cause a significant enough impact to justify the setbacks of increased grid capacity.

Furthermore, the revenue, cost and profits of regular charging poles are calculated using the same rates given in Section 4.4.2 and given in Table 4.12.

Table 4.12: Comparison and Breakdown of Charging Poles Revenues under Private Charging Load

Scenario	Revenue of Charging (€)	Cost of Electricity (€)	Daily Profit (€)	Yearly Profit (€)
Winter	335.68	79.86	255.82	93,374.3
Summer	335.68	55.79	279.89	102,159.85

Furthermore, the details about the maximum financial performance of the mobile system with 3 switchable units under private load are tabulated for different scenarios and grid capacities in Table 4.13.

Table 4.13: Comparison and Breakdown of Mobile System Revenues for Different Grid Capacities under Private Charging Load

Scenario	50 kW Grid Capacity			100 kW Grid Capacity		
	Revenue of Charging (€)	Revenue of Energy Arbitrage (€)	Cost of Electricity (€)	Revenue of Charging (€)	Revenue of Energy Arbitrage	Cost of Electricity (€)
Winter	545.48	0.19	72.04	545.48	0.39	58.63
Summer	545.48	0	5.45	545.48	39.57	3.58

Following the details given in Table 4.13, daily and yearly profits of the mobile system under a private charging load can be calculated. Calculated values are given in Table 4.14.

Table 4.14: Comparison and Breakdown of Mobile System Profits for Different Grid Capacities under Private Charging Load

Scenario	50 kW Grid Capacity		100 kW Grid Capacity	
	Daily Profit (€)	Yearly Profit (€)	Daily Profit (€)	Yearly Profit (€)
Winter	473.63	172,874.95	487.24	177,842.6
Summer	540.03	197,110.95	581.47	212,236.55

Compared to the profits obtained by the systems, mobile systems can significantly outperform regular charging poles, due to the higher revenues and lower cost of electricity resulting from the flexible operation. However, it is also important to note that the system results in a lower operational life due to the capacity fading, compared to the charging poles' 10 years of service period. Furthermore, as the maximum yearly ROI values are sometimes observed at 310 kWh, and in some cases the effect becomes minimal after 260 kWh, lifetime and yearly profit values with the total investment considering the costs associated with the hub are calculated for the mobile system. For comparison, the same metrics are also calculated for the charging poles, also considering the maintenance costs and given in Table 4.15.

Mobile System with Switchable Batteries					
Scenario	**Capacity (kWh)**	**Product Life (Year)**	**Total Investment (€)**	**Revenue Earned until End-of-Life (€)**	**Profit Earned until End-of-Life (€)**
Winter	260	2.06	266,648.58	391,357.02	124,708.45
Winter	310	2.46	290,091.86	466,476.88	176,385.02
Summer	260	2.07	266,650.46	439,946.29	173,295.83
Summer	310	2.44	290,086.27	523,241.06	233,154.79
Charging Poles					
Winter	-	10	317,863	933,743	615,880
Summer	-	10	317,863	1,021,598.5	703,735.5

Table 4.15: Comparison of Costs and Profits of Mobile Systems and Regular Charging Poles under Private Load

As shown in Table 4.15, the mobile system can bring along reductions in the initial investment. However, due to the capacity loss observed in the batteries, the system's operational life is significantly lower when compared to the regular charging poles. Therefore, the system returns considerably less profits until the batteries reach their end-of-life points. On the other hand, it is also important to note that the system with charging poles returns these higher profits over the course of a long period of 10 years. Consequently, when the yearly profits are considered, the mobile system can exhibit a good level of competitiveness, returning very close or slightly higher yearly profits. Again, it is important to note that the hub costs are one-off payments and no other costs are relevant after it is installed, except for the maintenance, while the batteries require reinvestment after they become retired. After that point, the investors can reinvest in the system to replace the batteries. This replacement cost is equal to €121,634.52 for the 260 kWh system while it is €144,933.71 for the 310 kWh system. The total amount of investment, cumulative revenue and profit values are calculated for each scenario regarding 3 reinvestment rounds for the mobile system and given in Tables 4.16, 4.17 and 4.18.

Mobile System with Switchable Batteries					
Scenario	**Capacity (kWh)**	**Service Life (Years)**	**Total Investment (€)**	**Total Revenue (€)**	**Total Profit (€)**
Winter	260	4.12	389,033.94	782,714.05	393,680.11
Winter	310	4.92	435,920.5	932,953.76	497,033.25
Summer	260	4.14	389,037.71	879,892.58	490,854.87
Summer	310	4.88	435,909.33	1,046,482.13	610,572.79

Table 4.16: Summary of Investment and Returns by the End of Reinvestment Period 1 under Private Load

Mobile System with Switchable Batteries					
Scenario	**Capacity (kWh)**	**Service Life (Years)**	**Total Investment (€)**	**Total Revenue (€)**	**Total Profit (€)**
Winter	260	6.19	511,419.31	1,174,071.07	662,651.77
Winter	310	7.38	581,749.15	1,399,430.64	817,681.49
Summer	260	6.2	511,424.96	1,319,838.87	808,413.91
Summer	310	7.33	581,732.39	1,569,723.19	987,990.79

Table 4.17: Summary of Investment and Returns by the End of Reinvestment Period 2 under Private Load

Mobile System with Switchable Batteries					
Scenario	**Capacity (kWh)**	**Service Life (Years)**	**Total Investment (€)**	**Total Revenue (€)**	**Total Profit (€)**
Winter	260	8.25	633,804.67	1,565,428.1	931,623.43
Winter	310	9.83	727,577.8	1,865,907.52	1,138,329.72
Summer	260	8.27	633,812.21	1,759,785.16	1,125,972.95
Summer	310	9.77	727,555.46	2,092,964.25	1,365,408.79

Table 4.18: Summary of Investment and Returns by the End of Reinvestment Period 3 under Private Load

As shown in Tables 4.16, 4.17 and 4.18, the mobile system's operational life can achieve similar values to that of charging poles at the end of the third reinvestment round. In this case, the total amount of investment is 1.99 to 2.29 times higher than that of charging poles, depending on the battery capacity. On the other hand, the potential profits are also 1.51 to 1.94 times higher. Furthermore, it is also important to note that these profits will be returned sooner than what is possible with the charging poles. Consequently, the mobile system sets an investment opportunity in which total higher profits can be earned even though more investments are required. Especially, the use of the mobile system almost doubles the yearly profits that can be earned when compared to the charging poles because the total return is obtained in a shorter amount of time. The difference in the total investments is more notable in the private load scenario. The main reason is in this scenario, all of the charging poles only support AC charging which is significantly cheaper than DC charging equipment. This allows the system to reduce the hardware costs. On the other hand, the mobile system offers a great reduction in the charging times due to the possibility of fast charging. This improved convenience can be highlighted as one of the main factors contributing to this difference. In addition, it is also important to remember that the investors are allowed to review their investment strategy with the help of reinvestment rounds or even redeploy the system to another location much more easily.

Comparing two different battery capacities, it is clear that employing 310 kWh capacity can significantly increase the system's operational life. By the end of the third reinvestment period, the system can reveal almost 9.8 years of operational life, which is very close to that of charging poles. Meanwhile, it can improve the total profits of the system by 22.2% in Winter and 21.3% in Summer due to longer service life at the end of the third reinvestment, when compared to the 260 kWh system. On the other hand, when the yearly profits are considered, this improvement is only 2.59% on average. Therefore, the 260 kWh system can exemplify a more compact system with 14.8% less investment costs, without compromising the yearly profits of the system very much. On the other hand, for investors who are willing to invest even more and yield the maximum returns that can be earned, the 310 kWh system could appear as a remarkable size.

5

Powertrain Specifications

This section discusses the powertrain requirements depending on different mobile charging robot configurations to answer Research Sub-Question 5. To achieve this, a realistic driving cycle is developed to simulate the travel of the units. In accordance, the required power that must be supplied by the traction motor and energy consumption are calculated. Finally, considering the purpose of the system, types of traction motors are introduced with a comparative analysis to guide the selection process.

5.1. Driving Cycle

One of the main objectives of the powertrain design process is to calculate the power required for the robots carrying the battery packages and the total energy consumption during the travel. To calculate these values in a realistic framework, it is crucial to design a driving cycle representing the robot's mobility throughout the operation. These travel instances mainly consist of two different types of journeys. First, the robot can travel from the hub to an EV to conduct a charging operation. Second, the robot can directly travel from one EV to another if it is more advantageous than taking a break at the hub to get the battery charged or switched. In both cases, the maximum speed, gradient and mass will be the same in both cases. However, these two scenarios mainly differ considering the energy spent for the travel, as the travelling time and distance depend. Nevertheless, for the calculations, the worst-case scenario is assumed, where the robot uses the maximum energy possible by travelling to the farthest lot from the hub before starting the charging operations.

When the location of the hub is assumed, as shown with a red pin in Figure 5.1, the distance between the hub and the closest car parked is measured at 170 m.

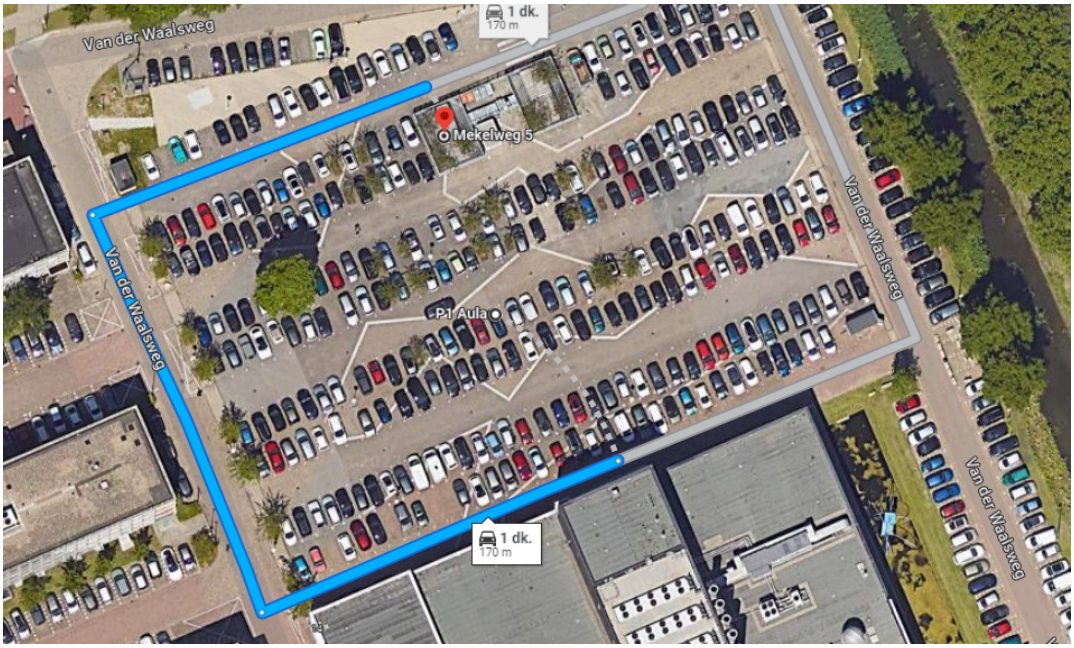

Figure 5.1: Assumed Hub Location and the Maximum Distance to an EV

While designing the driving cycle, it is crucial to address the safety expectations of the operations. Hence, it is important to remember that these operations occur in public spaces where people walk and drive freely, entrusting their personal vehicles to the safety of the area. At this point, the robot's mobility should not put any of these aspects in danger and conflict with the values of public space. Accordingly, the maximum speed of the robots is determined to be not far from the typical walking speed of a human, which is measured around 5 km/h [21]. Furthermore, when the robots' duty is summarized as a motorized autonomous vehicle using public space and displacing a certain mass to serve people, they can be found similar to the delivery robots used by cargo or food companies. Such robots are also equipped with batteries to feed electric motors and are responsible for taking a payload from a central location to specific customer locations by using roads and pavements. One of the most well-known examples of such robots is produced by Starship Technologies Ltd. These robots can cruise up to 6 km/h to travel within a 5 km radius and are specifically designed to cover this distance on pavements [93]. This further validates the safety of limiting the maximum speed of the robots to a typical walking speed.

Moreover, maximum travelling speeds of motorized vehicles are often regulated under the Traffic Acts to ensure public safety, even if such acts do not cover mobile robots as they are not very widespread as of today. For example, Dutch Traffic Regulations limit the maximum speed of motorized vehicles using pavements and footpaths to 6 km/h. However, these vehicles are only mentioned as disabled vehicles and motor-assisted bicycles [130]. On the other hand, autonomous robots operating in the public are subjected to regulations in the United States and their maximum speed is limited to 5 km/h [105], [195].

Considering these design parameters, an artificial driving cycle covering the maximum travelling distance is developed. In this cycle, it is determined that the robot will travel at 5 km/h, 1.389 m/s, maximum speed with $0.278\,\mathrm{m/s^2}$ maximum acceleration, equivalent to an increase of 1 km / h in speed per second, to cover the distance between the hub and the farthest parking lot shown in Figure 5.1. This maximum acceleration value is determined regarding the autonomous guidance requirements. It is reported that the sensitivity of the sensors in autonomously driven systems can greatly be affected by acceleration. At higher acceleration than $0.7\,\mathrm{m/s^2}$, it is reported the vibrations can distort the localisation and mapping ratings of the visual sensors [6]. In the literature, maximum acceleration values varying between 0.2 and $0.3\,\mathrm{m/s^2}$ are used and found adequate in different autonomous robot designs and some experiments to assess the sensitivity of the measurements [106], [205], [192]. As soon as the robot arrives at the lot, it waits for 4 seconds to detect and measure the distance between two vehicles parked one next to each other and decides on the manoeuvre strategy to reach the charging

port. Consequently, the robot's maximum speed is limited to 2.5 km/h, 0.694 m/s, while approaching the vehicles to make sure the sensors have enough time to intervene by steering or stopping the movement to avoid collision with any obstacle in the surroundings. All in all, the robot travels at 1.345 m/s average speed from the hub to the lot, and at 0.555 m/s while approaching the parking lot. The average speed observed in the full driving cycle, considering the acceleration, deceleration and waiting times, is calculated as 1.235 m/s. The designed driving cycle is plotted in Figure 5.2, showing the target speeds at the designated time.

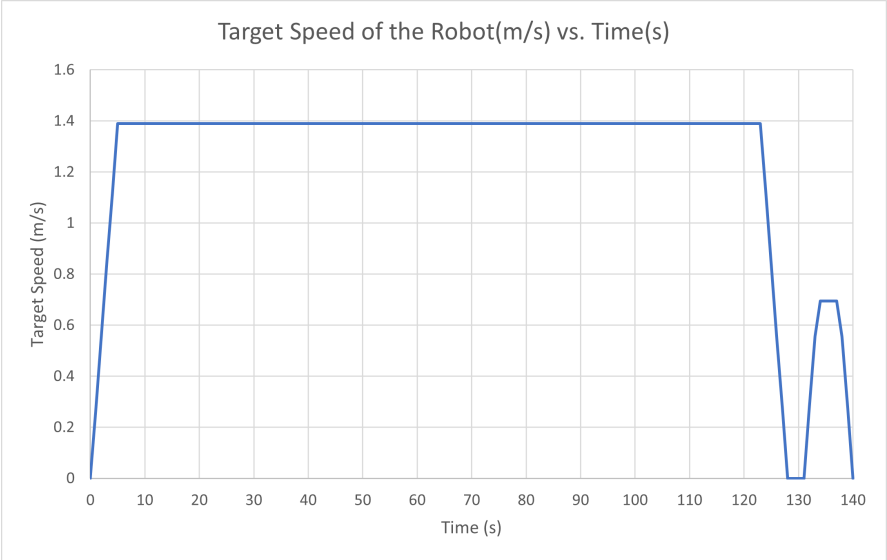

Figure 5.2: Designed Driving Cycle of the Robot on Duty

As this driving cycle only considers the travel between one service point to another, it can fully capture how much one built-in robot travels. For example, it can be either from the hub to the parking lot or vice versa. However, when a switchable configuration is used, it is important to note that this driving cycle is doubled. In this case, the carrier robot will follow this driving cycle by towing the battery unit to the service point, and proceed to the next service point after releasing the battery in a stand-alone condition. To achieve this, the energy requirement of the first cycle can be sourced by the battery unit, while the stand-alone travel can be powered by the smaller battery unit installed on the carrier unit. All in all, the driving cycle of the switchable configuration can be described as the double of the built-in one which first one requires the mobility of the battery unit and the carrier unit, while the second one only regards the mobility of the carrier unit.

5.2. Weight Estimation

In order to calculate how much a single unit weighs, the main components contributing significantly to the mass have to be classified. The most significant contributor is the battery itself. $LiFePO_4$ batteries are widely used in energy storage applications due to their high durability and lower cost. The energy density of such batteries is reported around 175 Wh/kg [119], [155]. However, this energy density further drops when it is packed due to the additional components implemented in the battery package. These elements are mainly the casing, BMS and cooling system [199]. The placement of additional elements causes the reported energy density to reduce to 125 Wh/kg [119], [150].

Other components are mainly the charger, robot platform or chassis with the wheels and sensors, the traction motor, robotic arm and DC/AC Converter. Considering the charger has to deliver the high power required by fast charging applications, adequate examples from the market have been studied. Furthermore, it is observed that it is possible to deliver power up to 175 kW by using a charger with 52 kg mass addition to the system. Moreover, the use of a switchable configuration requires the implementation of two different robotic platforms for each unit. In this case, the battery unit is heavier and therefore requires a chassis which can stand against heavier forces. At this point, a heavy-duty robotics platform will be used for the battery unit, while a lighter-duty chassis with less mass is enough to support

the components installed on the carrier unit. All the components mentioned and their corresponding masses are shown in Table 5.1.

Table 5.1: Bill of Materials for Built-in and Switchable Battery Configurations Regarding their Masses

Built-in Battery Configuration		
Unit Type	**Component Name**	**Mass**
Main Unit	$LiFePO_4$ Battery	125 Wh/kg
	DC/AC Converter	5 kg
	Motor	24 kg
	Heavy Duty Robot Platform	150 kg
	Robotic Arm	50 kg
	Onboard Charger	52 kg
Switchable Battery Configuration		
Unit Type	**Component Name**	**Mass**
Battery Unit	$LiFePO_4$ Battery	125 Wh/kg
	Heavy Duty Robot Platform	150 kg
	Onboard Charger	52 kg
Carrier Unit	$LiFePO_4$ Battery (10 kWh)	80 kg
	Lighter Duty Robot Platform	32 kg
	Motor	24 kg
	DC/AC Converter	5 kg
	Robotic Arm	50 kg

As shown in Table 5.1, the total mass of the main unit in the built-in configuration and the battery unit in the switchable configuration differs significantly for different battery capacities installed. On the other hand, the mass of the carrier unit is rather a constant and unchanging value of 191 kg. As the considered robotic platform can support carrying useful payloads up to 200 kg, the unit's total mass except the chassis suits the use of such a platform.

For the battery units in switchable configuration and the main unit in built-in configuration, the total mass, M can be expressed as a function of the battery capacity, Q in kWh. Meanwhile, for the carrier unit, a constant weight of 191 kg can be calculated. These functions are given in Equations 5.1 and 5.2.

$$M_{MainUnit}(Q) = \frac{1000 \cdot Q}{125} + 281kg \tag{5.1}$$

$$M_{BatteryUnit}(Q) = \frac{1000 \cdot Q}{125} + 202kg \tag{5.2}$$

As mentioned, in the built-in configuration, the travelling mass will be equal to the mass of the main unit given in Equation 5.1. On the other hand, in switchable configuration, the travelling mass will be equal to the sum of the mass of the battery unit given in Equation 5.2 and the carrier unit of 191 kg for one driving cycle, and only the carrier unit for another cycle. In this way, it can be expected that the switchable configuration requires slightly more energy due to the extended driving cycle, and higher overall mass getting mobilized during the first cycle.

5.3. Performance Requirements

The energy consumption of an electric drive train is dependent on various factors such as the forces exerted on the vehicle, and the degree of regenerative braking. Mainly, these forces and the resulting energy demand shape how much power and torque should be provided by the traction motor. Furthermore, in vehicle applications, the performance requirements of the drive line also impact the choice of traction motor and the required power and torque provided. Performance requirements could be described as top speed, gradability and acceleration [81].

5.3.1. Road Forces

The road forces applied on a mobile vehicle are rolling resistance force (F_{rr}), aerodynamic drag (F_{ad}), gradient force (F_{g}) and acceleration force (F_{a}). The total force exerted on a vehicle (F_{t}) can be calculated as the sum of these forces as shown in Equation 5.3.

$$F_{\mathsf{t}}(t) = F_{\mathsf{rr}}(t) + F_{\mathsf{ad}}(t) + F_{\mathsf{g}}(t) + F_{\mathsf{a}}(t) \tag{5.3}$$

Furthermore, the direction of these forces acting on the vehicle during travelling indicated in Equation 5.3, are demonstrated in Figure 5.3.

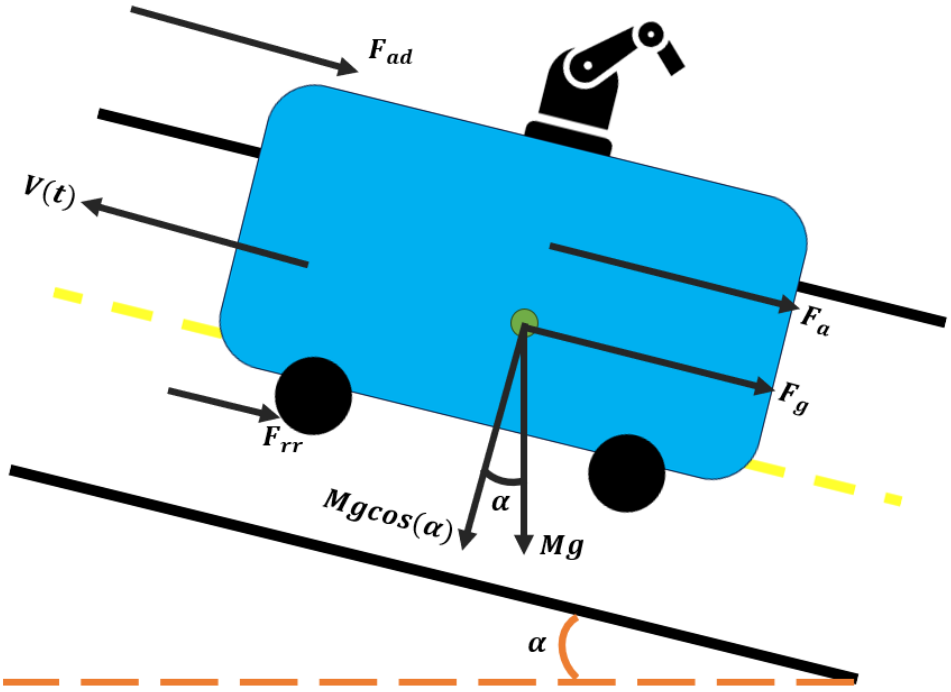

Figure 5.3: Forces Acting on the Unit while Travelling

Rolling resistance is primarily caused by the nonlinearities associated with the tire material during the rolling movement, due to the heterogeneous distribution of reaction force exerted by the ground observed in the contact patch. Next, the rolling resistance force can be calculated as introduced in Equation 5.4, where M denotes the mass of the vehicle, g is the gravitational acceleration and fr is the rolling resistance coefficient. The rolling resistance coefficient (f_{r}) varies with different road conditions and tyre properties such as inflation pressure and profile as well as the cruising speed. For the most common range of conditions, the coefficient can be approximated as a function of speed as shown in Equation 5.5 [51].

$$F_{\mathsf{rr}} = f_{\mathsf{r}} \times \mathsf{M} \times g \times \cos(\alpha) \tag{5.4}$$

$$f_{\mathsf{r}}(V) = 0.01 \times \left(1 + \frac{\mathsf{V}}{100}\right) \tag{5.5}$$

Furthermore, the aerodynamic drag force can be calculated by using Equation 5.6. This force is mainly a function of air density (ρ), drag coefficient (C_{D}), frontal area (A_{f}), velocity (V) and the wind speed acting on the vehicle (W). Air density can be calculated by using Ideal Gas Law as shown in Equation 5.7. In the equation, p represents the absolute pressure, M the molar mass, R the ideal gas constant, T the absolute temperature, T_0 the standard temperature at sea level, L the temperature lapse rate, h the altitude above sea level, and p_0 the standard atmospheric pressure at sea level. Next,

an assumption is made regarding the drag coefficient and the frontal area values, since there is no possibility of experimenting with these parameters. Consequently, practical applications are investigated and the literature is scanned to find adequate values that can realistically represent the system. Further observations indicate that a mobile autonomous charging robot with similar specifications can be realized with dimensions of 1850 mm in length, 950 mm in width, and 1500 mm in height [122]. The frontal area value is derived by using these specifications. Moreover, it is further witnessed that a drag coefficient of 0.6 is used in the studies analysing the aerodynamic performance of delivery robots [195]. Therefore, this value is processed in the calculations assuming that the same coefficient of drag value can be obtained by implementing a similar outer shell design. Lastly, regarding the maximum speed observed in the driving cycle, it is also acknowledged that the effect of aerodynamic drag will be minimal compared to the other sources of loss.

$$F_{\mathsf{ad}}(\rho, C_{\mathsf{D}}, A_{\mathsf{f}}, V) = 0.5 \times \rho \times C_{\mathsf{D}} \times A_{\mathsf{f}} \times (V - W)^2 \tag{5.6}$$

$$\rho = \frac{pM}{RT} = \frac{pM}{RT_0\left(1 - \frac{Lh}{T_0}\right)} = \frac{p_0 M}{RT_0}\left(1 - \frac{Lh}{T_0}\right)^{\frac{gM}{RL}-1} \tag{5.7}$$

The gradient force can be described as the extra force that has to be overcome while the vehicle is climbing uphill. This force can be towards the longitudinal direction if the vehicle is cruising downhill since gravity will act as a force speeding it up. The force can be calculated as a function of vehicle mass (M), gravitational acceleration (g) and the gradient angle (α) as shown in Equation 5.8. In this study, it is assumed that there is no considerably steep gradient in the parking place as is often the case and hence the angle α is taken as 0.

$$F_{\mathsf{g}} = \mathsf{M} \times g \times \sin(\alpha) \tag{5.8}$$

Lastly, the acceleration force can be calculated as shown in Equation 5.9 as a function of instantaneous acceleration.

$$F_{\mathsf{a}}(a) = \mathsf{M} \times a \tag{5.9}$$

5.3.2. Power Ratings and Energy Consumption

The total required power for the travel as a function of time can be calculated as shown in Equation 5.10.

$$P_{\mathsf{r}}(t) = (F_{\mathsf{rr}}(t) + F_{\mathsf{ad}}(t) + F_{\mathsf{g}}(t) + F_{\mathsf{a}}(t)) \times V(t) \tag{5.10}$$

However, the power drawn from the battery will be higher than the instantaneous power requirement due to the losses associated with the drive train. The efficiency of the traction motor and the mechanical losses due to the parts in contact can be classified as the root causes of this efficiency factor, denoted by η_{M}. This factor is taken as 0.9. Furthermore, there is also the auxiliary power, P_{aux}, consumed by the electronic appliances operating during the travel. An auxiliary power of 60W is considered in the system as this value is used in the studies focusing on the design of autonomous delivery robots [195]. These are mainly the sensors and lights that monitor the surrounding area ensuring safe operation. Lastly, a certain amount of power will be required to keep the cooling system operating, denoted by P_{cooling}. This system is crucial to keep the batteries at the optimal temperature to ensure both safety and efficiency. It is reported that the consumption associated with the cooling ranges between 1.3% and 11.2%, depending on the driving cycle, ambient temperature conditions and the refrigerant type used [113]. Following this interval, the power consumed by this system is assumed as 6.25% of the total power, which is the average reported value. When the efficiency, cooling and this auxiliary power are taken into consideration, the power drawn from the battery can be calculated by the following Equation 5.11.

$$P_{\mathsf{b}}(t) = \frac{P_{\mathsf{r}}(t)}{\eta_{\mathsf{M}}} + P_{\mathsf{aux}}(t) + P_{\mathsf{cooling}}(t) \tag{5.11}$$

Lastly, thanks to the use of an electric machine, a portion of the braking energy will be recuperated by using the motor as a generator. In this case, as the maximum regular deceleration of the driving

cycle is $0.278\,\mathrm{m/s^2}$, most of the braking power can be supplied by the motor, causing mechanical brakes to play a minimal role unless it is an emergency braking. Hence, it is assumed 70% of the energy will be regenerated as this ratio is also realisable in trained economic style driving in passenger cars [45]. This factor is denoted by η_{reg}. Consequently, the instantaneous energy regenerated at the instances of deceleration, E_{r}, is calculated as shown in Equation 5.12.

$$E_{\text{r}}(t) = \frac{1}{2} \times M \times [V(t+1)^2 - V(t)^2] \times \eta_{\text{reg}} \tag{5.12}$$

Then, the instantaneous energy spent travelling by the batteries can be calculated by the following Equation 5.13. It is important to note that the regenerated energy is in Joules, and therefore a conversion step to kWh is necessary as presented in the equation.

$$E_{\text{t}}(t) = P_{\text{b}}(t) \times \Delta t + E_{\text{r}}(t) \times 2.7778 \times 10^{-}7 \tag{5.13}$$

As soon as the energy required is calculated dependent on the speed and acceleration depicted on the driving cycle at each second, the total energy that will be spent on travelling during one travelling period can be calculated by summing up all the energy requirement values throughout the cycle. These energy consumption values are plotted for each battery capacity value and each different configuration, built-in and switchable. The resulting plot is shown in Figure 5.4.

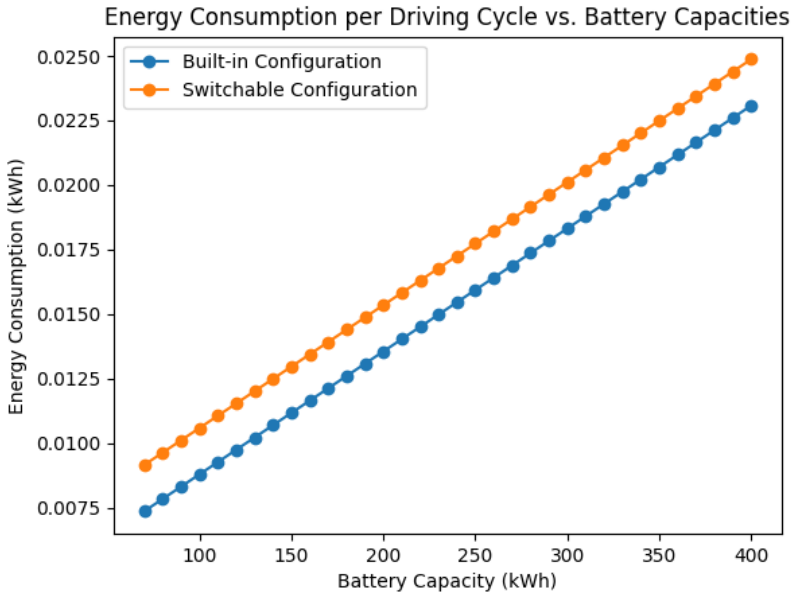

Figure 5.4: Total Energy Consumption during the Driving Cycle for Different Configurations and Battery Capacities

As shown in Figure 5.4, the amount of energy that will be fed by the battery differs between 0.0075 and 0.025 kWh, depending on the battery capacity and configuration used. As expected, the switchable configuration demands more energy per travel due to its extended driving cycle and slightly higher mass carried by the robot during the first cycle. For example, when a 270 kWh battery is used, the switchable configuration requires 10.53% more energy. In detail, this consumption is around 16.9 Wh for the built-in configuration, while it is 18.68 Wh for the switchable case. Hence, it can be concluded that even if the switchable configuration requires more energy due to the argued reasons, the difference is not significant especially compared to the other type of exchanges the battery undergo with 10s of kW power.

Sample values obtained in the literature focusing on similar analysis are researched to check the consistency of this calculated value. Similarly, in a study, a driving cycle is designed for an automated guided vehicle which carries a 1.2t payload to a designated point and comes back to the starting point unloaded [142]. Furthermore, the platform has a mass of 343 kg, which makes the total travelling weight around 1.5t [5]. The studied robot is further equipped with fuel cells and hydrogen storage

systems which contribute significantly to the overall weight, however, the physical parameters regarding these components are unspecified. The cycle takes around 125 seconds and the robot cruises with a velocity between 0.8 and 1 m/s. Following this route, the vehicle consumes 131.2 Wh of energy at the end of 5 cycles, which is equal to 26.24 Wh per cycle. Considering that this driving cycle bears similarities to the one designed for the switchable configuration, and 1.2t on payload can correspond to 150 kWh of battery storage, the calculated energy consumption per cycle is around 13 Wh for the mobile system. Although this value is comparable to that in the study, the reported value is higher because the vehicle's route includes lots of stop-and-go cycles [142]. This frequent acceleration causes higher energy consumption than mostly steady-speed cruising which is considered in this study. Another reason could be due to the unspecified mass of the components implemented in the system researched, which are heavy equipment powering a fuel cell system.

Furthermore, in order to represent the power drawn by the battery during the travel, the total energy spent on travelling is averaged over 5-minute time steps. The calculation method is shown in Equation 5.14.

$$P_{\mathrm{M_{avg}}} = \frac{\sum_{t=1}^{300} E_{\mathrm{t}}(t)}{\frac{5}{60}} \tag{5.14}$$

Even if the use of the switchable configuration does not significantly affect the total energy consumed in travel, its effect on the maximum power required by the traction motor is also investigated. As the total mass mobilized during the first cycle is slightly higher in this case, the required maximum power that will be delivered by the traction motor is calculated and compared for each configuration. As a result, maximum power requirement values are plotted for each case as a function of the battery capacity as presented in Figure 5.5. The shown data points represent the maximum values obtained in Equation 5.10 for each case.

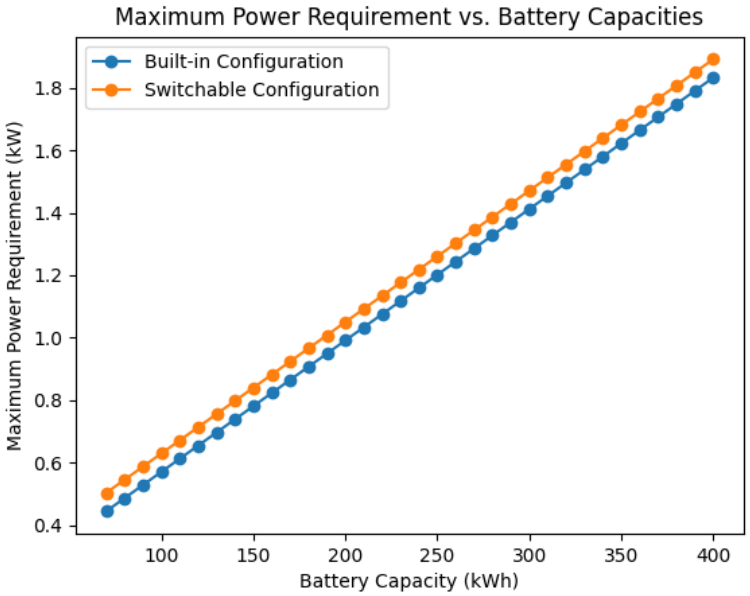

Figure 5.5: Maximum Power Requirement during the Driving Cycle for Different Configurations and Battery Capacities

As shown in Figure 5.5, the use of a switchable configuration requires the maximum power delivered by the traction motor to slightly increase. For example, for a 270 kWh main battery capacity, the built-in configuration requires 1.286 kW of peak power while this value for switchable configuration is around 1.34 kW. This change in the configuration requires 4.2% more peak power. However, this peak power is only required when the maximum acceleration of $0.278\,\mathrm{m/s^2}$ is attained just before the unit reaches its maximum velocity in the driving cycle. Considering that this acceleration rating is observed only for a few seconds, its effect on the total energy consumption is therefore limited.

In addition, this maximum power rating is also compared to the values reported in the literature. As a result, the study mentioned while comparing the energy consumption underscores a peak power rating of around 1.4 kW [142]. Even if the maximum acceleration which is the main factor describing the peak power is not specified in the study, it is observed that the reported value is within the calculated range shown in Figure 5.5.

Instantaneous power required by the traction motor throughout the driving cycle is plotted in Figure 5.6. The plot also shows the mentioned peak powers as well as when they are required for each configuration.

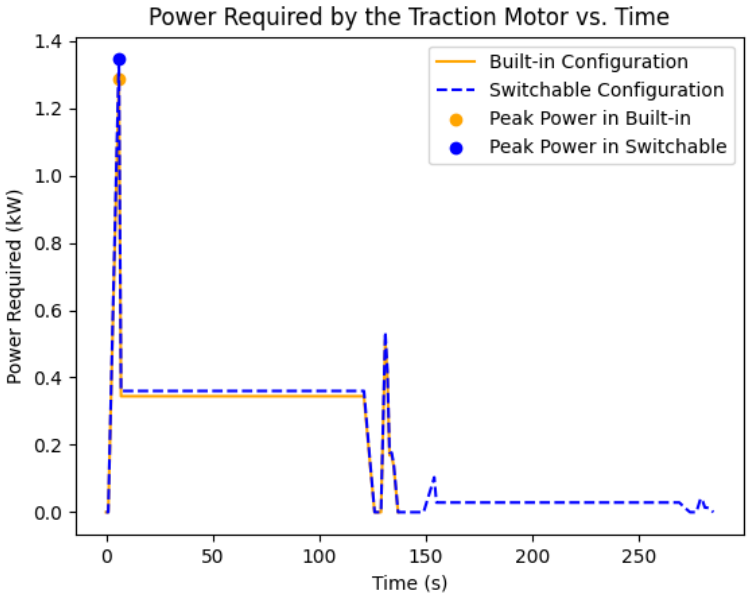

Figure 5.6: Power Requirement by the Traction Motor during the Driving Cycle for Different Configurations with 270 kWh Battery Capacity

As shown in Figure 5.6, the power required by the traction motor to realise the driving cycle increases as the unit accelerates. At this period, the power requirement increases due to the overcoming of the growing road forces as a consequence of the increase in cruising speed. Hence, the power is mostly determined by the road forces and acceleration force. At the peak point, the switchable configuration requires more power primarily due to the increase in mobilized mass. As soon as the unit reaches its maximum speed, it sustains a stable speed and hence the motor power is only used to overcome the road forces. As the vehicle decelerates, the road forces decrease and eventually become zero. Then, the unit accelerates again to manoeuvre towards the parking lot and reaches its secondary stable speed. This movement is presented by the second peak in the plot. Finally, after the unit sustains the second stable speed for a short amount of time, it comes to a full stop. With a switchable configuration, the battery unit is detached and docking takes place in this time interval to connect the charger to the EV. Following that, the carrier unit continues towards the second operation point in stand-alone operation mode. As the mobilized mass is much lower in this secondary cycle, the power requirement is proportionally much less.

5.4. Traction Motor Selection

Regarding the propulsion system of the units, there are lots of different options that can be implemented. Primarily, as the traction motor will be fed by a battery, which is a fundamental DC source, the traction motor can be chosen among AC and DC electric machines. In detail, a motor drive to invert DC to AC is required in between the battery and the traction machine if an AC motor is utilized. On the other hand, this inversion step can be excluded when a DC motor is used, rather a voltage and current regulator can be used to control the motor's speed and torque output.

DC motors have historically garnered attention due to their straightforward control and the ability

to separate flux and torque by controlling field and armature currents independently [88]. However, their reliance on brushes and rings for construction has led to maintenance challenges. As vector control for AC motors became more prominent, the appeal of DC motors faded, particularly in traction applications [88]. Despite this shift, DC motors remain viable for low-power tasks. The commutator serves as a durable inverter, simplifying and reducing the cost of power electronics devices [88].

Induction motors have emerged as a remarkable choice due to their reliability, durability, minimal maintenance requirements, and adaptability to harsh environments. Furthermore, flux weakening enables an expanded speed range within the constant power zone [88].

Permanent magnet synchronous motors (PMSM) are an important competitor of induction motors in traction applications. These motors offer several advantages, including higher power density, improved efficiency, and more efficient heat dissipation [88]. Despite their benefits, PMSMs are susceptible to demagnetization due to heat or armature reaction, which represents a notable drawback [88]. On the other hand, PMSMs typically rely on rare-earth magnets composed of metals such as neodymium, praseodymium, and dysprosium. These metals are often sourced through mining practices that pose environmental and ethical dilemmas.

Switched reluctance motors are increasingly gaining attention for use in traction systems. These motors offer a range of benefits including straightforward and robust construction, fault tolerance, easy control, and impressive torque-speed performance [88]. However, they come with some drawbacks such as high noise levels, significant torque ripple and susceptibility to electromagnetic interference [88].

Regarding the introduced traction motor types, the requirements for the mobile system's powertrain should be high efficiency, low cost, high power density and low maintenance. High efficiency is important to secure the energy stored in the batteries for the EVs and energy arbitrage in order to support the profitability of the system. Furthermore, the cost of the traction motor is significant to minimize the investment cost of the system. Moreover, considering that the selected motor will be used in a mobile application where size and compactness are an issue, the motor's power density bears significance to using the packaging area more efficiently. Lastly, low maintenance is a key parameter to minimize the operational costs associated with the system and avoid downtime.

Due to the maintenance challenges of the DC machine, it is not found suitable for this powertrain application. It is also noted that this challenge can be addressed by using brushless DC motors, however, due to their higher cost and lower power density in terms of mass and size, it is concluded that the use of this type of motor also brings additional challenges [26].

Compared to switched reluctance and brushless DC motors, induction motors appear as a remarkable choice due to their higher power density and lower costs [26]. The use of this type of motor can facilitate a better use of the packaging area of the robot. Especially, in the built-in configuration, effective packaging is vital due to the higher number of components embodied in the main unit. At this point, the induction motor can take up less space and mass, contributing to the efficient use of space and energy. Furthermore, it is important to note that as this type of motor has a wide range of applications in the industry, the technology is very mature enough to allow the manufacturing of reliable motors [26]. In terms of efficiency, PMSMs can outperform induction motors due to the hindrance of rotor losses [203]. However, the use of PMSM motors brings along higher investment costs and the use of precious metals which can raise questions about the sustainability of the system. The use of rare earth metals inherently conflicts with the main motivation of the system, which is acting as a step towards the sustainable mobility transformation. Despite its slightly lower efficiency, it can be concluded that the use of an induction machine in the system outperforms PMSM due to its lower cost, and robustness. It is also important to note that the effect of this slight inefficiency will not be very considerable when considering the fact that the total energy spent on travel is just a small and inconsiderable percentage of the total energy bought from the grid. For example, this percentage takes up around 0.12% - 0.2% of the total energy use, depending on the grid capacity, when a 270 kWh system is used.

6

Power Conversion

This section discusses the electronic power conversion topologies that can act as a bridge between the system and EVs. DC/DC converter topologies are introduced with their advantages and disadvantages. Reported performance critiques are demonstrated to highlight the most suitable converter in stationary and mobile applications to set a basis to answer Research Sub-Question 6.

An efficient power conversion topology is vital in Mobile EV Charging systems because there are different types of voltage and current ratings involved, flowing through multiple directions. To accomplish desired functionalities, there have to be different conversion steps, regulating the energy flow. The characteristics and the duties of the system directly affect the endpoints and how much energy should be flowing. In this particular system, the endpoints can be listed as the grid, battery, motor and EV. Furthermore, the battery can charge itself with the energy fed by the grid and discharge to sell to the grid, while powering the electric machine and recuperating. Therefore, the designed topology must be sufficient to facilitate bidirectional energy flows between the battery and the grid and between the battery and electric machine as well as a unidirectional flow between the battery and the EVs. These endpoints and flow directions are illustrated in Figure 6.1.

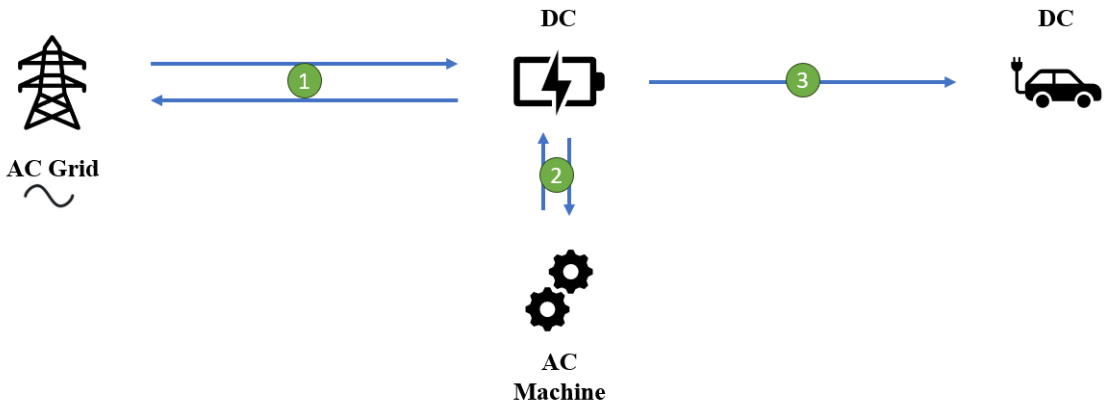

Figure 6.1: Illustration showing the energy flow directions and endpoints

As shown with number 1 in Figure 6.1, the battery will be charged by the energy flowing from the AC grid. Before getting stored in the battery, the energy has to go through two different conversion steps. First, alternating current must be converted to direct current and secondly, voltage and current ratings should be adjusted considering the DC line voltage. These two steps can be done in different sequences. At this point, two different topologies can be proposed. The first one suggests that the AC can go through a transforming step to adjust the voltage rating and then get rectified while the second one proposes a rectification step first followed by voltage stepping up and down. However, it is crucial to remember that the system is also able to do energy arbitrage and hence sell energy to the grid once

there is a price incentive. Thus, this flow and the topology implemented must be suitable for operating bidirectionally.

Moreover, the energy stored in the battery can be used for two more purposes such as powering the AC machine to travel between the parking lot and hub and vice versa as shown with number 2 in Figure 6.1, or charging the EV as shown with number 3. For number 2, an inversion step is necessary to feed the machine with AC as well as a frequency and voltage regulation to control the speed and torque of the machine. Furthermore, the machine can be used as a generator while braking to use the energy more efficiently, feeding a portion of the waste energy back to the battery, and pointing out a bidirectional operation again. For number 3, a unidirectional flow is observed while charging EVs with regulated power and voltage ratings by the Battery Management System (BMS) through the communication protocol.

To implement a suitable power electronics topology in the system, protocols and standards are vital to avoid compatibility issues. These industrial standards make the charging applications safe and accessible, paving the way for a high level of integration. They form a bridge between the EV manufacturers and charging applications so that the designed solutions can work seamlessly with different types and varieties of vehicles. International standards regulating the charging applications are SAE, IEC and CHAdeMO standards [83]. These standards and their respective power, voltage, current and location regulations are summarized in Figure 6.2.

Charging Power Levels	Location for charger	Expected power level
AC and DC Charging based on SAE STANDARDS		
Basic: Level 1 Charging • Vac = 230 (EU) • Vac = 120 (US)	Single Phase • On-board	• P = 1.4 kW with (12 A) • P = 1.9 kW with (20 A)
Main: Level 2 Charging • Vac = 400 (EU) • Vac = 240 (US)	Single Phase/Three Phase • On-board	▶ P = 4 kW with (17 A) ▶ P = 8 kW with (32 A) ▶ P = 19.2 kW with (80 A)
Fast: Level 3 Charging • Vac = 208–600	Three Phase • Located Off-Board	• P = 50 kW • P = 100 kW
Level 1: DC Charging • Vdc = 200–450	• Located Off-Board	• P = 40 kW with (80 A)
Level 2: DC Charging • Vdc = 200–450	• Located Off-Board	• P = 90 kW with (200 A)
Level 3: DC Charging • Vdc = 200–600	• Located Off-Board	• P = 240 kW with (400 A)
AC and DC Charging based on IEC STANDARDS		
AC Power Level 1	Single Phase • On-board	• P = 4–7.5 kW with (16 A)
AC Power Level 2	Single Phase/Three Phase • On-board	• P = 8–15 kW with (32 A)
AC Power Level 3	Three Phase • On-board	• P = 60–120 kW with (250 A)
DC Rapid Charging	• Off-Board	• P = 1000–2000 kW with (400A)
CHAdeMo Charging Standard		
DC Rapid Charging	• Off-Board	• 62.5 kW with (125 A)

Figure 6.2: Industry Standards for EV Charging Applications [83]

According to the standards in Figure 6.2, the Mobile EV Charging in the study is categorized as a DC Charger. These types of chargers are located off-board according to all three standards while their power outputs differ according to their levels. Since the aim of the system is to charge vehicles as fast as possible to spend the minimum amount of time outside of the hub to exchange energy with the grid when it is optimal, the charging activity can be classified as the highest level possible. In the Netherlands, the DC fast charging stations are equipped with 50 kW and 175 kW chargers. Furthermore, CharIN also announced an enhanced CCS standard realising charging powers up to 350 kW in 2017 [28], [76].

On the other hand, it is also important to analyse the maximum charging power of the 10 most popular vehicles used in the Netherlands. These power values are shown in Table 6.1.

Table 6.1: Electric Vehicle Models and Max DC Charging Powers [62][66][68][61][64][65][63][60][67][69]

EV Model	Max DC Power (kW)
Tesla Model 3	175
Kia Niro	80
Volkswagen ID3	124
Hyundai Kona	77
Renault Zoe	46
Skoda Enyaq	143
Nissan Leaf	46
Audi eTron	155
Tesla Model S	175
Volkswagen Golf	40

As Table 6.1 shows, the Tesla Model S has the highest charging power of 175 kW, when a CCS charger is used. Therefore, the system should be sufficient to support this charging power.

6.1. Charging System Architecture

The design choices branch under two different configurations. The first one requires a portable on-board charger implemented in the mobile system while the second requires a stationary application in which the charger is located beside the parking lot so that the mobile system gets autonomously connected. In both of the systems, as the endpoints of the charging activity are the batteries, the conversion will be from DC to DC. This power conversion topology has certain requirements regarding the industry standards and necessities of its duty. In order to successfully and effectively fulfil the duty necessities, it should efficiently regulate the voltage and current ratings according to the information acquired from both of the BMSs regulating the power. These ratings are primarily dependent on the SoC of the batteries as well as the cell conditions. Secondly, because the conversion will take place in a publicly available area, it should ensure safe operation and must not compromise security when unexpected accidents happen. This could be provided by galvanic isolation. Significant leakage current can be present in non-isolated chargers when they lack galvanic isolation. This leakage current poses safety hazards for the surroundings and the electronic components equipped [211]. The chosen architecture should also maximise the power quality, with a high power factor and hence control the injected harmonics as numerous regulations exhibit standards regarding the harmonic distortion, such as SAE: J2894 (Power Quality Requirements for Plug-In Electric Vehicle Chargers) [96] and IIEC 61000-3-2 (Electromagnetic compatibility (EMC)) [101], [84]. Furthermore, the selected topology must not compromise the efficiency of the system, minimizing conductive and switching losses. The physical parameters of the charger also bear significance such that the volume must be considered in mobile applications while the dimension of the charger matters in stationary applications to minimize public space use. Lastly, cost-effectiveness should also be an important criterion to attract the investor ground. In this regard, it is also important to note that the stationary application requires this topology to be located beside every parking lot, significantly increasing the costs associated with the system, while the mobile application can fulfil the bridging task by only requiring them to be implemented in the units. Stationary bridging also hinders the overall convenience of the system, requiring human intervention to do the plugging job, while the mobile application can do it autonomously.

6.2. Converter Topologies

Output power is a significant factor when deciding on the power electronics topology. Hence, converter applications' performance can mainly differ according to the charging power level. Some basic topologies of DC/DC converters can be listed as forward, fly-back, half-bridge, full-bridge and push-pull converters.

6.2.1. Basic Configurations

Flyback converters are generally cheaper and easier to install since they only require a single active switch. Therefore, their overall cost is lower and control is relatively easier. They also have galvanic isolation which is a necessary feature for the safety requirements. Furthermore, the overall number

of components involved in the topology is limited, supporting the cost-effectiveness and simplicity. On the other hand, this converter topology is widely used in low-power applications [84]. The primary reason for this is due to its reliance on one magnetic element such as a transformer. When the winding experiences high voltage resulting from high power applications, the core can reach saturation and therefore cause leakage flux inducing current nearby as well as causing distortion in the secondary winding [147]. This phenomenon could cause overheating, reduced efficiency and damage to the power electronics. Furthermore, in this topology, the primary switch is exposed to high-voltage stress during the switch-off state [84]. This stress gets even higher in high-power applications. Despite its simplicity and low cost, this kind of topology is not the best fit for the system considering its high power requirement. Meanwhile, similar issues can be faced in the forward converter due to its reliance on one transformer [84]. Additionally, the maximum duty cycle of the converter is limited by the reset time of the transformer, significantly limiting the maximum power it carries [84].

On the other hand, half-bridge, full-bridge and push-pull converters appear as a better choice for fast charging applications. One of the main reasons is unlike forward and flyback converters, the energy transfer takes place during the full input waveform, causing a better utilization of the magnetic core in the absence of a reset period. This also paves the way for higher duty cycles, realising higher power transfers. This is primarily accomplished by complementary switching. However, one notable limitation of push-pull topology is the voltage stress experienced by the input switch [84]. This stress can even reach higher than the input voltage when the switch is off due to the induced voltage by the energy stored in the transformer in the form of magnetic field [84]. The sudden change of current through the primary winding during switching is the main cause of this phenomenon. Meanwhile, this problem is not observed in the half-bridge converter. The main reason is when one of the switches is in the off state, the voltage is shared by two switches, reducing the voltage stress of the components during the complementary switching. However, the main problem associated with half-bridge topology is the intermittency of the output current during the step-up operation mode [84].

Despite the additional costs due to the higher number of switches and the relevant complexity, a full-bridge converter is also a popular option in high-power applications. Compared to half-bridge, two times higher voltage outputs can be obtained with the same input voltage, resulting in lower output currents and conductive losses [172]. This especially appears as a major benefit in high-power applications, since the same power can be transferred by less currents and losses.

Traditionally, the full-bridge converter topology has been the favoured option for achieving high-power DC–DC conversion [43]. Nevertheless, issues resulting from the transformer's leakage inductance and resulting reverse recovery dissipation issues in output diodes restrict the feasible switching frequency [13]. The presence of these challenges necessitated the exploration of alternative solutions to enhance performance. In response to the limitations posed by the conventional full-bridge converter, various solutions have been proposed. These include the implementation of active clamps and/or auxiliary circuits [47] [145]. These solutions aim to overcome the constraints on switching frequency, enabling higher rates. However, it is important to note that these enhancements come at a cost, involving the incorporation of additional components and potentially subjecting devices to increased stress [13]. Even if these techniques increase the power density of such applications at the expense of complexity, it is also noted that the resulting efficiencies are indifferent to the traditional switching techniques [13].

6.2.2. Dual Active Bridge (DAB) Converter

Some of the problems associated with Full Bridge Converter can be addressed in DAB converter topology, making higher switching frequencies and a subsequent increase in power density possible [13]. As a consequence, it is further noted that remarkable power densities around 11.13 kW/L can be achievable by implementing this converter in high-power applications in the literature depending on how efficient the cooling system is [146].

The DAB converter utilizes galvanically isolated dual full-bridge circuits to deliver high efficiency and enhanced switching performance through soft switching, alongside superior power density [77], [134]. This topology becomes a remarkable choice, especially in applications requiring bidirectional energy flow such as V2G applications. DAB converter's operation mode depends on the DC voltages of the input and output sources and it can either operate in buck or boost mode. Output power is generally controlled by modulating the phase shift between the input and output voltages. A circuit diagram corresponding to a conventional DAB converter is shown in Figure 6.3.

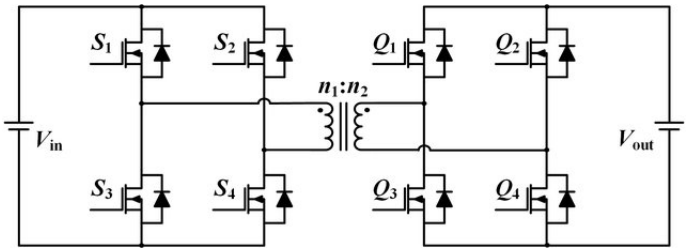

Figure 6.3: A Conventional Dual Active Bridge Converter Circuit Diagram [208]

In this topology, the output inductor can be in series with the leakage inductance resulting in the transfer of the energy stored to the output without increasing the reverse recovery losses in the output diodes, in contrast with conventional Full-Bridge Topology [13]. This supports a more efficient operation, reduces the stress on the diodes and makes higher switching frequencies possible. Furthermore, less number of passive components are employed in this topology, compared to the Full Bridge Converter, which is another advantage in terms of power density. However, it is also important to note that more switches are used in this converter [157]. Lastly, even though the DAB converter can achieve soft switching as explained in the next chapter, the operation range is limited by the transformer turns ratio and voltage gain [157].

6.2.3. Resonant Converters

Switching frequency is also a key factor affecting the power density of the equipment. Typically, the passive elements implemented in converters such as inductors charge and discharge energy during each cycle of switching. Hence, there exists an inverse proportion between the inductance and the switching frequency such that higher switching frequencies can result in less inductance and less space and weight [132]. This relation becomes even more important in mobile applications, where efficient packaging is key. On the other hand, the increase in switching frequency also escalates the associated losses and diminishes the overall efficiency of conversion. This trade-off sheds light on such techniques as Zero Voltage Switching (ZVS) and Zero Current Switching(ZCS). These methods can support high switching frequencies while not compromising efficiency, helping to achieve higher power densities [132]. Fundamentally, these soft switching methodologies set the switching to happen while the voltage or current across the devices is approaching or equal to zero to minimize the losses and eliminate the abrupt changes [132]. Employing these techniques minimizes the energy dissipation during switching, supporting the realisation of higher frequencies with a minimum amount of losses. Lastly, such techniques also help to reduce the abrupt changes in the voltage and current across the components, decreasing the ripple [84].

Among the various DC-DC converter technologies explored in the EV charging industry, particular attention has been directed towards resonant power converters. Improving the effectiveness of EV chargers requires careful attention to certain aspects. One important factor is the implementation of a soft switching technique in these converters. In this way, abrupt changes when the power devices switch can be smoothed out, leading to fewer losses during these transitions. Consequently, switching losses can be minimised. The outcome is an increase in overall efficiency during the charging process [84].

Additionally, a significant focus is placed on dealing with high voltage peaks in the charging system. Steps are taken to lessen these voltage peaks when the system converts alternating current to direct current resulting from the isolation, ensuring a more controlled and smoother power flow to the electric vehicle. Managing this aspect is critical for making sure the charging system performs reliably [84].

In connection with these considerations, the progress of EV chargers also involves expanding the range where the output voltage is controlled. This strategic approach offers more flexibility, allowing the EV charger to work well across a wider range of EV models and SoC conditions. By broadening this controlled range, the charging system becomes more adaptable and robust, handling different situations effectively. This, in turn, contributes to creating a dependable and efficient charging infrastructure for electric vehicles [84].

Among multiple options, one of the most popular choices for reducing both switching and conduction losses involves employing different soft-switching resonant techniques across various converter con-

figurations. The design of efficient and effective chargers for electric vehicles benefits significantly from resonant topologies, primarily due to their high-performance switching operations. Types of resonant converters that take part in EV charging applications are series resonant converters (SRC), parallel resonant converters (PRC), series-parallel resonant converters (SPRC) and LLC resonant converters [84]. The circuit diagrams corresponding to these four various types of resonant converter topologies are shown in Figures 6.4, 6.5, 6.6, 6.7.

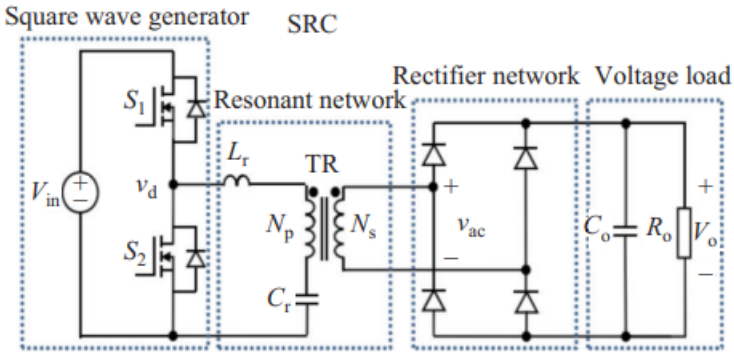

Figure 6.4: Series Resonant Converter Circuit Diagram
[84]

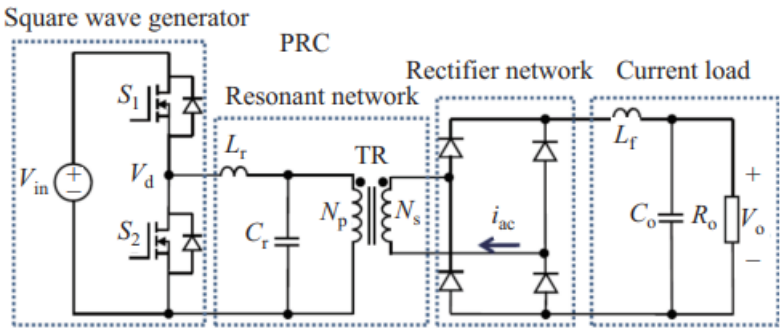

Figure 6.5: Parallel Resonant Converter Circuit Diagram
[84]

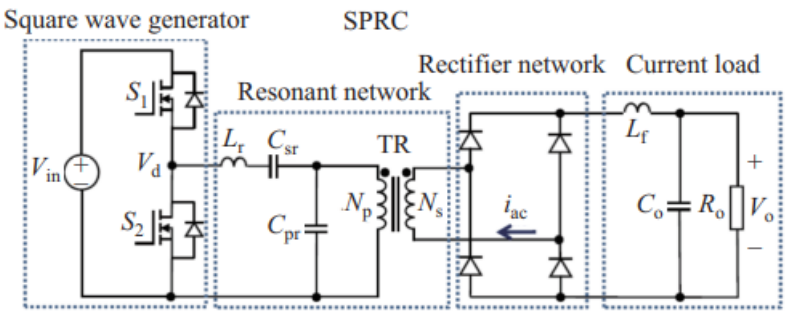

Figure 6.6: Series Parallel Resonant Converter Circuit Diagram
[84]

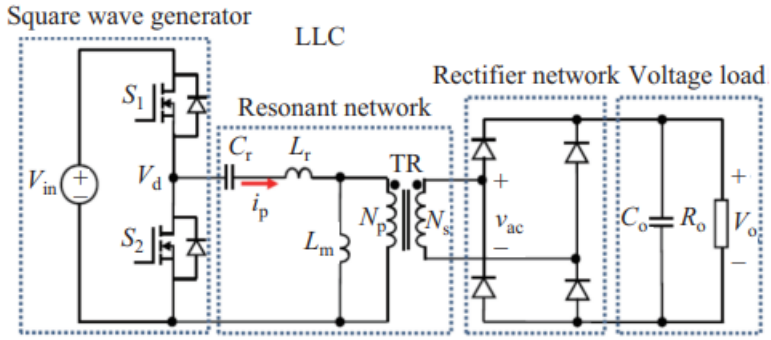

Figure 6.7: LLC Resonant Converter Circuit Diagram
[84]

A resonant power converter incorporates circuits that exhibit sinusoidal variations in voltage and current waveforms at specific points within the switching periods. In the context of power conversion applications, these converters demonstrate relatively low harmonic distortion due to resonant frequency-based switching [163]. While the use of electrical resonance is a prevalent method to achieve soft switching conditions, it brings about certain drawbacks when compared to traditional Pulse Width Modulation (PWM) converters such as the presence of additional reactive components, and observation of higher peak current or voltage [163]. Furthermore, limitations about the operating frequency of such converters, as well as the complexities in circuit controller design are the additional challenges introduced by such systems. Despite these limitations, resonant converters are gaining popularity due to their substantial contribution to reducing switching losses and improving waveform generation [163]. The mentioned sinusoidal waveforms are shown and associated switching losses are compared to a converter topology with hard switching in Figure 6.8.

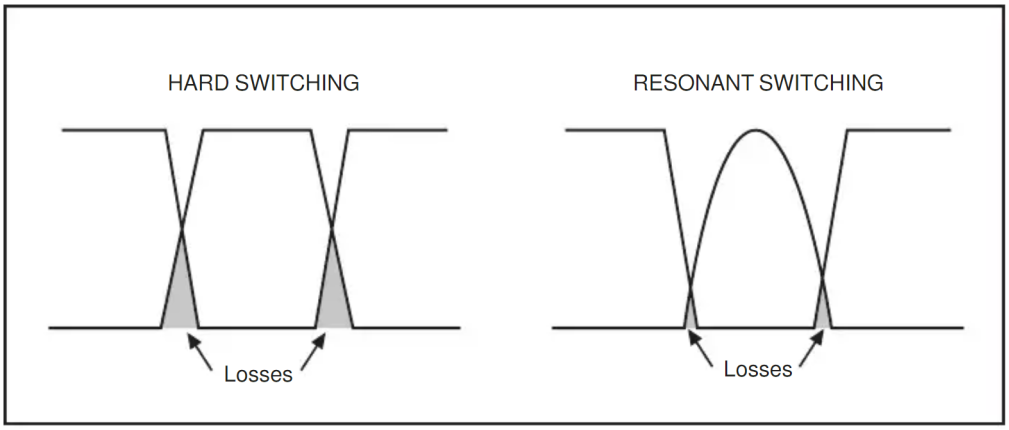

Figure 6.8: Difference in Switching Losses between Hard Switching and Soft Switching
[19]

As shown in Figure 6.8, the switching losses in a resonant switching converter are much lower due to ZVS and ZCS techniques employed.

A conventional Zero Current Switch setup comprises a switch positioned in series with the resonant inductor, while the resonant capacitor is connected in parallel [19]. During the switch's off state, the resonant capacitor undergoes charging with a relatively constant current, resulting in a linear rise in voltage across it. Upon switching on, the energy stored in the capacitor is transferred to the inductor, inducing a sinusoidal current [19]. In the negative half-wave, the current flows through the anti-paralleled diode, leading to a period where there is neither current through nor voltage across the switch. This facilitates turning off the switch without any energy dissipation [19].

On the other hand, a typical Zero Voltage Switch configuration consists of a switch in series with a diode [19]. The resonant capacitor is linked in parallel, while the resonant inductor is connected in series with this arrangement. A voltage source connected in parallel injects energy into this system.

During the switch's activation, a linear current traverses the inductor. After the switch turns off, the energy stored in the inductor flows into the resonant capacitor, generating a sinusoidal voltage across the capacitor and the switch [19]. The diode obstructs the negative half-wave of the voltage. In this interval, both the current and voltage in the switch hit zero, allowing for a lossless switch-on during this phase [19].

Series resonant converter employs a series connection of resonant inductor and capacitor. Despite its advantageous simplicity compared to other types of converters, it also brings about certain drawbacks. One of the major disadvantages of this topology lies in its nature. Since it acts as a voltage divider in steady state conditions, it brings about a lower average DC output voltage than the average input voltage [163]. This operational principle causes this topology to be insufficient by limiting the range of voltages the system can work with. For example, in this case, the maximum voltage that can be supplied is limited by the DC link voltage of the battery side and therefore can not be further increased. Lastly, ZVS can be sustained at higher frequencies than the resonance, while ZCS can be maintained at lower ratings, supporting efficient operation [163].

Meanwhile, this challenge of DC voltage gain is not observed in parallel resonant converters, allowing gain ratios larger than one [84]. The average DC voltage can be multiplied with the support of resonance-induced sinusoidal waveform [84]. On the other hand, the main challenge related to the use of parallel resonant converters is due to the higher energy flow exhibited during lighter load applications, limiting the operational range of the converter [84]. Similar issues can be observed while working with series resonant converters at no load condition, causing the regulation frequency to reach infinity, which can be solved by employing various control methodologies [84].

These challenges of high circulating energy flow and output voltage regulation under no load conditions can be addressed by series-parallel configurations connecting inductive and capacitive elements in series to the load and employing an output filter on the load side [84]. Furthermore, this topology is less dependent on the load changes, allowing an effective operation at a wider range of conditions and providing flexibility [9]. However, high input voltage ratings act as a source of switching loss, putting efficiency at stake [84].

Some of the main challenges associated with the mentioned resonant converters can be fixed by using LLC topology [84]. One major benefit of implementing this type of converter in EV charging applications is the flexibility of operation under different load conditions while maintaining a smaller switching frequency range [9], [84]. In resonant converters, the impedance of the resonant tank increases as the frequency increases due to the nature of the resonance phenomenon. The resonant frequency is the frequency at which the inductive and capacitive reactances are equal to each other. At resonance, the impedance of the tank circuit becomes purely resistive, and its magnitude is minimized. When the frequency increases beyond the resonance level, the capacitive reactance decreases, while the inductive reactance increases, resulting in a higher impedance and therefore higher energy circulation within the resonant tank. This brings about considerable losses in efficiency due to conductive losses [200], [84]. In LLC converters, it is possible to work under different loads while maintaining the frequency close to the optimal value, the resonance frequency [9]. Furthermore, in this application, zero voltage switching can be achieved within the whole operating range, including no load condition, decreasing the relevant switching losses and enhancing the overall efficiency [9], [84].

In the literature, high-power LLC converters examples are found with 98% peak efficiency and 42.7 kW/L power density [136].

6.3. Battery Charging Profile

While designing an EV charger, it is also crucial to address the typical charging profile of a Li-ion battery, equipped in vehicles. In order to decide on the best topology, analyzing the performance of various converters under different operation modes bears significance.

Typically, two different operation modes, Constant Current (CC) and Constant Voltage (CV), are employed in EV charging applications to maintain a good state of health of the battery by reducing cell degradation without compromising the charging speed [129]. CC mode consists of a stable current and gradually increasing voltage while CV mode starts as soon as the voltage reaches maximum with decreasing current. The maximum charging power is observed at the intersection point of current and voltage curves. In this operation mode, the cell voltages and currents are shown in Figure 6.9.

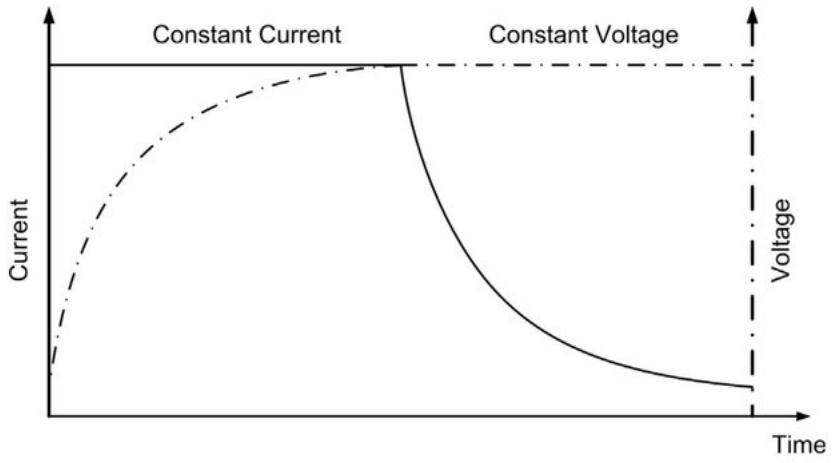

Figure 6.9: Typical Charging Profile of a Li-ion Battery
[129]

In a study to compare the performance of various resonant converters, a DC link voltage of 600V and primary resonance frequency of 200 kHz are designed to monitor and compare the switching frequencies of different topologies [200]. It is observed that the series resonant converter exhibits a switching frequency ranging between 219.9 kHz and 212.2 kHz during the CC mode, pointing out a close operation point to resonance frequency and therefore presenting a low circulating energy in the resonant tank. This paves the way for an efficient operation with reduced losses. On the contrary, a high switching frequency is observed during CV operation, around 370 kHz, showing an inefficient performance due to the enhanced switching losses even though the approximate circulating power is lower than parallel and series-parallel configurations. Its incapability of voltage regulation at low load is further noted. Due to these inadequacies, it is concluded that a series resonant converter is not a suitable choice in this kind of charging application [200].

Meanwhile, a switching frequency range between 221 kHz and 217 kHz is observed when a parallel resonant converter is used in CC mode. This proximity of value to the resonance frequency highlights the efficient performance of the conversion topology. Furthermore, it is also noted that the switching frequency ranged between 217 kHz and 233 kHz in CV mode, highlighting a much more efficient operation compared to series topology. On the other hand, its underperformance at low load conditions is further emphasized and 17 kVA of circulating power is approximated in the resonant tank, which is much larger than the calculated value in the series configuration, underscoring its poor efficiency [200].

Next, the switching frequency ranged between 277 kHz and 276.9 kHz in the series-parallel configuration test, exhibiting a higher value than the resonance frequency compared to the other two topologies tested in CC mode. This higher deviation from the optimal frequency demonstrates a higher circulating power in the resonant tank and results in less efficient operation. Further, in CV mode, the frequency ranged between 276.9 kHz and 325.3 kHz, operating at a much higher frequency than the ideal frequency. Circulated power is approximated as 14.1 kVA at low load conditions around 0.24 kW, highlighting the inefficient handling of low power, similar to the parallel configuration [200].

Finally, the LLC converter's switching frequency ranged between 193.3 kHz- 167.3 kHz at CC mode and 168 kHz- 176.3 kHz at CV mode, performing better than the other configurations tested. It further demonstrates a large slope of the voltage curve, proving a good voltage regulation performance at low loads, outperforming series configuration. Moreover, the circulating power in the resonant tank is approximated around 1.79 kVA, which is a much smaller value than the observed losses with parallel and series-parallel configurations at low loads. This value describes more efficient operation at CV mode [200].

6.4. Comparison of Power Converters

Discussed advantages and disadvantages of the converter topologies investigated in the previous sections are summarised in Table 6.2 to emphasize the differences in the most important selection criteria such as efficiency, and power density.

Considering the advantages and the drawbacks of the different converter types, the number of elements implemented in the system directly affects the system in terms of cost and power density as the elements take up space in the packaging area. However, the achievable frequency also matters to improve the power density of the converter topology. In this case, a higher number of elements could be compensated by higher operation frequency. Hence, the objective of the selection should be minimizing the cost while maximizing the efficiency and power density. Due to their outstanding properties in high-power applications, LLC, series resonant, full-bridge and DAB converters are remarkable and widely used topologies in the charging industry. Especially, in a mobile onboard charger where the dimensions of the converter play a key role, LLC resonant converter becomes prominent due to its high power density and efficiency values reported. However, compared to the other types, this converter has the most number of elements and therefore in stationary applications where high power density is not the priority, the simplicity of the DAB and full-bridge converter and their specifications can outweigh the advantages of a resonant converter. Even if it takes up slightly more space, the DAB converter's high efficiency and relatively small number of elements make it an excellent choice in charging applications where the equipment does not have to be mobilized. The number of switches can be further reduced by employing full-bridge topology. Especially, considering the stationary converter will be installed besides numerous parking lots, this could significantly reduce the associated costs. It is also important to note the control challenges associated with resonant converters. While they typically operate at the resonant frequency, a sophisticated controlling methodology has to be implemented to maintain ZVS and ZCS throughout the operating range with different load conditions. Resonant operation and nonlinearities due to the parasitic elements employed make it more complex to control LLC resonant converters in various load conditions while maintaining a good performance. Meanwhile, DAB and full-bridge converters may require a much simpler controlling methodology due to the nature of the bridge topology, possibly employing Pulse Width Modulation or Phase Shift Modulation techniques for controlling switches. This is also another advantage, making DAB and full-bridge converters a remarkable choice for applications where power density is not a priority. The research Sub-Question 6 can be answered in this way.

Table 6.2: Comparison of Various Converters

Converter	Advantages	Disadvantages	Efficiency	Power Density
Flyback	Requires only a single active switch, cheaper and easier to install and control. A limited number of components, cost-effective and simplicity[84].	Risk of saturation of magnetic core under high power applications [84].	-	-
Forward	Requires less number of switches, simple and cost-effective	Risk of saturation of magnetic core under high power applications. Limited duty cycle due to transformer reset time[84].	-	-
Push-Pull	Energy transfer occurs during full input waveform, better utilization of the magnetic core. Enables higher duty cycles and higher power transfers[84].	High voltage stress on the input switch[84].	-	-
Half Bridge	Voltage stress is shared by two switches during complementary switching, reducing stress on components[84].	Intermittent output current in boost operation[84].	-	-
Full Bridge	Allows for two times higher voltage outputs with the same input voltage, lower output currents and conductive losses[172]. High efficiency by ZVS [118].	Additional costs due to higher number of switches and increased complexity [172]. Leakage inductance of the transformer and related limits on switching frequency [13]. Voltage stress of the rectifier diode due to voltage oscillation [118].	97.2% @CC, 88% @CV [118], 97.25% [123]	6.56 kW/L [123]
DAB	Provides high efficiency and switching performance by ZVS [13].	Higher number of switches, more complex to control, limited soft-switching range [157].	96.6% @4 kW [82], 95.6% @80 kW [13]	11.3 kW/L [146], 7.1 kW/L [82]
Series Resonant	Simpler than other resonant converters [163].	Voltage divider in steady state conditions, lower average DC output voltage than the average input voltage [163]. Control challenges at no load condition[84].	High in CC, Moderate in CV [200]	2.38 kW/L [127]
Parallel Resonant	Allowing gain ratios larger than one[84].	High circulation of energy at light load [84].	High in CC, Low in CV [200]	0.97 kW/L [18]
Series-Parallel Resonant	Effective operation at a wider range of conditions, flexibility [9].	Higher number of elements [9]. Inefficient handling of low power	Moderate in CC, Low in CV [200]	10.2 kW/L [14]
LLC Resonant	Flexibility of operation under different load conditions while maintaining a smaller switching frequency range [9]. Zero voltage switching can be achieved within the whole operating range, including no load condition [84]	Complexity due to more elements, Challenging control	98% @ 3 kW [136], 97% @40 kW, 8.5 kHz [84] High in CC, Moderate in CV [200]	42.7 kW/L [136], 10.8 kW/L [94], 8.54 kW/L [133]

7

Conclusion

The thesis demonstrates an alternative solution to address the challenges associated with today's charging methodologies to further promote the widespread use of EVs. In this regard, the conducted analysis can set an example to highlight the effective and feasible use of robot-like mobile EV chargers along with the introduced benefits from different stakeholders' perspectives. In this regard, key findings and takeaways are presented to answer the Research Questions in Section 7.1 and future work is introduced in Section 7.2.

7.1. Answers to Research Questions

Introduced Research Questions can be answered below, combining the findings gathered from different approaches and analyses. The combination of answers to these sub-questions provides a comprehensive response to the Main Research Question, detailing the specifications of the developed mobile charging system.

1. **What are the challenges associated with today's EV charging systems? What alternative methods can be proposed instead of charging poles to address these challenges? What potential benefits can mobile charging bring along, compared to regular charging poles?**

   The main challenges associated with today's EV charging systems include long charging durations and a lack of available charging stations, often due to limited service or unnecessary occupation. Other issues involve cable handling, related safety and convenience problems, investment risks due to low utilization rates, urban space usage, and uncontrolled power and energy demand peaks on the grid. Introduced alternative methodologies are battery-less systems, large-scale battery-integrated systems, mobile or stationary battery swapping systems and robot-like systems with batteries (Section 2.2). Among these alternatives, robot-like systems demonstrate a remarkable solution to address the challenges associated with today's charging infrastructure, offering greater flexibility and convenience to drivers, supporting the electricity grid and exhibiting a remarkable investment opportunity. From the drivers' perspective, these systems can present reduced waiting times, improved availability and user-friendliness, contributing to the attractiveness of owning EVs while also offering slightly more affordable service compared to the fast charging alternatives offered today. From the grid's perspective, operating with a lower grid capacity such as 50 kW, the system can significantly reduce peak charging demand by 73%, decoupling the charging load from the grid, and potentially minimising the extra costs of improving the electricity infrastructure while still offering high power service. By engaging in energy arbitrage services, this integrated battery can also support the grid. The proposed system can store a portion of the surplus energy to be used during scarcity. This function can become very useful if renewable generation is the source of this surplus. The analysis demonstrates that this exchanged energy can reach up to 500 kWh when the system is allowed to utilize a high grid capacity of 100 kW. As a consequence, the developed system requires more investment when compared to the regular charging poles while yielding 40.7% to 61.82% more yearly profits, regarding the public and

workplace demand scenario. The system can also increase flexibility by allowing investors to redeploy more easily and review their investment decisions by dividing the total investment into smaller replacement rounds. In this way, the investment risks such as the uncertain price and interest factors can be avoided much more easily (Section 4). It is also important to note that this investment cost can also further decrease in the future as a consequence of steadily decreasing prices of components such as Li-ion batteries [174].

2. **What is the optimal configuration that can be suggested as a mobile charging solution in the urban setting?**

   Regarding the introduced mobile charging solutions, robot-like systems with batteries are remarkable solutions to reveal the full functionality of mobile charging while addressing the challenges associated with charging solutions applied today. These systems stand out for their ease of deployment and convenience in charging services, particularly suitable for the urban environment. Unlike large-scale battery-integrated systems, which may not be suitable due to scalability and integration challenges within limited service areas, robot-like systems offer a flexible and efficient alternative. Their relatively smaller battery size enables better performance in urban settings and requires less space. They also address the concerns associated with battery size, weight, and scalability issues that are present in other configurations such as battery swapping systems or charging vans. Furthermore, these robot-like systems are capable of providing fast charging options, helping to overcome some of the current challenges faced by drivers, such as the need for rapid charging to reach desired levels within a short timeframe. They also allow for effective energy arbitrage, thanks to their easier establishment of grid connections due to shorter service distances (Section 2). In addition, it is concluded that using a switchable battery configuration in robot-like systems can significantly minimise the amount of investment required to deploy the system. This configuration suggests the decoupling of the travelling necessity of the batteries from the units utilised, reducing the number of expensive components without sacrificing the full functionality. The investigation, which aims to show the frequency of concurrent movements, proves that 2 carrier units are sufficient to handle the mobility duties of 3 battery units without a significant service disruption. Using smaller carrier units to meet transportation requirements, it is revealed that this configuration can show the highest annual return on investment due to the possibility of showing the same effective operation at a lower cost (Section 4).

3. **How can a realistic demand estimation be conducted to identify the charging tasks the mobile system fulfils in a typical day?**

   A random demand sampling algorithm is developed to estimate the charging load on a typical day. This algorithm regards the probability of arrival times, energy demand, charging power and connection duration in a separate approach for private, public and workspace types of charging. Regarding this probabilistic data, the algorithm samples a set of charging operations in which the user input gives the number of daily operations. This number is determined by the capacity of the studied portion of the parking place, P1 at TU Delft Campus, along with the reported number of monthly public and workspace charging operations in the Netherlands. It further combines this sampled data with the specifications of the 10 most popular EV models used in the Netherlands and applies a correction to the sampled data. In addition, the algorithm accounts for the share of DC charging in public and workplace settings and incorporates fast charging by analyzing the charging profiles of ten studied EV models (Section 3).

4. **What could be an effective sizing strategy for this proposed mobile charging system? How many units should be considered and what should be the size of their batteries in the proposed configuration?**

   The sizing strategy should reveal an optimal balance regarding the profitability, investment costs and operational life period. In this regard, energy arbitrage acts as a source to maximise daily profits. Obtained data suggests that even though this method can pave the way for maximizing daily profits, more energy arbitrage brings along a heavy use of the batteries and therefore significantly limits the operational life and hence the total return of the system. Therefore, the findings suggest that, when a 50 kW grid capacity is used, the system can perform better in the long term

due to the longer service period while still doing limited energy arbitrage up to approximately 60 kWh. Consequently, the most effective strategy is highlighted, namely using the battery units mostly for charging EVs to utilize the invested material as profitably as possible, as realised with 50 kW capacity. This approach relies less on the electricity grid, realizing a significant reduction in peak demand, and supporting daily revenues through slight energy arbitrage, without heavily compromising the battery life. Furthermore, the obtained data reveals that with the use of 3 battery units and 2 carrier units in a switchable configuration, the system can yield a maximum yearly return on investment, which is an evaluation metric as a function of profits, battery life and investment cost. This configuration points out the greatest cash flow in unit time per amount invested, exhibiting an efficient business opportunity where maximum financial efficiency and sustainability are achieved. Under public and workspace charging demand, two battery capacities of 270 and 340 kWh are highlighted. The 270 kWh system demonstrates a more compact system, requiring 20% less investment without significant compromise on the yearly returns at the end of the third reinvestment round. Meanwhile, the 340 kWh system showcases 2.87% higher yearly profits on average, at the end of three reinvestment periods, even though it necessitates more investment. Furthermore, the system's performance is also evaluated under different input parameters. Load type is one of these parameters, changing the total amount of charging demand and schedule throughout the day. Accordingly, the system is tested under private load to represent a charging demand sourced by users unable to access a home charger at a residential location. In this case, the effect of energy arbitrage is verified and again 50 kW grid capacity is found as a better parameter in order to achieve longer operational life and more significant peak demand reduction. In addition, two battery capacities of 260 kWh and 310 kWh used in a switchable configuration made up of 3 batteries and 2 carrier units are highlighted to maximise the financial performance. The first capacity presents a more compact system with around 14.8% less investment cost while maintaining significant yearly profits, only 2.57% lower than the second suggested system (Section 4).

5. **How does the powertrain system need to be built to achieve the expected functionality and performance requirements, and what characteristics should the system possess to ensure suitability?**

   While investigating the performance requirements of the drivetrain, the effect of increasing the system's size and configuration on the total amount of energy consumed and peak power is analysed. To achieve this, an artificial driving cycle is developed to simulate its operation in the P1 Parking Area at TU Delft Campus. The results prove that using a switchable configuration increases the peak power demand by 4.2%, and energy consumption by 10.53%. However, as the total energy consumption values for the travel are not comparable to the other sources drawing power from the batteries, it is concluded that the advantages of this configuration can significantly outweigh this higher requirement. As a result, it is found that the system requires 1.34 kW of peak power while consuming 18.68 Wh per cycle when 270 kWh batteries are used. Accordingly, the traction motor types implemented in such applications are introduced and an adequate machine is selected for the system. As a result, the induction machine emerges as a notable option for meeting performance criteria while minimizing both initial investment and maintenance expenses. Its use promotes a more sustainable manufacturing process, aligning with the system's motivation by eliminating the need for rare earth elements. While the efficiency of this machine is slightly lower, its impact on the overall efficiency of the system is found negligible because travelling energy accounts for only 0.12-0.2% of the total energy intake when 270 kWh batteries are used (Section 5).

6. **How can the power conversion topology be implemented to act as a bridge between the system and EVs?**

   An effective power conversion is essential to support high-charging powers and the overall functionality of the system. In this regard, two different topologies are suggested to be used in stationary and mobile applications. The stationary application requires the charger topology to be located beside the designated parking lot to act as a bridge between the EV and the system. On the other hand, the mobile application requires the topology to be carried on board to facilitate a

fully autonomous docking process, without human intervention. The second one is found more advantageous in terms of charging convenience while it necessitates efficient unit packaging, since the additional hardware takes up space. Furthermore, the first one alleviates the concerns related to packaging while it exhibits a more costly solution due to the placement of the charger at every parking lot. In this regard, the LLC resonant converter is suggested as an adequate topology to be implemented in the mobile application due to its outstanding power density. In this way, high charging powers are achievable while allowing more efficient packaging and energy transfer with the help of ZVS and ZCS characteristics of this topology. The reported experimental data suggest that it is possible to obtain power densities up to 42.7 kW/L while not compromising the efficiency even though the control process is more complex [94], [207], [136]. On the other hand, for stationary applications where power density is less critical, DAB and full-bridge converters are recommended due to their simplicity and fewer components (Section 6).

In this way, the thesis demonstrates a multidisciplinary approach towards mobile EV chargers as an alternative to address today's necessities. It is proven that today's technology is well developed to realise such systems to operate in the urban environment and the economy is sufficiently scaled to make it profitable and viable, with potential for future improvement.

7.2. Future Work

To improve the analysis further, the following strategies can be taken into consideration.

- A simulation with more timesteps to represent a larger time horizon of a month or a year can be done with heuristics. Consequently, this way allows the capture of different price scenarios and circumstances, testing the resilience of the system in a complementary approach.
- When more computational resources are given, the analysis could be repeated with a higher time sensitivity, such as a minute. This way also allows capturing travelling durations more critically.
- Integrating renewable energy generation data would enable accurate measurement of the energy sourced from zero-emission sources, and facilitate a critical examination of the mobile system's performance in renewable energy integration. This data could be integrated by further developing the optimization model when more computational resources are allocated.
- Instead of relying on probabilistic data, real-time charging data taken from the site can be utilized. In this way, a more realistic approach, depending on the service location, could be developed. Instantaneous SoC data of the EVs could be further integrated to regulate the charging power of the mobile system if an effective linearization could be applied or a global solver with more time allocation is utilized.
- Conducting battery testing under conditions similar to those of the system could provide valuable insights and enhance the accuracy of lifetime calculations in future studies.
- An experimentation could also include the test of the proposed power converter topologies to examine their performances further under different CC and CV conditions and verify the reported values in the literature.

References

[1] Ahmed Abdulaal et al. “Solving the multivariant EV routing problem incorporating V2G and G2V options”. In: *IEEE Transactions on Transportation Electrification* 3.1 (2016), pp. 238–248.

[2] Shahab Afshar and Vahid Disfani. “A distributed ev charging framework considering aggregators collaboration”. In: *2021 IEEE Madrid PowerTech*. IEEE. 2021, pp. 1–6.

[3] Shahab Afshar et al. “A literature review on mobile charging station technology for electric vehicles”. In: *2020 IEEE transportation electrification conference & expo (ITEC)*. IEEE. 2020, pp. 1184–1190.

[4] Shahab Afshar et al. “Mobile charging stations for electric vehicles — A review”. In: *Renewable and Sustainable Energy Reviews* 152 (2021), p. 111654. ISSN: 1364-0321. DOI: https://doi.org/10.1016/j.rser.2021.111654. URL: https://www.sciencedirect.com/science/article/pii/S1364032121009291.

[5] AGV Network. URL: https://www.agvnetwork.com/robot-showroom-2/ad/platform,5/aformic-intralogistics-system,367.

[6] Vaibhav Ahluwalia et al. “Construction and benchmark of an autonomous tracked mobile robot system”. In: *Robotic Systems and Applications* 2 (Jan. 2022). DOI: 10.21595/rsa.2022.22336.

[7] Ali Ahmadian, Behnam Mohammadi-IVatloo, and Ali Elkamel. *Electric Vehicles in Energy Systems*. Springer, 2020.

[8] AI-WAYS EU. *Aiways granted patents for autonomous EV charging solution*. 2020. URL: https://media.ai-ways.eu/2020/aiways-granted-patents-for-autonomous-ev-charging-solution/.

[9] Nehmedo Alamir et al. “Fixed-frequency phase-shift modulated PVMPPT for LLC resonant converters”. In: *Journal of power electronics* 20 (Jan. 2020). DOI: 10.1007/s43236-019-00001-w.

[10] Muapper Alhadri et al. “Analysis of second-life of a lithium-ion battery in an energy storage system connected to a wind turbine”. In: *2019 IEEE Power and Energy Conference at Illinois (PECI)*. IEEE. 2019, pp. 1–8.

[11] All Charge Cards. *Shell Recharge*. 2024. URL: https://allchargecards.com/chargecard/5/Shell%20Recharge.

[12] Tinton Dwi Atmaja and Midriem Mirdanies. “Electric vehicle mobile charging station dispatch algorithm”. In: *Energy Procedia* 68 (2015), pp. 326–335.

[13] N.H. Baars et al. “A 80 kW isolated DC-DC converter for railway applications”. In: *2014 16th European Conference on Power Electronics and Applications*. 2014, pp. 1–10. DOI: 10.1109/EPE.2014.6910741.

[14] U. Badstuebner, J. Biela, and J. W. Kolar. “Power density and efficiency optimization of resonant and phase-shift telecom DC-DC converters”. In: *2008 Twenty-Third Annual IEEE Applied Power Electronics Conference and Exposition*. 2008, pp. 311–317. DOI: 10.1109/APEC.2008.4522739.

[15] M. R. Barzegaran, Hassan Zargarzadeh, and O.A. Mohammed. “Wireless Power Transfer for Electric Vehicle Using an Adaptive Robot”. In: *IEEE Transactions on Magnetics* 53.6 (2017), pp. 1–4. DOI: 10.1109/TMAG.2017.2664800.

[16] Madhur Behl et al. “Autonomous Electric Vehicle Charging System”. In: *2019 Systems and Information Engineering Design Symposium (SIEDS)*. 2019, pp. 1–6. DOI: 10.1109/SIEDS.2019.8735620.

[17] Marie Rajon Bernard, Nic Lutsey, and Dale Hall. *Update on electric vehicle uptake in European cities*. 2021. URL: https://theicct.org/sites/default/files/publications/ev-uptake-eu-cities-oct21.pdf.

[18] J. Biebach et al. “Compact modular power supplies for superconducting inductive storage and for capacitor charging”. In: *IEEE Transactions on Magnetics* 37.1 (2001), pp. 353–357. DOI: 10.1109/20.911853.

[19] M Bildgen. *Resonant converter topologies: Application note*. 1999. URL: https://www.scribd.com/document/416518682/5-10530.

[20] Christoph R. Birkl et al. “Degradation diagnostics for lithium ion cells”. In: *Journal of Power Sources* 341 (2017), pp. 373–386. ISSN: 0378-7753. DOI: https://doi.org/10.1016/j.jpowsour.2016.12.011. URL: https://www.sciencedirect.com/science/article/pii/S0378775316316998.

[21] British Heart Foundation. *Walks and treks faqs*. URL: https://www.bhf.org.uk/how-you-can-help/events/training-zone/walking-training-zone/walking-faqs.

[22] Thomas S. Bryden et al. “Lithium-ion degradation at varying discharge rates”. In: *Energy Procedia* 151 (2018). 3rd Annual Conference in Energy Storage and Its Applications, 3rd CDT-ESA-AC, 11–12 September 2018, The University of Sheffield, UK, pp. 194–198. ISSN: 1876-6102. DOI: https://doi.org/10.1016/j.egypro.2018.09.047. URL: https://www.sciencedirect.com/science/article/pii/S1876610218305915.

[23] Lluc Canals Casals, Beatriz Amante García, and Maria Margarita González Benítez. “Aging model for re-used electric vehicle batteries in second life stationary applications”. In: *Project Management and Engineering Research: AEIPRO 2016*. Springer. 2017, pp. 139–151.

[24] Lluc Canals Casals, B. Amante García, and Camille Canal. “Second life batteries lifespan: Rest of useful life and environmental analysis”. In: *Journal of Environmental Management* 232 (2019), pp. 354–363. ISSN: 0301-4797. DOI: https://doi.org/10.1016/j.jenvman.2018.11.046. URL: https://www.sciencedirect.com/science/article/pii/S0301479718313124.

[25] Bülent Çatay and İhsan Sadati. “An improved matheuristic for solving the electric vehicle routing problem with time windows and synchronized mobile charging/battery swapping”. In: *Computers and Operations Research* 159 (2023), p. 106310. ISSN: 0305-0548. DOI: https://doi.org/10.1016/j.cor.2023.106310. URL: https://www.sciencedirect.com/science/article/pii/S0305054823001740.

[26] L. Chang. “Comparison of AC drives for electric vehicles-a report on experts’ opinion survey”. In: *IEEE Aerospace and Electronic Systems Magazine* 9.8 (1994), pp. 7–11. DOI: 10.1109/62.311235.

[27] ChargePoint, Inc. *2017 Charging Forward Report All Roads Lead to e-Mobility*. 2018. URL: https://www.greeneconome.com/wp-content/uploads/2018/04/2017_ChargePoint_Charging_Forward_Report.pdf.

[28] Pradip Chatterjee. *Design considerations for Fast DC Chargers targeting 350 kW*. URL: https://www.infineon.com/dgdl/Infineon-Design_considerations_DC_chargers-ART-v01_00-EN.pdf?fileId=5546d46269e1c019016a2ab43fb22560.

[29] Vishal Chauhan and Arobinda Gupta. “Scheduling Mobile Charging Stations for Electric Vehicle Charging”. In: *2018 14th International Conference on Wireless and Mobile Computing, Networking and Communications (WiMob)*. 2018, pp. 131–136. DOI: 10.1109/WiMOB.2018.8589146.

[30] Huwei Chen et al. “Dynamic Charging Optimization for Mobile Charging Stations in Internet of Things”. In: *IEEE Access* 6 (2018), pp. 53509–53520. DOI: 10.1109/ACCESS.2018.2868937.

[31] Huwei Chen et al. “Optimal Approach to Provide Electric Vehicles with Charging Service by Using Mobile Charging Stations in Heterogeneous Networks”. In: *2016 IEEE 84th Vehicular Technology Conference (VTC-Fall)*. 2016, pp. 1–5. DOI: 10.1109/VTCFall.2016.7881135.

[32] Ming Cheng et al. “Sustainability evaluation of second-life battery applications in grid-connected PV-battery systems”. In: *Journal of Power Sources* 550 (2022), p. 232132. ISSN: 0378-7753. DOI: https://doi.org/10.1016/j.jpowsour.2022.232132. URL: https://www.sciencedirect.com/science/article/pii/S0378775322011090.

[33] Bentley C Clinton and Daniel C Steinberg. “Providing the Spark: Impact of financial incentives on battery electric vehicle adoption”. In: *Journal of Environmental Economics and Management* 98 (2019), p. 102255.

[34] Ryan Collin et al. “Advanced electric vehicle fast-charging technologies”. In: *Energies* 12.10 (2019), p. 1839.

[35] Commission for Electricity and Gas Regulation. *Study on the occurrence and impact of negative prices in the day-ahead market*. 2023. URL: https://www.creg.be/sites/default/files/assets/Publications/Studies/F2590EN.pdf.

[36] Continental AG. *Continental is jointly developing fully automatic charging robots for electric vehicles with Volterio*. 2022. URL: https://www.continental.com/en/press/press-releases/20220126-charging-robot/.

[37] Julian Conzade et al. *Europe's EV opportunity-and the charging infrastructure needed to meet it*. Nov. 2022. URL: https://www.mckinsey.com/industries/automotive-and-assembly/our-insights/europes-ev-opportunity-and-the-charging-infrastructure-needed-to-meet-it.

[38] Shaohua Cui et al. “Locating Multiple Size and Multiple Type of Charging Station for Battery Electricity Vehicles”. In: *Sustainability* 10.9 (2018). ISSN: 2071-1050. DOI: 10.3390/su10093267. URL: https://www.mdpi.com/2071-1050/10/9/3267.

[39] Muhammad Danial, Fatin Amanina Azis, and Pg Emeroylariffion Abas. “Techno-Economic Analysis and Feasibility Studies of Electric Vehicle Charging Station”. In: *World Electric Vehicle Journal* 12.4 (2021). ISSN: 2032-6653. DOI: 10.3390/wevj12040264. URL: https://www.mdpi.com/2032-6653/12/4/264.

[40] Christopher L Decker. *Electric vehicle charging and routing management via multi-infrastructure data fusion*. Rochester Institute of Technology, 2012.

[41] Boucar Diouf and Ramchandra Pode. “Potential of lithium-ion batteries in renewable energy”. In: *Renewable Energy* 76 (2015), pp. 375–380. ISSN: 0960-1481. DOI: https://doi.org/10.1016/j.renene.2014.11.058. URL: https://www.sciencedirect.com/science/article/pii/S0960148114007885.

[42] Scooter Doll. *Introducing ziggy: An Autonomous Robot that saves you a parking spot then charges your EV*. 2022. URL: https://electrek.co/2022/06/14/ziggy-autonomous-robot-charges-ev/.

[43] Rik W. de Doncker, Deepak Divan, and Mustansir Kheraluwala. “A three-phase soft-switched high power density DC/DC converter for high power applications”. In: *Conference Record of the 1988 IEEE Industry Applications Society Annual Meeting* (1988), 796–805 vol.1. URL: https://api.semanticscholar.org/CorpusID:16567803.

[44] Qingyin Dong et al. “Cost, energy, and carbon footprint benefits of second-life electric vehicle battery use”. In: *iScience* 26.7 (2023), p. 107195. ISSN: 2589-0042. DOI: https://doi.org/10.1016/j.isci.2023.107195. URL: https://www.sciencedirect.com/science/article/pii/S2589004223012725.

[45] Aisling Doyle and Tariq Muneer. “2 - Traction energy and battery performance modelling”. In: *Electric Vehicles: Prospects and Challenges*. Ed. by Tariq Muneer, Mohan Lal Kolhe, and Aisling Doyle. Elsevier, 2017, pp. 93–124. ISBN: 978-0-12-803021-9. DOI: https://doi.org/10.1016/B978-0-12-803021-9.00002-1. URL: https://www.sciencedirect.com/science/article/pii/B9780128030219000021.

[46] B. X. Du et al. “High thermal conductivity insulation and sheathing materials for electric vehicle cable application”. In: *IEEE Transactions on Dielectrics and Electrical Insulation* 26.4 (2019), pp. 1363–1370. DOI: 10.1109/TDEI.2019.008069.

[47] J. Dudrik, P. Spanik, and N.D. Trip. “Zero-Voltage and Zero-Current Switching Full-Bridge DC–DC Converter With Auxiliary Transformer”. In: *IEEE Transactions on Power Electronics* 21.5 (2006), pp. 1328–1335. DOI: 10.1109/TPEL.2006.880285.

[48] EFI Automotive. *Inductive Robot Charger*. Feb. 2023. URL: https://www.efiautomotive.com/en/produits/inductive-robot-charger/.

[49] EFI Automotive. *Press Kit EFI Automotive - CES 2023*. 2023. URL: https://www.efiautomotive.com/wp-content/uploads/2023/01/press-kit-CES2023.pdf.

[50] Ona Egbue and Suzanna Long. “Barriers to widespread adoption of electric vehicles: An analysis of consumer attitudes and perceptions”. In: *Energy Policy* 48 (2012). Special Section: Frontiers of Sustainability, pp. 717–729. ISSN: 0301-4215. DOI: https://doi.org/10.1016/j.enpol.2012.06.009. URL: https://www.sciencedirect.com/science/article/pii/S0301421512005162.

[51] M. Ehsani, Y. Gao, and A. Emadi. *Modern Electric, Hybrid Electric, and Fuel Cell Vehicles: Fundamentals, Theory, and Design, Second Edition*. Power Electronics and Applications Series. CRC Press, 2017. ISBN: 9781420054002. URL: https://books.google.nl/books?id=Rue_FhZsV40C.

[52] Hauke Engel, Patrick Hertzke, and Giulia Siccardo. *Second-life EV batteries: The newest value pool in Energy Storage*. 2019. URL: https://www.mckinsey.com/~/media/McKinsey/Industries/Automotive%20and%20Assembly/Our%20Insights/Second%20life%20EV%20batteries%20The%20newest%20value%20pool%20in%20energy%20storage/Second-life-EV-batteries-The-newest-value-pool-in-energy-storage.ashx.

[53] Envision Group. *Envision Group launches Green Charging Robot Mochi*. 2021. URL: https://www.prnewswire.com/news-releases/envision-group-launches-green-charging-robot-mochi-the-worlds-first-mass-produced-charging-robot-100-powered-by-green-electricity-301275227.html.

[54] Epex Spot. *Market data*. 2023. URL: https://www.epexspot.com/en/market-data?market_area=NL&trading_date=2023-12-09&delivery_date=2023-12-10&underlying_year=&modality=Intraday&sub_modality=DayAhead&technology=&product=60&data_mode=table&period=&production_period=.

[55] European Alternative Fuels Observatory. *Electric vehicle recharging prices*. 2024. URL: https://alternative-fuels-observatory.ec.europa.eu/consumer-portal/electric-vehicle-recharging-prices.

[56] European Automobile Manufacturers’ Association. *ACEA Position Paper Proposal for the Alternative Fuels Infrastructure Regulation (AFIR)*. Nov. 2021. URL: https://acea.auto/files/ACEA_Position_Paper-Alternative_Fuels_Infrastructure_Regulation.pdf.

[57] European Environment Agency. *New registrations of electric vehicles in Europe*. 2023. URL: https://www.eea.europa.eu/en/analysis/indicators/new-registrations-of-electric-vehicles?activeAccordion=309c5ef9-de09-4759-bc02-802370dfa366.

[58] European Parliament. *EU ban on the sale of new petrol and diesel cars from 2035 explained*. June 2023. URL: https://www.europarl.europa.eu/news/en/headlines/economy/20221019STO44572/eu-ban-on-sale-of-new-petrol-and-diesel-cars-from-2035-explained.

[59] Eurostat. *Passenger cars in the EU*. Mar. 2023. URL: https://ec.europa.eu/eurostat/statistics-explained/index.php/Passenger_cars_in_the_EU.

[60] EV Database. *Audi e-tron 55 quattro*. URL: https://ev-database.org/car/1355/Audi-e-tron-55-quattro.

[61] EV Database. *Hyundai Kona*. URL: https://ev-database.org/car/1423/Hyundai-Kona-Electric-64-kWh.

[62] EV Database. *Kia e-Niro*. URL: https://ev-database.org/car/1260/Kia-e-Niro-64-kWh.

[63] EV Database. *Nissan Leaf*. URL: https://ev-database.org/car/1656/Nissan-Leaf.

[64] EV Database. *Renault Zoe ZE50 R110*. URL: https://ev-database.org/car/1164/Renault-Zoe-ZE50-R110.

[65] EV Database. *Skoda Enyaq iV 80*. URL: https://ev-database.org/car/1280/Skoda-Enyaq-iV-80.

[66] EV Database. *Tesla Model 3*. URL: https://ev-database.org/car/1555/Tesla-Model-3.

[67] EV Database. *Tesla Model S*. URL: https://ev-database.org/car/1324/Tesla-Model-S-Performance.

[68] EV Database. *Volkswagen ID.3 Pro*. URL: https://ev-database.org/car/1202/Volkswagen-ID3-Pro.

[69] EV Database. *Volkswagen-e-Golf*. URL: https://ev-database.org/car/1087/Volkswagen-e-Golf.

[70] EV Safe Charge. *Ziggy*. 2023. URL: https://evsafecharge.com/ziggy/.

[71] EVAR Corp. *Parky- EV recharging robot*. URL: https://www.evar.co.kr/evar-robot.

[72] EVKX. *Tesla Model 3 charging curve and performance*. 2024. URL: https://evkx.net/models/tesla/model_3/model_3/chargingcurve/.

[73] Jim Eyer and Garth Corey. "Energy storage for the electricity grid: Benefits and market potential assessment guide". In: *Sandia National Laboratories* 20.10 (2010), p. 5.

[74] Hossein Farzin, Mahmud Fotuhi-Firuzabad, and Moein Moeini-Aghtaie. "A Practical Scheme to Involve Degradation Cost of Lithium-Ion Batteries in Vehicle-to-Grid Applications". In: *IEEE Transactions on Sustainable Energy* 7.4 (2016), pp. 1730–1738. DOI: 10.1109/TSTE.2016.2558500.

[75] Fastned. *Prices*. 2024. URL: https://fastnedcharging.com/en/ev-charging-price.

[76] Fastned Global. *Everything you've always wanted to know about fast charging*. 2022. URL: https://fastnedcharging.com/hq/everything-youve-always-wanted-to-know-about-fast-charging/.

[77] Hao Feng et al. "Passive Capacitor Voltage Balancing of SiC-Based Three-Level Dual-Active-Bridge Converter Using Hybrid NPC-Flying Capacitor Structure". In: *IEEE Transactions on Power Electronics* 37.4 (2022), pp. 4183–4194. DOI: 10.1109/TPEL.2021.3119210.

[78] P. Friedlingstein et al. "Global carbon budget 2022". In: *Earth System Science Data* 14 (11 2022), pp. 4811–4900. DOI: 10.5194/essd-14-4811-2022.

[79] Foad. H. Gandoman et al. "Quantitative analysis techniques for evaluating the reliability of Li-ion battery: challenges and solutions". In: *2020 IEEE Vehicle Power and Propulsion Conference (VPPC)*. 2020, pp. 1–5. DOI: 10.1109/VPPC49601.2020.9330994.

[80] Global Market Insights Inc. *Ev charging station market size, Forecast report 2032-2032*. May 2023. URL: https://www.gminsights.com/industry-analysis/electric-vehicle-charging-station-market.

[81] Emma Arfa Grunditz. *Design and assessment of battery electric vehicle powertrain, with respect to performance, energy consumption and electric motor thermal capability*. Chalmers Tekniska Hogskola (Sweden), 2016.

[82] Giuseppe Guidi et al. "Efficiency optimization of high power density Dual Active Bridge DC-DC converter". In: July 2010, pp. 981–986. DOI: 10.1109/IPEC.2010.5542146.

[83] Salman Habib et al. "Contemporary trends in power electronics converters for charging solutions of electric vehicles". In: *CSEE Journal of Power and Energy Systems* 6.4 (2020), pp. 911–929. DOI: 10.17775/CSEEJPES.2019.02700.

[84] Salman Habib et al. "Contemporary trends in power electronics converters for charging solutions of electric vehicles". In: *CSEE Journal of Power and Energy Systems* 6.4 (2020), pp. 911–929. DOI: 10.17775/CSEEJPES.2019.02700.

[85] Ahmad Hamidi, Luke Weber, and Adel Nasiri. "EV charging station integrating renewable energy and second-life battery". In: *2013 International Conference on Renewable Energy Research and Applications (ICRERA)*. IEEE. 2013, pp. 1217–1221.

[86] Hans Eric Melin. *The lithium-ion battery end-of-life market – A baseline study*. Tech. rep. Switzerland: World Economic Forum, Dec. 2018.

[87] Mohammed Hussein Saleh Mohammed Haram et al. "Feasibility of utilising second life EV batteries: Applications, lifespan, economics, environmental impact, assessment, and challenges". In: *Alexandria Engineering Journal* 60.5 (2021), pp. 4517–4536. ISSN: 1110-0168. DOI: https://doi.org/10.1016/j.aej.2021.03.021. URL: https://www.sciencedirect.com/science/article/pii/S1110016821001757.

[88] Nasser Hashemnia and Behzad Asaei. "Comparative study of using different electric motors in the electric vehicles". In: *2008 18th International Conference on Electrical Machines*. 2008, pp. 1–5. DOI: 10.1109/ICELMACH.2008.4800157.

[89] Fang He, Yafeng Yin, and Jing Zhou. “Deploying public charging stations for electric vehicles on urban road networks”. In: *Transportation Research Part C: Emerging Technologies* 60 (2015), pp. 227–240.

[90] Joachim Hentschel. *Volkswagen Konzern - AR 2017 - roadmap E: Full of energy!* 2017. URL: https://annualreport2017.volkswagenag.com/magazine/go-electric/roadmap-e-full-of-energy.html.

[91] Catherine Heymans et al. “Economic analysis of second use electric vehicle batteries for residential energy storage and load-levelling”. In: *Energy Policy* 71 (2014), pp. 22–30.

[92] Mario Hirz, Bernhard Walzel, and Helmut Brunner. “Autonomous Charging of Electric Vehicles in Industrial Environment”. In: *Tehnički glasnik* 15 (June 2021), pp. 220–225. DOI: 10.31803/tg-20210428191147.

[93] Thomas Hoffmann and Gunnar Prause. “On the Regulatory Framework for Last-Mile Delivery Robots”. In: *Machines* 6.3 (2018). ISSN: 2075-1702. DOI: 10.3390/machines6030033. URL: https://www.mdpi.com/2075-1702/6/3/33.

[94] Daocheng Huang et al. “High power density high efficiency dc/dc converter”. In: *2011 IEEE Energy Conversion Congress and Exposition*. 2011, pp. 1392–1399. DOI: 10.1109/ECCE.2011.6063942.

[95] Shisheng Huang et al. “Design of a Mobile Charging Service for Electric Vehicles in an Urban Environment”. In: *IEEE Transactions on Intelligent Transportation Systems* 16.2 (2015), pp. 787–798. DOI: 10.1109/TITS.2014.2341695.

[96] Hybrid - EV Committee. *Power Quality Requirements for Plug-In Electric Vehicle Chargers*. Jan. 2019. DOI: https://doi.org/10.4271/J2894/1_201901. URL: https://doi.org/10.4271/J2894/1_201901.

[97] Hyundai Motor Group. *EV Auto Charging Robot: Hyundai Motor Group: Robotics Lab*. 2022. URL: https://www.hyundaimotorgroup.com/tv/CONT0000000000044794.

[98] Hyundai Motor Group. *Hyundai Motor Group Shows Newly Developed Automatic Charging Robot for Electric Vehicles*. 2023. URL: https://www.hyundai.news/eu/articles/press-releases/newly-developed-automatic-charging-robot-for-electric-vehicles.html.

[99] Hyundai Robotics Lab. *Unveiled Robots: Service Robot: ACR*. URL: https://robotics.hyundai.com/en/unveiled-robots/service/acr.do.

[100] Internatinal Energy Agency. *Share of cumulative power capacity by technology, 2010-2027*. Dec. 2022. URL: https://www.iea.org/data-and-statistics/charts/share-of-cumulative-power-capacity-by-technology-2010-2027.

[101] International Electrotechnical Commission. *IEC 61000-3-2:2018*. 2018. URL: https://webstore.iec.ch/publication/28164.

[102] International Energy Agency. *CO2 emissions in 2022*. 2022. URL: https://www.iea.org/reports/co2-emissions-in-2022.

[103] International Energy Agency. *Global CO2 emissions from transport by sub-sector in the Net Zero Scenario, 2000-2030*. URL: https://www.iea.org/data-and-statistics/charts/global-co2-emissions-from-transport-by-sub-sector-in-the-net-zero-scenario-2000-2030-2.

[104] International Energy Agency. *Global EV Outlook 2021*. 2021. URL: https://www.iea.org/reports/global-ev-outlook-2021.

[105] Dylan Jennings and Miguel Figliozzi. “Study of sidewalk autonomous delivery robots and their potential impacts on freight efficiency and travel”. In: *Transportation Research Record* 2673.6 (2019), pp. 317–326.

[106] Anatol Pashkevich Jiuchun Gao Fabien Claveau and Philippe Chevrel. “Real-time motion planning for an autonomous mobile robot with wheel-ground adhesion constraint”. In: *Advanced Robotics* 37.10 (2023), pp. 649–666. DOI: 10.1080/01691864.2023.2186188. eprint: https://doi.org/10.1080/01691864.2023.2186188. URL: https://doi.org/10.1080/01691864.2023.2186188.

[107] Johan Cruijff Arena. *Innovation Lab - Energy Arena*. URL: https://www.johancruijffarena.nl/en/innovationlab/energyarena/.

[108] Peter Keil et al. “Calendar Aging of Lithium-Ion Batteries”. In: *Journal of The Electrochemical Society* 163.9 (July 2016), A1872. DOI: 10.1149/2.0411609jes. URL: https://dx.doi.org/10.1149/2.0411609jes.

[109] Wajahat Khan, Furkan Ahmad, and Mohammad Saad Alam. “Fast EV charging station integration with grid ensuring optimal and quality power exchange”. In: *Engineering Science and Technology, an International Journal* 22.1 (2019), pp. 143–152.

[110] Cosmin Koch-Ciobotaru et al. “Second life battery energy storage system for enhancing renewable energy grid integration”. In: *2015 IEEE Energy Conversion Congress and Exposition (ECCE)*. IEEE. 2015, pp. 78–84.

[111] Peng-Yong Kong. “Autonomous Robot-Like Mobile Chargers for Electric Vehicles at Public Parking Facilities”. In: *IEEE Transactions on Smart Grid* 10.6 (2019), pp. 5952–5963. DOI: 10.1109/TSG.2019.2893962.

[112] Alexandros-Michail Koufakis et al. “Towards an optimal EV charging scheduling scheme with V2G and V2V energy transfer”. In: *2016 IEEE International Conference on Smart Grid Communications (SmartGridComm)*. IEEE. 2016, pp. 302–307.

[113] Imke Krüger and Gerhard Schmitz. “Energy Consumption Of Battery Cooling In Hybrid Electric Vehicles”. In: Jan. 2012.

[114] KUKA AG. *Volkswagen Group Research and Automation Specialist kuka conclude new cooperation contract*. 2017. URL: https://www.kuka.com/en-de/company/press/news/2017/07/kuka-und-vw-schliessen-neuen-kooperationsvertrag.

[115] Gillian Lacey, Ghamin Putrus, and Anwar Salim. “The use of second life electric vehicle batteries for grid support”. In: *Eurocon 2013*. IEEE. 2013, pp. 1255–1261.

[116] Fred Lambert. *Tesla deploys new mobile supercharger powered by Megapack instead of diesel generators*. 2019. URL: https://electrek.co/2019/11/29/tesla-mobile-supercharger-megapack/.

[117] Henry Lee and Alex Clark. “Charging the future: Challenges and opportunities for electric vehicle adoption”. In: (2018).

[118] Min-Su Lee et al. “A High Efficiency Phase-Shift Full-Bridge Converter With Improved Clamping Circuit to Eliminate Oscillation for EV Battery Charger”. In: *2020 IEEE 9th International Power Electronics and Motion Control Conference (IPEMC2020-ECCE Asia)*. 2020, pp. 1696–1701. DOI: 10.1109/IPEMC-ECCEAsia48364.2020.9367647.

[119] Jingkun Li and Zi-Feng Ma. “Past and Present of LiFePO4: From Fundamental Research to Industrial Applications”. In: *Chem* 5.1 (2019), pp. 3–6. ISSN: 2451-9294. DOI: https://doi.org/10.1016/j.chempr.2018.12.012. URL: https://www.sciencedirect.com/science/article/pii/S2451929418305758.

[120] Qi Liu et al. “Towards an Efficient and Real-Time Scheduling Platform for Mobile Charging Vehicles”. In: *Algorithms and Architectures for Parallel Processing*. Ed. by Jaideep Vaidya and Jin Li. Cham: Springer International Publishing, 2018, pp. 402–416. ISBN: 978-3-030-05057-3.

[121] Ya’Nan Lou and Shichun Di. “Design of a Cable-Driven Auto-Charging Robot for Electric Vehicles”. In: *IEEE Access* 8 (2020), pp. 15640–15655. DOI: 10.1109/ACCESS.2020.2966528.

[122] Shangai JIYU Technology Co. Ltd. *Autonomous Driving EV Charging Robot*. URL: http://en.shanghaijiyu.com/p-cproduct.html.

[123] Dingsihao Lyu, Thiago Batista Soeiro, and Pavol Bauer. “Multi-objective Design and Benchmark of Wide Voltage Range Phase-Shift Full Bridge DC/DC Converters for EV Charging Application”. In: *IEEE Transactions on Transportation Electrification* (2023), pp. 1–1. DOI: 10.1109/TTE.2023.3254203.

[124] Lukas Mauler, Fabian Duffner, and Jens Leker. “Economies of scale in battery cell manufacturing: The impact of material and process innovations”. In: *Applied Energy* 286 (2021), p. 116499. ISSN: 0306-2619. DOI: https://doi.org/10.1016/j.apenergy.2021.116499. URL: https://www.sciencedirect.com/science/article/pii/S030626192100060X.

[125] Mohsen Mazidi et al. “Optimal allocation of PHEV parking lots to minimize distribution system losses”. In: *2015 IEEE Eindhoven PowerTech*. IEEE. 2015, pp. 1–6.

[126] Garth P. McCormick. “Computability of global solutions to factorable nonconvex programs: Part I — Convex underestimating problems”. In: *Mathematical Programming* 10 (1976), pp. 147–175. URL: https://api.semanticscholar.org/CorpusID:12478942.

[127] M. M. McQuage et al. “High Power Density Capacitor Charging Power Supply Development for Repetitive Pulsed Power”. In: *Conference Record of the 2006 Twenty-Seventh International Power Modulator Symposium*. 2006, pp. 368–371. DOI: 10.1109/MODSYM.2006.365261.

[128] Danielle Meyer and Jiankang Wang. “Integrating ultra-fast charging stations within the power grids of smart cities: a review”. In: *IET Smart Grid* 1.1 (2018), pp. 3–10. DOI: https://doi.org/10.1049/iet-stg.2018.0006. URL: https://ietresearch.onlinelibrary.wiley.com/doi/abs/10.1049/iet-stg.2018.0006.

[129] Jerome Mies, Jurjen Helmus, and Robert van den Hoed. “Estimating the Charging Profile of Individual Charge Sessions of Electric Vehicles in The Netherlands”. In: *World Electric Vehicle Journal* 9 (June 2018), p. 17. DOI: 10.3390/wevj9020017.

[130] Ministry of Infrastructure and the Environment. *Road traffic signs and regulations in the Netherlands*. URL: https://www.universiteitleiden.nl/binaries/content/assets/customsites/study-abroad-exchange-students/road_traffic_signs_and_regulations_jan_2013_uk.pdf.

[131] Valeh Moghaddam et al. “Dispatch management of portable charging stations in electric vehicle networks”. In: *ETransportation* 8 (2021), p. 100112.

[132] Jeffrey Morroni and Pradeep Shenoy. *Understanding the Trade-offs and Technologies to Increase Power Density*. 2023. URL: https://www.ti.com/lit/wp/slyy193c/slyy193c.pdf?ts=1705712679676.

[133] Seyed Abolfazl Mortazavizadeh et al. “High Frequency, High Efficiency, and High Power Density GaN-Based LLC Resonant Converter: State-of-the-Art and Perspectives”. In: *Applied Sciences* 11.23 (2021). ISSN: 2076-3417. DOI: 10.3390/app112311350. URL: https://www.mdpi.com/2076-3417/11/23/11350.

[134] Mahdi Mosayebi et al. “Smart Emergency EV-to-EV Portable Battery Charger”. In: *Inventions* 7.2 (2022). ISSN: 2411-5134. DOI: 10.3390/inventions7020045. URL: https://www.mdpi.com/2411-5134/7/2/45.

[135] NaaS Technology Inc. *Naas unveils first automatic charging robot*. 2023. URL: https://ir.enaas.com/news-releases/news-release-details/naas-unveils-first-automatic-charging-robot/.

[136] Ahmed Nabih et al. “High Power Density 1 MHz 3 kW 400 V-48 V LLC Converter for Datacenters with improved Core Loss and Termination Loss”. In: *2021 IEEE Applied Power Electronics Conference and Exposition (APEC)*. 2021, pp. 304–309. DOI: 10.1109/APEC42165.2021.9487232.

[137] Nationale Agenda Laadinfrastructuur. *Dutch National Charging Infrastructure Agenda*. May 2023. URL: https://nederlandelektrisch.nl/u/images/nal-english-may-2023.pdf.

[138] Netherlands Enterprise Agency. *Electric Vehicles Statistics in the Netherlands*. Mar. 2023. URL: https://www.rvo.nl/sites/default/files/2023-03/Statistics-Electric-Vehicles-and-Charging-in-The-Netherlands-up-to-and-including-February-2023.pdf.

[139] Jeremy Neubauer et al. *Identifying and overcoming critical barriers to widespread second use of PEV batteries*. Tech. rep. National Renewable Energy Lab.(NREL), Golden, CO (United States), 2015.

[140] New West Technologies, LLC and U.S Department of Energy. *Costs Associated With Non-Residential Electric Vehicle Supply Equipment*. 2015. URL: https://afdc.energy.gov/files/u/publication/evse_cost_report_2015.pdf.

[141] Michael Nicholas. *Estimating electric vehicle charging infrastructure costs across major U.S. metropolitan areas*. 2019. URL: https://theicct.org/sites/default/files/publications/ICCT_EV_Charging_Cost_20190813.pdf.

[142] Roman Niestrój, Tomasz Rogala, and Wojciech Skarka. “An Energy Consumption Model for Designing an AGV Energy Storage System with a PEMFC Stack”. In: *Energies* 13.13 (2020). ISSN: 1996-1073. DOI: 10.3390/en13133435. URL: https://www.mdpi.com/1996-1073/13/13/3435.

[143] B. Padmavathi et al. *Implementation of Charging an Electric Vehicle Using an Adaptive Robot*. 2018. URL: https://acadpubl.eu/hub/2018-118-24/2/373.pdf.

[144] Geerte L. Paradies et al. “Falling short in 2030: Simulating battery-electric vehicle adoption behaviour in the Netherlands”. In: *Energy Research & Social Science* 97 (2023), p. 102968. ISSN: 2214-6296. DOI: https://doi.org/10.1016/j.erss.2023.102968. URL: https://www.sciencedirect.com/science/article/pii/S2214629623000282.

[145] O.D. Patterson and D.M. Divan. “Pseudo-resonant full bridge DC/DC converter”. In: *IEEE Transactions on Power Electronics* 6.4 (1991), pp. 671–678. DOI: 10.1109/63.97767.

[146] Martin Pavlovsky, Sjoerd Walter Hero de Haan, and Jan Abraham Ferreira. “Reaching High Power Density in Multikilowatt DC–DC Converters With Galvanic Isolation”. In: *IEEE Transactions on Power Electronics* 24.3 (2009), pp. 603–612. DOI: 10.1109/TPEL.2008.2008650.

[147] Sarath Perera and Sean Elphick. “Chapter 7 - Implications of equipment behaviour on power quality”. In: *Applied Power Quality*. Ed. by Sarath Perera and Sean Elphick. Elsevier, 2023, pp. 185–258. ISBN: 978-0-323-85467-2. DOI: https://doi.org/10.1016/B978-0-323-85467-2.00002-0. URL: https://www.sciencedirect.com/science/article/pii/B9780323854672000020.

[148] Scott B. Peterson, J.F. Whitacre, and Jay Apt. “The economics of using plug-in hybrid electric vehicle battery packs for grid storage”. In: *Journal of Power Sources* 195.8 (2010), pp. 2377–2384. ISSN: 0378-7753. DOI: https://doi.org/10.1016/j.jpowsour.2009.09.070. URL: https://www.sciencedirect.com/science/article/pii/S0378775309017303.

[149] Andreas Podias et al. “Sustainability assessment of second use applications of automotive batteries: Ageing of Li-ion battery cells in automotive and grid-scale applications”. In: *World Electric Vehicle Journal* 9.2 (2018), p. 24.

[150] Hakan Polat et al. “A Review of DC Fast Chargers with BESS for Electric Vehicles: Topology, Battery, Reliability Oriented Control and Cooling Perspectives”. In: *Batteries* 9.2 (2023). ISSN: 2313-0105. DOI: 10.3390/batteries9020121. URL: https://www.mdpi.com/2313-0105/9/2/121.

[151] Premium Power Corporation. *TransFlow 2000: Utility Scale Mobile Energy Storage System*. 2009. URL: http://www.premiumpower.com/product/TF2000-2-pager.pdf.

[152] Roberto Quilez et al. “Docking autonomous robots in passive docks with Infrared sensors and QR codes”. In: (June 2015). DOI: 10.4108/icst.tridentcom.2015.259673.

[153] Maria-Simona Răboacă et al. “An Optimization Model for the Temporary Locations of Mobile Charging Stations”. In: *Mathematics* 8.3 (2020). ISSN: 2227-7390. DOI: 10.3390/math8030453. URL: https://www.mdpi.com/2227-7390/8/3/453.

[154] *Rainflow 3.2.0*. URL: https://pypi.org/project/rainflow/.

[155] Brindha Ramasubramanian et al. “Recent Development in Carbon-LiFePO4 Cathodes for Lithium-Ion Batteries: A Mini Review”. In: *Batteries* 8.10 (2022). ISSN: 2313-0105. DOI: 10.3390/batteries8100133. URL: https://www.mdpi.com/2313-0105/8/10/133.

[156] Rijksdienst voor Ondernemend Nederland. *Nationaal Laadonderzoek 2022 - RVO*. 2022. URL: https://www.rvo.nl/sites/default/files/2022-09/Nationaal-laadonderzoek-2022.pdf.

[157] Leandro Roggia et al. “Comparison between full-bridge-forward converter and DAB converter”. In: *2013 Brazilian Power Electronics Conference*. 2013, pp. 224–229. DOI: 10.1109/COBEP.2013.6785119.

[158] Bram Rotthier et al. “Home charging of electric vehicles in Belgium”. In: *2013 World Electric Vehicle Symposium and Exhibition (EVS27)*. IEEE. 2013, pp. 1–6.

[159] Hedayat Saboori and Shahram Jadid. “Optimal scheduling of mobile utility-scale battery energy storage systems in electric power distribution networks”. In: *Journal of energy storage* 31 (2020), p. 101615.

[160] Hedayat Saboori, Shahram Jadid, and Mehdi Savaghebi. “Optimal Management of Mobile Battery Energy Storage as a Self-Driving, Self-Powered and Movable Charging Station to Promote Electric Vehicle Adoption”. In: *Energies* 14.3 (2021). ISSN: 1996-1073. DOI: 10.3390/en14030736. URL: https://www.mdpi.com/1996-1073/14/3/736.

[161] Andoni Saez-de-Ibarra et al. “Sizing study of second life Li-ion batteries for enhancing renewable energy grid integration”. In: *IEEE Transactions on Industry Applications* 52.6 (2016), pp. 4999–5008.

[162] Zafer Sahinoglu, Zhifeng Tao, and Koon Hoo Teo. “Off-grid portable EV charging network management with dynamic energy pricing”. In: *13th International IEEE Conference on Intelligent Transportation Systems*. 2010, pp. 403–408. DOI: 10.1109/ITSC.2010.5625299.

[163] Mohamed Salem et al. “A Review of an Inductive Power Transfer System for EV Battery Charger”. In: *European Journal of Scientific Research* 134 (Aug. 2015), pp. 41–56.

[164] Jan Schöberl et al. “Thermal runaway propagation in automotive lithium-ion batteries with NMC-811 and LFP cathodes: Safety requirements and impact on system integration”. In: *eTransportation* 19 (2024), p. 100305. ISSN: 2590-1168. DOI: https://doi.org/10.1016/j.etran.2023.100305. URL: https://www.sciencedirect.com/science/article/pii/S2590116823000802.

[165] Sven Schoenberg and Falko Dressler. “Reducing Waiting Times at Charging Stations With Adaptive Electric Vehicle Route Planning”. In: *IEEE Transactions on Intelligent Vehicles* 8.1 (2023), pp. 95–107. DOI: 10.1109/TIV.2022.3140894.

[166] Andreas Schroeder and Thure Traber. “The economics of fast charging infrastructure for electric vehicles”. In: *Energy Policy* 43 (2012), pp. 136–144.

[167] Yuanyuan Shi et al. “A Convex Cycle-based Degradation Model for Battery Energy Storage Planning and Operation”. In: *2018 Annual American Control Conference (ACC)*. 2018, pp. 4590–4596. DOI: 10.23919/ACC.2018.8431814.

[168] Aviral Shukla, Joseph Pekny, and Venkat Venkatasubramanian. “An optimization framework for cost effective design of refueling station infrastructure for alternative fuel vehicles”. In: *Computers and Chemical Engineering* 35.8 (2011). Energy and Sustainability, pp. 1431–1438. ISSN: 0098-1354. DOI: https://doi.org/10.1016/j.compchemeng.2011.03.018. URL: https://www.sciencedirect.com/science/article/pii/S0098135411001086.

[169] Margaret Smith. *Level 1 electric vehicle charging stations at the workplace*. Tech. rep. Energetics Incorporated, Columbia, MD (United States), 2016.

[170] Tiago JC Sousa et al. “New perspectives for vehicle-to-vehicle (V2V) power transfer”. In: *IECON 2018-44th Annual Conference of the IEEE Industrial Electronics Society*. IEEE. 2018, pp. 5183–5188.

[171] Julian Spector. *FreeWire technologies raises* $25M, starts shipping battery-boosted fast chargers.$ 2020. URL: https://www.greentechmedia.com/articles/read/freewire-technologies-raises-25-million-as-it-ships-battery-boosted-fast-chargers.

[172] A Srisawang, S Panaudomsup, and Y Prempraneerach. “Comparison of EMI Performance of Full-Bridge and Half-Bridge Power Converter”. In: *International Symposium on Nonlinear Theory and its Applications* (2002). URL: https://www.ieice.org/~nolta/symposium/archive/2002/nolta_pdf/4204.pdf.

[173] Stanwell. *Negative prices: how they occur, what they mean*. URL: https://www.stanwell.com/our-news/energy-explainer/negative-prices/.

[174] Statista. *Battery price per kwh 2023*. en. Accessed: 2024-3-5. URL: https://www.statista.com/statistics/883118/global-lithium-ion-battery-pack-costs/.

[175] Statista. *Europe: number of electric vehicle charging stations 2022*. en. https://www.statista.com/statistics/955443/number-of-electric-vehicle-charging-stations-in-europe/. Accessed: 2023-11-5.

[176] Statista. *Monthly wholesale electricity prices in the Netherlands 2019-2023*. https://www.statista.com/statistics/1314549/netherlands-monthly-wholesale-electricity-price/.

[177] Marco Stecca et al. “Lifetime Estimation of Grid-Connected Battery Storage and Power Electronics Inverter Providing Primary Frequency Regulation”. In: *IEEE Open Journal of the Industrial Electronics Society* 2 (2021), pp. 240–251. DOI: 10.1109/OJIES.2021.3064635.

[178] Daniel Ioan Stroe. *Lifetime Models for Lithium-ion Batteries used in Virtual Power Plant Applications*. English. Nov. 2014.

[179] Bo Sun et al. “Optimal scheduling for electric vehicle charging with discrete charging levels in distribution grid”. In: *IEEE Transactions on Smart Grid* 9.2 (2016), pp. 624–634.

[180] Goro Tamai. “What are the hurdles to full vehicle electrification?[technology leaders]”. In: *IEEE Electrification Magazine* 7.1 (2019), pp. 5–11.

[181] Peng Tang et al. “Online-to-offline mobile charging system for electric vehicles: Strategic planning and online operation”. In: *Transportation Research Part D: Transport and Environment* 87 (2020), p. 102522. ISSN: 1361-9209. DOI: https://doi.org/10.1016/j.trd.2020.102522. URL: https://www.sciencedirect.com/science/article/pii/S1361920920307094.

[182] Tesla. *Charger prototype finding its way to Model S*. YouTube, Aug. 2015. URL: https://www.youtube.com/watch?v=uMM0lRfX6YI.

[183] Tesla. *Charging*. URL: https://www.tesla.com/support/charging.

[184] Trin Thananusak et al. “The Development of Electric Vehicle Charging Stations in Thailand: Policies, Players, and Key Issues (2015–2020)”. In: *World Electric Vehicle Journal* 12.1 (2021). ISSN: 2032-6653. DOI: 10.3390/wevj12010002. URL: https://www.mdpi.com/2032-6653/12/1/2.

[185] The International Council on Clean Transportation. *European Union CO2 Standards for New Passenger Cars and Vans*. June 2021. URL: https://theicct.org/wp-content/uploads/2021/12/eu-co2-FS1-jun2021.pdf.

[186] The Society of Automotive Engineers. *SAE charging configurations and ratings terminology*. 2011. URL: https://www-sae-org.tudelft.idm.oclc.org/standards/development/sae-involvement-smart-grid.

[187] Transport & Environment. *“Charging” for phase-out*. Sept. 2022. URL: https://www.transportenvironment.org/discover/charging-for-phase-out/.

[188] U.S. Department of Energy. *Operation and maintenance for Electric Vehicle Charging Infrastructure*. URL: https://afdc.energy.gov/fuels/electricity_infrastructure_maintenance_and_operation.html.

[189] Falko Ueckerdt et al. “System LCOE: What are the costs of variable renewables?” In: *Energy* 63 (2013), pp. 61–75. ISSN: 0360-5442. DOI: https://doi.org/10.1016/j.energy.2013.10.072. URL: https://www.sciencedirect.com/science/article/pii/S0360544213009390.

[190] United Nations Environment Programme. *Paris Agreement*. 2015. URL: https://wedocs.unep.org/20.500.11822/20830.

[191] US Department of Energy. *Evaluating Electric Vehicle Charging Impacts and Customer Charging Behaviors-Experience from Six Smart Grid Investment Grant Projects, Office of Electricity Delivery and Energy Reliability, US Department of Energy*. 2014.

[192] E.J. Van Henten et al. “An Autonomous Robot for Harvesting Cucumbers in Greenhouses.” In: *Auton. Robots* 13 (Nov. 2002), pp. 241–258. DOI: 10.1023/A:1020568125418.

[193] Vattenfall | InCharge. *Our charging rates*. 2024. URL: https://incharge.vattenfall.nl/en/charge-on-the-go/our-rates.

[194] Sai Krishna Vempalli, K Deepa, et al. “A novel V2V charging method addressing the last mile connectivity”. In: *2018 IEEE International Conference on Power Electronics, Drives and Energy Systems (PEDES)*. IEEE. 2018, pp. 1–6.

[195] Jari Vepsäläinen. “Energy Demand Analysis and Powertrain Design of a High-Speed Delivery Robot Using Synthetic Driving Cycles”. In: *Energies* 15.6 (2022). ISSN: 1996-1073. DOI: 10.3390/en15062198. URL: https://www.mdpi.com/1996-1073/15/6/2198.

[196] Volkswagen Newsroom. *Initial contact: The Mobile Charging Robot – presenting a vision*. 2020. URL: https://www.volkswagen-newsroom.com/en/press-releases/initial-contact-the-mobile-charging-robot-presenting-a-vision-6736.

[197] Bernhard Walzel et al. *Automated robot-based charging system for electric vehicles*. Mar. 2016. DOI: 10.1007/978-3-658-13255-2_70.

[198] Faping Wang et al. "Location optimization of electric vehicle mobile charging stations considering multi-period stochastic user equilibrium". In: *Sustainability* 11.20 (2019), p. 5841.

[199] Fenfen Wang, Yelin Deng, and Chris Yuan. "Comparative Life Cycle Assessment of Silicon Nanowire and Silicon Nanotube Based Lithium Ion Batteries for Electric Vehicles". In: *Procedia CIRP* 80 (Jan. 2019), pp. 310–315. DOI: 10.1016/j.procir.2019.01.004.

[200] Haoyu Wang and Alireza Khaligh. "Comprehensive topological analyses of isolated resonant converters in PEV battery charging applications". In: *2013 IEEE Transportation Electrification Conference and Expo (ITEC)*. 2013, pp. 1–7. DOI: 10.1109/ITEC.2013.6574496.

[201] Jos Warmerdam, Jorden van der Hoogt, and Richard Kotter. *Final report – Johan Cruijff ArenA operational pilot: Johan Cruijff ArenA case study*. English. Interreg, North Sea Region, Oct. 2020.

[202] Lei Wen et al. "Open-pore LiFePO4/C microspheres with high volumetric energy density for lithium ion batteries". In: *Particuology* 22 (2015), pp. 24–29. ISSN: 1674-2001. DOI: https://doi.org/10.1016/j.partic.2014.11.002. URL: https://www.sciencedirect.com/science/article/pii/S1674200114002090.

[203] J.G.W. West. "DC, induction, reluctance and PM motors for electric vehicles". In: *Power Engineering Journal* 8.2 (1994), pp. 77–88. DOI: 10.1049/pe:19940203.

[204] Zijin Yan. "Design of base station backup power system constructed with ladder battery". In: *IOP Conference Series: Materials Science and Engineering*. Vol. 677. 3. IOP Publishing. 2019, p. 032011.

[205] Gil Jin Yang, Raimarius Delgado, and Byoung Wook Choi. "A Practical Joint-Space Trajectory Generation Method Based on Convolution in Real-Time Control". In: *International Journal of Advanced Robotic Systems* 13.2 (2016), p. 56. DOI: 10.5772/62722. eprint: https://doi.org/10.5772/62722. URL: https://doi.org/10.5772/62722.

[206] Laurance Yap. *Volkswagen's EV charging robots: GreenCars*. 2023. URL: https://www.greencars.com/news/volkswagens-ev-charging-robots.

[207] Tianlong Yuan et al. "Design of an Integrated Transformer With Parallel Windings for a 30-kW LLC Resonant Converter". In: *IEEE Transactions on Power Electronics* 38.11 (2023), pp. 14317–14333. DOI: 10.1109/TPEL.2023.3291954.

[208] Hyeok-Jin Yun et al. "A DAB Converter with Common-Point-Connected Winding Transformers Suitable for a Single-Phase 5-Level SST System". In: *Energies* 11 (Apr. 2018), p. 928. DOI: 10.3390/en11040928.

[209] Hongcai Zhang et al. "PEV Fast-Charging Station Siting and Sizing on Coupled Transportation and Power Networks". In: *IEEE Transactions on Smart Grid* 9.4 (2018), pp. 2595–2605. DOI: 10.1109/TSG.2016.2614939.

[210] Yaoli Zhang et al. "Mobile charging: A novel charging system for electric vehicles in urban areas". In: *Applied Energy* 278 (2020), p. 115648. ISSN: 0306-2619. DOI: https://doi.org/10.1016/j.apenergy.2020.115648. URL: https://www.sciencedirect.com/science/article/pii/S0306261920311454.

[211] Yue Zhang et al. *Leakage Current Mitigation of Non-Isolated Integrated Chargers for Electric Vehicles*. 2019. DOI: 10.1109/ECCE.2019.8913245.